EARLY-AGE SHRINKAGE OF ULTRA HIGH-PERFORMANCE CONCRETE: MITIGATION AND COMPENSATING MECHANISMS

(Spine title: Early-age shrinkage of ultra high-performance concrete)

(Thesis format: Integrated Article)

by

AHMED MOHAMMED **SOLIMAN**

Graduate Program in Engineering Science

Department of Civil and Environmental Engineering

A thesis submitted in partial fulfillment
of the requirements for the degree of
Doctor of Philosophy

The School of Graduate and Postdoctoral Studies
The University of Western Ontario
London, Ontario, Canada

THE UNIVERSITY OF WESTERN ONTARIO
School of Graduate and Postdoctoral Studies

CERTIFICATE OF EXAMINATION

Supervisor   **Examiners**

_____   _____
Dr. Moncef L. Nehdi   Dr. Tim A. Newson

                                                         _____
                                                         Dr. Julie Q. Shang

                                                         _____
                                                         Dr. Robert J. Klassen

                                                         _____
                                                         Dr. Medhat Shetata

The thesis by

Ahmed Mohammed Soliman

entitled:

**Early-Age Shrinkage of Ultra High-Performance Concrete:
Mitigation and Compensating Mechanisms**

is accepted in partial fulfillment of the
requirements for the degree of
Doctor of Philosophy

_____   _____
          Date   Chair of the Thesis Examination Board

Abstract

The very high mechanical strength and enhanced durability of ultra high-performance concrete (UHPC) make it a strong contender for several concrete applications. However, UHPC has a very low water-to-cement ratio, which increases its tendency to undergo early-age shrinkage cracking with a risk of decreasing its long-term durability. To reduce the magnitude of early-age shrinkage and cracking potential, several mitigation strategies have been proposed including the use of shrinkage reducing admixtures, internal curing methods (e.g. superabsorbent polymers), expansive cements and extended moist curing durations. To appropriately utilize these strategies, it is important to have a complete understanding of the driving forces behind early-age volume change and how these shrinkage mitigation methods work from a materials science perspective to reduce shrinkage under field like conditions.

This dissertation initially uses a first-principles approach to understand the interrelation mechanisms between different shrinkage types under simulated field conditions and the role of different shrinkage mitigations methods. The ultimate goal of the dissertation is to achieve lower early-age shrinkage and cracking risk concrete along with reducing its environmental and economic impact. As a result, a novel environmentally friendly shrinkage reducing technique based on using partially hydrated cementitious materials (PHCM) from waste concrete is proposed. The PHCM principle, mechanisms and efficiency were evaluated compared to other mitigation methods. Furthermore, the potential of replacing cement with wollastonite microfibers was investigated as a new strategy to produce UHPC with lower carbon foot-print, through reducing the cement production. Finally, an artificial neural networks (ANN) model for early-age autogenous shrinkage of concrete was proposed.

The evidence and insights provided by the experiments can be summarized in: drying and autogenous shrinkage are dependant phenomena and applying the conventional superposition principle will lead to an overestimation of the actual autogenous shrinkage, adequately considering in-situ conditions in testing protocols should allow gaining a better understanding of shrinkage mitigation mechanisms, the

PHCM technique provides a passive internal restraining system that resists deformation as early as the cementitious materials are mixed, wollastonite microfibers can act as an internal restraint for shrinkage, reinforcing the microstructure at the micro-crack level and leading to an enhancement of the early-age engineering properties, along with gaining environmental benefits, and ANN showed success in predicting autogenous shrinkage under simulated field conditions.

Co-Authorship Statement

This thesis has been prepared in accordance with the regulation of integrated-article format stipulated by the Faculty of Graduate Studies at The University of Western Ontario. Substantial parts of this thesis were either published in or submitted for publication to peer-reviewed technical journals and an international conference. All experimental work, data analysis, modeling process and writing of initial versions of all publications listed below were carried out by the candidate himself. The contribution of his research advisor and any other co-author, if applicable, consisted of either providing advice, and/or helping in the development of the final versions of publications:

1. Nehdi, M. L. and **Soliman, A. M.** (Accepted 2009) " Early-age properties of concrete: Overview of fundamental concepts and state-of-the art research," Construction Materials, ICE., Vol. 164, Issue CM2, April 2011, pp. 55-77.

2. **Soliman, A. M.** and Nehdi, M. L. (2009) "Effect of drying conditions on autogenous shrinkage of ultra-high performance concrete at early-age," Materials and Structures, RILEM. **In Press** (published on line in 2011-DOI: 10.1617/s11527-010-9670-0).

3. **Soliman, A. M.** and Nehdi, M. L. (Accepted 2011) "Early-age shrinkage of ultra high performance concrete under drying/wetting cycles and submerged conditions," ACI Materials Journal, American Concrete Institute. **Accepted.**

4. **Soliman, A. M.** and Nehdi, M. L. (Accepted 2010) "Self-accelerated reactive powder concrete using partially hydrated cementitious materials," ACI Materials Journal, American Concrete Institute. **In Press** (to appear in 2011).

5. **Soliman, A. M.** and Nehdi, M. L. (2010) "Self-restraining concrete: mechanisms and Evidence," Cement and Concrete Research, Elsevier Science. **Submitted.**

6. **Soliman, A. M.** and Nehdi, M. L. (2010) "Can partially hydrated cementitious materials mitigate early-age shrinkage in ultra-high Performance concrete?," Cement and Concrete Research, Elsevier Science. **Submitted.**

7. **Soliman, A. M.** and Nehdi, M. L. (2010) "Influence of natural wollastonite microfiber on early-age behaviour of ultra high-performance concrete," Journal of Materials in Civil Engineering, ASCE. **Submitted.**

8. **Soliman, A. M.** and Nehdi, M. L. (2011) "Shrinkage behaviour of ultra high performance concrete with shrinkage reducing admixture and wollastonite microfiber," Cement and Concrete Composites, Elsevier Science. **Submitted.**

9. **Soliman, A. M.** and Nehdi, M. L. (2011) "Artificial neural network modeling of early-age autogenous shrinkage of concrete," ACI Materials Journal, American Concrete Institute. **Submitted.**

10. **Soliman, A. M.** and Nehdi, M. L. (2010) "Performance of shrinkage reducing admixture under drying/wetting cycles and submerged conditions," 2nd International Structures Specialty Conference, Winnipeg, Manitoba, Canada, (ST-30-1: ST-30-7). **Published.**

11. **Soliman, A. M.** and Nehdi, M. L. (2010) "Effect of Shrinkage Mitigation Methods on Early-Age Shrinkage of UHPC under simulated field conditions," 8th International Conference on. Short and Medium Span Bridges, Niagara Falls, Ontario, Canada, 2010, pp. (83-1 :83-8) **Published.**

12. **Soliman, A. M.** and Nehdi, M. L. (2012) "Early-age behaviour of wollastonite microfiber UHPC," Twelfth International Conference on Recent Advances in Concrete Technology and Sustainability Issues, Prague, Czech Republic, 2012. **Submitted.**

13. **Soliman, A. M.** and Nehdi, M. L. (2012) "Performance of concrete shrinkage mitigation admixtures under simulated field conditions," Proceeding of the Tenth International Conference on Superplasticizer and Other Chemical Admixtures in Concrete to be held in Prague, Czech Republic, October 28 to 31, 2012. **Submitted.**

14. **Soliman, A. M.** and Nehdi, M. L. (2011), "Environmentally friendly self-accelerated concrete," Proceedings of 2nd International Engineering Mechanics and Materials Specialty Conference, Ottawa, Ontario, Canada. **Submitted.**

15. **Soliman, A. M.** and Nehdi, M. L. (2011), "Early-age behaviour of shrinkage reducing admixture and wollastonite microfibers in UHPC," Proceedings of 2nd International Engineering Mechanics and Materials Specialty Conference, Ottawa, Ontario, Canada. **Submitted.**

16. **Soliman, A. M.** and Nehdi, M. L. (2011), "Effect of exposure conditions on early-age shrinkage of UHPC thin elements," Proceedings of 2nd International Engineering Mechanics and Materials Specialty Conference, Ottawa, Ontario, Canada. **Submitted**.

To: *My Father Mohammed Salah El-Din,(God bless his soul)*

My Mother Nemat,

My Sisters Rania, Yara, and Nanies

My Beloved Wife Noha,

My Beloved Daughter Malak,

And My Beloved Son Youssef.

Acknowledgments

TABLE OF CONTENTS

CHAPTER ONE

INTRODUCTION

CHAPTER TWO

EARLY-AGE PROPERTIES OF CONCRETE: OVERVIEW

CHAPTER THREE

INTERACTIONS MECHANSIMS OF EARLY-AGE SHRINKAGE OF UHPC UNDER SIMULATED DRYING CONDITIONS

CHAPTER FOUR

INFLUENCE OF SHRINKAGE MITIGATION TECHNIQUES ON EARLY-AGE SHRINKAGE INTERRELATION UNDER DRYING CONDITIONS

CHAPTER FIVE

EARLY-AGE SHRINKAGE OF UHPC UNDER DRYING/WETTING CYCLES AND SUBMERGED CONDITIONS

CHAPTER SIX

SELF-RESTRAINING SHRINKAGE CONCRETE: MECHANISMS AND EVIDENCE

CHAPTER SEVEN

EVALUATION OF SELF-RESTRAINING SHRINKAGE TECHNIQUE COMPARED TO CONVENTIONAL METHODS IN UHPC: INDIVDUALLY AND COMBINED

CHAPTER EIGHT

INFLUENCE OF NATURAL WOLLASTONITE MICROFIBERS ON EARLY-AGE BEHAVIOUR OF UHPC

CHAPTER NINE

SHRINKAGE BEHAVIOUR OF UHPC WITH SHRINKAGE REDUCING ADMIXTURE AND WOLLASTONITE MICROFIBERS

CHAPTER TEN

ARTIFICIAL NEURAL NETWORK MODELING OF EARLY-AGE AUTOGENOUS SHRINKAGE OF CONCRETE

CHAPTER ELEVEN

SUMMARY, CONCLUSIONS AND RECOMMENDATIONS

LIST OF TABLES

LIST OF FIGURES

LIST OF APPENDICES

CHAPTER ONE

INTRODUCTION

1.1. ULTRA HIGH PERFORMANCE CONCRETE (UHPC)

Over the last few decades, concrete technology has experienced substantial advances, resulting in innovative uses and unconventional applications of concrete. The use of supplementary cementitious materials and additives has developed new generations of concrete with enhanced properties, which can be used in areas that were dominated by metals and ceramics. These new generations of concrete can be categorized based on compressive strength development. Starting by Normal Concrete (NC) (20 to 40 MPa) passing by high-performance concrete (HPC) (40 to 80 MPa), very high performance concrete (VHPC) (100 to <150 MPa) and ultra high performance (≥ 150 MPa), which represents a leap development in concrete technology.

In the early 1990's, researchers at Bouygues company were the first to develop ultra high-performance concrete (UHPC) (Richard and Cheyrezy, 1995). UHPC is characterized by a very specific mixture design, which gives it a superior performance compared to that of conventional concrete. The main concept behind UHPC mixture is to minimize the number of defects, such as voids and internal micro-cracks, and to achieve a greater percentage of the ultimate load capacity of its components (Acker and Behloul, 2004). This can be reached by enhancing homogeneity and increasing the packing density

through optimization of the granular mixture and elimination of coarse aggregates (Holschemacher and Weiße, 2005), producing a very dense and strong structure of the hydration products using very low water-to-cement ratio (w/c) (about 0.20 to 0.25) (Schmidt and Fehling, 2005).

The main characteristics of UHPC include very high compressive strength, a relatively high tensile strength and enhanced durability compared even with that of HPC. These outstanding properties make it a promising material for different concrete applications (Tang, 2004). Nowdays, UHPC is used for producing special pre-stressed and precast concrete members (Yazici, 2007). Applications include the production of nuclear waste storage facilities (Yazici *et al*., 2009), precast pre-stressed concrete highway bridge girders (Garas *et al*., 2009), pedestrian footbridges (Shah and Weiss, 1998), inner wedges and outer barrel of nonmetallic anchorage systems (Reda *et al*., 1999), rehabilitation and retrofitting of concrete structures (e.g. waterproofing layer in bridge decks, protection layer on a crash barrier walls and strengthening of industrial floors) (Brühwiler and Denarié, 2008). Although there are only a few applications for these concretes due to its high production cost, some economical advantages do exist in UHPC applications (Yazici *et al*., 2009). For instance, it is possible to reduce maintenance costs relative to steel and conventional concrete bridge girders (Garas *et al*., 2009). Moreover, due to the ultra-high mechanical performance, the thickness of UHPC elements can be reduced, which results in materials and cost savings (Yazici *et al*., 2009) and increased useful space in buildings.

Indeed, it has been possible since several years ago to produce in the laboratory concrete with a compressive strength as high as 700 MPa. But to reproduce it in a job site

would be questionable due to uncontrolled in-situ conditions. Therefore, understanding the influence of in-situ environmental conditions on UHPC behaviour is essential before taking UHPC technology from the laboratory to full-scale field construction, rehabilitation and retrofitting of concrete structures.

1.2. EARLY-AGE SHRINKAGE

In the literature, there is no agreed upon definition of the early-age period for concrete; it highly depends on the investigated property. The early-age can be the first few hours or days after casting concrete that are characterized by two main processes: setting (progressive loss of fluidity) and hardening (gaining strength) (Pane and Hansen, 2002). Generally, shrinkage can be divided into two main types: early-age shrinkage, which represents shrinkage during the first 24 hours after the first contact between cement and water, and can extend up to 7 days (Holt, 2001, Wongtanakitcharoen and Naaman, 2007, Khan, 1995), and long-term shrinkage, which extends beyond the early-age period (Holt, 2001). The total shrinkage of concrete must be considered as the summation of both. However, there is no clear relationship between the magnitudes of these two types of concrete shrinkage.

Concrete shrinkage is a complex phenomenon that is affected by many factors including drying and internal self-desiccation deformations, curing procedure and ambient environmental conditions. Concrete shrinkage is generally assumed to begin at the time of loading or drying, however, it actually starts as early as the cement and water come in contact during concrete mixing. Early-age shrinkage is typically ignored in

design codes of concrete structures since its magnitude is assumed to be much less than long-term shrinkage (William *et al*., 2008). However, this can be erroneous since the early-age shrinkage can be equivalent to or even more than the long-term one. New generations of concrete are characterized by very low w/c (approximately below 0.40), thus a high portion of measured shrinkage (i.e. up to 80%) can be a result of self-desiccation shrinkage. Furthermore, a significant portion of this self-desiccation shrinkage takes place during the early-age period (Holt, 2001).

Many serviceability and durability problems of concrete can be attributed to the early formation of cracks as a result of concrete shrinkage. Recent studies have shown that this can also significantly affect the initial term response of structures (Bischoff and Johnson 2007). (Brown *et al*., 2007) reported that early-age cracking resulting from drying shrinkage affects more than 100,000 bridge decks in the US. Therefore, several shrinkage mitigation strategies have been proposed. These include adding shrinkage reducing admixtures (SRA) (Tazawaa and Miyazawaa, 1995), controlling the binder particle size distribution (Bentz *et al*., 2001), modifying the chemical composition of the binder (Tazawaa and Miyazawaa, 1995), adding of saturated lightweight aggregates (LWA) (Bentur *et al*., 2001) and superabsorbent polymers (SAP) (Igarashi and Watanabe, 2006).

Substantial research has focused on predicting the early-age shrinkage behaviour and evaluating the efficiency of various shrinkage mitigation methods under laboratory conditions. Conversely, very limited research has explored that early-age shrinkage behaviour under field-like conditions, whether with or without applying shrinkage mitigation methods. This probably led to a misevaluation of the actual early-age

shrinkage behaviour of different concrete mixtures and the real performance of shrinkage mitigation methods.

1.3.   NEED FOR RESEARCH

Despite the current knowledge and specifications for early-age shrinkage and mitigation techniques, numerous early-age shrinkage cracking cases for different concrete structures have been reported, indicating the existence of high shrinkage stresses (Brown *et al.*, 2007). It seems that the difference between the well defined curing conditions inside the lab and the actual field conditions had contributed to a clear discrepancy between laboratory measured performance and the actual performance of concrete mixtures in-situ. Moreover, several studies have been conducted to quantify the shrinkage behaviour of UHPC either under heat curing or constant temperature and relative humidity. Therefore, a proper understanding for the effect of field exposure conditions still needs to be gained, and the actual mechanisms that govern UHPC shrinkage of structural elements cast in-situ is still largely unexplored.

On the other hand, several shrinkage mitigation techniques have been proposed and are being used in various applications. The mechanisms of these shrinkage mitigation techniques are based on certain chemical and physical processes that take place within the cementitious material microstructure. Any factors that affect these processes are expected to affect the efficiency and mitigation mechanisms of the used techniques. Hence, a better understanding of the role and efficiency of these shrinkage mitigation

techniques in UHPC, which exhibits more complex chemical and physical processes compared to that of conventional concrete, under different exposure conditions is needed.

UHPC has a relatively high carbon-footprint and environmental impact due to its high cement content, which leads to high energy consumption and CO_2 emissions associated with cement production. Hence, finding new strategies to produce more environmentally friendly concrete, which exhibits lower or at least similar cracking tendency to traditional cement-based materials, is our obligation to future generations (Naik and Moriconi, 2005).

1.4.   OBJECTIVES AND SCOPE

To address the aforementioned research needs, the fundamental theme of this research is improving the current level of knowledge on the early-age shrinkage behaviour of UHPC and evaluating the efficiency of shrinkage mitigation methods under realistic field conditions. The specific objectives of the research are multi-fold:

- Introducing fundamental knowledge on the relationship between different types of early-age shrinkage of UHPC under a wide range of simulated field conditions.

- Evaluating the influence of exposure conditions on the efficiency and mechanisms of different shrinkage mitigation techniques.

- Implementing new environmentally-friendly shrinkage mitigation techniques that can utilize the superior performance of UHPC along with achieving economical and environmental benefits compared to that of convention mitigation techniques.

- Investigating the synergetic effects of different shrinkage mitigation techniques in order to identify optimum combinations that achieve efficient performance under realistic field exposure conditions.

- Building modeling systems that are capable of predicting the early-age shrinkage of a wide range of UHPC mixtures under various curing conditions.

To achieve the above objectives, the scope of this research includes:

- A wide range of simulated field-like conditions: the key variables included the temperature (10°C, 20°C and 40°C) and ambient humidity (40, 60, 80 and 100%). In the case of drying/wetting cycles, switching between a drying condition and a submerging condition was conducted. For submerged conditions, specimens were stored under water.

- Active shrinkage mitigation techniques: these include techniques that directly deal with shrinkage sources and try to minimize their effects, including chemical admixtures (i.e. shrinkage reducing admixture), since it reduces the surface tension of the pore solution; and chemical additives (i.e. superabsorbent polymer) that acts as an internal source of water.

- Passive shrinkage mitigation techniques: these include techniques that have indirect effect on the developed shrinkage, including internal passive restraint systems, and the addition of natural microfibers (e.g. wollastonite microfibers).

- Combined shrinkage mitigation techniques: since each shrinkage mitigation technique has its benefits and drawbacks, combining two or more of the techniques above may

optimize the gained benefits and minimize the drawbacks along with achieving better

shrinkage mitigation behaviour.

- Modelling: a model based on an artificial neural network (ANN), an emerging computational intelligence-based tool in concrete technology research, was developed to predict the shrinkage of the different types of concrete mixtures under the effect of environmental exposure. The model was applied to the case of variable simulated curing humidity and temperature including cold, normal and arid conditions. Based on the experimental database and developed ANN model, a parametric analysis was conducted to investigate the influences of different mixture criteria on the shrinkage behaviour.

1.5.   STRUCTURE OF THESIS

This thesis has been prepared according to the guidelines of the Faculty of Graduate Studies at the University of Western Ontario for an integrated-article format. It comprises 11 chapters, 9 of which display the progress in the experimental program starting by enhancing the fundamental knowledge about shrinkage and its mitigation techniques, moving to introducing and evaluating new shrinkage mitigation techniques, followed by modelling. Substantial parts of these chapters have been either published, accepted, or submitted for possible publication in peer-reviewed technical journals and national and international conferences.

Chapter 2 contains a state-of-the-art review of the current knowledge on early-age properties of concrete, their relationships, influences of various shrinkage mitigation

techniques and different proposed models. Chapter 3 discusses the interaction mechanisms between different types of UHPC shrinkage under the effect of various exposure conditions. In chapters 4 and 5, the role of different shrinkage mitigation techniques and their performance under simulated field-like conditions are discussed. Chapter 6 introduces a new concept for inducing an internal passive restraint to mitigate UHPC shrinkage at the micro-structural level. The basic phenomena and experimental results that demonstrate the concept are presented in this chapter. The performance of the new shrinkage mitigation technique and its efficiency compared to that of conventional mitigation techniques are described in Chapter 7. The benefits of adding different sizes and contents of natural wollastonite microfibers to UHPC as partial volume replacement for cement are presented in Chapter 8. Chapter 9 evaluates the performance of UHPC incorporating different combinations of shrinkage mitigation techniques discussed in previous chapters. The development of an artificial neural network model and parametric analysis are presented in Chapter 10. Finally, general and specific conclusions drawn from the research study along with recommendations for future research are included in Chapter 11.

1.6.   ORIGINAL CONTRIBUTIONS

This research introduces a series of fundamental investigations related to the early-age shrinkage and the role of different shrinkage mitigation techniques under field-like conditions. It explores the influence of a wide range of field-like conditions and the efficiency of available shrinkage mitigation strategies. Moreover, it proposes new

strategies to produce concrete with lower shrinkage and risk of cracking, yet with a smaller environmental impact. Specific original contributions of this dissertation include:

1. Developing a large and comprehensive database on the early-age shrinkage of UHPC under a wide range of environmental conditions.

2. Identifying the interaction mechanisms between different types of UHPC shrinkage under simulated field-like conditions. Specifically, it was revealed that: (i) autogenous and drying strains in UHPC specimens are dependent phenomena; (ii) autogenous strains under sealed conditions differ from that under drying conditions; (iii) applying the superposition principle without considering the effect of drying conditions will result in overestimating autogenous strains.

3. Evaluating the performance and efficiency of different shrinkage mitigation techniques and their interaction with the surrounding environmental. Specifically, it was found that: (i) adequate external curing is essential for shrinkage mitigation methods to work properly; (ii) drying conditions jeopardize the effect of SAP as a shrinkage mitigating method; (iii) the efficiency of SRA admixtures is highly affected by the ambient relative humidity, (iv) under submerged conditions, initial early swelling results in very low net shrinkage strains; (v) the washout behaviour of SRA under submerged and drying/wetting cycles was documented for the first time; (vi) the washout of SRA can dismiss its effectiveness in mitigating shrinkage strains; and (vii) combining SRA and SAP has a strong potential for developing a new generation of high-performance shrinkage mitigation admixture with dual effect.

4. Developing for the first time an innovative shrinkage mitigation technique capable of improving the mechanical properties along with reducing shrinkage strains and solving the economical and environmental problems associated with waste concrete. More specifically: (i) the concept of self-retraining concrete was pioneered based on using partially hydrated cementitious material (PHCM); (ii) it was demonstrated for the first time that PHCM has a high potential for reducing shrinkage through providing internal passive restraining system; (iii) left-over and/or returned concrete can be used as PHCM, thus enhancing concrete sustainability and preventing waste and disposal; (iv) PHCM showed a hydration acceleration effect, which has a potential to replace conventional chloride-based accelerating admixtures, particularly in the pre-cast industry; (v) combining PHCM and SRA mitigated the drawbacks of SRA including delays in setting time and significant reduction in early-age compressive strength; and (vi) combining PHCM and SAP reduced porosity and mass loss during drying in UHPC.

5. Implementing the use of wollastonite microfibers in UHPC as a replacement of cement, which has economical and environmental benefits along with enhancing the early-age properties. In particular, (i) wollastonite microfibers enhanced the early age compressive strength of UHPC mixtures incorporating SRA; (ii) wollastonite microfibers promote pore discontinuity, leading to lower mass loss, drying shrinkage and reduced SRA washing out; (iii) wollastonite microfibers act as passive internal restraint leading to lower shrinkage; (iv) at early-age, the low elastic modulus of the cementitious matrix increases the shrinkage restraining effect of wollastonite microfibers; and (v) wollastonite microfibers delay the coalescence of micro-cracks.

6. Advancing the promising use of artificial neural networks for predicting and estimating the shrinkage behaviour of different concrete mixtures that are used in concrete structures serving in different environments.

1.7.   REFERENCES

Acker, P. and Behloul, M., (2004), "Ductal ® technology: A large spectrum of properties, a wide range of applications," *Proceedings of the International Symposium on UHPC*, Kassel, Germany, pp. 11-23.

Bentur, A., Igarashi, S. and Kovler, K., (2001), "Prevention of autogenous shrinkage in high strength concrete by internal curing using wet lightweight aggregates," *Cement and Concrete Research*, Vol. 31, No. 11, pp. 1587-1591.

Bentz, D.P., Jensen, O.M., Hansen, K.K., Olesen, J.F., Stang, H., and Haecker, C.J., (2001), "Influence of cement particle-size distribution on early-age autogenous strains and stresses in cement-based materials," *Journal of American Ceramic Society,* Vol. 84, No. 1, pp. 129-135.

Bischoff, P.H., Johnson, R.D., (2007), "Effect of shrinkage on short-term deflection of reinforced concrete beams and slabs," In: *Proceeding of structural implications of shrinkage and creep of concrete* , Gardner, J., Chiorino, M.A. (eds.) ACI International, SP-246, pp. 167–180.

Brown, M.D., Smith, C.A., Sellers, J.G., Folliard, K.F. and Breen, J.E., (2007), "Use of alternative materials to reduce shrinkage cracking in bridge decks," *ACI Materials Journal*, Vol. 104, No. 6, pp. 629-637.

Brühwiler, E. and Denarié, E., (2008), "Rehabilitation of concrete structures using Ultra-High Performance Fiber-Reinforced Concrete," In: *Proceeding of 2nd International Symposium on UHPC*, Kassel, Germany, pp. 1-8.

Garas, V.Y., Kahn, L.F. and Kurtis, K.E., (2009), "Short-term tensile creep and shrinkage of ultra-high performance concrete," *Cement and Concrete Composites*, Vol. 31, No. 3, pp. 147-152.

Holschemacher, K. and Weiße, D., (2005), "Economic mix design of ultra high strength concrete," *In: Proceedings of the 7th International Symposium on Utilization of High-Strength/ High-Performance Concrete*, Washington D.C., Vol. 2, pp.1133-1144.

Holt, E.E., (2001), "Early age autogenous shrinkage of concrete," *Espoo 2001*. Technical Research Centre of Finland, VTT Publications 446, 184 p.

Igarashi, S. and Watanabe, A., (2006), "Experimental study on prevention of autogenous deformation by internal curing using super-absorbent polymer particles," In: *Proceedings of the International RILEM Conference - Volume Changes of Hardening Concrete: Testing and Mitigation*, O.M. Jensen, P. Lura, and K. Kovler (eds.), RILEM Publications, pp. 77-86.

Khan, A.A., (1995), "Concrete properties and thermal stress analysis of members at early-ages," *PhD Thesis*, McGrill University, Canada.

Naik, T., R., Moriconi, G., (2005), "Environmental-friendly durable concrete made with recycled material for sustainable concrete construction," In Proceeding of international symposium on sustainable development of cement, concrete and concrete structures, Toronto, Canada, pp. 277-291.

Pane, I. and Hansen, W., (2002), "Early-age creep and stress relaxation of concrete containing blended cements," *Materials and Structures*, Vol. 35, No. 2, 92-96.

Reda, M.M., Shrive, N.G. and Gillott, J.E., (1999), "Microstructural investigation of innovative UHPC," *Cement and Concrete Research*, Vol. 29, No. 3, 1999, pp. 323-329.

Richard, P. and Cheyrezy, M., (1995), "Composition of reactive powder concrete Research," *Cement and Concrete Research*, Vol. 25, No. 7, pp. 1501-1511.

Schmidt, M. and Fehling, E., (2005), "Ultra-high-performance concrete: research, development and application in Europe" I*n: Proceedings of the 7th International Symposium on Utilization of High-Strength/ High-Performance Concrete*, Washington D.C., Vol. 1, pp. 51-77.

Shah, S.P. and Weiss, W.J., (1998), "Ultra high strength concrete; looking toward the future," In: *ACI Special Proceedings from the Zia Symposium*, Huston, Texas, USA.

Tang, M.C., (2004), "High performance concrete – past, present and future," In: *Proceedings of the International Symposium on UHPC*, Kassel, Germany, pp. 3-9.

Tazawaa, E. and Miyazawaa, S., (1995), "Influence of cement and admixture on autogenous shrinkage of cement paste," *Cement and Concrete Research*, Vol. 25, No. 2, pp. 281-287.

William, G.W., Shoukry, S.N. and Riad, M.Y., (2008), "Development of early age shrinkage stresses in reinforced concrete bridge decks," *Mechanics of Time-Dependent Materials*, Vol. 12, No. 4, pp. 343-356.

Wongtanakitcharoen, T. and Naaman, A.E., (2007), "Unrestrained early-age shrinkage of concrete with polypropylene, PVA, and carbon fibers," *Materials and Structures*, Vol. 40, No. 3, pp. 289-300.

Yazici, H., (2007), "The effect of curing conditions on compressive strength of ultra high strength concrete with high volume mineral admixtures," *Building and Environment*, Vol. 42, No. 5, pp. 2083-2089.

Yazici, H., Yardımcı, H.Y., Aydın, S. and Karabulut, A., (2009), "Mechanical properties of reactive powder concrete containing mineral admixtures under different curing regimes," *Construction and Building Materials*, Vol. 23, No. 3, pp. 1223-1231.

CHAPTER TWO

EARLY-AGE PROPERTIES OF CONCRETE: OVERVIEW*

The long-term performance of concrete structures is affected to a large extent by the properties and behaviour of concrete at early-age. However, the fundamental mechanisms affecting the early-age behaviour of concrete have not yet been fully understood. This is due to the various highly interrelated factors influencing it, and the complexity of testing techniques needed for its investigation. With modern developments in concrete technology, it has become essential to evaluate the influence of these interrelated factors and their implications for the service life of concrete structures. Thus, a more fundamental approach for investigating the early-age behaviour of concrete, along with more reliable testing techniques is required. This chapter provides a critical overview of research on the mechanisms that affect the properties of concrete and its performance at early-age. It provides useful, concise and coherent information on the behaviour of concrete at early-age, which should enhance the understanding of the implications of such behaviour on the service life performance of concrete structures.

2.1. INTRODUCTION

Concrete is the most widely used construction material in the world. Its service life is considered synonymous to its mechanical strength, durability and serviceability. The selection of proper ingredients and mixture proportions are important to produce concrete

---

that can meet strength and durability requirements. However, achieving a high quality concrete may be elusive if adequate attention is not paid to its early-age properties. For instance, the mechanical performance and long-term durability of concrete can be seriously compromised due inadequate curing or insufficient compaction during placement. Moreover, accelerated construction schedules aiming at economic gains have led to tragic failures during construction due to inadequate knowledge of the concrete behaviour at early-age (Oluokun *et al.*, 1990). Therefore, a fundamental understanding of the behaviour of concrete at early-age is essential to assure safety during construction, as well as adequate durability and long-term properties.

There is no agreed upon definition of the early-age period for concrete; indeed it depends on the investigated property. In other words, the time required to achieve a certain level of a desired property is perceived as the early-age (Mehta and Monteiro, 2006). **Table 2-1** summarizes the early-age period as considered by different researchers (Mehta and Monteiro, 2006, RILEM, 1981, Kahouadji *et al.*, 1997, Holt, 2001, Wongtanakitcharoen and Naaman, 2007, Brooks and Megat-Johari, 2001, Holt and Leivo, 2004, Altoubat, 2002, Østergaard *et al.*, 2001, Khan, 1995, Oluokun *et al.*,1991, Nassif *et al.*, 2003, Kovler *et al.*, 1999, Pane and Hansen, 2002, Bissonnette and Pigeon, 1995). Generally, the early-age is the first few hours or days after casting concrete that are characterized by two main processes: setting (progressive loss of fluidity) and hardening (gaining strength). During these processes, the fluid multiphase structure of the fresh concrete transforms into a hardened structure due to the progress of hydration reactions, leading to the development of mechanical properties, heat liberation and deformations (Pane and Hansen, 2002). This heat liberation and water loss, due to either

evaporation or consumption by hydration reactions, leads to internal/external deformations. Hence, the coupling between thermal and mechanical characteristics of early-age concrete is more critical compared to that in mature concrete. Furthermore, proper curing after placement is crucial to maintain a satisfactory moisture content and adequate temperature in concrete during this early stage so that the desired properties can develop later (Huo and Wong, 2006).

Table 2-1: Definition of early-age period.

Early-age period	Field of study	Reference.
First 1-2 days	Concrete properties	(Mehta and Monteiro, 2006)
Up to 48 hrs	Concrete properties	(RILEM, 1981)
4 days after casting	Strength	(Kahouadji *et al.*, 1997)
24 hrs after placing concrete	Shrinkage	(Holt, 2001, Wongtanakitcharoen and Naaman, 2007)
	Shrinkage and creep	(Brooks and Megat-Johari, 2001)
	Creep and relaxation	(Holt and Leivo, 2004)
5 days after casting	Shrinkage and creep	(Altoubat, 2002)
	Creep	(Østergaard *et al.*, 2001)
3 days after placing concrete	Strength	(Khan, 1995, Oluokun *et al.*,1991)
Up to 7 days after casting	Shrinkage	(Nassif *et al.*, 2003)
	Strength	(Kovler *et al.*, 1999)
	Creep and relaxation	(Pane and Hansen, 2002)
	Creep	(Bissonnette and Pigeon, 1995)

2.2.   EARLY-AGE PROPERTIES

2.2.1.   Early-Age Thermal Properties

Because of the significant role of the heat of hydration at early-age, basic thermal data for concrete are of a vital importance. These data are essential to predict the temperature and thermally induced stress and strain distributions within a concrete member in order to

avoid thermal cracking. Generally, the thermal properties of concrete reflect those of its constituents, i.e. the cement paste (including cement, water, chemical and mineral admixtures) and aggregates, and these depend on the mixture proportions and type of constituents (RILEM, 1981).

2.2.1.1 Heat of Hydration

The amount and kinetics of heat generated by cement hydration is an important parameter for predicting the temperature development and its distribution within a concrete member. The hydration of Portland cement is a highly exothermic chemical reaction (Neville, 1996). Usually, about one-half of the total heat of hydration is evolved between 1 and 3 days after mixing cement with water (Oluokun *et al.*, 1990). At early-age, the rate and total heat of hydration are mainly influenced by the type, total content, and chemical composition of cement, the ambient temperature and the admixtures used (Khan, 1995). Cements with a high Dicalcium Silicate (C_2S) and/or Tetracalcium Aluminoferrite (C_4AF) content can usually be considered as low heat cements, while cements high in Tricalcium Silicate (C_3S) and Tricalcium Aluminate (C_3A) typically exhibit high heat liberation (RILEM, 1981). **Table 2-2** shows the typical heat of hydration for each of the main cement phases (McCullough and Rasmussen, 1999). For instance, the ASTM C150 (Standard Specification for Portland Cement) limited the C_3S and C_3A contents for low-heat cement (Type IV) to 35% and 7%, respectively (ASTM, 2007). Furthermore, the use of mineral admixtures, such as blast furnace slag (BFS), fly ash (FA) and other supplementary cementing materials (SCM), in combination with ordinary portland cement (Type I) in a blended cement, have proven to be a cost-effective method for controlling the heat of hydration, which led to stopping the manufacture of the low heat

cement Type IV. The hydration process in blended cements is relatively more complex than that of the ordinary cement. It involves hydration reactions of the mineral additives (pozzolanic reactions) resulting in heat liberation, in addition to that of the portland cement hydration (Pane and Hansen, 2005). Generally, the total amount of heat liberated will depend on the pozzolanic activity and proportion of the added mineral (Snelson *et al.*, 2008). For example, adding silica fume can accelerate the hydration of cement resulting in a higher rate of heat of hydration, while adding BFS usually exhibit an opposite trend (Alshamsi, 1997).

Table 2-2: Heat of hydration of cement compounds [after (McCullough and Rasmussen, 1999), (Lea, 2004)].

Compound	Heat of Hydration (J/g)
C_3S (Tricalcium Silicate)	500-520
C_2S (Dicalcium Silicate)	260
C_3A (Tricalcium Aluminate)	850-910
C_4AF (Tetracalcium Aluminoferrite)	420
C (Free Lime)	1165
MgO (Magnesium Oxide)	850

The ambient temperature has a significant effect on the rate of hydration and heat liberation during early-ages. **Figure 2-1** illustrates the effect of the temperature on the heat of hydration for different types of Portland cement. In hot weather, the hydration rate increases leading to more rapid heat generation. Conversely, in a cold climate, the hydration rate slows down and lower heat is liberated. Hence, rapid hydrating cements are used in such-conditions to avoid excessive set retardation and strength gain delays. Moreover, chemical admixtures that affect the kinetics of hydration reactions normally change the rate of heat liberation (Schindler, 2004). For instance, retarding agents slow

the rate of hydration reactions at early-age; consequently, the rate and amount of heat liberated will decrease. Conversely, accelerating admixtures increase the hydration rate. However, the total long-term heat generated usually remains almost unchanged (RILEM, 1981).
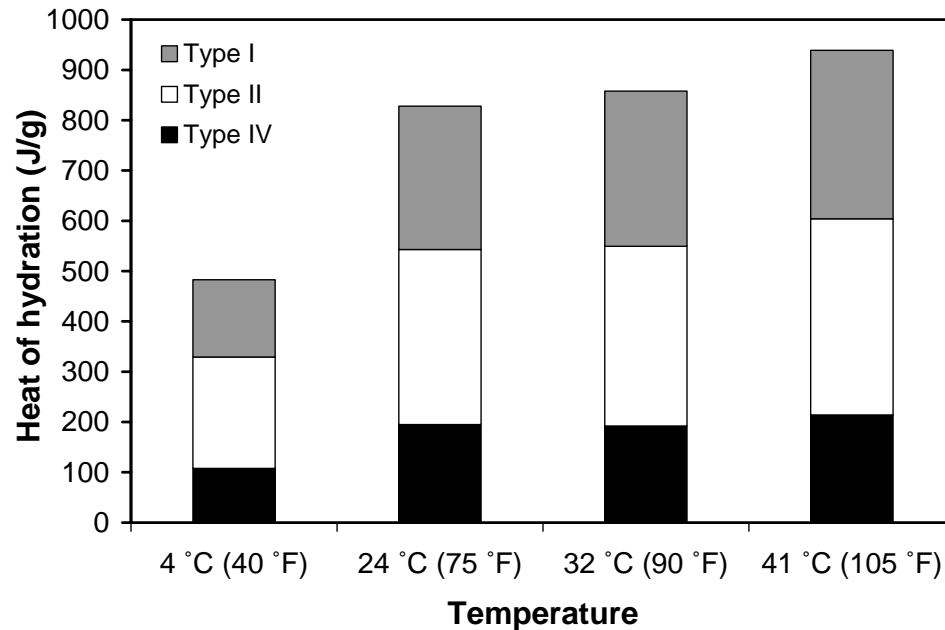
Figure 2-1: Heat of hydration developed after 72 hours at different temperatures (Type I: Ordinary Portland cement, Type II: Moderate sulfate resistance portland cement, Type IV: Low heat portland cement) [adapted after (Neville, 1996)].

There are generally three commonly used methods for evaluating the heat liberated from the hydration of cement (Khan, 1995), namely: conduction calorimetry, heat of solution, and the adiabatic/semi-adiabatic method. Conduction calorimetry measures the rate of heat released under nearly isothermal conditions. This method is preferable for determining the heat of hydration at very early-ages (even less than 0.5 hour). For the heat of solution method, the heat of hydration is determined by the

difference between the heat of solution of the dry cement and a hydrated cement paste immersed in acid, respectively. This method is not suited for early-ages because of the limited amount of heat being liberated. The adiabatic/semi-adiabatic methods measure the temperature rise under insulated conditions, which simulates curing conditions at the center of large concrete elements at early-ages. Generally, in the adiabatic method the temperature of the sample surrounding environment must be equal to the temperature of the concrete at any time. This condition requires that additional heat be supplied from the outside. In the semi-adiabatic method, a maximum heat loss from the hydration specimen less than 100 J/(h.K) is accepted. Therefore, the sample is insulated to minimize the rate of heat loss (RILEM, 1997). The rate of hydration can be obtained from the product of the specific heat, concrete density and the rate of change in the measured adiabatic temperature curve.

2.2.1.2 *Specific Heat Capacity*

The specific heat (C_p) of a material is the amount of heat required to change a unit mass of the material by one degree in temperature (Goldsmid, 1965). For concrete, C_p depends on the mixture composition, moisture content and ambient temperature. The specific heat of water is about 5 times greater than that of the un-hydrated cement and most aggregates (Khan, 1995). Thus, the moisture content of concrete has a major effect on its specific heat capacity at early-age as it changes significantly due to hydration and drying. A linear reduction of the specific heat with the degree of hydration was reported (Bentur, 2003). Generally, a decrease in the specific heat of concrete with age was consistently reported by several researchers, while the opposite trend was not reported (Bentur, 2003). However, there has been no general agreement concerning the magnitude of this decrease

due to differences in the testing procedures and materials used. **Table 2-3** summarizes

values of decrease of specific heat capacity with time reported by different researchers

(RILEM, 1981, Brown and Javaid, 1970, Mounanga, 2004). Moreover, the specific heat

of concrete was found to increase by about 3 % to 3.5 % per 10°C increase in temperature

(RILEM, 1981). However, little attention has been paid to the effect of the curing

conditions, including the ambient temperature and relative humidity on C_p. The curing

condition is expected to have a significant effect on the specific heat of concrete as it

directly affects the concrete moisture content and temperature. Therefore, a more

comprehensive study of the effects of different curing conditions on the development of

the specific heat of concrete at early-age is needed.

Table 2-3: Values of specific heat investigated by different researchers.

Age	Initial Value	Age	Later Value	Units	Reduction (%)*	Sample	Reference
3 days	1180	10 days	1160	J/kg per $^\circ$C	-1.70	Mortar	(RILEM, 1981)
6 hrs	1151	24 hrs	1122		-2.52	Concrete	(Brown and Javaid, 1970)
		7 days	888		-22.85		
6 hrs	1076	24 hrs	1055		-1.95	Mortar	
		7 days	871		-19.05		
6 hrs	2.6	24 hrs	2.35	10^6 J/m^3 per K	- 9.62	Paste	(Mounanga, 2004)

*Related to the Initial measured value.

2.2.1.3 Thermal Conductivity

The thermal conductivity (κ) is the rate of heat transmission across a unit cross-section

area when there is a unit temperature gradient perpendicular to that area, and is usually

expressed as the ratio of the flux of heat to the temperature gradient (Goldsmid, 1965). It significantly influences temperature gradients, thermal strains, warping, and cracking in early-age concrete (Neville, 1996). A decrease in the thermal conductivity of concrete by about 10 to 40% with age within the first week of hydration was observed (Østergaard, 2003). Conversely, other researchers stated that the thermal conductivity of concrete does not change significantly with age, and may be considered constant (RILEM, 1981, Khan, 1995). The density, water content, temperature and mineralogical characteristics of aggregates (see **Table 2-4**) significantly influence the thermal conductivity of concrete (Khan, 1995). The thermal conductivity of cement paste is a resultant of the thermal conductivity of its constituents, including un-hydrated cement, hydration products, and that of the air and moisture contained in pores (Uysal *et al.*, 2004). Air has a low thermal conductivity; while water has about 25 times the thermal conductivity of air and less than half that of the hydrated cement (Neville, 1996). Therefore, it is expected that the thermal conductivity changes during the early period of hydration as the concrete phases change (Khan, 1995). During this process, the air in pores is being partially displaced by water or moisture; which in turn reacts with cement and is replaced by hydrated cement, leading to greater thermal conductivity (Uysal *et al.*, 2004). Therefore, variation in both the moisture content and density of concrete can drastically affect the thermal conductivity of concrete (Brown and Javaid, 1970). On the other hand, silica fume, latex, and methylcellulose were found to decrease the thermal conductivity of concrete (Xu and Chung, 1999, Fu and Chung, 1997). This is mainly due to the relatively low thermal conductivity of these admixtures.

Table 2-4: Thermal properties of concrete with different aggregate types [after (Mehta and Monteiro, 2006)].

Aggregate Type	Thermal conductivity (W/m.K)	Thermal diffusivity (m²/h)	Coefficient of thermal expansion (microstrain /°C)
Quartzite	3.5	0.0054	≈ 12.0
Dolomite	3.2	0.0047	----
Limestone	2.6-3.3	0.0046	≈ 6.0
Granite	2.6-2.7	0.0040	≈ 8.0
Rhyolite	2.2	0.0033	----
Basalt	1.9-2.2	0.0030	≈ 7.0

There are mainly three common methods for measuring the thermal conductivity of concrete (Kook-Han *et al.*, 2003), namely the two-linear parallel-probe (TLPP) method, the plane-heat-source (PHS) method, and the hot-guarded plate (HGP) method. The required sample preparation was the main obstacle for applying these methods to concrete at early stages. However, a new experimental device based on the basic principle of the TLPP method was recently developed. It showed reasonable reliability for measuring the thermal conductivity of concrete at very early-age (Kook-Han *et al.*, 2003). Moreover, Bentz (Bentz, 2007) demonstrate the applicability of the transient plane source method (TPS) for measuring the thermal conductivity of hardening concrete. These developments should provide useful tools for investigating the thermal conductivity of different concrete mixtures during early-ages and significant research work is still needed in this area.

2.2.1.4 *Thermal Diffusivity*

The thermal diffusivity (k_d) of a material represents the rate at which temperature changes within its mass (Goldsmid, 1965). It measures the rapidity of heat propagation through a

material. It is an important property in problems involving non-steady state heat conduction. The thermal diffusivity of ordinary concrete generally depends on the aggregate type used (see **Table 2-4**) and water content (Mehta and Monteiro, 2006, Neville, 1996). Only limited and conflicting data are available on the thermal diffusivity of concrete at early-age. Constant thermal diffusivity values through the hardening process were observed, as well as increasing and decreasing trends (De Schutter and Taerwe, 1995). Generally, the thermal diffusivity is related to the thermal conductivity and specific heat by the following mathematical formula (Goldsmid, 1965):

$$k_d = \frac{\kappa}{\rho \cdot C_p} \qquad (m^2/s) \qquad \textbf{Eq. 2-1}$$

Where, k_d is the thermal diffusivity (m^2/s), κ is the thermal conductivity (W/(m.K)), ρ is the bulk density (kg/m^3), and C_p is the specific heat (J/(kg.K)). **Table 2-5** summarizes values for the thermal diffusivity of concrete reported by various researchers (RILEM, 1981, Bentur, 2003, Brown and Javaid, 1970).

The conflicting data of thermal diffusivity of concrete can be attributed to differences in the testing methods, mixture proportions and constituents of tested concrete, and curing conditions. These factors have a significant effect on the degree and rate of concrete phase development, which can lead to diverse thermal characteristics. Even applying the above mathematical relationship (**Eq. 2-1**) is expected to give different thermal diffusivity values since it depends on the thermal conductivity and specific heat, which do not have a well-defined trend during early-age.

Table 2-5: Values of thermal diffusivity obtained by different researchers.

Age	Value (m^2/hr)	Trend	Sample	Reference
1 day	0.00370	Constant	Concrete	(RILEM, 1981)
7 days	0.00370			
1 hr	0.00336	Decrease (-15.85%)	Concrete	(Brown and Javaid, 1970)
7 days	0.00283			
1 day	0.00255	Increase (16.08%)	Mortar	
7 days	0.00296			
Within 1000 hrs	0.85000	Increase (23.53 %)	Paste	(Mounanga, 2004)
	1.05000			

2.2.1.5 Coefficient of Thermal Expansion

The coefficient of thermal expansion (CTE) of a material is the change in a unit length of the material per one degree of temperature change (Goldsmid, 1965). The CTE of concrete depends on different parameters, including the type and content of cement, aggregate type (see **Table 2-4**), w/c, age, temperature, and relative humidity (Østergaard, 2003). The CTE of concrete can be estimated from the volumetrically weighted average of the coefficients of thermal expansion of its mixture components (Kada *et al.*, 2002).

At early-age, especially during the first ten hours, an important variation in the CTE of concrete occurs, and then it stabilizes (see **Fig. 2-2**). This variation is essentially caused by variation in the amount of water that is not yet chemically bound since water has a CTE up to 20 times greater than that of other concrete constituents (Kada *et al.*, 2002). Hence, it is believed that the CTE of concrete at early-age, when concrete typically has a higher free water content, is several times higher than that of the hardened concrete (Østergaard, 2003, Kada *et al.*, 2002), and can be estimated to be 3 to 4 times that of the hardened concrete at the onset of setting, then decreases until the end of the

setting period to remain nearly constant thereafter (Kada *et al.*, 2002). **Table 2-6** summarizes CTE values of concrete as a function of its age (RILEM, 1981, Khan, 1995, Bentur, 2003, Østergaard, 2003, Kada *et al.*, 2002, Cusson and Hoogeveen, 2006, Sellevold and BjØntegaard, 2006). Generally, a decreasing trend of CTE with age was observed, however its amount is highly varied. This can be attributed to the ongoing hydration, change in primary constituents and surrounding conditions, which affect the amount of free water and proportion of concrete constituents at the testing age.
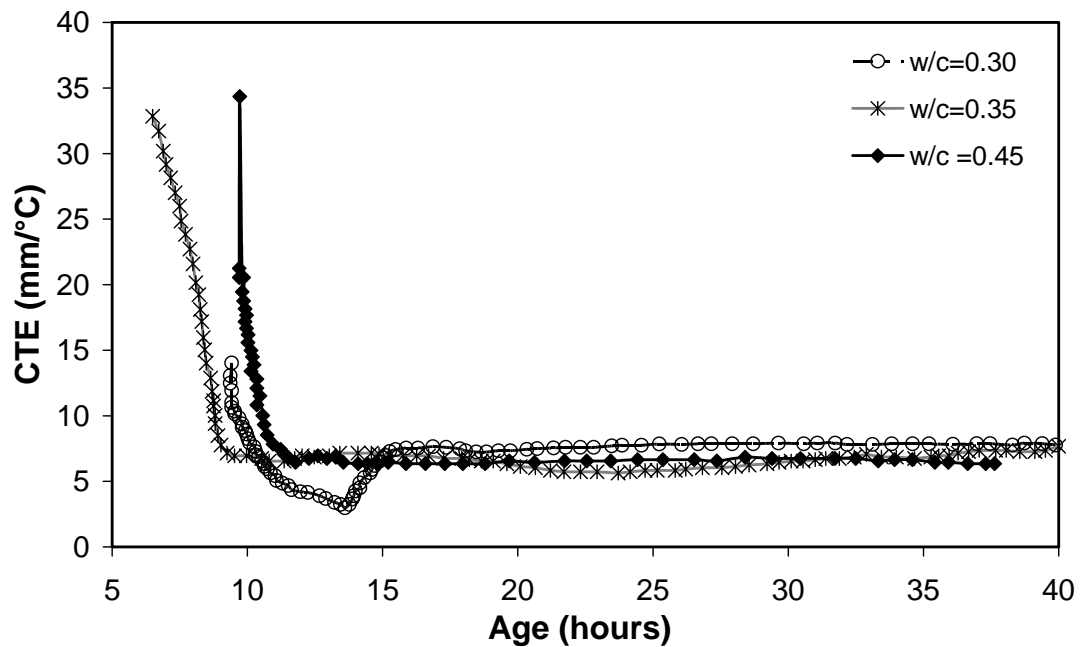
Figure 2-2: Evaluation of the coefficient of thermal expansion of concrete during hydration [adapted after (Kada *et al.*, 2002)].

Table 2-6: Values of coefficient of thermal expansion obtained by different researchers.

Age	/ °C × 10⁻⁶	Reference
4 hrs	70.00	(Østergaard, 2003)
≥120 hrs	12.00	
7 hrs	24.00	(Khan, 1995)
≥ 13 hrs	10.00	
1 day	6.00	(Cusson and Hoogeveen, 2006)
4 days	8.00	
Fresh concrete	20.00	(RILEM, 1981)
8-24 hrs	15.00	
1 -6 days	12.00	
10-24 hrs	≈ 9.10 to 12.30	(Bentur, 2003)
1 day – 4 days	≈ 8.50to 8.10	
> 4 days	≈ 8.00	
8 hrs	≈ 22.11	(Kada *et al.*, 2002)
12 hrs	≈ 7.12	
≥ 1 day	≈ 5.79	
Before setting	20.00	(Sellevold and BjØntegaard, 2006)
Final set	7.00	
11 weeks	11.00	
> 11 weeks	7.00	

In addition, during the hydration period, the accuracy of measuring small displacements in concrete is strongly dependent on its stiffness, which presents the main difficulty during the testing stage. On the other hand, dealing with a heterogeneous, porous and aging material such as concrete, presents other difficulties during the analysis stage. Thus, a special extensometer with a sufficiently low stiffness (1 GPa) was used to monitor the concrete strain at very early-age (Kada *et al.*, 2002). This method allows monitoring the evolution of the CTE from the onset of concrete hardening. In order to maximize the accuracy of readings, an experimental approach to determine the coefficient of thermal expansion of concrete at early-age under stress-free and isothermal

conditions using high accuracy LVDTs was developed (Cusson and Hoogeveen, 2006).
As a result, the evolution of CTE as a function of time after casting could be monitored.
Nevertheless, it was not possible to accurately measure the CTE before the final setting.
(Viviani *et al.*, 2006) introduced a system of optical fiber sensors to monitor the evolution
of CTE based on determine the kinetic parameters of hardening materials. However the
measurement system allows rapid and efficient predictions of CTE under laboratory
conditions, its potential for in-situ application is still need to be investigated (Viviani *et
al.*, 2006).

2.2.2.   Early-Age Mechanical Properties

The mechanical properties of concrete at early-age depend, to a large extent, on the
development of the hydrated cementitious microstructure as a function of the achieved
degree of hydration. However, the rate of development differs from one mechanical
property to another. Since the interrelations between these mechanical properties are
affected by numerous factors such as the mixture proportions, w/c, age, curing
conditions, rate of loading, it is difficult to formulate a unique relationship between such
properties.

2.2.2.1 *Compressive Strength*

The compressive strength is considered as a key property of concrete. It provides a
general indication of concrete quality. The gain in compressive strength is typically rapid
at early-age, and then becomes slower at later ages. This early rapid increase in strength
is directly related to the increase in the calcium silicate hydrate (CSH) gel/space ratio
(Neville, 1996). Compressive strength is influenced by several factors; most notably the

w/c, type of cement, additives, and curing conditions (Østergaard, 2003). Rapid hydration of cement results in a higher degree of hydration and consequently higher early-age strength for a given w/c ratio (Mehta and Monteiro, 2006).

Curing conditions, i.e. the availability of moisture and the temperature profile, drastically affect the compressive strength gain. At a very early-age, the absence of moisture usually has a limited effect on the early strength gain, because concrete is still wet. However, inadequate moisture curing during the first day after casting concrete could lead to noticeable strength loss at later ages (RILEM, 1981). Furthermore, a high initial curing temperature speeds up the hydration reactions and the formation of the hydrated cement paste structure at early-age. Thus, it enhances the early-age compressive strength of concrete. However, it decreases the strength at later ages due to the lower quality of hydration products microstructure formed at higher temperature (Kahouadji *et al.*, 1997).

Pozzolanic materials can also contribute to the early-age strength through improving the particle packing density (filler effect) and densifying the aggregate-cement paste interfacial transition zone (Neville, 1996). In addition, the type and level of addition of pozzlans have a significant influence on the compressive strength development. For instance, concrete incorporating class C (high calcium oxide) fly ash generally develops higher early-age strength than that of concrete made with class F (low calcium oxide) fly ash (Kosmatka *et al.*, 2002). Moreover, other pozzolanic materials such as blast furnace slag were found to slightly improve the early-age strength compared to its more significant contribution to the later strength, which can be ascribed to its slow hydration rate (Shan-bin and Zhao-jia, 2002). However, applying the crystal seed technology, i.e.

addition of hydrated micro-crystals, for this type of pozzolanic materials was found to improve its early strength contribution significantly (Prusinski, 2006). Generally, using pozzolanic materials may result in higher or lower early compressive strength of concrete depending on their type, addition rate, mineralogy, particle shape and fineness, and pozzolanic activity.

Several methods have been developed to predict the compressive strength of concrete at early-age. One of the well-known methods is the maturity or the "equivalent age" method, which is expressed as a function of the time and temperature of curing as follows:

$$M(t) = \sum (T_a - T_0) \cdot \Delta t$$ **Eq. 2-2**

Where Δt is the time interval, T_a is the average concrete temperature during the time interval Δt, and T_0 is the datum temperature (Mehta and Monteiro, 2006).

At early-ages, maturity is low, especially in the first two days after casting, and the relation between compressive strength and maturity is not fully linear. Thus, for accurate compressive strength prediction at early-age using the maturity concept, the heat of hydration should be considered during the calculation of maturity (Oluokun *et al.*, 1990). **Figure 2-3** shows the average additional maturity due to the heat of hydration with respect to concrete strength (σ_c). Moreover, a more fundamental approach to evaluating the compressive strength development as a function of the degree of hydration, taking into account the w/c as a parameter, was introduced (De Schutter and Taerwe, 1996). Good agreement with the available data was obtained based on following formula:

$$\frac{f_c(r)}{f_c(r=1)} = \left(\frac{r-r_o}{1-r_o}\right)^a$$

Eq. 2-3

Where $f_c(r)$ is the compressive strength at degree of hydration r, $f_c(r=1)$ is the compressive strength at a degree of hydration $r=1$, r_o and a are parameters that depend on the cement type and w/c (De Schutter and Taerwe, 1996).
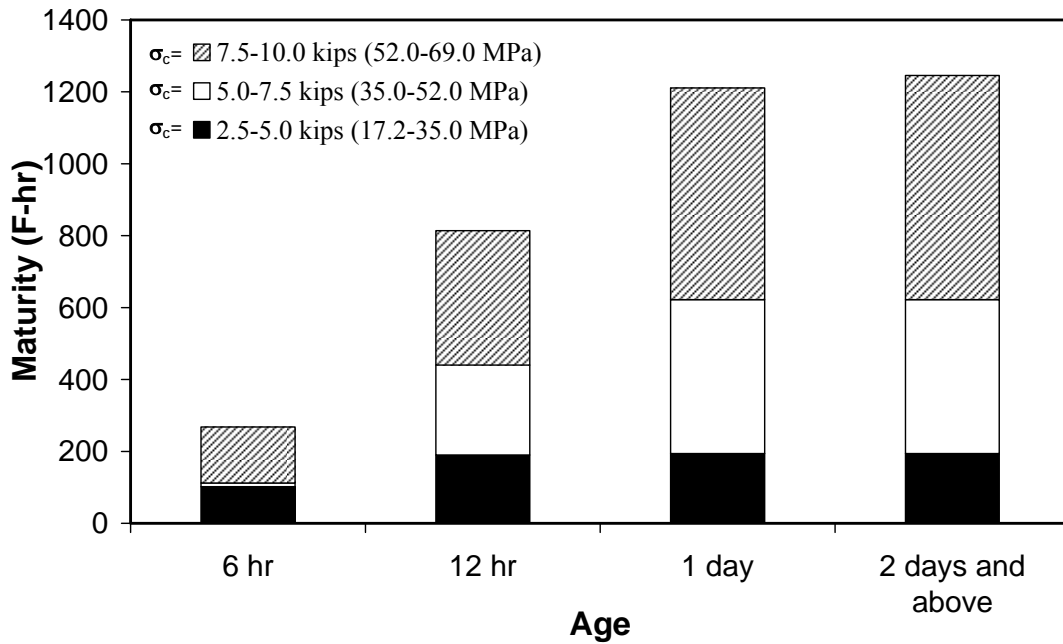
Figure 2-3: Average additional maturity, (F-hr), due to hydration [adapted after (Oluokun *et al.*, 1990)].

2.2.2.2 Tensile Strength

Tensile strength is a key property of early-age concrete; it has a chief influence on the resistance of concrete to plastic shrinkage, thermal stresses during hydration, and early-age loading and cracking which can affect the stiffness of the structure (Zhao, 1990). Measuring the early-age tensile strength of concrete is complicated since concrete is

viscous and inelastic at that stage (Abel and Hover, 1998). Several methods have been developed in an attempt to evaluate this property including uniaxial tensile test, splitting test, and flexural test. Results obtained by the uniaxial tensile test can be characterized as the real tensile strength of concrete. However, the specimen's self-weight for the vertical testing position or the friction against the sub-base for the horizontal testing position induce a significant error (Østergaard, 2003). The splitting tensile test (Brazilian test) and the three point flexural test rely on linear elastic formulas with empirical correction factors, which make their applicability for early-age concrete questionable. Fracture mechanics testing methods, e.g. the crack mouth opening displacement (CMOD), have increasingly been applied to evaluate the early-age tensile strength (Østergaard, 2003).

The development of tensile and compressive strength is generally affected by similar factors. Thus, the tensile strength of concrete can be related to its compressive strength. This relationship is influenced by age, grading, type and density of aggregates, curing conditions, and the strength evaluation method. At early-age, the tensile strength tends to increase more rapidly than the compressive strength (RILEM, 1981, Bentur, 2003, De Schutter and Taerwe, 1996). Conversely, some researcher found that the tensile strength increases at a lower rate than that of the compressive strength (Swaddiwudhipong *et al.*, 2003), and that the ratio between the two properties decreases from 0.1 to 0.04 as the concrete matures. This discrepancy can be attributed to differences in the starting age of the test and quality of concrete. (Kasai *et al.*, 1972) reported a higher increasing rate for the tensile strength compared to that of the compressive strength during the very early age up to around 0.5 day. Thereafter, the

tensile strength increasing rate became lower than that of the compressive strength, as shown in **Fig. 2-4**.
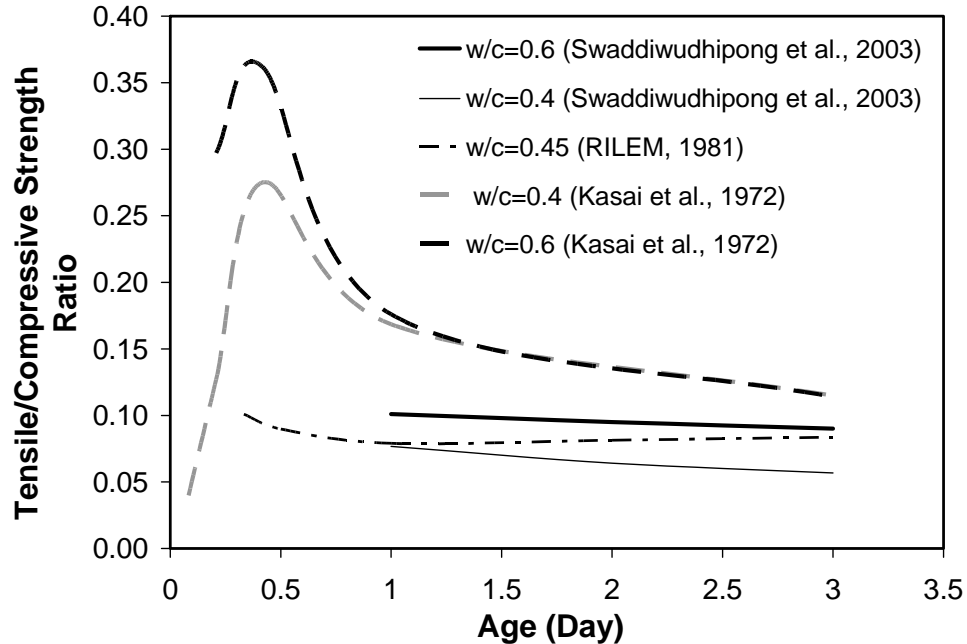
Figure 2-4: Tensile / compressive strength of concrete versus age.

The tensile strength can be expressed as a function of the compressive strength as follows (Neville, 1996):

$$f_t = k \cdot (f_c)^n$$ **Eq. 2-4**

Where f_t is the tensile strength, f_c is the compressive strength, and *k* and *n* are relation coefficients as shown in **Table 2-7** (Zhao, 1990, ACI, 2005, Raphael, 1984, CEB-FIP, 1991). This relationship was obtained for matured concrete. Yet, previous research has indicated its validity at early-ages and under various conditions (Zhao, 1990).

Table 2-7: Different suggested values for *k* and *n*.

	Direct tensile strength		Modulus of rupture		Splitting tensile strength	
k	0.5	0.7	0.3	0.95	6.7	0.33
n	0.5	2/3	2/3	2/3	0.5	2/3
Ref.	(Zhao, 1990)	(Raphael, 1984)	(CEB-FIP, 1991)	(Raphael, 1984)	(ACI, 2005)	(CEB-FIP, 1991)

The tensile strength evolution between the ages of 2 and 8 hrs after mixing concrete was investigated by (Abel and Hover, 1998). A dormant period of tensile strength gain was observed from the age of 2 hrs to 4 hrs at which tensile strength was infinitely low. This period was followed by a very rapid tensile strength development starting at the point of initial setting. However, it is difficult to monitor this dormant period for mixtures characterized by a delayed setting. On the other hand, the tensile strain capacity (strain at maximum stress) starts with a very high value before the initial setting and continues to decrease beyond that, reaching a minimum value later (**Fig. 2-5**) (Hammer *et al.*, 2007).
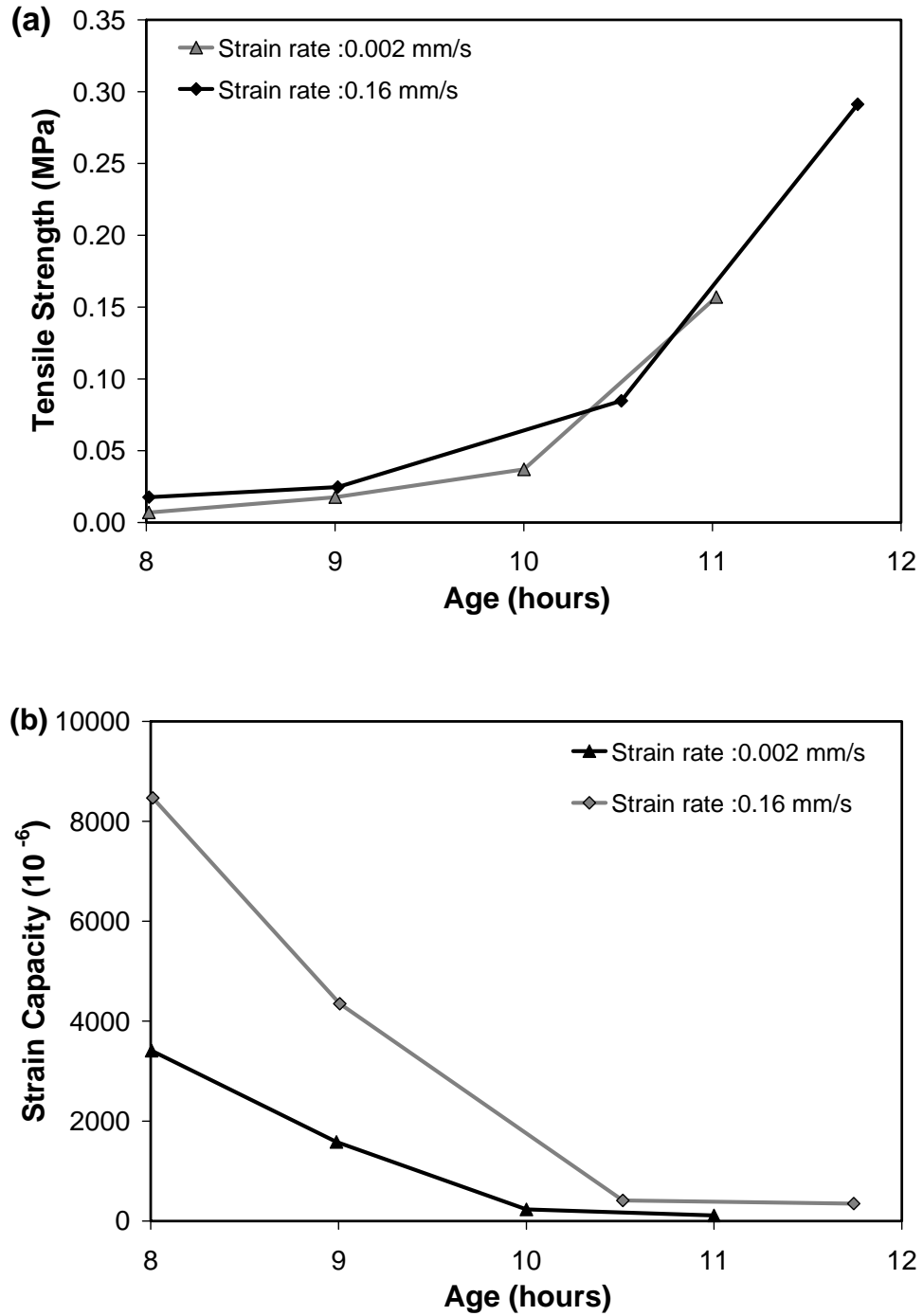
Figure 2-5: a) Uniaxial tensile strength, and b) Uniaxial tensile strain capacity [adapted after (Hammer *et al*., 2007)].

Decreasing the w/c was reported to increase the early-age tensile strength development (**Fig. 2-6**) (Abel and Hover, 1998). Using shrinkage reducing admixtures (SRA) was found to have a non significant effect on the early-age tensile strength of concrete at different w/c as shown in **Fig. 2-7** (D'Ambrosia *et al.*, 2001, D'Ambrosia *et al.*, 2002)**.**
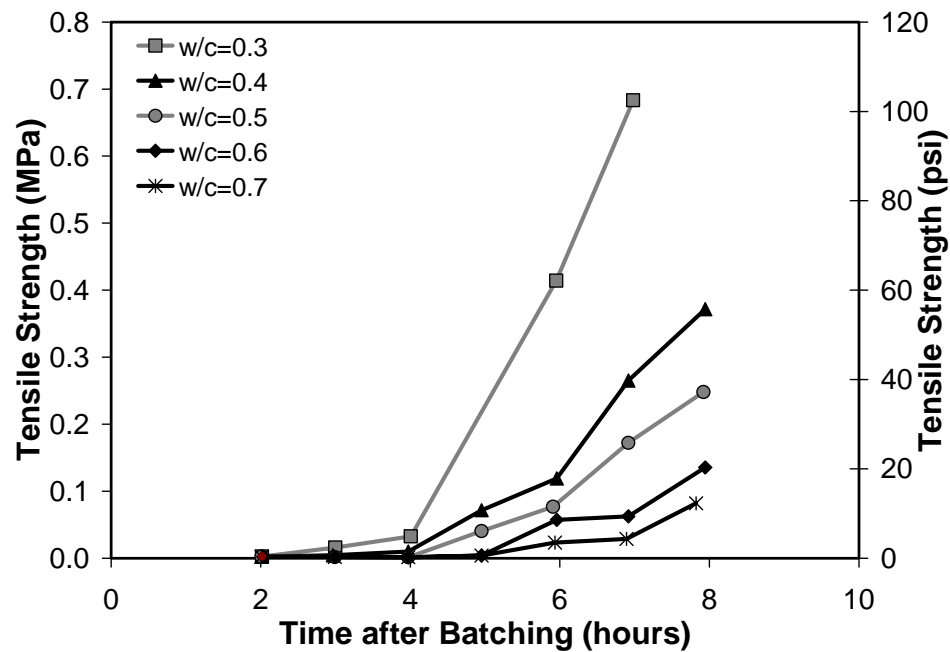
Figure 2-6: Tensile strength of concrete with different water/cement ratio [after (Abel and Hover, 1998)].
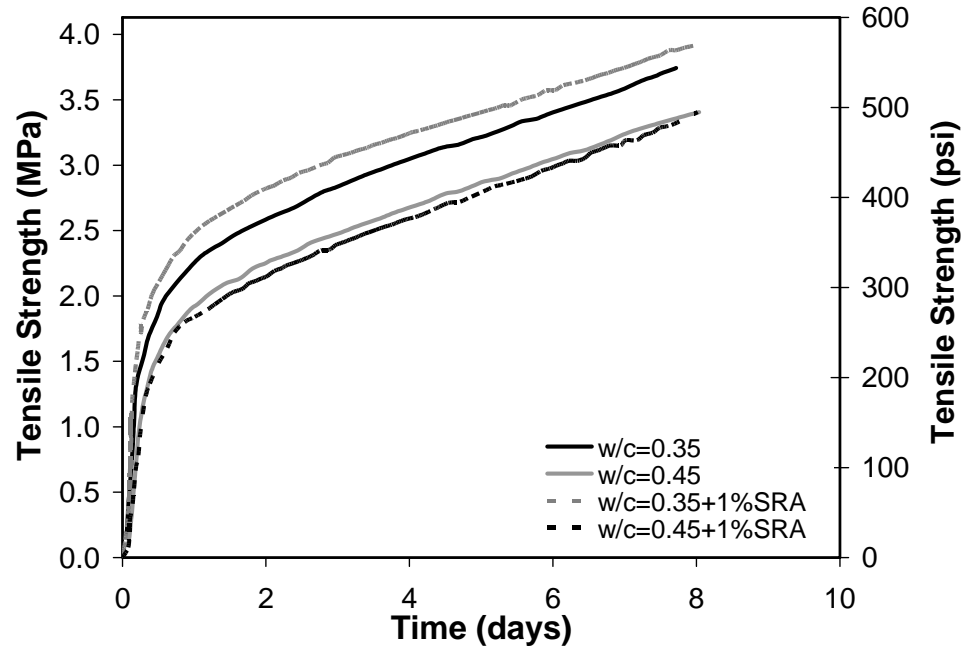
Figure 2-7: Tensile strength of concrete with shrinkage reducing admixture [adapted after (D'Ambrosia, 2002)].

2.2.2.3 Modulus of Elasticity

The modulus of elasticity is a principle property of concrete; it indicates the concrete's capability to deform elastically and thus is related to its serviceability. Generally, it is obtained from the stress-strain curve at a certain stress level relative to the ultimate strength (Tia *et al.*, 2005). This stress value is 40% of the ultimate strength according to ASTM C 469-94 (Standard Test Method for Static Modulus of Elasticity and Poisson's Ratio of Concrete in Compression) (ASTM, 1994), and about 33% in the British Standards (BS 1881: part 121:1983: Method for determination of static modulus of elasticity in compression) (BSI, 1983). On the other hand, researchers have tried to monitor the evolution of the elastic modulus at early-age using ultrasonic waves and to formulate a relationship between the measured dynamic modulus values (E_d) and the

static modulus (E_c), especially for high-performance concrete. A relationship between the dynamic and elastic modules was given by (Mesbah *et al.*, 2002):

$$E_c = 9 \times 10^{-11} (65E_d + 1600)^{3.2}$$ **Eq. 2-5**

The proposed correlation was obtained based on experiential results, which makes it limited to the used aggregates and cement type. However, it indicates the possibility of establishing a relationship between the concrete's dynamic and static modules of elasticity at early-age.

Several formulas have been proposed to express the modulus of elasticity of concrete at any age as a function of its compressive strength (**Table 2-8**) (Zhao, 1990, Ghali and Favre, 1994, Gardner and Zhao, 1993). However, the change in the concrete elastic modulus with respect to its compressive strength at early-ages is affected by several parameters, including the w/c, temperature; cement type, properties of aggregates, and curing conditions (Neville, 1996). Decreasing the w/c enhances the modulus of elasticity as a result of developing a denser microstructure (Østergaard, 2003). The age of concrete at the time of testing was not found significantly to affect the relationship between the modulus of elasticity and compressive strength as shown in **Fig. 2-8** (Zhao, 1990). This is due to the very rapid development rate of the modulus of elasticity of concrete at early-age compared to that of compressive strength. About 90% or more of the elastic modulus value is achieved within the first 24 hours after casting (Myers, 1999). Consequently, the risk of cracking at early-age rises since the stress generated depends on the modulus of elasticity, whereas the resistance to cracking depends on the development of tensile strength (Atrushi, 2003).

Table 2-8: Modulus of elasticity as a function of compressive strength of concrete at any age.

Equation		Reference
$$E(t_0) = 57000\sqrt{f_c'}\ \sqrt{\left(\dfrac{t_o}{4+0.85t}\right)}$$		(Ghali and Favre, 1994)
Where E (t_0) = modulus of elasticity at age t_0, f_c' = compressive strength (psi), and t = age of concrete.		
$$E_c = 3500 + 4300\sqrt{f_{cm}'}$$		(Gardner and Zhao, 1993)
Where E_c = time dependent modulus, f_{cm}' = compressive strength (MPa)		
$$E_c = 3.0(f_{cm}')^{2/3}$$	for $f_{cm}' \leq 27$ MPa	(Zhao, 1990)
$$E_c = 9.0(f_{cm}')^{1/3}$$	for $f_{cm}' > 27$ MPa	
Where E_c = modulus of elasticity, f_{cm}' = compressive strength at test time.		
$$E_{c,t} = 8 + 0.08 f_{cu,28}' + 0.12 f_{cu,t}' + 1.2\left(f_{cu,t}'/f_{cu,28}'\right)$$		
Where $E_{c,t}$ = modulus of elasticity at age t, $f_{cu,28}'$ = compressive strength at 28 days, $f_{cu,t}'$ = compressive strength at age t days, and $t \geq 3$ days.		
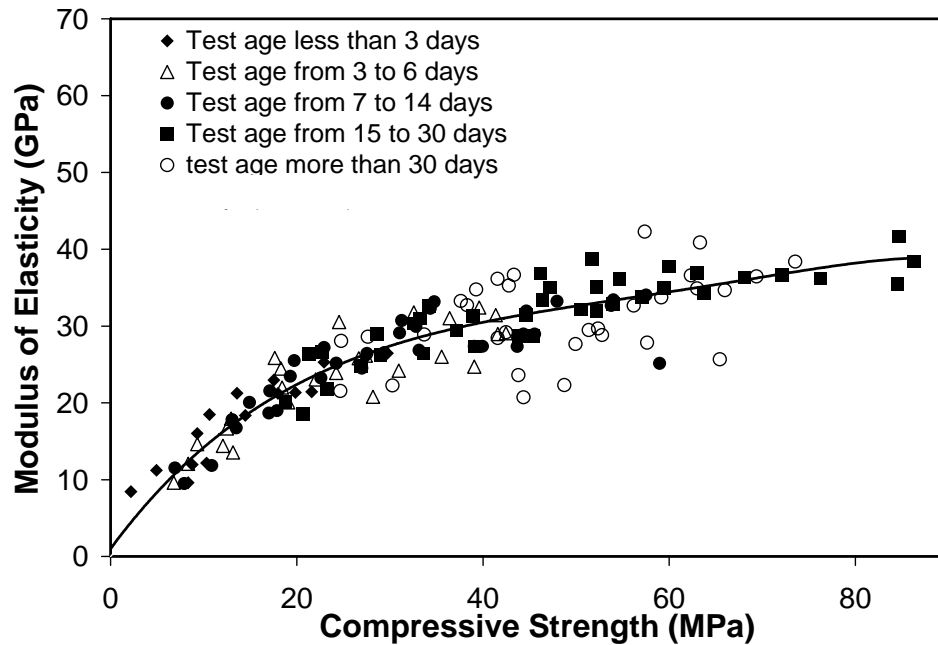
Figure 2-8: Modulus of elasticity to compressive strength ratio data classified by concrete age [after Zhao, 1990].

2.2.2.4. Poisson's Ratio

Poisson's ratio is the ratio between the lateral and longitudinal strains under the same uniaxial load (Neville, 1996). Limited research focused on the evolution of the Poisson's ratio of concrete at early-ages. A review of previous studies showed that the Poisson's ratio changes with time. It starts with a high value at early stage, then it decreases sharply until it reaches a low value during the first 24 hours, then it starts to increase again (Mesbah *et al.*, 2002, Byfors, 1980). Conversely, other researchers stated that the Poisson's ratio of concrete does not change significantly with age, and may be considered constant (Oluokun *et al.*, 1991). Considering the assumption that the deformation of fresh concrete occurs without volume changes, the Poisson's ratio can be taken equal to 0.5 (De Schutter and Taerwe, 1996). **Table 2-9** gives typical Poisson's ratio values observed by different researchers (RILEM, 1981, Mesbah *et al.*, 2002, Byfors, 1980, Oluokun *et al.*, 1991). It was found that the Poisson's ratio does not change significantly with the increase of the cement content (Oluokun *et al.*, 1991, Oluokun, 1989). Moreover, tests conducted on concrete specimens at different ages (1, 3, 7, 14, 28, 90 and 180 days) have shown an insignificant effect of the moisture content and ambient temperature on Poisson's ratio (Downie, 2005). Generally, the Poisson's ratio can be evaluated as a function of the degree of hydration as follows:

$$v(r) = 0.18 \cdot \sin\left(\frac{\pi \cdot r}{2}\right) + 0.5 \cdot e^{-10 \cdot r} \qquad \textbf{Eq. 2-6}$$

Where $v(r)$ is the Poison's ratio at a degree of hydration r (De Schutter and Taerwe, 1996).

Table 2-9: Poisson's ratio values.

Initial value	Minimum value*	Reference
0.23	0.14	(Mesbah *et al.*, 2002)
0.40	0.20	(RILEM, 1981)
0.48	0.13	(Byfors, 1980)
0.19		(Oluokun *et al.*, 1991)

*Minimum measured value during the first 24 hr

2.2.3. Early-Age Shrinkage of Concrete

Shrinkage of concrete is the main cause for several types of cracks which influence the serviceability and durability of concrete. Shrinkage can be divided into two main types: early-age which represents shrinkage during the first 24 hours after the first contact between cement and water (Holt, 2001, Wongtanakitcharoen and Naaman, 2007, Khan, 1995), and long-term shrinkage, which extends beyond the first day (Holt, 2001). The total shrinkage of concrete must be considered as the summation of both. However, there is no clear relationship between the magnitudes of these two types of shrinkage. At rapid drying conditions, the magnitude of the early-age shrinkage can easily exceed that of the long-term shrinkage. **Figure 2-9** illustrates this behaviour for different environmental conditions (Holt, 2005). Due to its low strength and strain capacity at early-age, concrete is very sensitive to internal stresses. Thus, any induced tensile stress greater than the tensile strength will cause either cracks comparable to those that occur at later ages, or internal and microscopic cracks which can be reactivated at later ages, causing serious problems (Holt and Leivo, 2004). Stresses that lead to early-age cracking are typically the result of a combination of three types of deformation: thermal dilation, drying shrinkage, and autogenous shrinkage.
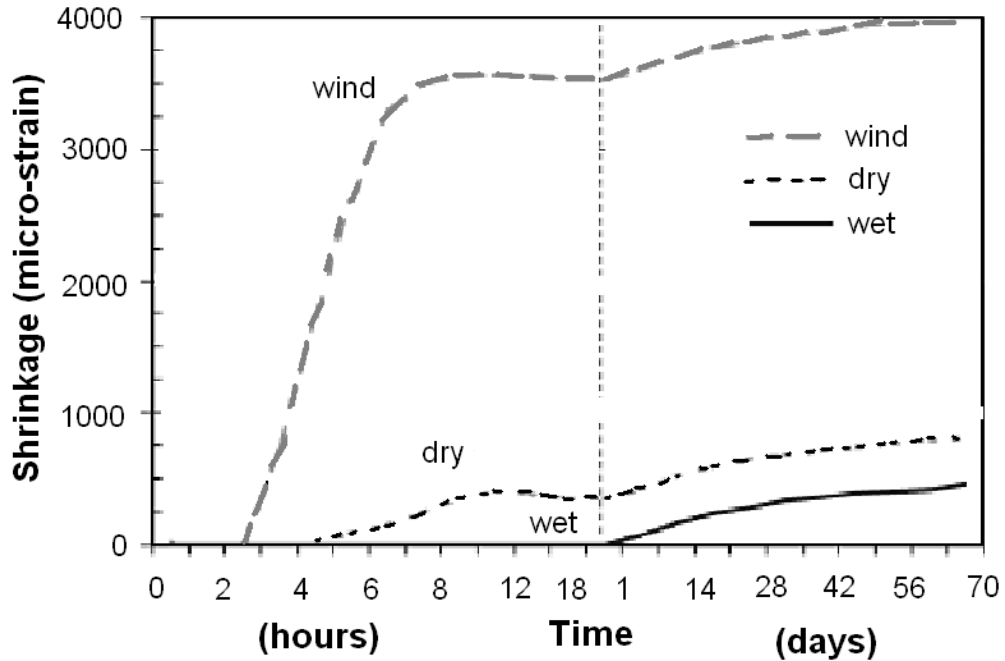
Figure 2-9: Accumulation of early-age and long-term shrinkage, with various curing environments (Wind = 2 m/s (4.5 mph), dry = 40% RH, wet = 100% RH) [after (Holt, 2005)].

2.2.3.1 Thermal Dilation

Thermal dilation is induced by inadequate heat dissipation during the cement hydration and cooling of concrete. It can be observed as an expansion and/or contraction deformation. During the hydration of cement at early-age, the liberated heat increases the concrete temperature causing thermal expansion. As the hydration reactions reach its peak, the rate of heat liberation decreases and concrete starts to dissipate heat and cools down, causing contraction or thermal shrinkage (Holt, 2001). In massive concrete however, the difference in the rate of heat dissipation between the interior and exterior concrete can induce a thermal gradient, leading to thermal strains, and associated stresses that can cause cracking (Holt, 2001, Neville, 1996). Because the coefficient of thermal

expansion varies during early-ages, the traditional method of multiplying the temperature change by an average value of the coefficient of thermal expansion is not accurate for the evaluation of the early-age thermal dilation. Other approaches including the Poly-isothermal test and Saw-toothed test were introduced (Bjøntegaard and Sellevold, 2001). In these methods, the tested specimen is subjected to a realistic temperature history, comprising of temperature steps. The basic idea behind these new approaches is that thermal dilation can be measured directly during each temperature step. Therefore, thermal dilation can be separated from other early-age deformations.

2.2.3.2 Drying Shrinkage

Drying shrinkage is the reduction in the concrete volume due to moisture loss at constant temperature and relative humidity. It is mainly affected by the total moisture loss, rate of evaporation and bleeding. If the bleeding rate is higher than the evaporation rate, drying shrinkage will not occur since the excess water will be sufficient for further evaporation and can act as a curing layer (Holt, 2001, Holt, 2005). When the reverse behaviour occurs, the extra water required for evaporation will be extracted from the internal pores. Losing water from capillary pores at early-age will cause plastic shrinkage and subsequent internal stresses, leading to early-age surface cracks (Khan, 1995). The particle size distribution and quantity of cement, w/c and aggregates have an essential role in controlling bleeding, which in turn controls the mechanism of drying shrinkage on the macro-level. However, it is believed that the drying shrinkage mechanism on the nano-level is a combination of four well-known mechanisms (Bentur, 2003), namely: surface free energy, capillary tension, movement of interlayer water, and disjoining pressure. This combination was found to be highly affected by the relative humidity of

concrete (Bentur, 2003), which varies drastically during early ages. In addition, it should be noted that the measured shrinkage strain of drying concrete specimens under isothermal conditions is not representative of the net drying shrinkage. This measured shrinkage includes drying shrinkage and shrinkage due to cement hydration (so-called autogenous shrinkage), especially at low w/c concrete mixtures.

2.2.3.3   *Autogenous Shrinkage*

Autogenous shrinkage of concrete can be defined as the macroscopic volume change that occurs after the initial setting as a result of the withdrawal of moisture from capillary pores to continue cement hydration reactions (Mihashi and Leite, 2004). Chemical shrinkage, which is the reduction in the volume of hydration products compared with that of the reacting constituents, can be considered as the main driving mechanism behind autogenous shrinkage (Tazawa, 1999). However, autogenous shrinkage is considered as an external volume change (apparent volume change), while chemical shrinkage is considered as an internal volume reduction (absolute volume change), as shown in (**Fig. 2-10**) (Holt, 2001, Mihashi and Leite, 2004, Tazawa, 1999, Esping, 2007).
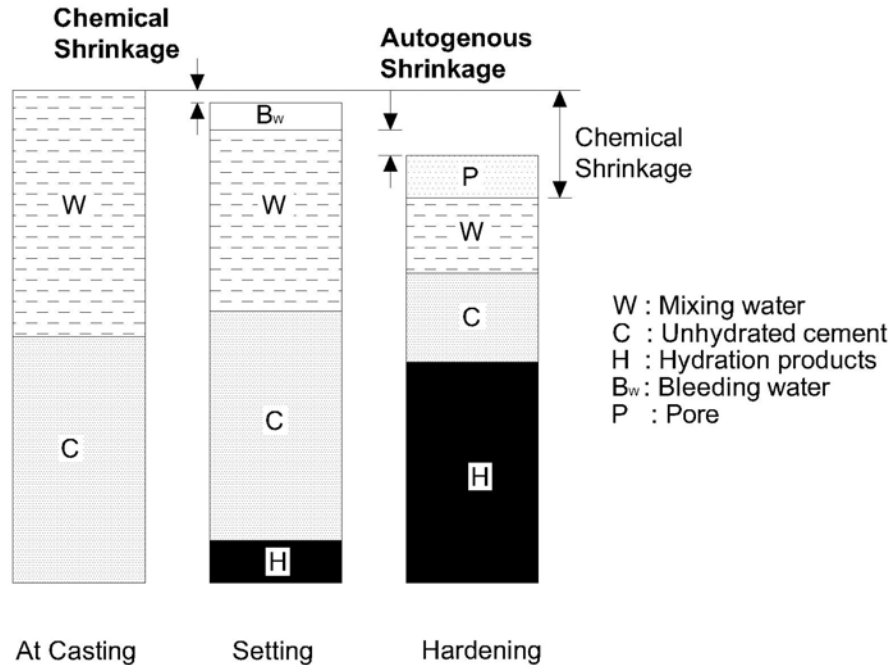
Figure 2-10: Chemical shrinkage and autogenous shrinkage of concrete[adapted after Mihashi and Leite (2004)].

During early-age, concrete undergoes three phases including particulate suspension, skeleton formation, and initial hardening (**Fig. 2-11**). At the initial phase, concrete is still plastic without a permanent internal structure, and autogenous shrinkage is equivalent to chemical shrinkage (part AB in **Fig. 2-11**). Consequently, any applied stresses will cause movement of the body. A few hours after casting, the development of a skeleton starts due to the formation of hydration products. During this stage, the setting will occur, and concrete can resist some of the chemical shrinkage. At this moment, the so-called mineral percolation threshold, autogenous shrinkage starts to diverge from chemical shrinkage (part BC in **Fig. 2-11**). Finally, the hardening stage starts and autogenous shrinkage becomes increasingly restrained due to stiffening of the cement paste (part C in **Fig. 2-11**) (Holt, 2001, Bentur, 2003, Tazawa, 1999, Esping, 2007).
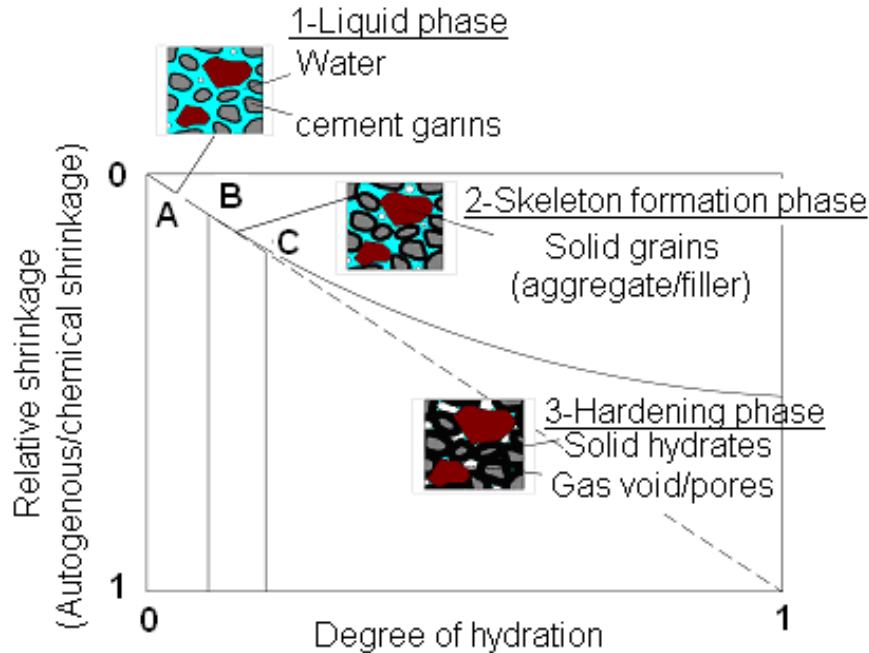
Figure 2-11: Autogenous and chemical shrinkage during different stages, as a function of degree of hydration [adapted after (Holt, 2001, Esping, 2007)].

Measuring autogenous shrinkage should start as soon as possible after mixing the concrete since there is no general agreement on the starting point of autogenous deformation (the time zero (t_0)) (Esping, 2007). While autogenous shrinkage has been known for a long time, it's practical importance and effects have only been recognized with the development of low w/c concrete mixtures (w/c below 0.42) (Aitcin, 2003). Autogenous shrinkage can have nearly the same value as drying shrinkage for low w/c concrete under normal condition (20°C and RH=50%) (Tazawa and Miyazawa, 1995).

Several methods for measuring the early-age shrinkage of concrete have been reported by several researchers. It is believed that the difference between the various measuring methods is largely responsible for variations in results. **Table 2-10** summarizes the common methods for measuring early-age shrinkage and their main

features (Tazawa, 1999, Bjøntegaard *et al.*, 2004, Lee *et al.*, 2003, Termkhajornkit *et al.*, 2005, Hansen and Jensen, 1997, Lokhorst, 1999, Glišic and Simon, 2000, Jensen and Hansen, 1995, Østergaard and Jensen, 2003, Gagné *et al.*, 1999, Lura and Jensen, 2007, Slowik *et al.*, 2004, Gary-Ong and Myint-Lay, 2006, Igarashi and Kawamura, 2002, Lura *et al.*, 2007, Turcry and Loukili, 2006).

Table 2-10: Methods used for measuring shrinkage at early-age.

Shrinkage	Sample size (mm)	Sample Shape	Material	Measuring approach	Reference
Autogenous	100 x100 x 500	Prism	Concrete	Inductive displacement transducer &LVDTs	(Bjøntegaard *et al.*, 2004)
	100 x 100 x 400	Prism		LVDTs & Embedded strain gauge	(Lee *et al.*, 2003)
	Diameter:125 Height: 250	Cylinder		Embedded strain gauge	(Termkhajornkit *et al.*, 2005)
	270 x 270 x 100	Slab		Vertical cast-in bars & LVDTs	(Tazawa, 1999)
	Diameter:100 Length: 375	Flexible tube		- LVDTs	(Hansen and Jensen, 1997)
	150 x 150 x 375	Beam		- Horizontal cast-in bars & LVDTs	(Lokhorst, 1999)
	380 x 1100 x 2000	Slab		- Fiber optical sensors	(Glišic and Simon, 2000)
Total	100 x 100 x 500	Prism		- High resolution digital camera	(Gary-Ong and Myint-Lay, 2006)
Autogenous and Total	70 x 70 x 1000	Dog bone		- LVDTs	(Igarashi and Kawamura, 2002)

Table 2-10 Cont'd: Methods used for measuring shrinkage at early-age.

Shrinkage	Sample size (mm)	Sample Shape	Material	Measuring approach	Reference
Plastic	355 x 100 x 560	Slab with stress riser	Mortar	- Automated image analysis	(Lura *et al.*, 2007)
	70 x 70 x 280	Prism	Concrete	- Laser sensors	(Turcry and Loukili, 2006)
Autogenous	40 x 40 x 160	Prism	Mortar	- Laser sensors	(Tazawa, 1999)
	Diameter:30 Length: 300	Corrugated tube	Cement Paste	- Inductive displacement transducer	(Jensen and Hansen, 1995)
	Diameter:30 Length: 350	Corrugated tube		- Thermal comparator sensor	(Østergaard and Jensen, 2003)
	Diameter:76 Length: 305 Membrane thickness:0.64	Flexible cylindrical latex membrane		- Dual-compartment cell	(Gagné *et al.*, 1999)
	Polyurethane membrane with thickness 0.04	----		- Buoyancy method	(Lura and Jensen, 2007)
	30 x 30 x 90	Prism		- Fiber optical sensors	(Slowik *et al.*, 2004)

2.2.3.4   Factors Affecting Early-Age Shrinkage

The parameters that affect early-age shrinkage of concrete differ according to the driving forces behind each shrinkage mechanism. Drying shrinkage is mainly attributed to environmental conditions. Thus, problematic factors are those that affect the rate of

evaporation, i.e. relative humidity, air velocity, air and concrete temperature (Esping, 2007). Additionally, the materials used in concrete have a parallel effect through controlling the quantity and duration of bleeding and setting time (Holt and Leivo, 2004). On the other hand, autogenous shrinkage is influenced by the type and properties of the binder, mixture proportions, and admixtures that can refine the pore structure. Although the early-age autogenous shrinkage is fully attributed to chemical shrinkage, it may behave differently than chemical shrinkage with respect to some factors especially those that affect the setting time and formation of a restraining structure (Esping, 2007). Generally, the early-age shrinkage is affected by the following parameters:

a) The binder type, content and rate of hydration: A higher rate of hydration results in higher autogenous and drying shrinkage due to the decreased volume of hydration products relative to their constituents and the higher water consumption, which in turn reduces bleeding and increases the concrete temperature (Bentur, 2003, Holt, 2005, Tazawa, 1999, Esping, 2007, Topçu and Elgün, 2004).

b) The aggregate content: aggregates reduce shrinkage, and act as an internal restraint. It also reduces the volume of cement paste, leading to lower chemical shrinkage (Holt, 2001, Esping, 2007). Furthermore, light-weight aggregates with high absorption were found to reduce autogenous shrinkage as it acts as an internal curing source (Nassif *et al.*, 2003, Mihashi and Leite, 2004, Tazawa, 1999, Zhutovsky *et al.*, 2002, Duran-Herrera *et al.*, 2007).

c) The water content: it has a major role during early-age shrinkage through controlling the amount of free water, and the development of the microstructure and pore

system, which consequently affects the capillary tension and meniscus development (autogenous shrinkage).

d) Admixtures: a shrinkage reducing admixture (SRA) can decrease the surface tension of the capillary pore solution resulting in a reduction of the capillary tension. It was found to reduce both autogenous and drying shrinkage strains (Bentur, 2003, D'Ambrosia, 2002, Holt, 2005, Esping, 2007, Lura *et al.*, 2007, Bentza *et al.*, 2001). About 60% reduction in the early-age unrestrained shrinkage due to an SRA dosage of 1-2% by mass of the cement was observed within the first week after casting concrete (D'Ambrosia, 2002). SRA has a more significant effect at low w/c as shown in **Fig. 2-12**. Moreover, SRA was found to induce early expansion after the time of set, maintain a higher relative humidity level in the concrete, and to facilitate water loss from smaller pores, which results in reducing the concrete shrinkage as discussed by (Weiss *et al.*, 2008). Greater early-age shrinkage was observed with the addition of superplasticizer (SP) as a result of improving cement dispersion, which consequently increases the rate of hydration reactions (Holt, 2005, Esping, 2007). In addition, it was pointed out that excessive SP dosage would delay the setting time and result in higher early-age drying shrinkage (Holt and Leivo, 2004). Scattered data on the effect of using air entraining admixtures on the early-age shrinkage were observed (Hammer and Fosså, 2006). However, the general trend was an increase of the autogenous shrinkage rate before it diverged from chemical shrinkage, and then it decreased thereafter. Conversely, air entraining admixtures were found by others to cause a considerable decrease in early-age shrinkage (Kronlof *et al.*, 1995).
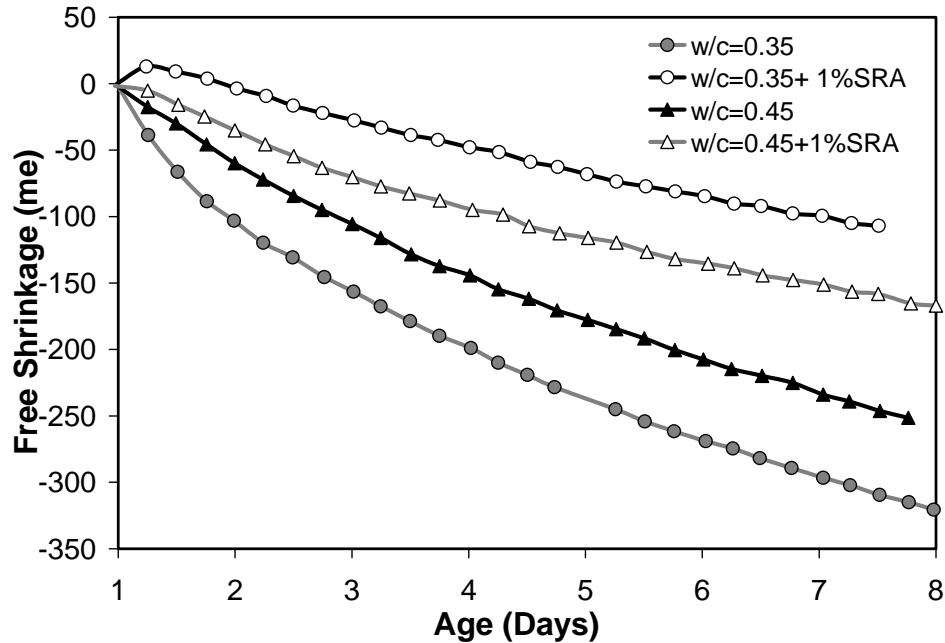
Figure 2-12: Free shrinkage with different w/c and 1% shrinkage reducing admixture [adapted after (D'Ambrosia, 2002)].

e) Pozzolanic materials: the type, fineness, and percentage of cement replacement are the main parameters controlling the effect of pozzolanic materials on early-age shrinkage. Silica fume was found to increase the autogenous shrinkage significantly due to refining the pore structure of concrete (Tazawa, 1999, Wiegrink *et al.*, 1996). Similar behaviour was observed for ground granulated blast furnace slag (Lee *et al.*, 2006, Lim and Wee, 2000). A high level of cement replacement by metakaolin (MK) (10-15%) was found to reduce both autogenous and drying shrinkage at early-age. This reduction may be a result of the dilution effect of reducing the cement content (Brooks and Megat-Johari, 2001, Kinuthia *et al.*, 2000). Conversely, Gleize *et al.* (Gleize *et al.*, 2007) observed an increase in autogenous shrinkage due to MK addition, which was interpreted as a result of the heterogeneous nucleation of hydration products on the surface of MK particles. Fly ash

was also found to reduce the autogenous shrinkage of concrete (Lee *et al.*, 2003, Termkhajornkit *et al.*, 2005). In contrast, it was reported that very fine fly ash had a similar effect to that of silica fume (Tazawa, 1999).

f) Curing conditions: the curing method, duration and temperature have a significant effect on early-age shrinkage. Shrinkage was found to increase with increasing curing temperature during the first 5 to 10 hours after casting, and then it decreased with temperature increase. This may be attributed to an increase in moisture loss at high curing temperature, leading to an increase in the development of plastic shrinkage (Zhao, 1990). Additionally, moist curing with burlap and/or cotton mats was found to effectively reduce the early-age shrinkage and to increase water retention compared with other curing methods (Nassif *et al.*, 2003, Huo and Wong, 2006). Furthermore, the longer the curing period, the lower was the shrinkage deformation (Tazawa, 1999).

2.2.3.5 Compensating for Early-Age Shrinkage

Different methods have been developed to compensate for and/or reduce early-age shrinkage. **Table 2-11** summarizes some of these different methods (Mehta and Monteiro, 2006, Wongtanakitcharoen and Naaman, 2007, Brooks and Megat-Johari, 2001, Bentur, 2003, D'Ambrosia, 2002, Holt, 2005, Mihashi and Leite, 2004, Tazawa, 1999, Esping, 2007, Lura *et al.*, 2007, Duran-Herrera *et al.*, 2007, Bentza *et al.*, 2001, Kronlof *et al.*, 1995, Kinuthia *et al.*, 2000, Sule and van Breugel, 2001, Weiss, 1999). However, the shrinkage of concrete cannot be completely avoided; it will occur at least due to the volume reduction resulting from the hydration of cement and water (chemical shrinkage also called Le Chatelier's contraction).

Table 2-11: Shrinkage compensating methods.

Method	Effective parameter	Action	Reference
Low and moderate heat cement	High C_2S content & formation of ettringite	Expansion	(Tazawa, 1999)
Expansive cement (Type K)	Formation of ettringite Hydration of hard-burnt CaO.	Expansion and chemical pre-stress level	(Mehta and Monteiro, 2006)
Shrinkage reducing admixture	Reduce surface tension of pore solution.	Reduce capillary tension	(Bentur, 2003, D'Ambrosia, 2002, Holt, 2005, Esping, 2007, Lura *et al.*, 2007, Bentza *et al.*, 2001)
Fiber	High elastic modulus.	Resist exceeded tensile stress	(Wongtanakitcharoen and Naaman, 2007, Kronlof *et al.*, 1995)
Internal curing	Soaked lightweight agg Water soluble, chemicals (self-curing admixture), Smart parafine microcapsule, Superabsorbent polymer.	Store water for internal curing, increase water retention, Mitigate rapid temperature change.	(Mihashi and Leite, 2004, Esping, 2007, Duran-Herrera *et al.*, 2007)
Increase w/c	Free water.	Sufficient amount of water for hydration and bleeding	(Tazawa, 1999)
Reinforcement schemes	Light reinforcement bars.	Resist exceeded tensile stress	(Sule and van Breugel, 2001, Weiss, 1999)
Additive	Expansive additive, gypsum, fly ash, metakaolin, water repellent powder.	Hydration product with tendency to volume increase	(Brooks and Megat-Johari, 2001, Tazawa, 1999, Kinuthia *et al.*, 2000)

2.2.4. Early-Age Creep of Concrete

Creep is a complex phenomenon, particularly at early-age, due to the rapid changes in concrete properties (Khan, 1995) and the difficulty to clearly distinguish between instantaneous elastic strains and early-age creep (Neville, 1996). The total creep, either

under tensile or compressive load, is the sum of two main components: basic creep (without external moisture loss), and drying creep (Pickett effect), which is an additional creep due to moisture loss during loading. However, the tensile creep has greater importance at early-age when the crack potential is to be determined (Altoubat, 2002, Bissonnette and Pigeon, 1995).

The mechanism of early-age creep is not completely understood. Several mechanisms have been proposed including real and apparent mechanisms. Real mechanisms, involving the viscous flow theory, plastic flow, and seepage of gel water, are related to cement hydration and can be considered as material properties (Bentur, 2003). Apparent mechanisms are associated with micro-cracking and stress-induced shrinkage (Altoubat, 2002). Generally, creep is a combination of these two categories of mechanisms. Several mathematical formulas were proposed to predicate and model early-age creep, see (Springenschmid, 1998). However, the accuracy of these formulas in capturing and simulating the early-age behaviour of concrete is still questionable and need more investigation (Springenschmid, 1998).

Creep is mainly affected by the mixture composition of concrete, loading age and duration, water migration, temperature, moisture conditions, and the stress level (Neville, 1996). The earlier the loading age, the higher the creep strain values due to the low modulus of elasticity of concrete (Bissonnette and Pigeon, 1995, Neville, 1996). Furthermore, no relationship between the applied stress and the resultant creep strain was found for specimens loaded at an age of 24 hours (Østergaard *et al.*, 2001). Increasing the temperature was found to enhance the early-age creep rate, which is contrary to its effect at later ages (Neville, 1996). However, high temperature is expected to reduce the early-

age creep value as a result of accelerating the hydration process (Springenschmid, 1998).

Moreover, the early-age creep of restrained concrete was found to be inversely related to

the w/c (Altoubat, 2002).

Generally, mineral additives such as fly ash, metakaolin and slag were found to

reduce the tensile creep and relaxation of concrete at early-age (Brooks and Megat-

Johari, 2001, Pane and Hansen, 2002, Li *et al.*, 2002), while silica fume showed an

opposite trend (Kovler *et al.*, 1999, Bissonnette and Pigeon, 1995, Pane and Hansen,

2002, Li *et al.*, 2002). The spherical shape and smooth surface of un-reacted silica fume

particles at early-age were suggested as a reason for this behaviour (Kovler *et al.*, 1999).

Autogenous shrinkage was found to affect basic creep significantly, especially at

low w/c (Pane and Hansen, 2002, Li *et al.*, 2002). Autogenous shrinkage is a material

property that is not dependent on the applied stress. Thus, it should be subtracted from

the total creep strain (see **Eq. 2-7**) (Lee *et al.*, 2006). Consequently, the measured creep

can be categorized into real creep (excluding autogenous shrinkage), and apparent creep

(including autogenous shrinkage) (**Fig. 2-13**). One interesting observation is that SRA

was found to reduce the total tensile creep as well as the early-age shrinkage, but to a less

extent. This can be a benefit if creep is considered to offset the induced tensile stress due

to shrinkage (D'Ambrosia, 2002).

$$J_{real}(t,t') = \frac{\varepsilon_{total}(t,t') - \varepsilon_{autogenous}(t,t')}{\sigma(t')} \qquad \textbf{Eq. 2-7}$$

Where, $J_{real}(t,t')$ is the real compliance function, $\varepsilon_{total}(t,t')$ is the total strain of a

concrete specimen measured from the basic creep test at time t caused by an amount of

constant stress applied at age t', $\varepsilon_{autogenous}(t,t')$ is the autogenous shrinkage strain at time t, σ is the total applied stress.
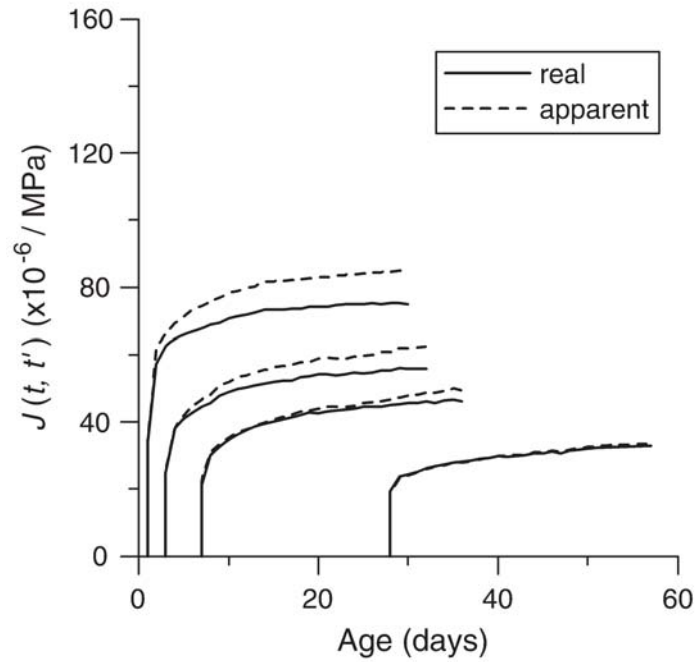
Figure 2-13: Apparent and real creep compliance function [after (Lee *et al*., 2006)].

Furthermore, the sustained mechanical loading at early-age seems to increase the degree of hydration during early-age creep (Tamtsia *et al.*, 2004). It was also shown that biaxial sustained compressive load would promote hydration reactions (Liu *et al.*, 2002). Enhancing the hydration process involves the formation of more calcium silicate hydrate (CSH) gel, which gradually carries load leading to stress reduction in the originally loaded CSH gel and consequently reduced creep at early-age (Springenschmid, 1998).

2.3.   MODELS FOR SIMULATION AND ANALYSIS OF EARLY-AGE PROPERTIES

Several complex and interacting factors affect the early-age properties of concrete, but the hydration process is generally considered as the main indication of early-age behaviour. Hydration of cement is a progressing system of reactions concurrent with a nonlinear temperature rise, thermal expansion, micro-structural changes, water loss and autogenous deformation. Therefore, developing accurate models for the early-age behaviour of hydrated cement should be based on an accurate simulation of the cement hydration process. Several analytical models for simulating the cement hydration process have been developed. According to the scale at which the hydration process is described, these models were classified into micro-scale, meso-scale, and macro-scale models (Mihashi and Leite, 2004). In addition, a digital-image-based model using the so-called "*cellular automata*" was introduced to study the hydration process, formation of microstructure, growth of void structures, strength development, and shrinkage (Bentz and Garboczi, 1993). However, this model was not able to simulate the hydration process at different material scales. Therefore, a multi-scale modeling approach was introduced to overcome this limitation, where separate models at different material scales are developed and then connected with each other (Bentz and Garboczi, 1996). This can better characterize for the hydration process of cement versus time.

Several other models have been introduced to predict the early-age concrete deformation, including thermal, autogenous, drying, and creep deformations. The basic concepts for some of these models that deal mainly with various types of early-age deformations are reviewed hereafter.

A thermo-dynamic model was proposed to describe the autogenous deformation of hardening cement paste. This model was based on reaching thermo-dynamic equilibrium in the capillary pore system, which continuously changes as a result of the hydration progress and autogenous shrinkage. The pore water surface tension was considered as the main reason for autogenous shrinkage (Koenders and van Breugel, 1997). However, the formula used to evaluate autogenous shrinkage is only valid for low relative humidity (< 40%). Moreover, a macro-scale model to explain autogenous shrinkage of cement paste was introduced (Hual *et al.*, 1995). In this model, microscopic stresses due to capillary depression were considered as the main driving force for autogenous shrinkage. This model was further enhanced to estimate autogenous shrinkage at the scale of hydrating grains (Hual *et al.*, 1997). Likewise, a multi-scale model for early-age autogenous shrinkage was proposed (Pichler *et al.*, 2007). It demonstrates the role of capillary depression and ettringite formation pressure on autogenous shrinkage.

On the other hand, the Kelvin chain model was modified to simulate basic creep in early-age concrete (De Schutter, 1999). The modified Kelvin chain model units have variable parameters that vary depending on the degree of hydration. As a result, the model was able to simulate the visco-elastic behaviour of early-age concrete and a good agreement with experimental results was observed. More recently, a hygro-thermo-chemo-mechanical model for early-age creep was introduced. In this model, creep was described based on the micro-pre-stress-solidification theory, which was modified to take into account the effect of relative humidity on the cement hydration rate and the associated hygro-thermal phenomena (Gawin *et al.*, 2006). The good agreement with

experimental data indicates a potential of this model to analyze creep phenomena at different ages and environmental conditions.

Generally, a challenge remains as to how to deal with the nonlinear ageing behaviour of concrete, and how to characterize the behaviour of its constituents at the microscopic and nano-scale levels under field mechanical and environmental conditions. Generally, a smart model which can predicate and demonstrate the interaction effects between different types of deformations (i.e. shrinkage and creep) during early-age of cement-based materials still remain to be developed.

2.4.   CONCLUDING REMARKS

It is widely accepted that the early-age period of concrete has a substantial influence on the long-term service life performance of concrete structures. During early-age, continuous and rapid changes in the concrete microstructure and constituents proportions (un-hydrated and hydrated cement, water content, etc.) take place. Consequently, the early-age characteristics of concrete, including thermal, mechanical and deformation properties, can have different development rates, relationships and values compared to that of the later age properties. Moreover, early-age properties are generally more sensitive to the curing regime (i.e. temperature and relative humidity), early-age loading rate and value, and the use of chemical and mineral admixtures. Several models for the early-age behaviour of concrete have been proposed. It appears that simulating the cement hydration process on a multi-scale level is a useful modeling method for predicting the early-age behaviour as it captures the microscopically ageing cement-based materials behaviour.

For a better understanding and control of the early-age properties of cement-based materials, especially new and emerging materials such as ultra-high performance concrete, the following remarks are noteworthy:

1) Optimization of the binder composition (e.g. use of SCMs) can allow achieving superior early-age performance along with avoiding various divergent effects on early-age properties.

2) There is a need for improving measuring techniques to capture the early-age properties precisely as early as possible and for developing standard testing methods to avoid conflicting data of various non-standardized test methods.

3) Early-age properties of concrete should be investigated under simulated field-like conditions to capture the real behaviour of cement-based materials and to develop more realistic predictive models and relationships.

4) Relationships between early-age concrete properties are greatly affected by the quality of concrete, which is influenced by several factors including the mixture proportions, constituent quality, ageing, etc. Hence, existing formulas for these properties in the literature should be calibrated to the actual concrete mixture and exposure conditions.

5) Mitigating the cracking of concrete should be studied in a holistic manner including thermal strains, drying and autogenous shrinkage.

6) Coupling new modeling tools such as artificial intelligence with existing empirical models may facilitate capturing the interactions between different early-age properties of concrete.

2.5.   REFERENCES

Abel, J. and Hover, K., (1998), "Effect of water/cement ratio on the early-age tensile strength of concrete," *Transportation Research Record: Journal of the Transportation Research Board*, No. 1610, pp. 33-38.

ACI Committee 318, (2005). Building Code Requirements for Structural Concrete (ACI 318-05) and Commentary (ACI 318R-05). 2nd ed., American Concrete Institute, Michigan.

Aitcin, P.C., (2003), "The durability characteristics of high performance concrete: a review," *Cement and Concrete Composites*, Vol. 25, No. 4–5, 409-420.

Alshamsi, A.M., (1997), "Microsilica and ground granulated blast furnace slag effects on hydration temperature," *Cement and Concrete Research*, Vol. 27, No. 12, pp. 1851-1859.

Altoubat, S.A., (2002), "Early-age stresses and creep-shrinkage interaction of restrained concrete," PhD Thesis, University of Illinois at Urbana-Champaign, United States.

ASTM American Society for Testing and Materials, (2007). Standard Specification for Portland Cement. ASTM International, West Conshohocken, ASTM C150 - 07.

ASTM American Society for Testing and Materials, (1994). Standard Test Method for Static Modulus of Elasticity and Poisson's Ratio of Concrete in Compression. ASTM International, West Conshohocken, ASTM C 469-1994.

Atrushi, D.S., (2003), "Tensile and compressive creep of early-age concrete: testing and modeling," PhD Thesis, The Norwegian University of Science and Technology, Norway.

Bentur, A. (ed.), (2003). Early-age Cracking in Cementitious Systems. RILEM Technical Committee 181-EAS: Early-age Shrinkage Induced Stresses and Cracking in Cementitious Systems. RILEM, Report 25, 335 p.

Bentz, D.P. and Garboczi, E.J., (1993), "Digital-image-based computer modelling of cement-based materials," In: *Digital Image Processing: Techniques and Application in Civil Engineering* (Frost, J. D. & Wright, J. R. (ed.)). ASCE, New York, pp. 44-51.

Bentz, D.P. and Garboczi, E.J., (1996), "Digital-image-based computer modelling and visualization of cement-based materials," In: *Transportation Research Record: Emerging technology in Geotechnical Engineering,* No. 1526, National Academy Press, Washington DC., pp. 129-134.

Bentz, D.P., (2007), "Transient plane source measurements of the thermal properties of hydrating cement pastes," *Materials and Structures*, Vol. 40, No. 10, pp. 1073-1080.

Bentza, D.P., Geiker, M.R. and Hansen, K.K., (2001), "Shrinkage-reducing admixtures and early-age desiccation in cement pastes and mortars," *Cement and Concrete Research*, Vol. 31, No. 7, pp. 1075-1085.

Bissonnette, B. and Pigeon, M., (1995), "Tensile creep at early-ages of ordinary, silica fume and fiber-reinforced concretes," *Cement and Concrete Research,* Vol. 25, No. 5, pp. 1075-1085.

Bjøntegaard, Ø. and Sellevold, E.J., (2001), "Interaction between thermal dilation and autogenous deformation in high-performance concrete," *Materials and Structures*, Vol. 34, No. 5, pp. 266-272.

Bjøntegaard, Ø., Hammer, T.A. and Sellevold, E. J. (2004), "On the measurement of free deformation of early-age cement paste and concrete," *Cement and Concrete Composites***,** Vol. 26, No. 5, pp. 427-435.

Brooks, J.J. and Megat-Johari, M.A., (2001), "Effect of metakaolin on creep and shrinkage of concrete," *Cement and Concrete Composite*, Vol. 23, No. 6, pp. 495-502.

Brown, T.D. and Javaid, M.Y., (1970), "The thermal conductivity of fresh concrete," *Materials and Structures*, Vol. 3, No. 6, pp. 411-416.

BSI British Standards. (1983). Method for Determination of Static Modulus of Elasticity in Compression. BSI, London, BS 1881: Part 121.

Byfors, J. (1980), "Plain Concrete at Early-ages," *Swedish Cement and Concrete Institute*, Stockholm, Technical Report, 345 p.

CEB-FIP Model Code for Concrete Structures 1990. (1991), Evaluation of the Time Dependent Behaviour of Concrete. Bulletin d' Information No. 199, Comité Europeen Du Béton / Fédération Internatonale De La Précontrainte, Lausanne.

Cusson, D. and Hoogeveen, T.J., (2006), "Measuring early-age coefficient of thermal expansion in high-performance concrete," In: *Proceeding of the International RILEM Conference on Volume Changes of Hardening Concrete: Testing and Mitigation*. Denmark RILEM Publications SARL, Lyngby, pp. 321-330.

D'Ambrosia, M., (2002), "Early-age Tensile Creep and Shrinkage of Concrete with Shrinkage Reducing Admixtures," Master Thesis, University of Illinois at Urbana-Champaign, United States.

D'Ambrosia, M., Altoubat, S.A., Park, C. and Lange, D.A., (2001), "Early-age tensile creep and shrinkage of concrete with shrinkage reducing admixtures. In *Creep, Shrinkage and Durability Mechanics of Concrete and other Quasi-Brittle Materials* (Ulm, F. J., Bazant, Z. P. & Wittman, F. H. (ed.)). Elsevier, Cambridge MA, pp. 645-651.

De Schutter, G. and Taerwe, L., (1995), "Specific heat and thermal diffusivity of hardening concrete," *Magazine of Concrete Research,* Vol. 47, No. 172, pp. 203-208.

De Schutter, G. and Taerwe, L., (1996), "Degree of hydration-based description of mechanical properties of early-age concrete," *Materials and Structures*, Vol. 29, No. 6, pp. 335-344.

De Schutter, G., (1999), "Degree of hydration based Kelvin model for the basic creep of early-age concrete," *Materials and Structures*, Vol. 32, No. 4, pp. 260-265.

Downie, B., (2005), "Effect of moisture and temperature on the mechanical properties of concrete," Master Thesis, West Virginia University, West Virginia, United States.

Duran-Herrera, A., Aitcin, P.C. and Petrov, N., (2007), "Effect of saturated lightweight sand on shrinkage in 0.35 w/b concrete," *ACI Materials Journal*, Vol. 104, No. 1, pp. 48-52.

Esping, O., (2007), "Early-age properties of self-compacting concrete - Effects of fine aggregate and limestone filler," PhD Thesis, Department of Civil and Environmental Engineering, Chalmers University of Technology, Sweden.

Fu, X. and Chung, D.D.L., (1997), "Effects of silica fume, latex, methycellulose, and carbon fibers on the thermal conductivity and specific heat of cement paste," *Cement and Concrete Research*, Vol. 27, No. 12, pp. 1799-1804.

Gagné, R., Aouad, I., Shen, J. and Poulin, C., (1999), "Development of a new experimental technique for the study of the autogenous shrinkage of cement paste," *Materials and Structures*, Vol. 32, No. 9, pp. 635-642.

Gardner, N.J. and Zhao, J.W., (1993), "Creep and shrinkage revisited," *ACI Materials Journal*, Vol. 90, No. 3, pp. 236-246.

Gary-Ong, K.C. and Myint-Lay, K., (2006), "Application of image analysis to monitor very early-age shrinkage," *ACI Materials Journal*, Vol. 103, No. 3, pp. 169-176.

Gawin, D., Pesavento, F. and Schrefler, B.A., (2006), "Hygro-thermo-chemo-mechanical modelling of concrete at early ages and beyond Part II: Shrinkage and creep of concrete," *International Journal for Numerical Methods in Engineering*, Vol. 67, No. 3, pp. 332-363.

Ghali, A. and Favre, R. (ed.) (1994). Concrete Structures: Stresses and Deformations, 3rd edn., Taylor, London.

Gleize, P.J.P., Cyr, M. and Escadeillas, G., (2007), "Effects of metakaolin on autogenous shrinkage of cement pastes," *Cement and Concrete Composites*, Vol. 29, No. 2, pp. 80-87.

Glišic, B. and Simon, N., (2002), "Monitoring of concrete at very early-age using stiff SOFO sensor," *Cement and Concrete Composites*, Vol. 22, No. 2, pp. 115-119.

Goldsmid, H. J. (ed.) (1965). The Thermal Properties of Solids. 1th edn., Routledge and Kegan Paul, London.

Hammer, T.A. and Fosså, K.T., (2006), "Influence of entrained air voids on pore water pressure and volume change of concrete before and during setting," *Materials and Structures*, Vol. 39, No. 9, pp. 801-808.

Hammer, T. A., Fosså, K. T. and Bjøntegaard, Ø., (2007), "Cracking tendency of HSC: Tensile strength and self generated stress in the period of setting and early hardening," *Materials and Structures*, Vol. 40, No. 3, pp. 319-324.

Hansen, K.K. and Jensen, O.M., (1997), "Equipment for measuring autogenous RH-change and autogenous deformation in cement paste and concrete," In: *Proceedings of the 1st International Research Seminar on Self-desiccation and its Importance in Concrete Technology* (Persson, B. and Fagerlund, F. (ed.)). Lund, pp. 27-30.

Holt, E. and Leivo, M., (2004), "Cracking risks associated with early-age shrinkage," *Cement and Concrete Composite*, Vol. 26, No. 5, pp. 521-530.

Holt, E.E., (2001a). "Early-age autogenous shrinkage of concrete," PhD Thesis, University of Washington, United States.

Holt, E.E., (2001b), "Early age autogenous shrinkage of concrete," *Espoo 2001*. Technical Research Centre of Finland, VTT Publications 446, 184 p.

Holt, E.E., (2005), "Contribution of mixture design to chemical and autogenous shrinkage of concrete at early-ages," *Cement and Concrete Research*, Vol. 35, No. 3, pp. 464-472.

Hual, C., Ehrlacher, A. and Acker P., (1997), "Analyses and models of the autogenous shrinkage of hardening cement paste: II. Modelling at scale of hydrating grains," *Cement and Concrete Research*, Vol. 27, No. 2, pp. 245-258.

Hual, C., Ehrlacher, A. and Acker, P., (1995), "Analyses and models of the autogenous shrinkage of hardening cement paste: I. Modeling at microscopic scale," *Cement and Concrete Research*, Vol. 25, No. 7, pp. 1457-1468.

Huo, X.S. and Wong, L.U., (2006), "Experimental study of early-age behavior of high-performance concrete deck slabs under different curing methods," *Construction and Building Materials*, Vol. 20, No. 10, pp. 1049-1056.

Igarashi, S. and Kawamura, M., (2002), "Effects of microstructure on restrained autogenous shrinkage behavior in high strength concretes at early-ages," *Materials and Structures*, Vol. 35, No. 2, pp. 80-84.

Jensen, O.M. and Hansen, P.F., (1995), "A dilatometer for measuring autogenous deformation in hardening Portland cement paste," *Materials and Structures*, Vol. 8, No. 7, pp. 406-409.

Kada, H., Lachemi, M., Petrov, N., Bonneau, O. and Aïtcin, P.C., (2002), "Determination of the coefficient of thermal expansion of high-performance concrete from initial setting," *Materials and Structures*, Vol. 35, No. 1, pp. 35-41.

Kahouadji, A., Clastres, P. and Debicki, G., (1997), "Early-age compressive strength prediction of concrete - application on a construction site," *Construction and Building Materials*, Vol. 11, No. 7-8, pp. 431-436.

Kasai, Y., Yokoyama, K. and Matsui, T., (1974), "Tensile properties of early-age concrete," In: *Proceedings of the 1974 Symposium on Mechanical Behaviour of Materials*. Kyoto, pp. 433-441.

Khan, A.A., (1995), "Concrete properties and thermal stress analysis of members at early-ages," PhD Thesis, McGrill University, Canada.

Kinuthia, J.M., Wild, S., Sabir, B.B. and Bai, J., (2000), "Self-compensating autogenous shrinkage in Portland cement-metakaolin-fly ash pastes," *Advances in cement research*, Vol. 12, No. 1, pp. 35-43.

Koenders, E.A.B. and van Breugel, K., (1997), "Numerical modeling of autogenous shrinkage of hardening cement paste," *Cement and Concrete Research*, Vol. 27, No. 10, pp. 1489-1499.

Kook-Han, K., Sang-Eun, J., Jin-Keun, K. and Sungchul, Y., (2003), "An experimental study on the thermal conductivity of concrete," *Cement and Concrete Research*, Vol. 33, No. 3, pp. 363-371.

Kosmatka, S.H., Kerkhoff, B., Panarese, W.C., Macleod, N.F. and McGrath, R.J. (ed.) (2002), "Design and Control of Concrete Mixtures," *Cement Association of Canada*, 7th Edition.

Kovler, K., Igarashi, S. and Bentur, A., (1999), "Tensile creep behavior of high-strength concretes at early-ages," *Materials and Structuresl*, Vol. 32, No. 5, pp. 383-387.

Kronlof, A., Leivo, M. and Sipari, P., (1995), "Experimental study on the basic phenomena of shrinkage and cracking of fresh mortar," *Cement and Concrete Research*, Vol. 25, No. 8, pp. 1747-1754.

Lea, F.M., (2004). Lea's Chemistry of Cement and Concrete, 4th Edition, (ed.) P.C. Hewlett, Elsevier Ltd., Oxford, UK, 1057 p.

Lee, K.M., Lee, H.K., Lee, S.H., Kim, G.Y., (2006), "Autogenous shrinkage of concrete containing granulated blast-furnace slag," *Cement and Concrete Research*, Vol. 36, No. 7, pp. 1279-1285.

Lee, K., Lee, K.M. and Kim, B.K., (2003), "Autogenous shrinkage of high-performance concrete containing fly ash," *Magazine of Concrete Research*, Vol. 55, No. 6, pp. 507-515.

Lee, Y., Yi, S.T., Kim, M.S. and Kim, J.K., (2006), "Evaluation of basic creep model with respect to autogenous shrinkage," *Cement and Concrete Research*, Vol. 36, No. 7, pp. 1268-1278.

Li, H., Wee, T.H., Wong, S.F., (2002), "Early-age creep and shrinkage of blended cement concrete," *ACI Materials Journal*, Vol. 99, No. 1, pp. 3-10.

Lim, S.N. and Wee, T.H., (2000), "Autogenous shrinkage of ground-granulated blast-furnace slag concrete," *ACI Materials Journal*, Vol. 97, No. 5, pp. 587-593.

Liu, G.T., Gao, H., Chen, F.Q., (2002), "Microstudy on creep of concrete at early-age under biaxial compression," *Cement and Concrete Research*, Vol. 32, No. 12, pp. 1865-1870.

Lokhorst, S.J., (1999), "Deformational behavior of concrete influenced by hydration-related changes of the microstructures," Delft University of Technology, Netherlands, Research Report 25.5-99-5.

Lura, P. and Jensen, O.M., (2007), "Measuring techniques for autogenous strain of cement paste," *Materials and Structures*, Vol. 40, No. 4, pp. 431-440.

Lura, P., Pease, B., Mazzotta, G., Rajabipour, F. and Weiss, J., (2007), "Influence of shrinkage-reducing admixtures on the development of plastic shrinkage cracks," *ACI Materials Journal*, Vol. 104, No. 2, pp.187-194.

McCullough, B.F. and Rasmussen, R.O., (1999), "Fast track paving: concrete temperature control and traffic opening criteria for bonded concrete overlays,"

Federal Highway Administration, Washington D.C., Report FHWA RD 98-167, 191 p.

Mehta, P.K. and Monteiro, P.J.M. (ed.), (2006). Concrete: Microstructure, Properties, and Materials. 3rd edn. McGraw-Hill, New York.

Mesbah, H.A., Lachemi, M. and Aïtcin, P.C., (2002), "Determination of elastic properties of high-performance concrete at early-age," *ACI Materials Journal*, Vol. 99, No. 1, pp. 37-41.

Mihashi, H. and Leite, J.P., (2004), "State-of-art Report on Control of Cracking in Early-age Concrete," *Journal of Advanced Concrete Technology*, Vol. 2, No. 2, pp. 141-154

Mounanga, P., (2004), "Étude Expérimentale du Comportement des Pâtes de Ciment au Très Jeune Age: Hydratation, Retraits, Propriétés Thermo-physiques," PhD Thesis, University of NANTES, France.

Myers, J.J., (1999). How to achieve a higher modulus of elasticity. Publication – HPC Bridge Views, FHWA, Sponsored, NCBC Co-Sponsored Newsletter, No. 5, pp. 1-3.

Nassif, H.H., Suksawang, N. and Mohammed, M., (2003), "Effect of curing method on early–age drying shrinkage of high-performance concrete," *Transportation Research Record: Journal of the Transportation Research Board,* No. 1834, TRB, National Research Council, Washington, D.C., pp. 48-58.

Neville, A.M. (ed.), (1996). Properties of Concrete. 4th Edition. Wiley, New York.

Oluokun, F.A., (1989), "Investigation of physical properties of concrete at early-ages," PhD Thesis, The University of Tennessee, United States.

Oluokun, F.A., Burdette, E.G. and Deatherage, J.H., (1991), "Elastic modulus, Poisson's ratio, and compressive strength relationships at early-ages," *ACI Materials Journal*, Vol. 88, No. 1, pp. 3-10.

Oluokun, F.A., Burdette, E.G. and Deatherage, J.H., (1990), "Early-age concrete: Strength prediction by maturity – another look," *ACI Materials Journal*, Vol. 87, No. 6, pp. 565-572.

Oluokun, F.A., Burdette, E.G. and Deatherage, J.H., (1991), "Splitting tensile strength and compressive strength relationships at early-ages," *ACI Materials Journal*, Vol. 88, No. 2, pp. 115-121.

Østergaard, L., (2003), "Early-age Fracture Mechanics and Cracking of Concrete, Experiments and Modeling," PhD Thesis, Technical University of Denmark, Denmark.

Østergaard, L., Lange, D.A., Altoubat, S.A. and Stang, H., (2001), "Tensile basic creep of early-age concrete under constant load," *Cement and Concrete Research*, Vol. 31, No. 12, pp. 1895-1899.

Østergaard, T. and Jensen, O.M., (2003), "A thermal comparator sensor for measuring autogenous deformation in hardening Portland cement paste," *Materials and Structures*, Vol. 36, No. 10, pp. 661-665.

Pane, I. and Hansen, W., (2002), "Early-age creep and stress relaxation of concrete containing blended cements," *Materials and Structures*, Vol. 35, No. 2, pp. 92-96.

Pane, I. and Hansen, W., (2005), "Investigation of blended cement hydration by isothermal calorimetry and thermal analysis," *Cement and Concrete Research*, Vol. 35, No. 6, pp. 1155-1164.

Pichler, C., Lackner, R. and Mang, H.A., (2007), "A multiscale micromechanics model for the autogenous-shrinkage deformation of early-age cement-based materials," *Engineering Fracture Mechanics*, Vol. 74, No. 1-2, pp. 34-58.

Prusinski, J.R. (2006), "Chapter 44: Slag as a cementitious material," In *Significance of Tests and Properties of Concrete and Concrete-making Materials (Lamond, J. F. and Pielert, J. H. (ed.))*. ASTM International, West Conshohocken, pp. 512-531.

Raphael, J.M., (1984), "Tensile strength of concrete," *ACI Materials Journal*, Vol. 81, No. 2, pp.158-165.

RILEM Commission 42-CEA, (1981), "Properties of set concrete at early-ages," *Materials and Structures*, Vol. 14, No. 84, pp. 399-460.

RILEM TC119-TCE., (1997), "Avoidance of Thermal Cracking in Concrete at Early Ages (Recommendation: TCE1: Adiabatic and Semi-adiabatic Calorimetry to Determine the Temperature Increase in Concrete Due to Hydration Heat of the Cement)," *Materials and Structures Journal*, Vol. 30, No. 202, pp. 451-464.

Schindler, A.K., (2004), "Effect of temperature on hydration of cementitious materials," *ACI Materials Journal*, Vol. 101, No. 1, pp. 72-81.

Sellevold, E.J. and BjØntegaard, Ø., (2006), "Coefficient of thermal expansion of cement paste and concrete: mechanisms of moisture interaction," *Materials and Structures Journal*, Vol. 39, No. 9, pp. 809-815.

Shan-bin, M. and Zhao-jia, Z., (2002), "The early strength of slag cements with addition of hydrate microcrystals," *Journal of Wuhan University of Technology-Material Science Edition*, Vol. 17, No. 2, pp. 83-85.

Slowik, V., Schlattner, E. and Klink, T., (2004), "Experimental investigation into early-age shrinkage of cement paste by using fiber Bragg gratings," *Cement and Concrete Composites*, Vol. 26, No. 5, pp. 473-480.

Snelson, D., Wild, S. and O'Farrell, M., (2008), "Heat of hydration of portland cement-metakaolin-fly ash (PC–MK–PFA) blends," *Cement and Concrete Research*, Vol. 38, No. 6, pp. 832-840.

Springenschmid, R. (ed.) (1998), "Prevention of Thermal Cracking in Concrete at Early Ages," *RILEM Technical Committee 119*, Avoidance of Thermal Cracking in Concrete at Early Ages. RILEM, Report 15, 348 p.

Sule, M. and van Breugel, K., (2001), "Cracking behavior of reinforced concrete subjected to early-age shrinkage," *Materials and Structures Journal*, Vol. 34, No. 5, pp. 284-292.

Swaddiwudhipong, S., Lu, H.R. and Wee, T.H., (2003), "Direct tension test and tensile capacity of concrete at early-age," *Cement and Concrete Research*, Vol. 33, No. 12, pp. 2077-2084.

Tamtsia, B.T., Beaudoin, J.J. and Marchand, J., (2004), "The early-age short-term creep of hardening cement paste: load-induced hydration effects," *Cement and Concrete Composites*, Vol. 26, No. 5, pp. 481-489.

Tazawa, E. and Miyazawa, S., (1995), "Experimental study on mechanism of autogenous shrinkage of concrete," *Cement and Concrete Research*, Vol. 24, No. 8, pp. 1633-1638.

Tazawa, E. (ed.) (1999). Autogenous Shrinkage of Concrete. *Proceedings of the International Workshop organized by the Japan Concrete Institute,* Taylor, New York.

Termkhajornkit, P., Nawa, T., Nakai, M. and Saito, T., (2005), "Effect of fly ash on autogenous shrinkage," *Cement and Concrete Research*, Vol. 35, No. 3, pp. 473-482.

Tia, M., Liu, Y. and Brown, D. (2005), "Modulus of elasticity, creep and shrinkage of concrete," Department of Civil and Coastal Engineering, University of Florida, Florida, United States, Report U.F. Project No. 49104504973-12, 165 p.

Topçu, İ.B. and Elgün, V.B., (2004), "Influence of concrete properties on bleeding and evaporation," *Cement and Concrete Research*, Vol. 34, No. 2, pp. 275-281.

Turcry, P. and Loukili, A., (2006), "Evaluation of plastic shrinkage cracking of self-consolidating concrete," *ACI Materials Journal*, Vol. 103, No. 4, pp. 272-279.

Uysal, H., Demirbog, R., Sahin, R. and Gűl, R., (2004), "The effects of different cement dosages, slumps, and pumice aggregate ratios on the thermal conductivity and density of concrete," *Cement and Concrete Research*, Vol. 34, No. 5, pp. 845-848.

Viviani, M., Glisic, B., Smith, I.F.C., (2006), "System for monitoring the evolution of the thermal expansion coefficient and autogenous deformation of hardening materials," *Smart Materials and Structures*, Vol. 15, No. 6, pp. N137-N146.

Weiss, J., Lura, P., Rajabipour, F. and Sant, G., (2008), "Performance of Shrinkage-Reducing Admixtures at Different Humidities and at Early Ages," *ACI Materials Journal*, Vol. 105, No. 5, pp. 478-486.

Weiss, W.J., (1999), "Prediction of Early-age Shrinkage Cracking in Concrete Elements," PhD Thesis, Northwestern University, United States.

Wiegrink, K., Marikunte, S. and Shah, S.P., (1996), "Shrinkage cracking of high-strength concrete," *ACI Materials Journal*, Vol. 93, No. 5, pp. 1-8.

Wongtanakitcharoen, T. and Naaman, A.E., (2007), "Unrestrained early-age shrinkage of concrete with polypropylene, PVA, and carbon fibers," *Materials and Structures*, Vol. 40, No. 3, pp. 289-300.

Xu, Y. and Chung, D.D.L., (1999), "Increasing the specific heat of cement paste by admixture surface treatments," *Cement and Concrete Research*, Vol. 29, No. 7, pp. 1117-1121.

Zhao, J., (1990). "Mechanical properties of concrete at early-ages," Master Thesis, University of Ottawa, Canada.

Zhutovsky, S., Kovler, K. and Bentur, A., (2002), "Efficiency of lightweight aggregates for internal curing of high strength concrete to eliminate autogenous shrinkage," *Materials and Structures*, Vol. 35, No. 2, pp. 97-101.

CHAPTER THREE

INTERACTION MECHANSIMS OF EARLY-AGE SHRINKAGE OF UHPC UNDER SIMULATED FIELD-LIKE DRYING CONDITIONS*

This chapter provides a fundamental investigation for the evaluation of different early-age shrinkage of UHPC and their interaction mechanisms under field-like conditions. UHPC specimens were exposed to different simulated field-like conditions including temperatures, namely, 10, 20 and 40°C and relative humidity (RH) ranging from 40 to 80%.

3.1.   INTRODUCTION

Ultra high-performance concrete (UHPC) represents a leap development in concrete technology. Its high strength and enhanced durability make it the ultimate building material for the construction, strengthening and rehabilitation of bridges and other transportation infrastructure (Tang, 2004). However, UHPC is affected by high self-desiccation and autogenous shrinkage due its low water-to-binder ratio (w/b) (Ichinomiya *et al.*, 2005). Moreover, exposure to drying conditions and moisture loss during early-ages are of particular concern in thin applications of UHPC, such as in slabs on grade, repairs and overlays, where the exposed surface area per unit volume of material is high.

Contrary to conventional drying, self-desiccation is an internal drying (without mass loss) of capillary pores as a result of water consumption by the hydration of cement

---

(Aïtcin, 1999). Moreover, the hydration of cement results in chemical shrinkage, which is the driving force for self-desiccation shrinkage (Jensen and Hansen, 1999). Therefore, self-desiccation shrinkage can be evaluated based on the progress of hydration reactions (i.e. increase of the chemically bound water) (Yang *et al.*, 2005, Tazawa, 1999). Nevertheless, drying and self-desiccation shrinkage occur with similar phenomena, especially for low w/b concrete. Since low w/b concrete typically has low bleeding, the evaporation from its surface at low RH conditions will extract water from the internal mass, causing moisture loss and menisci formation (Holt, 2001). This process will extend until equilibrium is achieved between the capillary pore pressure and the vapour pressure above the menisci (Kovler and Zhutovsky, 2006). Generally, more evaporation during early stages will result in more shrinkage. On the other hand, localized water loss due to hydration process will result in the formation of internal water menisci. As hydration proceeds, the menisci radius will decrease, leading to higher capillary stresses, and consequently to higher self-desiccation shrinkage (Holt, 2005, Jensen and Hansen, 1996).

In concrete exposed to field conditions during early-ages, water evaporates from the surface along with self-desiccation due to the progress of hydration reactions (Yuasa *et al.*, 1999). Therefore, a better understanding of the combined effects of drying and autogenous shrinkage, and their interaction mechanisms under field-like conditions is needed. Furthermore, an accurate evaluation of the associated deformations is useful to seek best solutions for reducing early-age deformations and the associated cracking, thus leading to stronger, more durable and maintenance free structures.

Substantial research has focused on evaluating the autogenous shrinkage of different concrete mixtures under sealed conditions, while limited research has explored

the influence of drying conditions and moisture loss on the autogenous shrinkage behaviour during early-age. In addition, only a few studies have been conducted in environments other than 20°C and 50% RH. The present study explores the combined effects of drying and autogenous shrinkage in UHPC and their mutual interactions under different drying conditions.

3.2.   RESEARCH SIGNIFICANCE

Several studies have been conducted to quantify autogenous strains in UHPC, either under sealed condition without accounting for the moisture exchange between concrete and its surrounding, or assuming that autogenous and drying strains can be superimposed. This study adopts a more fundamental approach based on the progress of hydration reactions in an attempt to capture the effects of ambient conditions, including temperature and RH, on the development of autogenous strains in UHPC. The results should have important implications in better understanding for the evolution of early-age deformations under field-like conditions.

3.3.   METHODOLOGY

To clarify the relationship between autogenous strains under sealed and drying conditions, this relationship will be evaluated based on the superposition principle and the degree of hydration method. The degree of hydration method will be applied in this study as follows: First, the progress of hydration under different curing conditions will be quantitatively evaluated based on the amount of chemically bound water (BW). Simultaneously, autogenous and total strains under identical curing conditions will be

measured. Subsequently, a relationship between autogenous strains under sealed conditions and BW will be established. Finally, the contribution of autogenous strains to total strains under drying conditions will be evaluated.

3.4.   EXPERIMENTAL PROGRAM

3.4.1.   Materials and Mixture Proportions

An ordinary portland cement (OPC) was used. Silica fume (SF) was added in a dry powder form as partial replacement for cement. The chemical and physical properties of the various binders are listed in **Table 3-1**. The high SF content was chosen within the optimum SF content recommended by (Youhua, 2000, Schachinger *et al.*, 2004) and used in a wide range of UHPC applications to achieve the required mechanical properties (Graybeal and Hartmann, 2005, Katrin *et al.*, 2006). According to the suggestions of (Cheyrezy *et al.*, 1995), coarse aggregate was not used. Quartz sand having a particle size in the range of 0.1 to 0.8 mm was used. A polycarboxylate-based high-range water-reducing admixture (HRWRA) was added at a rate of 3% by mass of cement. Water from the HRWRA was included in the specified water to cement ratio (w/c). The mixture compositions of the control UHPC mixtures with a target compressive strength of 150 MPa are shown in **Table 3-2**.

3.4.2.   Environmental Conditions

To understand the mechanisms that govern UHPC shrinkage, it is necessary to understand the real effects that exist in structural elements cast in-situ as well as in precast elements subjected to heat curing. Heat curing of UHPC usually consists of steam

curing at 90°C for two days, which is not always easy to apply in the precast industry or

in-situ. Therefore, different curing conditions (i.e. temperature and RH) were applied in

the present study in order to investigate the influence of in-situ environmental conditions

and normal temperature curing regimes during early-age on UHPC deformations (**Table

3-3**). At cold curing conditions, maintaining the RH as low as 40% inside the walk-in

environmental chamber was not feasible. Therefore, this condition was excluded from the

experimental program.

Table 3-1: Chemical and physical properties of cement and Silica fume

	OPC	Silica Fume
SiO_2 (%)	19.8	94.0
CaO (%)	63.2	0.4
Al_2O_3 (%)	5.0	0.1
Fe_2O_3 (%)	2.4	0.1
MgO (%)	3.3	0.4
K_2O (%)	1.2	0.9
SO_3 (%)	3.0	1.3
Na_2O (%)	0.1	0.1
TiO_2 (%)	0.3	0.3
$CaCO_3$ (%)	--	--
Loss on ignition (%)	2.5	4.7
Specific surface area (m^2/kg)	410	19530
Specific gravity	3.17	2.12
C_3S	61	--
C_2S	11	--
C_3A	9	--
C_4AF	7	--

Table 3-2: Composition of control mixture.

Material	(mass/cement mass)
Cement	1.00
Silica fume	0.30
Quartz sand (0.1-0.5 mm)	0.43
Quartz sand (0.3-0.8 mm)	1.53
water	0.22 / 0.25
HRWRA	0.03

Table 3-3: Simulated environmental conditions.

Curing condition	Temperature (°C)	Ambient humidity (%)
Cold	10	60 / 80
Normal	20	40 / 60 / 80
Hot	40	40 / 60 / 80

3.4.3.   Preparation of Test Specimens and Testing Procedures

Cubic specimens (50×50×50 mm) were used to determine the compressive strength at 1, 3, 7 and 28 days according to ASTM C109/C109M-08 (Standard Test Method for Compressive Strength of Hydraulic Cement Mortars (Using 2-in. or [50-mm] Cube Specimens)). Prismatic specimens (25×25×280 mm) were used to measure autogenous and total strains. Identical size specimens were used to measure the mass loss, coefficient of thermal expansion (CTE) and thermo-gravimetric analysis (TGA) tests in order to dispel the effect of the specimen size on the results. Microanalysis was conducted on a chip of specimen from selected UHPC mixtures. The fracture surfaces were examined

using scanning electron microscopy coupled with energy dispersive X-ray analysis (SEM/EDX) using a Hitatchi S-4500 Field Emission SEM.

All UHPC specimens were taken from a single batch of the tested mixture. Specimens were cast in layers and compacted on a vibrating table. After casting, specimens were maintained at ambient temperature (i.e. 20 ±1 °C) and covered with polyethylene sheets until demolding to avoid any moisture loss. All specimens were demolded at the final setting time and initial readings were taken before moving specimens to the pre-determined curing conditions inside the walk-in environmental chamber (*Note: strains will be used hereafter to account for both shrinkage and expansion deformations*).

3.4.3.1 Chemically Bound Water and Degree of Hydration

Thermo-gravimetric and derivative thermo-gravimetric analyses (TGA/DTG) were used to determine the evolution of the BW content during hydration. This indirect method has been commonly used (e.g. Loukili *et al.*, 1999, Mounanga *et al.*, 2004) to quantify the degree of hydration. Since only one binder composition was used, a linear correlation between the amount of BW and the degree of hydration was assumed, in agreement with previous studies (Loukili *et al.*, 1999, Mounanga *et al.*, 2004, Kjellsen and Detwiler, 1992, Lam *et al.*, 2000, Pane and Hansen, 2005). At the specific testing age, small pieces were sliced from (25×25×280 mm) specimens and submerged in an isopropanol solvent to stop hydration. They were subsequently dried using a desiccator until a constant mass was achieved. Immediately before testing, the dried samples were ground and sieved on a No. 350 sieve. The tested samples, weighing up to 40 mg, were heated from 20 to 1100°C under nitrogen gas flow at a heating rate of 10°C/min. All TGA/DTG curves,

mass changes, and temperature peaks were calculated using a TGA software. The amount

of BW and degree of hydration were related based on the Powers' relation given in **Eq. 3-1** (Loukili *et al.*, 1999, Mounanga *et al.*, 2004):

$$\alpha(\%) = \frac{BW(t)}{W(t_\infty)} \times 100 \qquad\qquad \textbf{Eq. 3-1}$$

Where α is the degree of hydration, $BW(t)$ is the amount of chemically bound water at

time t and $W(t_\infty)$ is the amount of water required for complete hydration. For the binder

used in this study, $W(t_\infty)$ was evaluated to be approximately 0.223 (g/g binder) using 18

months age specimens. The starting temperature for calculating the BW ranges from 103

to 112°C according to DTG results, which was within the temperature range used in

previous studies on UHPC (Loukili *et al.*, 1999). However, if the tested sample is dried

well, then the induced error by the difference in the starting temperature will be

negligible (Pane and Hansen, 2005). Furthermore, the measured $BW(t)$ was corrected to

consider the mass loss due to CO_2 release between 600 and 780°C as a result of calcite

decomposition (Mounanga *et al.*, 2004, Pane and Hansen, 2005).

3.4.3.2 Strain Measurements

For each mixture, four (25×25×280 mm) specimens per curing condition were made

according to ASTM C 157 (Standard Test Method for Length Change of Hardened

Hydraulic-Cement Mortar and Concrete). Immediately after demolding, specimens for

autogenous strain measurements were wrapped with four layers of polyethylene sheets

and a layer of paraffin wax membrane to prevent moisture loss. Specimens for total strain

measurements were exposed to different curing conditions inside the walk-in

environmental chamber. The measured unrestrained one-dimensional deformations have

been measured using a comparator provided by a dial gauge with an accuracy of 10 µm/m. Moreover, Type-T thermocouples were inserted in the specimens to monitor internal temperature changes from the onset of tests. Small cross-section prismatic (25×25×280 mm) specimens were chosen to reduce the moisture gradients effect induced by drying (Lam, 2005) and to assure quick dissipation of the hydration heat (Bao-guo, *et al.*, 2007, Baroghel-Bouny *et al.*, 2006). In addition, the high surface area to volume ratio of the tested specimens was intended to enhance the effect of drying conditions through reaching moisture equilibrium between the specimen and it's surrounding in a shorter time.

3.4.3.3 Moisture Loss

Prismatic specimens (25×25×280 mm) were made for each mixture and demolded at the time of starting total strain measurements. Prisms were transferred to the walk-in environmental chamber after measuring the initial mass of each prism using a balance with an accuracy of 0.01 g. The mass measurements were taken for all prisms along with measurements of the total strains. Each mass loss test result in this study represents the average value obtained on four identical prisms.

3.4.3.4 Coefficient of Thermal Expansion

The coefficient of thermal expansion (CTE) was measured based on the temperature variations method introduced by (Cusson and Hoogeveen, 2006, Cusson and Hoogeveen, 2007). In this method, tested specimens were subjected to a realistic temperature history including small range temperature cycles. Three sealed concrete prisms (25×25×280 mm) from each mixture were tested simultaneously in the walk-in environmental chamber from the demolding time up to 48 hrs during which an important variation in CTE

occurred before it stabilized thereafter. During the 25-30°C temperature cycles, the temperature was maintained constant at each temperature step for 3 hrs, including a 15 minute ramp between each temperature step, thus resulting in 4 completed cycles per day.

Each specimen was fixed to an invar frame at one end and was free to deform over two invar rods at the other end. The longitudinal deformation of the concrete prism was measured using a high accuracy (0.001mm) LVDT located at the ends of the invar frame. A foam rubber pad was placed between the test setup and the floor of the walk-in environmental chamber to eliminate ambient vibrations. The concrete temperature was measured using Type-T thermocouples embedded at the centre of the UHPC specimens. In addition, the temperature inside the walk-in environmental chamber was monitored using other thermocouples. **Figure 3-1** presents a diagram of the test setup. The test setup was calibrated under similar experimental conditions in order to eliminate undesirable temperature effects induced by LVDT sensors and the metal and geometry of the test apparatus. All measurements were corrected based on the calibration factor obtained (**Eq. 3-2**). Further details on the CTE calculation method can be found in (Cusson and Hoogeveen, 2006).

$$\varepsilon_c = \kappa\varepsilon_m + \alpha \times 10^{-6}\Delta T \qquad\qquad \textbf{Eq. 3-2}$$

Where ε_c is the corrected strains, ε_m is the measured strains, κ is a calibration factor (0.9925), and α is the coefficient of thermal expansion of the calibrated test apparatus (1.267 x10^{-6} /°C).
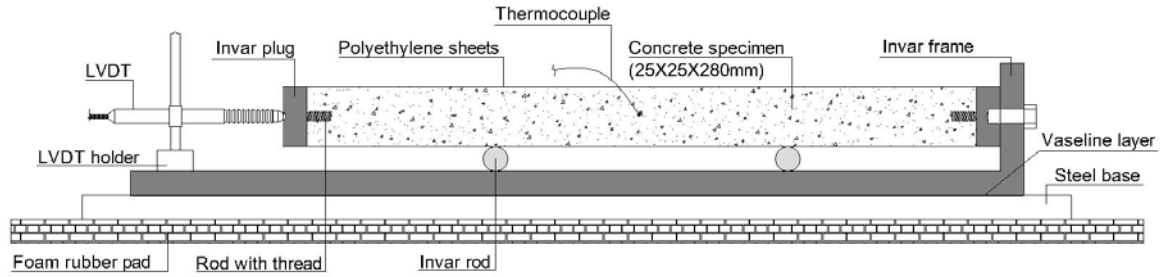
Figure 3-1: Coefficient of thermal expansion test setup.

3.5.   RESULTS AND DISCUSSION

The discussion below will focus on the influence of drying conditions, including the ambient temperature and relative humidity, on the measured autogenous strains of UHPC specimens. The thermal strain evaluated based on the temperature change at the centre of the tested specimens and the corresponding CTE was excluded from the total measured strain. (Note: CTE results are included in **Appendix A**).

3.5.1.   Compressive Strength

Compressive strength is considered as a key property of UHPC. Results indicate that curing conditions, including the availability of moisture and temperature profile, can significantly affect the early-age compressive strength of UHPC. **Figure 3-2** shows the effect of the curing temperature on the compressive strength development of UHPC. Higher curing temperature resulted in higher compressive strength, especially during the first 24 hrs. The compressive strength at 24 hrs for specimens cured at 10 and 20°C achieved only 45% and 70% of that cured at 40°C, respectively. However, the rate of strength gain was lower at later age for specimens cured at 40°C compared with that at 10

and 20°C. For instance, the strength gain at 40°C between ages 3 and 7 days was only about 9%, while it was about 29% at 20°C.
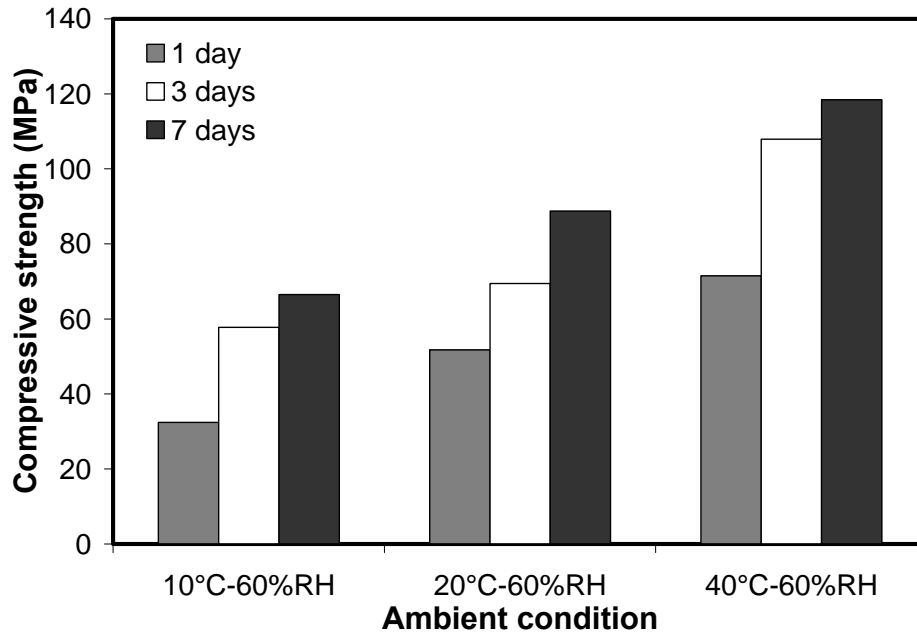
Figure 3-2: Effect of curing temperature on compressive strength for mixtures with w/c=0.25.

During early-age, higher ambient humidity led to higher compressive strength, while at latter age, this effect started to diminish as shown in **Fig. 3-3**. The strength gained during the first 24 hrs at 20°C and 40% ambient humidity was about 25% lower than that gained under 80% ambient humidity, while this difference was only 10 and 7% at 3 and 7 days, respectively. This is likely due to the fact that for UHPC a lower amount of hydration is required to gain higher strength since space between cement particles and porosity to be filled by hydration products are relatively low. In addition, at later ages the depercolation of capillary pores will reduce moisture exchange between the core of the specimens and it's surrounding (Bentz and Garboczi, 1991).
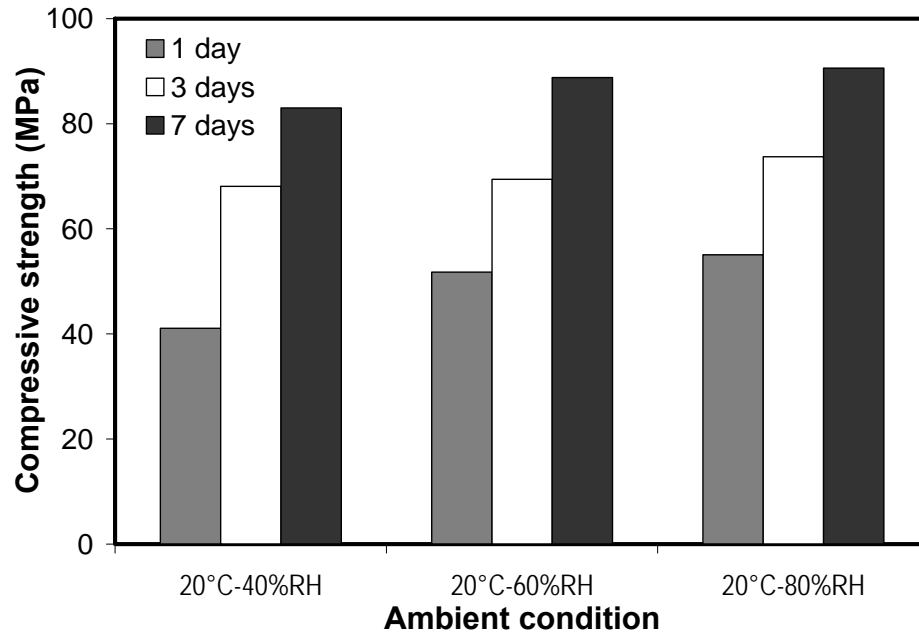
Figure 3-3: Effect of ambient humidity on compressive strength for mixtures with w/c=0.25.

Generally, decreasing the w/c resulted in greater compressive strength. However, the compressive strength results for the control mixture with w/c=0.22 were comparable to that of the control mixture with w/c=0.25 as shown in **Fig. 3-4**. For instance, the percentage difference in early-age compressive strength between control mixtures with w/c=0.22 and 0.25 after 7 days under different curing conditions, ranged from about (-5.0%) to (+4.0%). Moreover, this difference decreased further at 28 days (ranged from (-3.2%) to (+2.0%)). Not achieving significantly greater compressive strength with lower w/c can be ascribed to the agglomeration of SF particles which reduced its effectiveness. The agglomerated grains of silica fume have less effective pozzolanic activity than that of individual grains (Yajun and Cahyadi, 2003). In addition, the size of such agglomerates often exceeds that of Portland cement particles, thus limiting the benefits attributed to the fine particle filler effect (Diamond and Sahu, 2006), leading to higher porosity. However,

such porosity may provide more space for further hydration products, leading to retrieval

of strength at later ages. It was observed by (Korpa and Trettin, 2004, Diamond *et al.*,

2004) that at later age, the pozzolanic reaction of large silica fume particles can attain a

considerable degree, contributing remarkably to the development of mechanical

properties.
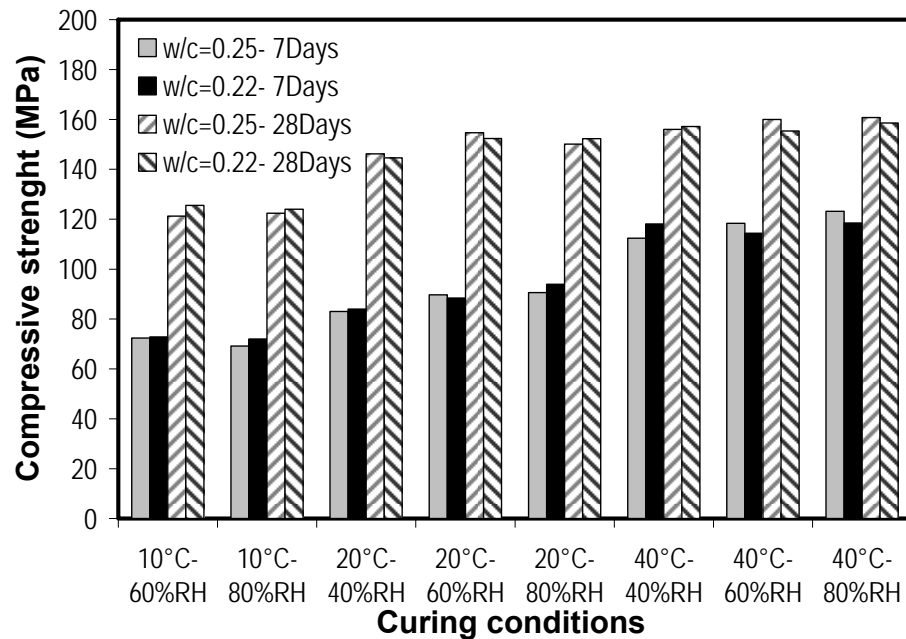
Figure 3-4: Effect of w/c on compressive strength.

3.5.2. Total Strain

3.5.2.1 Influence of Curing Temperature and Ambient Humidity on Total Strain

The total amount of strain mainly depends on the exposure conditions and concrete

mixture design (Mönnig and Lura, 2007). **Figure 3-5** illustrates the effect of exposure

conditions on the measured total strains for control UHPC mixtures. At higher

temperature, specimens were found to exhibit higher total strains compared to that of

specimens exposed to lower temperature, regardless of the RH. In addition, under the

same exposure temperature, lowering the RH increased the total strains. This increase was more significant at high temperature as shown in **Fig. 3-5**. Moreover, mixtures with w/c=0.22 showed lower total strain compared to that of mixtures with w/c=0.25. This can be attributed to lower water content of w/c=0.22 mixtures and consequently lower evaporable water.

3.5.3.   Autogenous Strain

3.5.3.1 *Effect of Curing Temperature and w/c*

Figure 3-6 shows the autogenous strain for the control mixture (w/c=0.25) under sealed conditions for the first 7 days at different curing temperatures. Increasing the temperature from 20 to 40°C accelerated the autogenous strain rate during the first 24 hours, which could be explained by the acceleration of hydration reactions, resulting in higher chemical shrinkage. The latter is considered as the main driving force for shrinkage until an internal rigid skeleton is formed (Jensen and Hansen, 1999, Mounanga *et al.*, 2004, Acker, 2004, Kamen *et al.*, 2008).

While the rate of autogenous strain at 40°C started to decrease after the first day of hydration, this took more than 4 days at 20°C. This could be attributed to the dual action of temperature on the microstructure of the cementitious matrix. High curing temperature motivates the development of a strong solid skeleton (Kamen *et al.*, 2008), which resists autogenous strain (Yang *et al.*, 2005, Esping, 2007). Simultaneously, the high curing temperature results in a coarser porous structure (larger pore radius) (Neville and Brooks, 1991, Cao and Detwiler, 1995), leading to lower capillary stresses as shown by the Kelvin-Laplace equations (Hua *et al.*, 1995). Consequently, autogenous strain will develop with a lower rate (Kamen *et al.*, 2008).
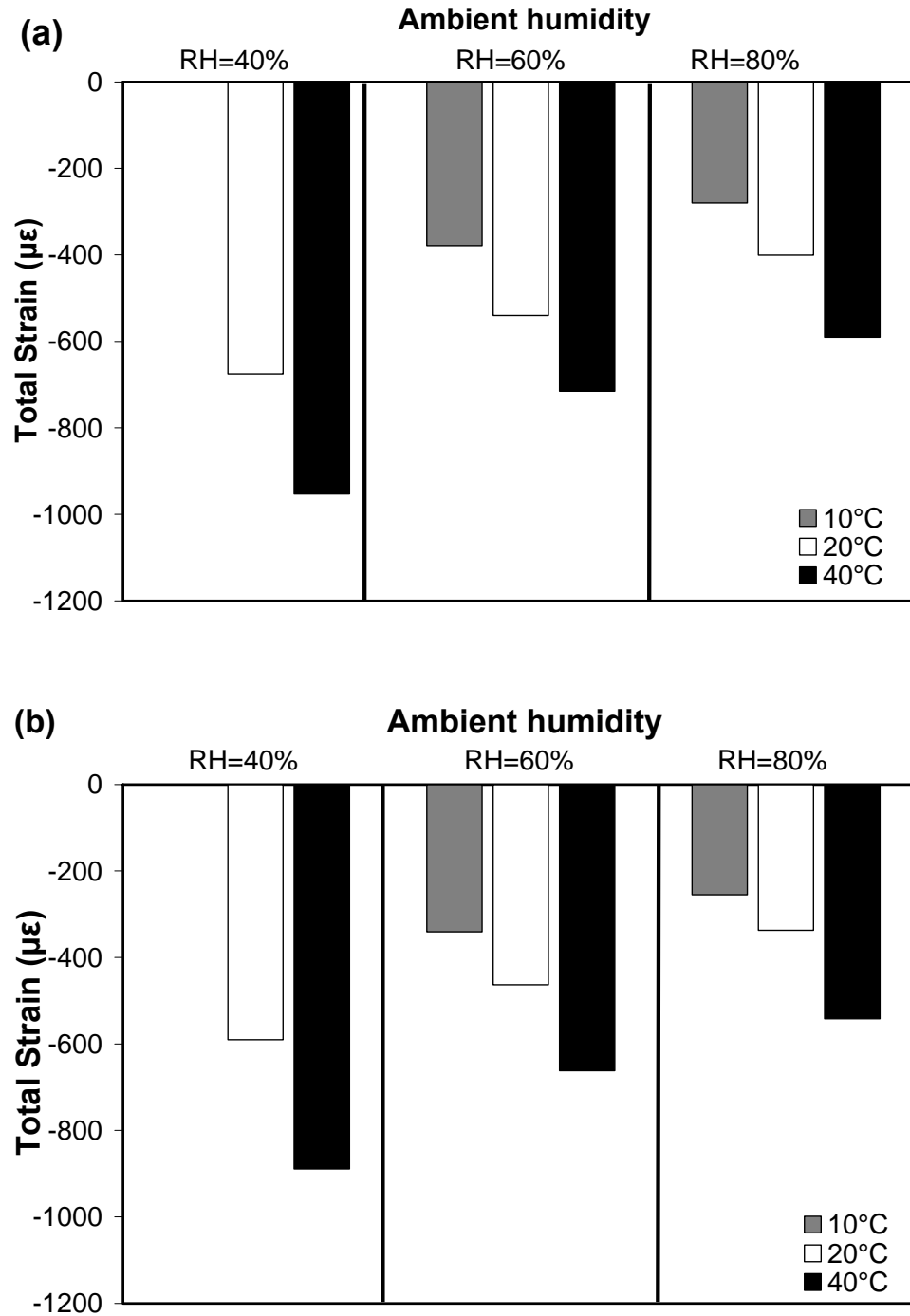
Figure 3-5: Total strains Vs. ambient humidity at different curing temperatures for a) w/c=0.25 and b) w/c=0.22 mixtures at age of 7-days.
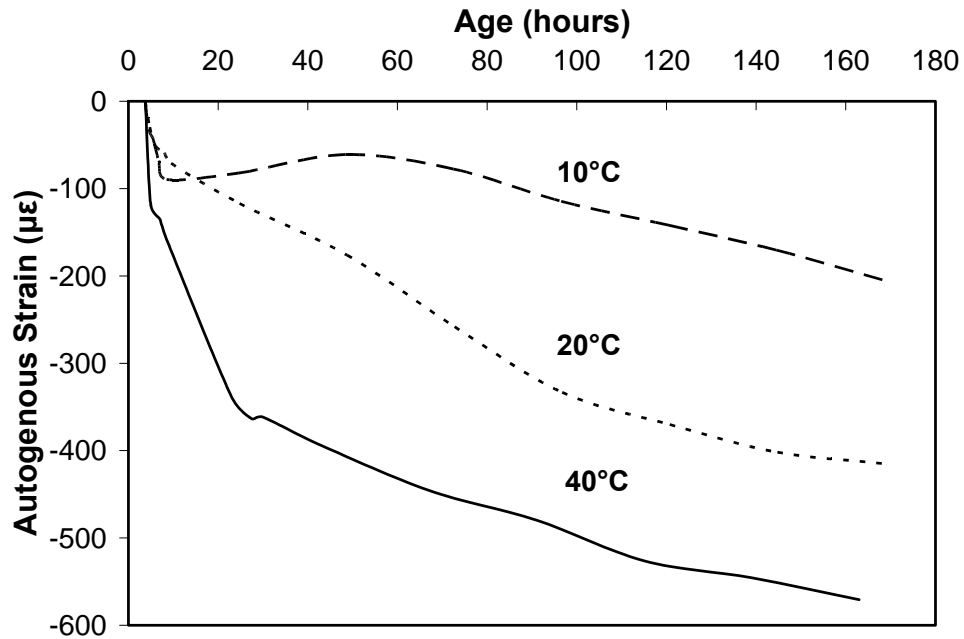
Figure 3-6: Autogenous strains for the control mixture (w/c=0.25) at 10, 20 and 40°C.

At 10°C, the developed strain showed a near plateau after a few hours from the setting time, then started to expand slightly, before autogenous shrinkage strain increased again. This expansion could not be attributed to the thermal effect of hydration reactions since the specimen cross-section was small (Baroghel-Bouny *et al.*, 2006), but could occur likely due to the formation of ettringite (Loukili *et al.*, 1999, Baroghel-Bouny *et al.*, 2006, Bentz *et al.*, 2001a).

Generally, decreasing the w/c results in greater autogenous strains (Holt, 2001, Zhang *et al.*, 2003, Holt and Leivo, 2004). However, comparable strains were observed for mixtures with w/c=0.22 and 0.25 at different temperatures as shown in **Fig. 3-7**. This can be ascribed to the high SF content (>25%), which was reported to reduce the autogenous strains for extremely low w/b mixtures as a result of the inadequate packing

and agglomeration of SF particles, which consequently leads to higher porosity (Baroghel-Bouny and Kheirbek, 2000, Yajun and Cahyadi, 2003).
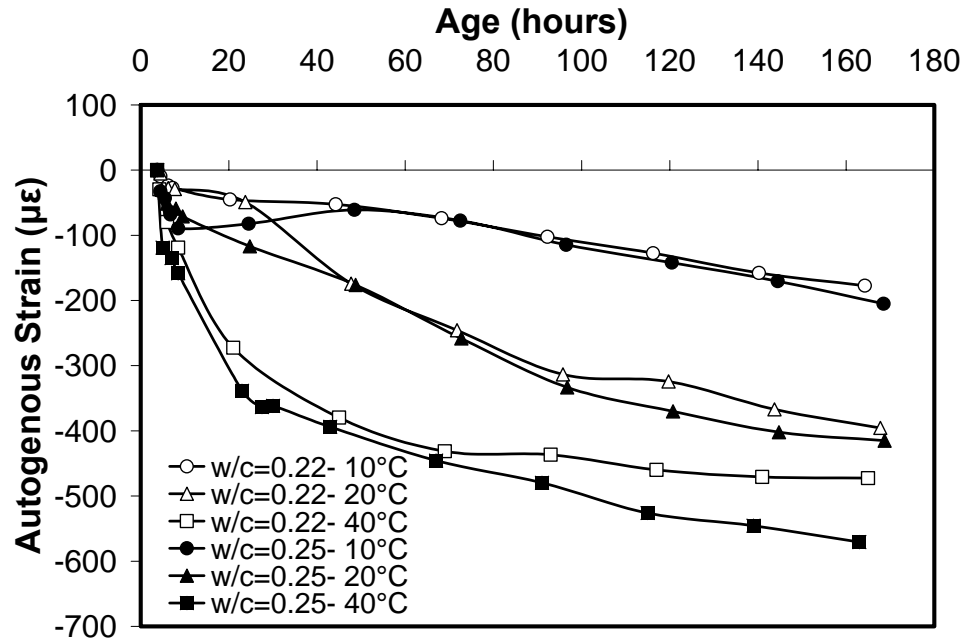
Figure 3-7: Autogenous strains for mixtures with w/c=0.22 and 0.25 at different temperatures.

Furthermore, for high SF/cement mixtures, calcium hydroxide (CH) crystals dissolve to provide calcium ions during the pozzolanic reaction. If the resulting calcium silicate hydrate (CSH) products do not fill the space of dissolved CH crystals, porosity can be created (Baroghel-Bouny and Kheirbek, 2000). This can partially explain the absence of expansion at 10°C for w/c=0.22 mixtures since more pore space could have been created. **Figure 3-8** shows SEM and EDX microanalysis results (conducted at Surface Science Western at The University of Western Ontario), which substantiate this hypothesis in w/c=0.22 UHPC control mixtures. Spatial elemental distribution by EDX revealed high intensity of silicon (Si) in the circular body representing an agglomerated

SF particle. The agglomerated SF particle is encapsulated by a rich media of calcium (Ca), silicon (Si) and oxygen (O) forming a halo of CSH.

(a)

(b)
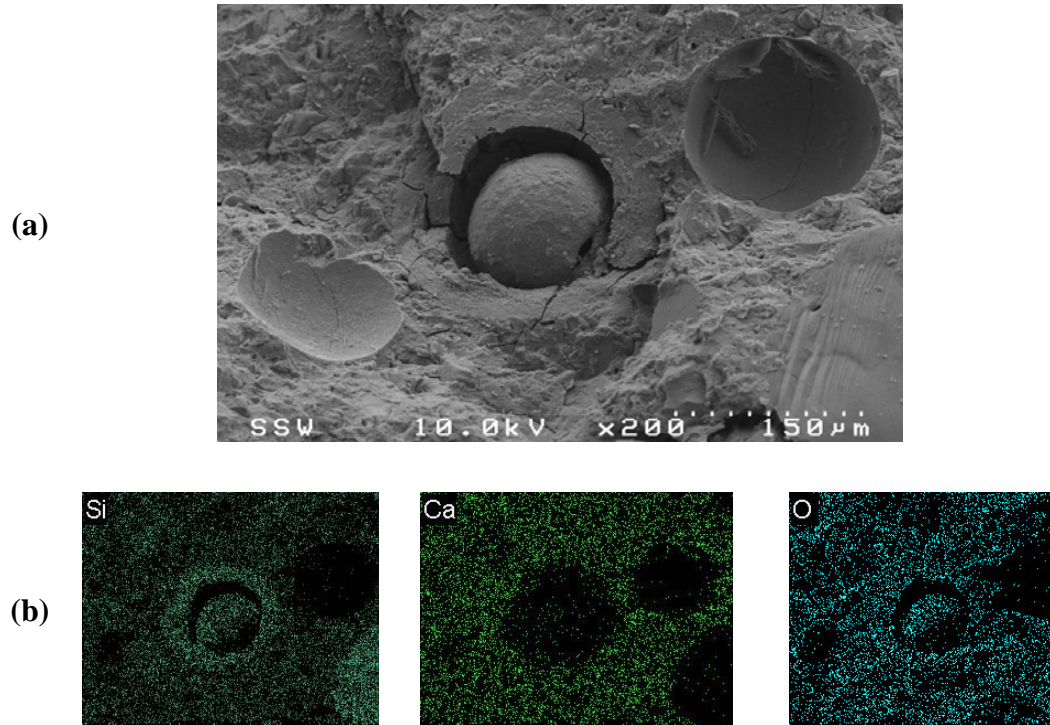
Figure 3-8: Scanning electron micrograph for w/c =0.22 UHPC specimens: (a) agglomerated silica fume encapsulated with C-S-H, (b) elemental distribution.

3.5.4.   Degree of Hydration

3.5.4.1 Under Sealed Condition

The hydration of cement is highly sensitive to the w/c and curing temperature (Mounanga *et al.*, 2004, Lothenbach *et al.*, 2007, Escalante-Garcia and Sharp, 2000, Slamecka and Škvara, 2002). The hydration kinetics increases with increasing w/c and/or curing temperature (Mounanga *et al.*, 2004). TGA was used to investigate the hydration evolution for samples taken from the cementitious matrix of the tested UHPC specimens. The measured degree of hydration versus age is shown in **Fig. 3-9**. For all mixtures, the

hydration rate increased with increasing temperature, which is in agreement with previous work (Mounanga *et al.*, 2004, Escalante-Garcia and Sharp, 2000). Reducing the w/c from 0.25 to 0.22 did not cause a significant reduction in the degree of hydration (**Fig. 3-9(b)**). This can be attributed to the fact that at very low w/c, the content of un-hydrated phases, which could exceed 42% (Acker, 2004), may restrict the further development of hydration products (Lothenbach *et al.*, 2007).

(a)
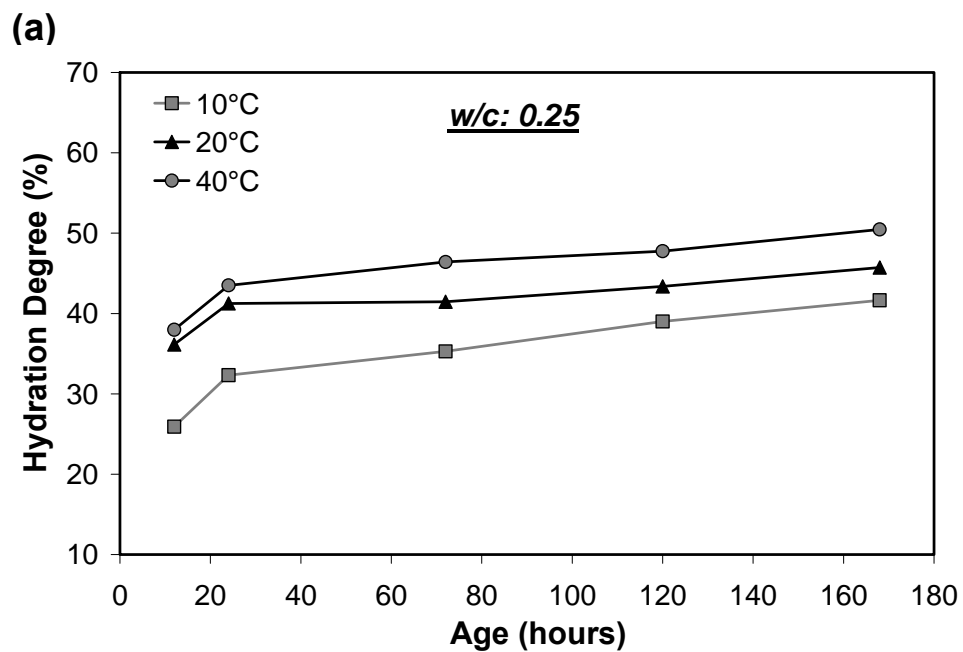
Figure 3-9: Evaluation of degree of hydration Vs. age for control mixtures a) w/c=0.25 and b) w/c= 0.22.

(b)
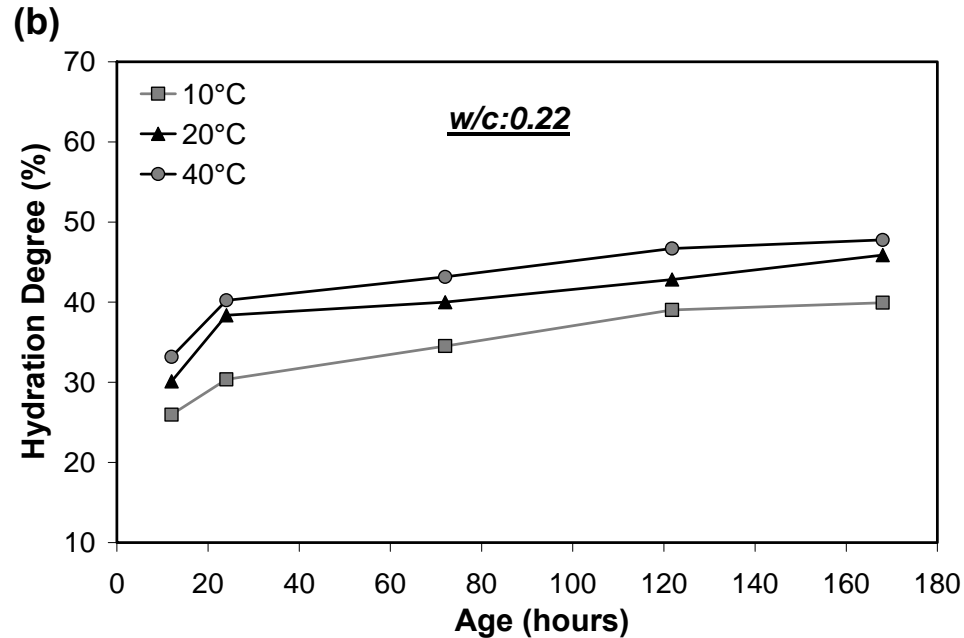
Figure 3-9 Contd': Evaluation of degree of hydration Vs. age for control mixtures a) w/c=0.25 and b) w/c= 0.22.

3.5.4.2 Under Drying Condition

Concrete is usually exposed to ambient air at early-ages, and a moisture exchange between concrete and its environment occurs. Hence, the amount of water available for hydration reactions will be altered. Generally, a reduction in water content at drying conditions takes place, with an adverse effect on the hydration process of cement. Accordingly, the amount of hydration products and BW will be changed (Bentz *et al.*, 2001b). **Figure 3-10** shows cross sections for sealed and exposed to drying specimens. The difference in the colors would indicate the difference in the hydration degree between the two specimens.
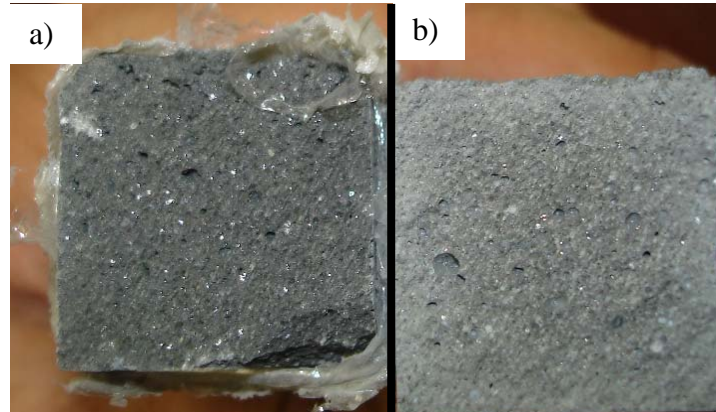
Figure 3-10: Cross sections for a) sealed and b) exposed to drying specimens after 7 days.

Figure 3- 11 (a,b,c) shows the effect of the curing conditions on the BW. At 10°C, the change in RH induced a slight difference in the degree of hydration achieved. This could be attributed to the low rate of evaporation and hydration (Escalante-Garcia and Sharp, 2000), which slowed down the reduction of internal RH (Jensen and Hansen, 1999). In addition, the rate of hydration seemed to be similar over the investigated period. At higher curing temperatures, the RH had a pronounced effect on both the rate of hydration and the degree of hydration achieved. Low RH enhances the moisture transfer from the specimen to its surrounding, which disturbs the hydration process, leading to a lower degree of hydration. Generally, curing at high temperature induces a competition for the mixing water between evaporation and hydration. High curing temperatures usually result in a more porous and continuous pore structure, which facilitates evaporation (Cao and Detwiler, 1995). Conversely, high curing temperature enhances the hydration rate causing more water to bond chemically and physically to hydration products, leaving a lower amount of evaporable water (Mounanga *et al.*, 2004). The rate of change of the internal RH, which is controlled by the hydration rate (Jensen and

Hansen, 1999) and external RH level, will dominate the water exchange between the tested specimen and its surrounding.

(a)

(b)
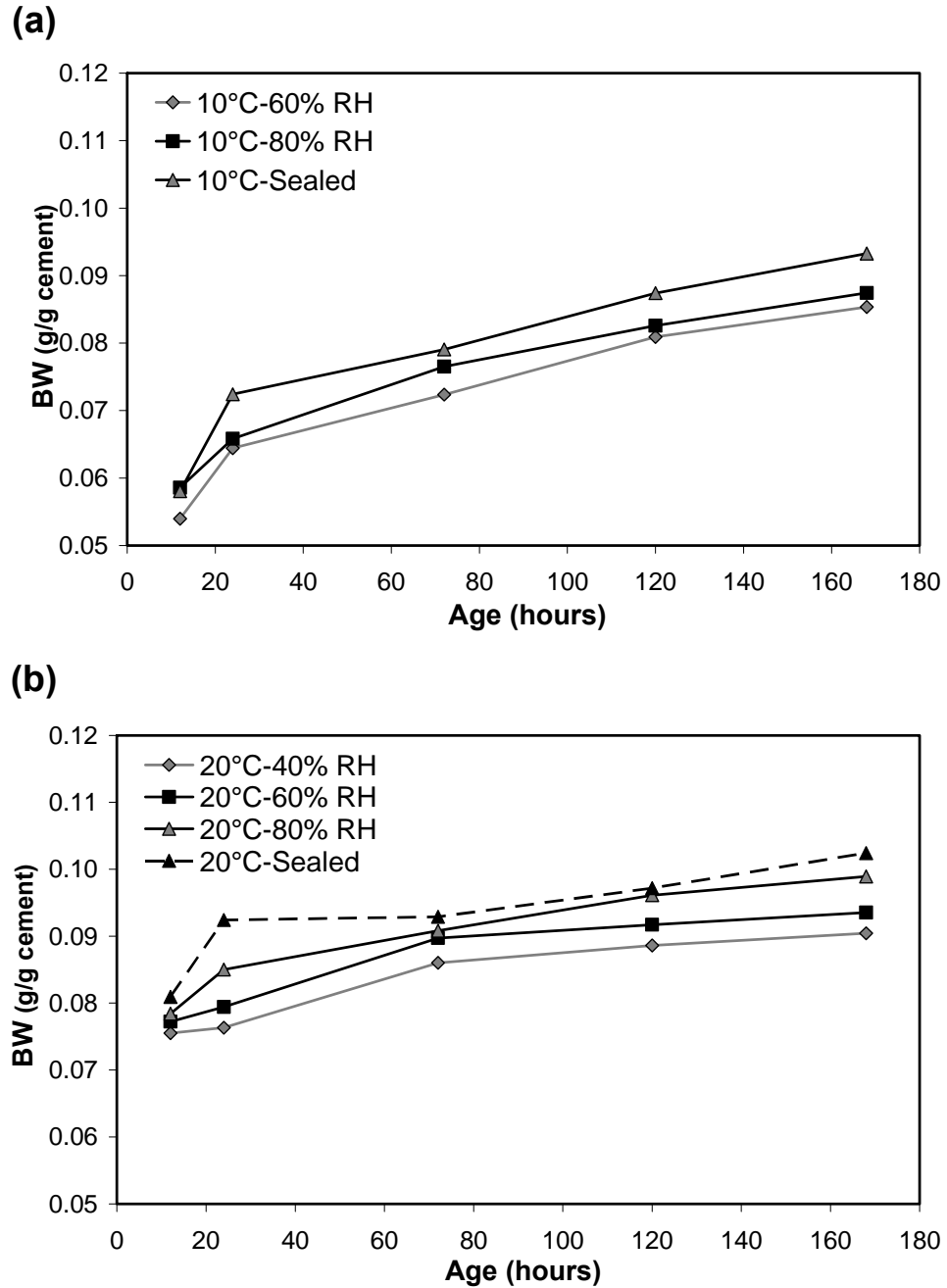
Figure 3-11: Change in BW Vs. ambient humidity for w/c=0.25 control mixtures at a) 10°C, b) 20°C, and c) 40°C.

(c)
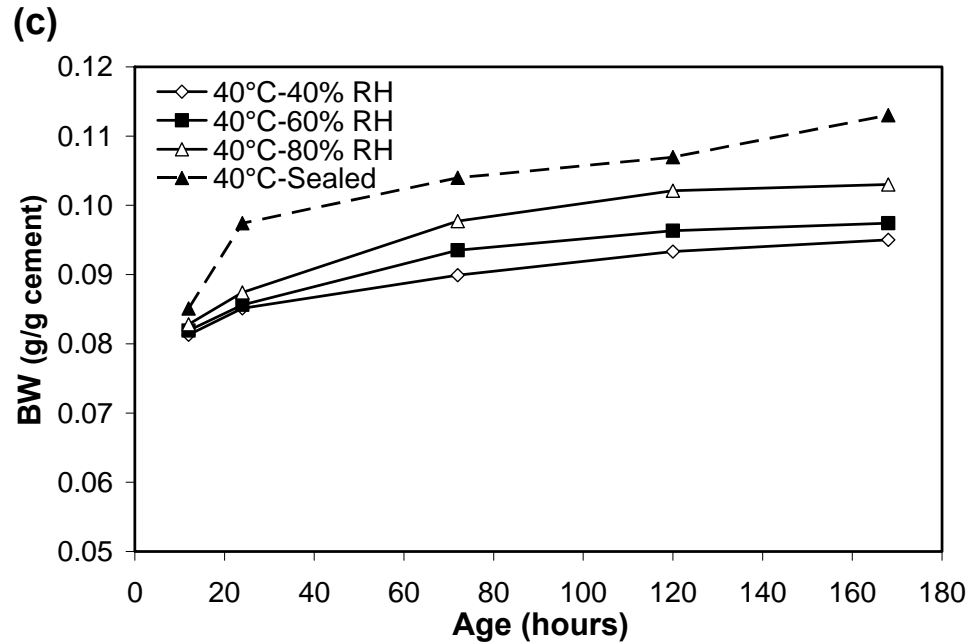
Figure 3-11 Cont'd: Change in BW Vs. ambient humidity for w/c=0.25 control mixtures at a) 10°C, b) 20°C, and c) 40°C.

BW results were consistent with mass loss measurements as shown in **Fig. 3-12 (a,b,c)**. While UHPC specimens cured at 10°C showed a slight increase in mass loss with decreasing RH, significant variations in mass loss were observed at higher temperature. Increasing the curing temperature and decreasing the RH enhanced the evaporation rate, resulting in higher mass loss, which is in agreement with previous studies (Almusallam, 2001, Bissonnette *et al.*, 1999, Al-Saleh and Al-Zaid, 2006).
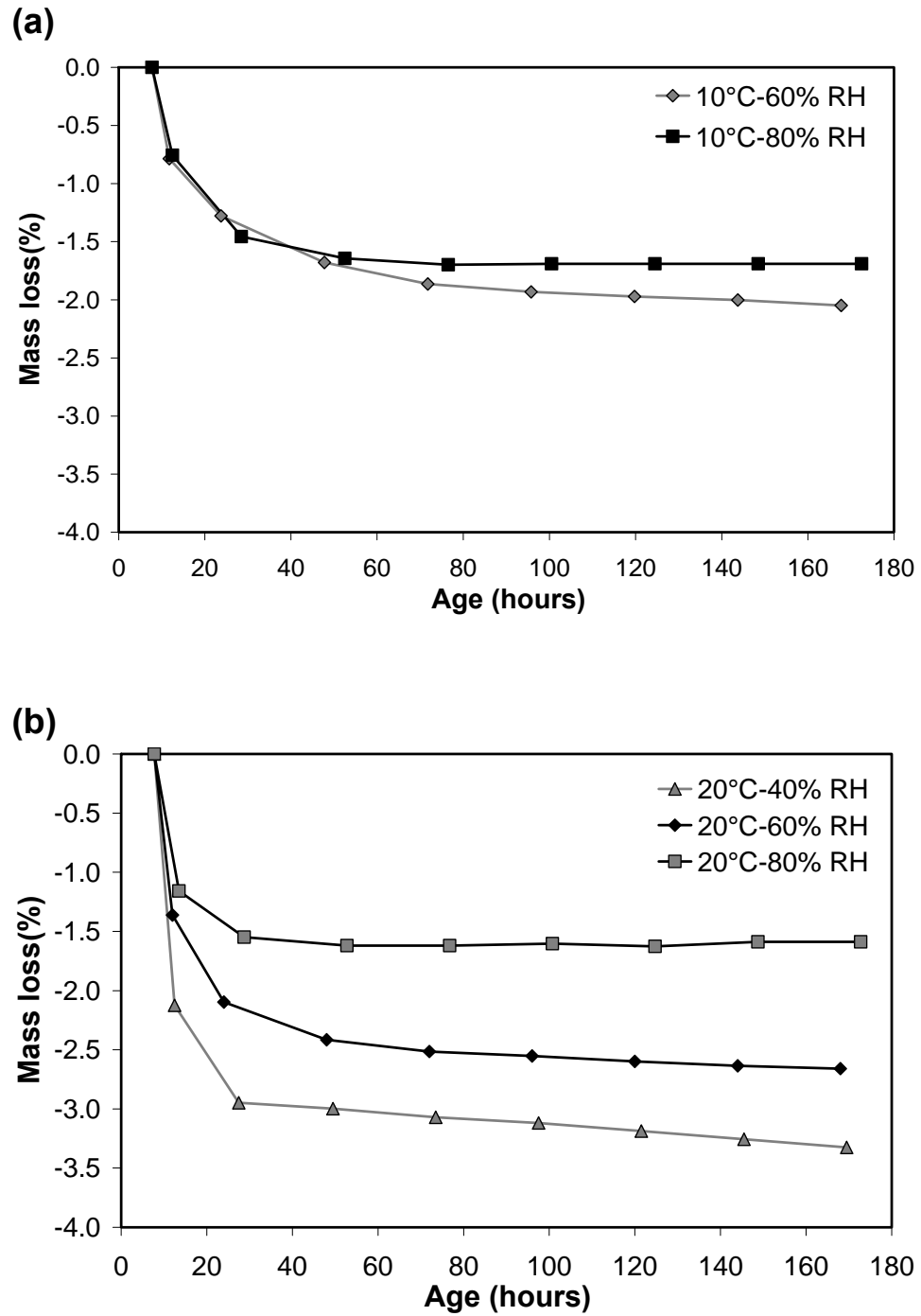
Figure 3-12: Change in mass loss Vs. ambient humidity for w/c=0.25 control mixtures at a) 10°C, b) 20°C, and c) 40°C.

(c)
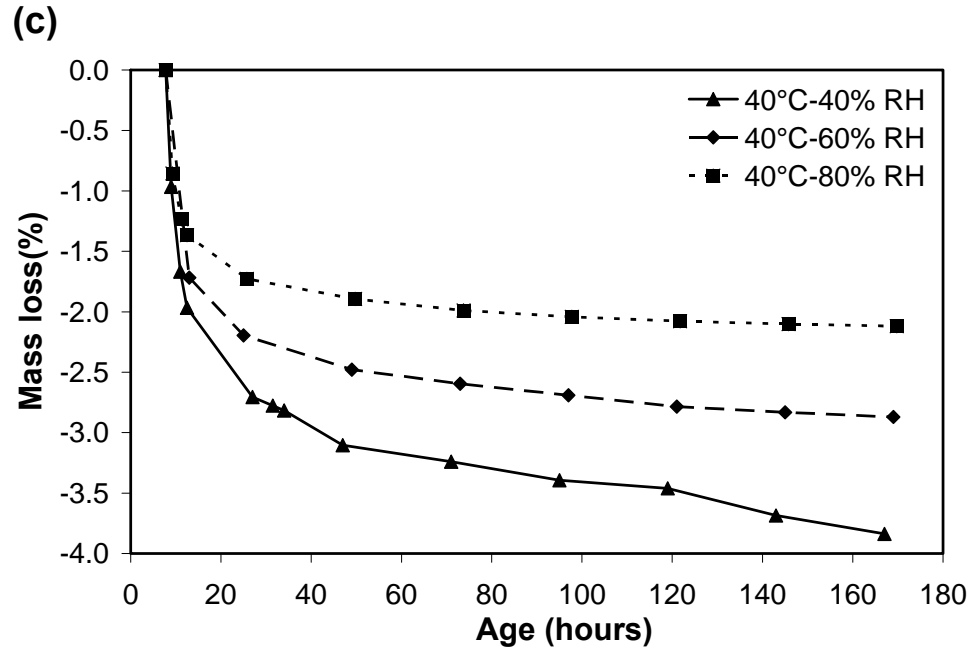
Figure 3-12 Cont'd : Change in mass loss Vs. ambient humidity for w/c=0.25 control mixtures at a) 10°C, b) 20°C, and c) 40°C.

3.5.5.   Correlation between Autogenous Strain and Achieved Degree of Hydration under Sealed Condition

Autogenous strains were plotted in **Fig. 3-13** for mixtures with w/c=0.22 and 0.25 cured at 10, 20 and 40°C as a function of the amount of BW determined by TGA tests. The amount of BW was fixed at zero at the start of autogenous strain measurements. Thus, BW will be considered as the relative chemically bound water (RBW) in the proposed relationship. The experimental results revealed a good correlation between the measured autogenous strains and the RWB, as shown in **Fig. 3-13.**
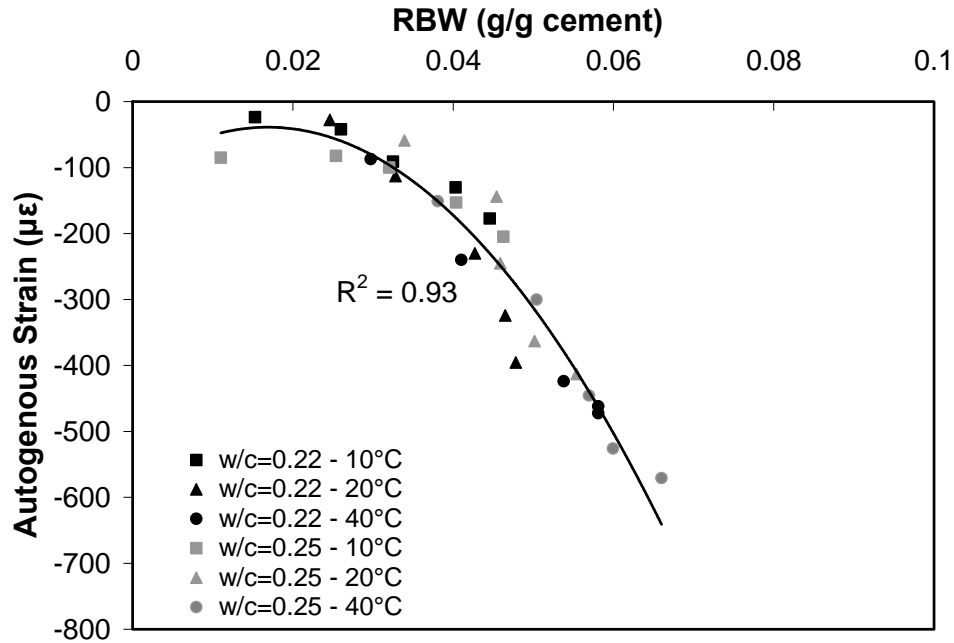
Figure 3-13: Correlation between autogenous strains and RBW for control mixtures cured at 10, 20 and 40°C.

3.5.6.   Predicting Drying and Autogenous Strains under Different Curing

Conditions

To investigate the effect of drying conditions on the contribution of both drying and autogenous strains to the total strains, the drying strains were determined based on the superposition principle and the evaluated degree of hydration.

3.5.6.1 Superposition Principle

The superposition principle is based on the assumption that autogenous and drying strains could be superimposed, and that autogenous strains in an exposed specimen are similar to that in a sealed specimen. Thus, drying strains can be determined by subtracting the autogenous strains in a sealed specimen from the total strains after applying the thermal

strains correction (Tazawa *et al.*, 2000). **Figure 3-14** illustrates the drying strains in the control specimens under different curing conditions. As the RH increased, drying strains decreased, which is consistent with previous results (Bao-guo *et al.*, 2007, Hansen, 2005, Almusallam, 2001, Holt and Leivo, 2000, Tazawa and Miyazawa, 1999, Bazant and Wittmann, 1982).

The effect of the temperature on drying strains at different RH did not exhibit a clear trend. At RH=40%, drying strains increased as the curing temperature increased, which is consistent with previous observation (Almusallam, 2001). At RH=60 and 80%, specimens cured at 10°C showed higher drying strains than that of specimens cured at 20 and 40°C. These results are in agreement with measurements performed in a previous study at 5, 20 and 30°C (Weiss and Berke,2003). It was argued that the delay in developing a strong microstructure to resist deformations at low curing temperature was the main reason for this behaviour.
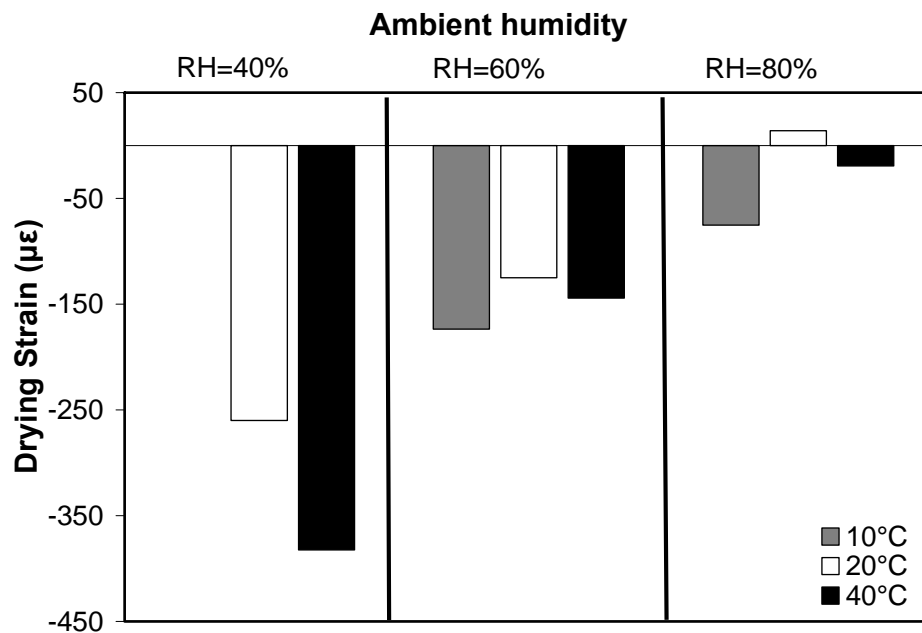
Figure 3-14: Drying strains for w/c=0.25 control mixtures based on the superposition principle at age of 7-days.

At RH=80% and 20°C, the calculated drying strains based on the superposition principle indicated swelling, which confirms that autogenous strains were higher than the total strains. Similar results were reported by others (Tazawa *et al.*, 2000, Tazawa and Miyazawa, 1999) who attributed this behaviour to the moisture movement from the high RH environment into the concrete specimens, driven by the lower intrinsic humidity developed due to the effect of self-desiccation.

3.5.6.2 Degree of Hydration Method

In the degree of hydration method, autogenous strains under different exposure conditions were evaluated based on the achieved degree of hydration (i.e. amount of RBW) of the exposed specimen and the relationship between the degree of hydration and the corresponding autogenous strain under sealed condition (Kovler and Zhutovsky, 2006). Consequently, the reductions in the autogenous strains due to the drying effect are considered. **Figure 3-15** shows the autogenous strains evaluated based on the degree of hydration at different exposure conditions. It can be observed that autogenous strains calculated based on the superposition principle under drying conditions were overestimated as compared with that calculated using the degree of hydration. The overestimation ratio (β) calculated by **Eq. 3-3** is listed in **Table 3-4**, in which autogenous strains at 7 days are used for calculations.

$$\beta = \frac{\varepsilon_s - \varepsilon_w}{\varepsilon_w}$$
Eq. 3-3

Where ε_s is the autogenous strain under sealed conditions, ε_w is the autogenous strain under drying conditions obtained based on the evaluated degree of hydration. The lower

the RH, the more pronounced was the difference between the autogenous strains obtained

by the two methods. It should be noted that the early-age exposure to drying increased the

overestimation ratio, since it interrupts the hydration process and the development of

denser microstructure, thus resulting in higher porosity.
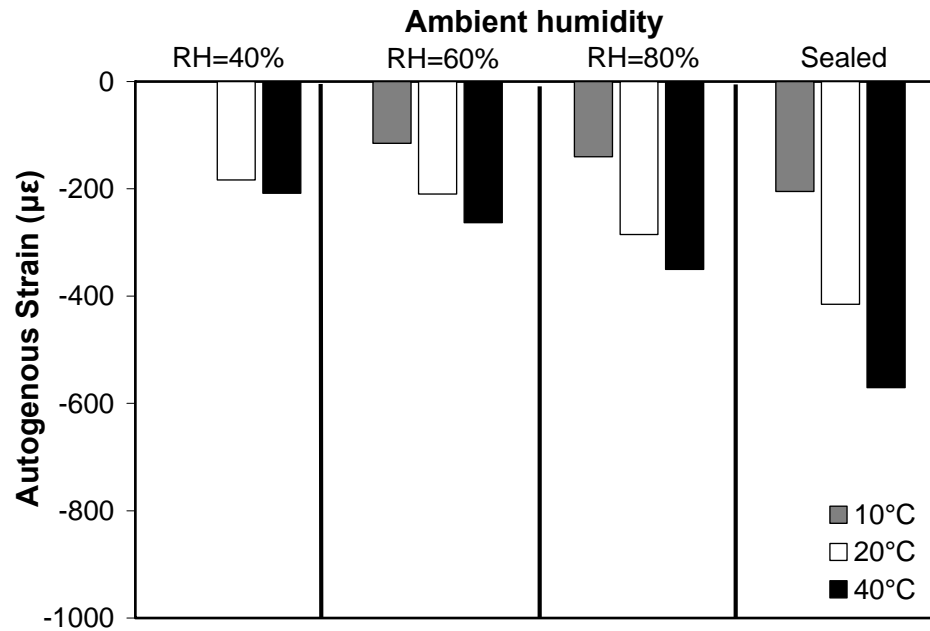
Figure 3-15: Autogenous strains evaluated based on achieved degree of hydration for w/c=0.25 UHPC mixtures at age 7 days.

Table 3-4: Overestimation ratios for autogenous strains under different curing conditions.

Mixture	Temp.°C/RH%	Overestimation ratio		
		40	60	80
w/c=0.25	10	----*	0.78	0.46
	20	1.26	0.98	0.45
	40	1.74	1.17	0.63
w/c=0.22	10	----*	0.80	0.51
	20	1.32	0.97	0.49
	40	1.89	1.22	0.65

* Condition is not feasible.

Figure 3-16 shows the drying strains determined by subtracting autogenous strains from the total measured strains, after considering the reduction in the autogenous strains due to the drying effect. Comparing **Figs. 3-14** and **3-16**, a significant increase in the contribution of drying strains to the total measured strains can be observed. For instance, at 40°C and RH=40%, the calculated drying strains based on the superposition principle represented about 40% of the total measured strains, compared to about 78% based on the evaluated degree of hydration. Moreover, no swelling was observed at high RH, which is consistent with the expected denser structure for the tested mixtures (Esping, 2007). Generally, a good agreement exists between the determined drying strains and mass loss results (**Fig. 3-12(a,b,c)** and **3-16**).
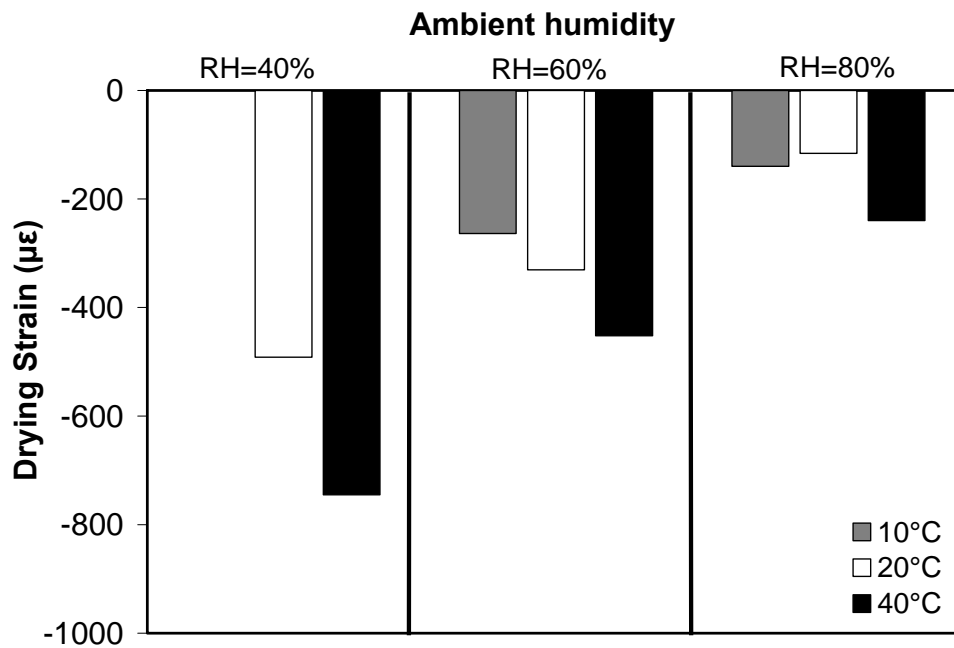
Figure 3-16: Drying strains evaluated based on achieved degree of hydration for w/c=0.25 UHPC mixtures at age 7 days.

3.6.   CONCLUSIONS

Using the amount of chemically bound water to assess autogenous and drying strains in ultra high-performance concrete specimens was explored in this chapter. The following conclusions can be drawn from the experimental results:

1) Ambient conditions, including temperature and relative humidity, can significantly affect the development of early-age compressive strength of UHPC cast in-situ, especially in cold temperature for which the achieved strength was only about 52% of the target strength.

2) Autogenous and drying strains in UHPC specimens are dependent phenomena; therefore the behaviour of autogenous strains under sealed conditions will differ from that under drying conditions.

3) Autogenous shrinkage strain and drying shrinkage strain of concrete under drying conditions can be separated from total shrinkage strain based on the evaluated degree of hydration based on BW

4) Applying the superposition principle without considering the effect of drying conditions will result in overestimating autogenous strains, especially in arid conditions.

5) For thin UHPC sections, drying dominates the total deformation and reduces the development of autogenous strains, leading to lower autogenous contribution to the total deformation.

3.7.   REFERENCES

Acker, P., (2004), "Swelling, shrinkage and creep: a mechanical approach to cement hydration," *Materials and Structures*, Vol. 37, No. 4, pp. 237-243.

Aïtcin, P.C., (1999), "Demystifying autogenous shrinkage," *Concrete International,* Vol. 21, No. 11, pp. 54-56.

Al-Saleh, S.A.and Al-Zaid, R.Z., (2006), "Effects of drying conditions, admixtures and specimen size on shrinkage strains," *Cement and Concrete Research*, Vol. 36, No. 10, pp. 1985-1991.

Almusallam, A.A., (2001), "Effect of environmental conditions on the properties of fresh and hardened concrete," *Cement and Concrete Composites*, Vol. 23, No. 4-5, pp. 353-361.

Bao-guo, M., Xiao-dong, W., Ming-yuan, W., Jia-jia, Y. and Gao, X-j., (2007), "Drying Shrinkage of Cement-Based Materials Under Conditions of Constant Temperature and Varying Humidity," *Journal of China University of Mining and Technology*, Vol. 17, No. 3, pp. 428-431.

Baroghel-Bouny, V. and Kheirbek, A., (2000), "Effect of mix-parameters on autogenous deformations of cement pastes - Microstructural interpretations," In: V. Baroghel-Bouny and P.C. Aïtcin, Editors, Proceedings of the Int. RILEM Workshop on Shrinkage of Concrete "Shrinkage 2000", Paris, France, RILEM Publication.

Baroghel-Bouny, V., Mounanga, P., Khelidj, A., Loukili, A. and Rafai, N., (2006), "Autogenous deformations of cement pastes: Part II. W/C effects, micro–macro correlations, and threshold values," *Cement and Concrete Research*, Vol. 36, No. 1, pp. 123-136.

Bazant, Z.P. and Wittmann, F.H, (1982). Creep and Shrinkage in Concrete Structures, John Wiley and Sons, Chichester.

Bentz, D.P. and Garboczi, E.J., (1991), "Percolation of phases in a three-dimensional cement paste microstructural model," *Cement and Concrete Research*, Vol. 21, No. 2-3, pp. 325-344.

Bentz, D.P., Hansen, K.K., Madsen, H.D., Vallee, F. and Griese, E.J., (2001b), "Drying/hydration in cement pastes during curing," *Materials and Structures*, Vol. 34, No. 9, pp. 557-565.

Bentz, D.P., Jensen, O.M., Hansen, K.K., Olesen, J.F., Stang, H. and Haecker, C-J., (2001a), "Influence of cement particle-size distribution on early age autogenous strains and stresses in cement-based materials," *Journal of American Ceramic Society*, Vol. 84, No. 1, pp.129-135.

Bissonnette, B., Pierre, P. and Pigeon, M., (1999), "Influence of key parameters on drying shrinkage of cementitious materials," *Cement and Concrete Research*, Vol. 29, No. 10, pp.1655-1662.

Cao, Y. and Detwiler, R.J., (1995), "Backscattered electron imaging of cement pastes cured at elevated temperatures," *Cement and Concrete Research*, Vol. 25, No. 3, pp. 627-638.

Cheyrezy, M., Maret, V. and Frouin, L., (1995), "Microstructural analysis of RPC (Reactive Powder Concrete)," *Cement and Concrete Research*, Vol. 25, No. 7, pp. 1491-1500.

Cusson, D. and Hoogeveen, T.J., (2006), "Measuring early-age coefficient of thermal expansion in high-performance concrete," In: *Proceeding of International RILEM Conference on Volume Changes of Hardening Concrete: Testing and Mitigation*, Lyngby, Denmark, RILEM Publication.

Cusson, D. and Hoogeveen, T.J., (2007), "An experimental approach for the analysis of early-age behaviour of high-performance concrete structures under restrained shrinkage," *Cement and Concrete Research*, Vol. 37, No. 2, pp. 200-209.

Diamond, S., Sahu, S. and Thaulow, N., (2004), "Reaction products of densified silica fume agglomerates in concrete," *Cement and Concrete Research*, Vol. 34, No. 9, pp.1625-1632.

Diamond, S. and Sahu, S., (2006), "Densified silica fume: particle sizes and dispersion in concrete," *Materials and Structures*, Vol. 39, No. 9, pp. 849-859.

Escalante-Garcia, J.I. and Sharp, J.H., (2000), "The effect of temperature on the early hydration of Portland cement and blended cements," *Advanced Cement Research.*, Vol. 12, No. 3, pp. 121-130.

Esping, O., (2007). "Early-age properties of self-compacting concrete - Effects of fine aggregate and limestone filler," PhD Thesis, Department of Civil and Environmental Engineering, Chalmers University of Technology.

Graybeal, B.A. and Hartmann, J.L., (2005), "Construction of an optimized UHPC vehicle bridge," *Proceedings of the Seventh International Symposium on Utilization of high-strength/ high performance concrete*, Washington D.C., USA, Vol. 2, pp.1109-1118.

Hansen, W., (2005), "Drying shrinkage mechanisms in portland cement paste," *Journal of American Ceramic Society*, Vol. 70, No. 50, pp. 323-328.

Holt, E. and Leivo, M.T., (2000), "Methods of reducing early-age shrinkage," *Proceedings of the International RILEM Workshop on Shrinkage of Concrete*

"Shrinkage 2000", V. Baroghel-Bouny and P.C. Aïtcin (ed.), Paris, France, RILEM Publication, 435-448.

Holt, E., (2001) "Early Age Autogenous Shrinkage of Concrete," PhD Thesis, University of Washington.

Holt, E. and Leivo, M., (2004), "Cracking risks associated with early age shrinkage," *Cement and Concrete Composites*, Vol. 26, No. 5, pp. 521-530.

Holt, E., (2005), "Contribution of mixture design to chemical and autogenous shrinkage of concrete at early ages," *Cement and Concrete Research*, Vol. 35, No. 3, pp. 464-472.

Hua, C., Acker, P. and Ehrlacher, A., (1995), "Analyses and models of the autogenous shrinkage of hardening cement paste: I. Modelling at macroscopic scale," *Cement and Concrete Research*, Vol. 25, No. 7, pp. 1457-1468.

Ichinomiya, T., Hishiki, Y., Ohno, T., Morita, Y. and Takada, K., (2005), "Experimental study on mechanical properties of ultra-high-strength concrete with low-autogenous-shrinkage," *American Concrete Institution, Special Publication, No. SP-228*, pp. 1341-1352.

Jensen, O.M. and Hansen, P.F., (1996), Autogenous deformation and change of the relative humidity in silica fume-modified cement paste, *ACI Materials Journal*, Vol. 93, No. 6, pp.1-5.

Jensen, O.M. and Hansen, P.F., (1999), "Influence of temperature on autogenous deformation and relative humidity change in hardening cement paste," *Cement and Concrete Research*, Vol. 29, No. 4, pp. 567-575.

Kamen, A., Denarié, E., Sadouki, H. and Brühwiler, E., (2008), "Thermo-mechanical response of UHPFRC at early age - Experimental study and numerical simulation," *Cement and Concrete Research*, Vol. 38, No. 6, pp. 822-831.

Katrin, H., Marco, V., Emmanuel, D. and Eugen, B., (2006), "Development of the mechanical properties of an Ultra-High Performance Fiber Reinforced Concrete (UHPFRC)," *Cement and Concrete Research*, Vol. 36, No.7, pp. 1362-1370.

Kjellsen, K.O. and Detwiler, R.J., (1992), "Reaction kinetics of Portland cement mortars hydrated at different temperatures," *Cement and Concrete Research*, Vol. 22, No. 1, pp. 112-120.

Korpa, A. and Trettin, R., (2004), "The use of synthetic colloidal silica dispersions for making HPC and UHPC systems, preliminary comparison results between colloidal silica dispersions and silica fumes (SF)," In: *Proceedings of the Int. Symposium on Ultra High Performance Concrete*, Kassel, Germany, pp. 155-163.

Kovler, K. and Zhutovsky, S., (2006), "Overview and future trends of shrinkage research," *Materials and Structures,* Vol. 39, No. 9, pp. 827-847.

Lam, H., (2005), "Effects of internal curing methods on restrained shrinkage and permeability," Master Thesis., University of Toronto.

Lam, L., Wong, Y.L. and Poon, C.S., (2000), "Degree of hydration and gel/space ratio of high-volume fly ash/cement systems," *Cement and Concrete Research*, Vol. 30, No. 5, pp. 747-756.

Lothenbach, B., Winnefeld, F., Alder, C., Wieland, E. and Lunk, P., (2007), "Effect of temperature on the pore solution, microstructure and hydration products of Portland cement pastes," *Cement and Concrete Research,* Vol. 37, No. 4, pp 483-491.

Loukili, A., Khelidj, A. and Richard, P., (1999), "Hydration kinetics, change of relative humidity, and autogenous shrinkage of ultra-high-strength concrete," *Cement and Concrete Research*, Vol. 29, No. 4, pp. 577-584.

Lura, P. and Jensen, O.M., (2007), "Measuring techniques for autogenous strain of cement paste," *Materials and Structures*, Vol. 40, No. 4, pp. 431-440.

Mönnig, S. and Lura, P., (2007), "Superabsorbent Polymers - An Additive to Increase the Freeze-Thaw Resistance of High Strength Concrete," In: *Advances in Construction Materials*, Part V, Springer Berlin Heidelberg, pp. 351-358.

Mounanga, P., Khelidj, A., Loukili, A. and Baroghel-Bouny, V., (2004), "Predicting $Ca(OH)_2$ content and chemical shrinkage of hydrating cement pastes using analytical approach," *Cement and .Concrete Research*, Vol. 34, No. 2, pp. 255-265.

Neville, A.M. and Brooks, J., (1991). Concrete Technology. Longman Scientific and Technical, Harlow, Essex, UK.

Pane, I. and Hansen, W., (2005), "Investigation of blended cement hydration by isothermal calorimetry and thermal analysis," *Cement and Concrete Research*, Vol. 35, No. 6, pp. 1155-1164.

Schachinger, I., Schubert, J. and Mazanec, O., (2004), "Effect of mixing and placement methods on fresh and hardened ultra high performance concrete (UHPC)," *Proceedings of the International Symposium on Ultra High Performance Concrete*, Kassel, Germany, pp. 575-586.

Slamecka, T. and Škvara, F., (2002), "The effect of water to cement ratio on the microstructure and composition of the hydration products of Portland cement pastes," *Ceramics − Silikáty*, Vol. 46, No. 4, pp. 152-158.

Tang, M.C., (2004), "High Performance Concrete – Past, Present and Future," *Proceedings of the International Symposium on Ultra High Performance Concrete*, Kassel, Germany, pp. 3-9.

Tazawa, E., (1999). Autogenous Shrinkage of Concrete. *Proceedings of the International Workshop* Organized by the Japan Concrete Institute, Hiroshima, Japan.

Tazawa, E. and Miyazawa, S., (1999), "Effect of constituents and curing condition on autogenous shrinkage of concrete," In: *Autogenous Shrinkage of Concrete: Proceedings of the International Workshop*, Eiichi Tazawa, (ed), Taylor & Francis, pp. 269-280.

Tazawa, E., Sato, R., Sakai, E. and Miyazawa, S., (2000). Work of JCI committee on autogenous shrinkage. In: *Proceedings of the International RILEM Workshop on Shrinkage of Concrete "Shrinkage 2000"*, V. Baroghel-Bouny and P.C. Aïtcin (ed.), Paris, France, RILEM Publ., pp. 21-40.

Weiss, J. and Berke, N. (2003), "Admixtures for reduction of shrinkage and cracking," In: *Early Age Cracking in Cementitious Systems: Report of RILEM Technical Committee 181-EAS*, Bentur A; (ed.), pp. 323–335.

Yang, Y., Sato, R. and Kawai, K., (2005), "Autogenous shrinkage of high-strength concrete containing silica fume under drying at early ages," *Cement and Concrete Research*, Vol. 35, No. 3, pp. 449-456.

Yajun, J. and Cahyadi, J.H., (2003), "Effects of densified silica fume on microstructure and compressive strength of blended cement pastes," *Cement and Concrete Research*, Vol. 33, No. 10, pp. 1543-1548.

Yuasa, N., Kasai, Y. and Matsui, I., (1999), "Inhomogeneous distribution of the moisture content and porosity in concrete," Proceedings of the International Conference, R.K. Dhir and M.J. McCarthy (Ed.), The University of Dundee, Scotland, United Kingdom, Thomas Telford Publication, pp. 93-101.

Youhua, Y., (2000), "Manufacturing Reactive Powder Concrete using common new Zealand materials," Master thesis, University of Auckland.

Zhang, M.H., Tam, C.T. and Leow, M.P., (2003), "Effect of water-to-cementitious materials ratio and silica fume on the autogenous shrinkage of concrete," *Cement and Concrete Research*, Vol. 33, No. 10, pp.1687-1694.

CHAPTER FOUR

**INFLUENCE OF SHRINKAGE MITIGATION
TECHNIQUES ON EARLY-AGE SHRINKAGE
INTERRELATION UNDER DRYING CONDITIONS***

In the preceding chapter (3), the combined effect of drying and autogenous shrinkage, and their interaction mechanisms was investigated. It was proven that autogenous and drying shrinkage are dependent phenomena. Reduction in the water content under drying conditions, due to evaporation, had an adverse effect on hydration process and development of autogenous shrinkage. However, the role of commonly used shrinkage mitigation methods, including shrinkage-reducing admixture (SRA) and a superabsorbent polymer (SAP), on these previous findings in Chapter 3 is not clear. Hence, this Chapter provides fundamental investigation for the effect of ambient conditions on these shrinkage mitigation methods mechanisms, suitable conditions for each mitigation method and how to optimize its benefit in reducing shrinkage strains.

4.1.   INTRODUCTION

General literature pertinent to UHPC self-desiccation, autogenous and drying shrinkage behaviour during early-ages has been given in Chapter 3 (Section 3.1). It had pointed out that early-age shrinkage and high cracking potential can defeat the purpose of using UHPC. Hence, several shrinkage mitigation strategies have been proposed to reduce shrinkage development and avoid crack formation. Among these, the most commonly used is the addition of shrinkage-reducing admixtures (SRAs). SRAs directly influence

---

shrinkage by decreasing the surface tension of the pore solution, leading to lower capillary stresses and consequently reduced shrinkage. Moreover, a new method using superabsorbent polymers (SAPs) particles as a concrete admixture has been proposed. SAPs are a group of polymeric materials that have the ability to absorb a significant amount of liquid from the surrounding environment and to retain it within their structure without dissolving. The SAP shrinkage mitigation technique is similar to using saturated lightweight aggregate (LWA) particles but in a better controlled manner. However, the efficacy of these mitigation techniques under field-like conditions is not guaranteed, since it was evaluated under controlled laboratory conditions. In concrete exposed to field conditions during early-ages, multi-mechanisms affect shrinkage behaviour simultaneously (Yuasa *et al.*, 1999). Hence, in this study a more realistic behaviour and efficiency of SRA and SAP under simulated field-like conditions was investigated.

4.2.   RESEARCH SIGNIFICANCE

Several studies have evaluated efficiency of various shrinkage mitigations techniques in reducing shrinkage strains in UHPC under controlled curing condition without accounting for the effect of the surrounding environment. A more realistic behaviour and efficiency for SRA and SAP was evaluated based on degree of hydration approach (described in previous chapter). Efficiency of SRA and SAP was found to be highly influenced by exposure conditions. Field conditions should given a greater attention while choosing the shrinkage mitigation method.

4.3.   METHODOLOGY

Basically, the same methodology discussed in Chapter 3 was followed (see section 3.3).

4.4. EXPERIMENTAL PROGRAM

4.4.1. Materials and Mixture Proportions

The materials used in this chapter were similar to that used in Chapter 3 (refer to Section 3.4.1). Four UHPC mixture incorporating 2% SRA or 0.6% SAP with w/c= 0.22 and 0.25 were tested in order to investigate the effect of both shrinkage mitigation techniques. The chemical and physical properties of the used binders have been given in Chapter 3 (refer to Table 3-1). A commercially available SRA composed mainly of poly-oxyalkylene alkyl ether was used in this study. A 2% SRA by mass of cement was added as partial replacement for mixing water, in agreement with previous works (Bentz et al., 2001a, Bentz, 2006, Loser and Leemann, 2009). SAP is a covalently cross-linked polyacrylic acid, suspension polymerized, white spherical particles with a particle size in the range of 100 to 140 μm. SAP was added at a rate of 0.6% by weight of cement as this value had shown a great influence in diminishing shrinkage and reducing the cracking potential in previous research (Jensen and Hansen, 2002, Lam, 2005, Lura and Jensen, 2007). Mixtures with SAP contain an additional entrained water to offset self-desiccation. The w/c of mixture incorporating SAP was increased to account for the amount of water that will be absorbed by SAP particles to offset self-desiccation (Jensen and Hansen, 2001).

4.4.2. Environmental Conditions

The environmental conditions applied in this chapter were similar to that used in Chapter 3 (refer to Section 3.4.2).

4.4.3. Preparation of Test Specimens and Testing Procedures

Testing samples were prepared and tested following the same procedure discussed in Chapter 3 (refer to Section 3.4.3).

4.5. RESULTS AND DISCUSSION

4.5.1. Compressive Strength

Addition of SRA reduced the rate of cement hydration and strength development in concrete. This led to a delay in setting and a reduction in the early-age compressive strength compared to that of control specimens with similar w/c as shown in **Fig. 4-1**. Moreover, reducing the ambient humidity had a minor effect on the achieved strength for SRA mixtures compared to that for control mixtures. This can be ascribed to the sharp drying front induced by SRA at low ambient humidity, which led to lower water loss (Bentz *et al.*, 2001a, Bentz, 2006).

Mixtures incorporating SAP exhibited lower compressive strength compared to that of other mixtures, as shown in **Fig. 4-1**. However, SAP incorporated higher water content, which enhanced the hydration process; it resulted in higher total porosity. At low ambient humidity, water evaporates faster leading to more porosity and lower development of hydration.
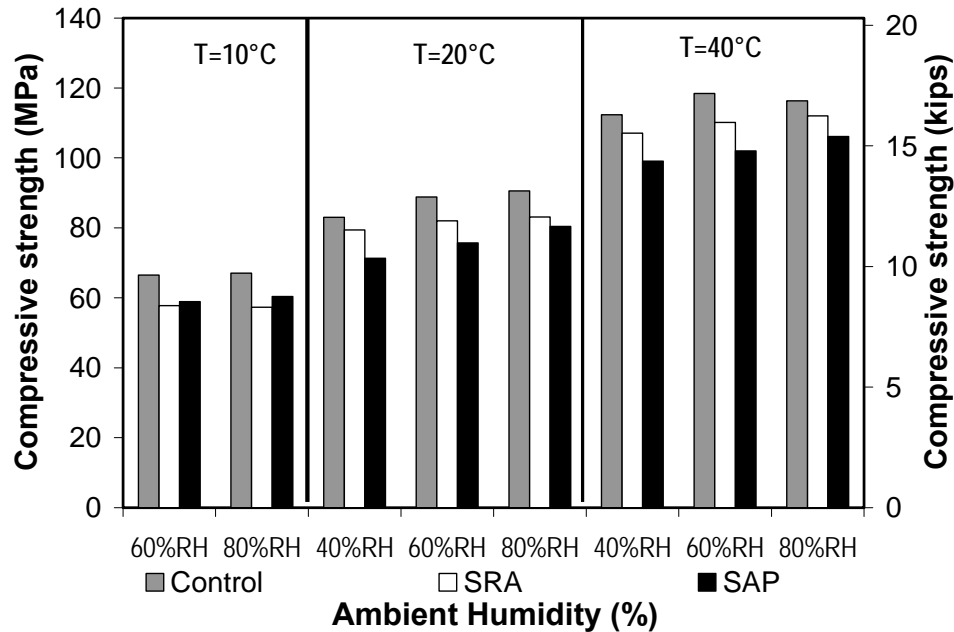
Figure 4-1: Effect of adding 2% SRA and 0.6%SAP on compressive strength after 7 days for mixtures with w/c=0.25.

As expected, SRA reduced the 28 days compressive strength. The reduction in the strength ranged between -5.8% to -11.0%. This is in agreement with ranges reported in previous study on low w/c concrete (Weiss and Berke, 2003). The reduction in the achieved strength can be attributed to the retardation effect induced by SRA addition. On the other hand, mixtures incorporating SAP exhibited higher compressive strength reduction (ranged between -12 to -22%) compared to SRA mixtures. Addition of SAP induced higher and continuous porosity that facilitates water exchange with the surrounding environments. As a result, higher porosity is required to be filled by hydration product to gain strength compared to that of control mixtures. This is consistent with previous findings which indicate that porosity has a dominate effect on the achieved strength (Odler and Rößler, 1985, Mikhail *et al.*, 1977).

4.5.2 Total Strain

Generally, SRA mixtures exhibited lower total strain compared to that of control mixtures (**Fig. 3-5(a)** & **Fig. 4-2(a)**). The reduction in total strain increased at higher curing temperature and/or lower RH. For instance, the reduction in the total strain was about 325 µε and 267 µε at (40°C and RH=40%) and (20°C and RH=40%) than that of control mixtures, respectively. Conversely, SAP mixtures showed higher total strain compared to that of control mixtures (**Fig. 3-5(a)** & **Fig. 4-2(b)**). Moreover, a higher total strain was exhibited with higher curing temperature and/or lower RH. For instance, the increase in the total strain was about 109 µε and 71 µε at (40°Cand RH=40%) and (20°C and RH=40%) than that of control mixtures, respectively.
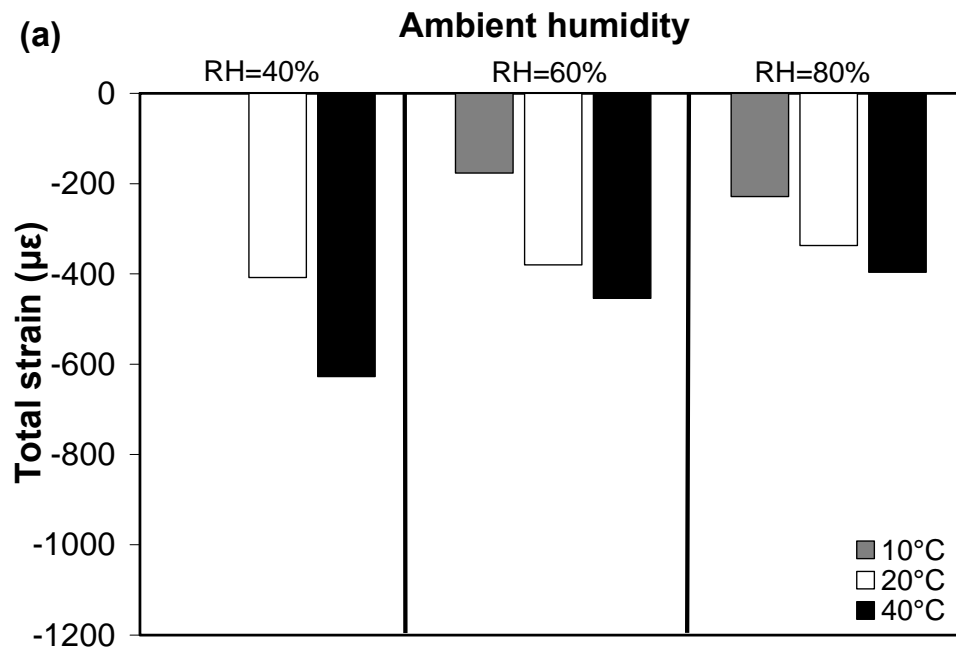
Figure 4-2: Total strains Vs. ambient humidity at different curing temperatures for w/c=0.25 mixtures at age of 7-days: a) SRA and b) SAP.

(b)
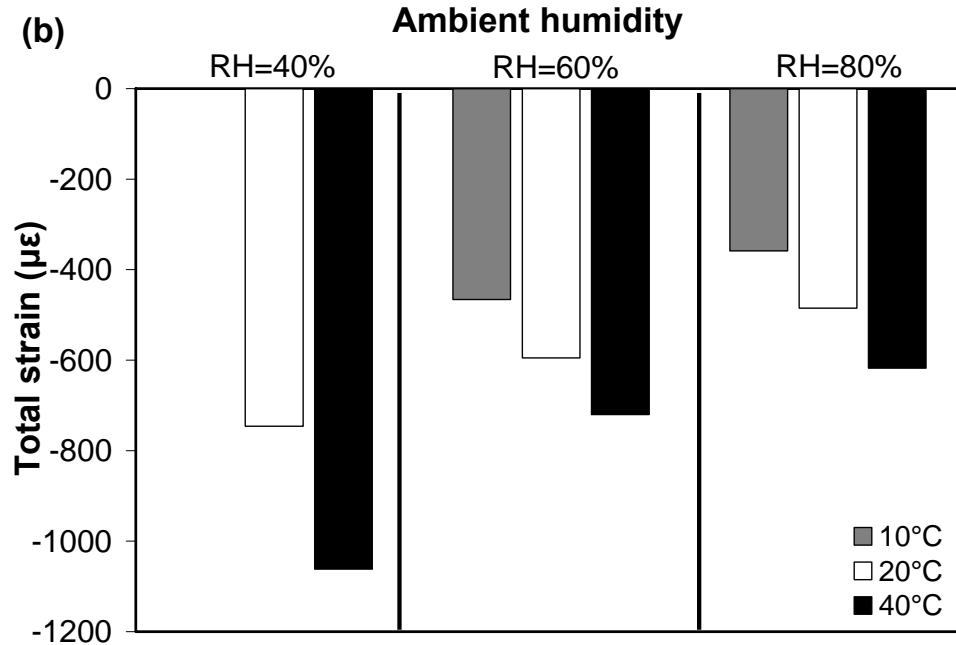
Ambient humidity

Figure 4-2 Contd': Total strains Vs. ambient humidity at different curing temperatures for w/c=0.25 mixtures at age of 7-days: a) SRA and b) SAP.

4.5.3. Autogenous Strain

4.5.3.1 *Effect of Curing Temperatures*

The effect of adding 2% SRA and 0.6% SAP on autogenous strains at 10, 20, and 40°C for UHPC mixtures made with w/c=0.25 is shown in **Fig. 4-3**. It can be observed that SRA and SAP reduced autogenous strains effectively, though SRA achieved more significant reduction. Moreover, the effect of SRA was more significant at higher temperature (40°C) where the reduction in autogenous strains was about 55% compared with 34% and 32% at 10 and 20°C, respectively. This is believed to be due to the increase of SRA concentration in the pore solution as a result of the accelerated hydration reactions at high temperature. Indeed, hydration reactions consume mixing water, while

SRA remains or would be consumed at a slower rate compared to that of water (Rajabipour *et al*., 2008), thus leading to higher SRA concentration.
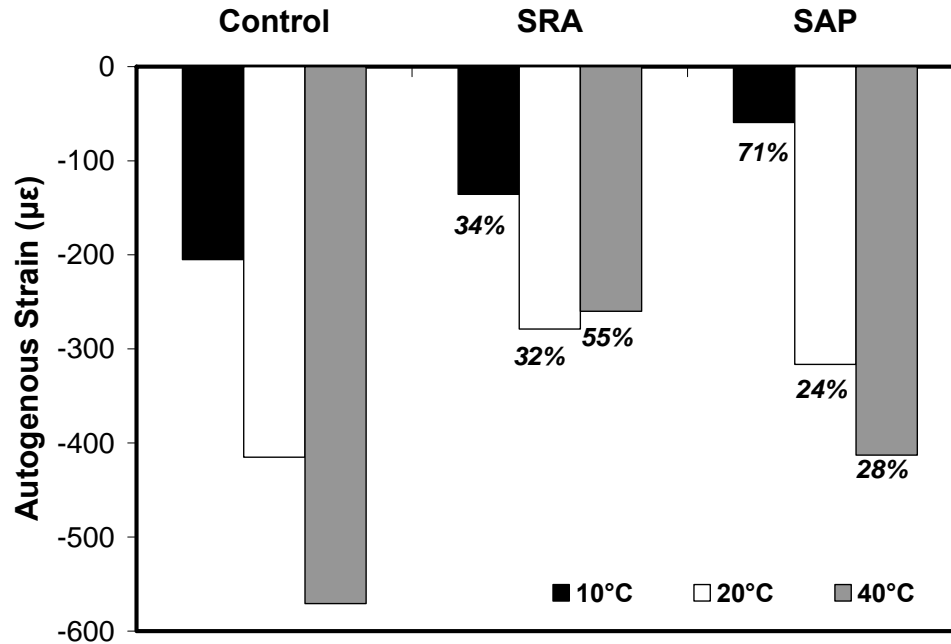
Figure 4-3: Autogenous strains after 7 days for mixtures with w/c=0.25.

Conversely, SAP appeared to be more effective at 10°C. It reduced autogenous strains by about 71% compared to that of the control mixture. The reason for this behaviour lays in the early expansion as shown in **Fig. 4-4(a)**. To capture this effect, the autogenous shrinkage curves were initiated to zero at the end of expansion as shown in **Fig. 4-4(b)**. The reduction in autogenous contraction after the early expansion was about 31 and 38% for SRA and SAP mixtures, respectively. Different phenomena are believed to induce this early expansion including ettringite formation, expansion due to the absorption of the internal curing water from SAP by the cement gel (Jensen and Hansen, 2002), and the relatively low stiffness of the specimens at early-age which permits such an expansion (Baroghel-Bouny *et al*., 2006, Cusson and Hoogeveen, 2007). In addition,

another mechanism can be hypothesized as follows: SAP particles release part of its entrained water as hydration progresses (Wang *et al*., 2009), the vapour pressure in the capillary pores increases and menisci curvature changes to have a large radius (Kovler, 1996). This will release the capillary surface tension, leading to capillary distension and consequently expansion.

Indeed, autogenous shrinkage and expansion occur simultaneously during early-ages. Early expansion along with autogenous shrinkage reduction due to SRA and/or SAP can result in lower net autogenous strains. This is in agreement with previous findings (Baroghel-Bouny *et al*., 2006, Cusson and Hoogeveen, 2007, Kamen *et al*., 2008, Weiss *et al*., 2008).
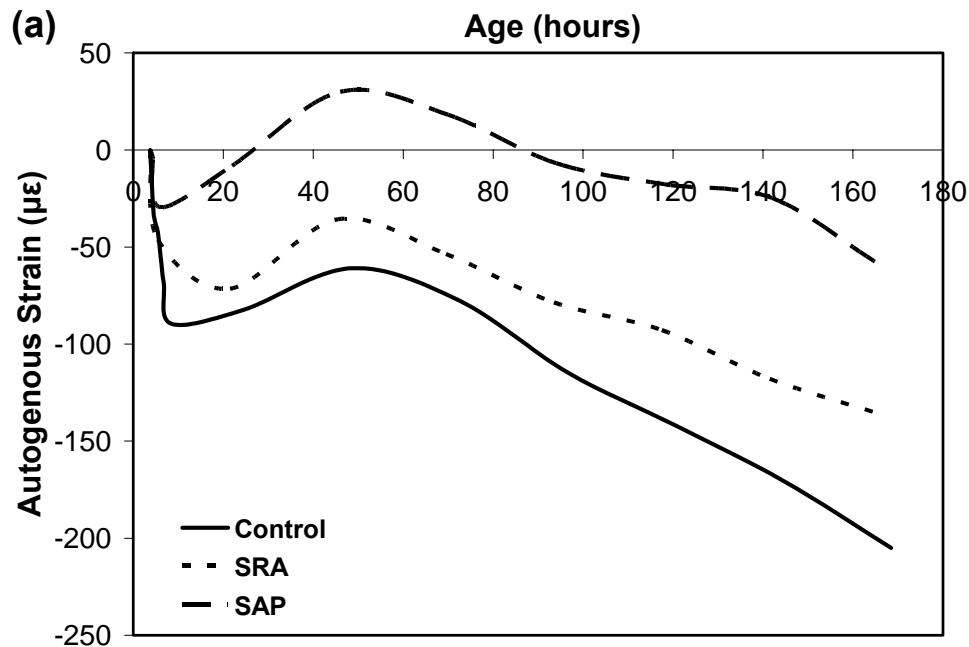
Figure 4-4: Autogenous strains at 10°C: a) observed, and b) after expansion for mixtures with w/c=0.25.

(b)
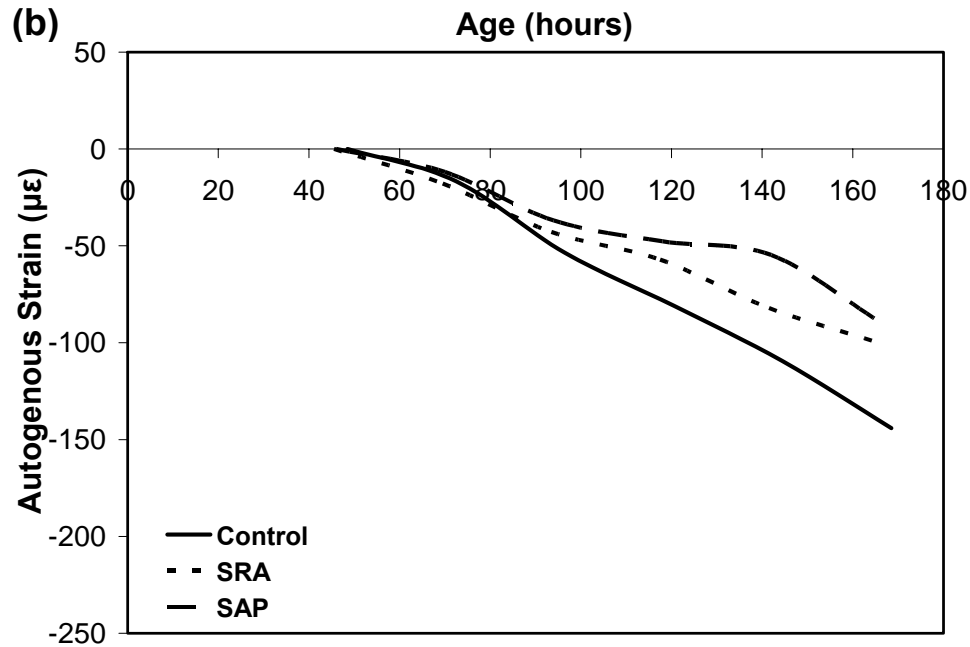
**Figure 4-4 Contd': Autogenous strains at 10°C: a) observed, and b) after expansion
for mixtures with w/c=0.25.**

4.5.3.2 *Effect of w/c under Different Curing Temperatures*

It was reported that SRA is more effective in reducing shrinkage at lower w/c
(D'Ambrosia, 2002). Conversely, SRA mixtures with w/c=0.22 showed higher
autogenous strain than that with w/c=0.25. In SRA mixtures, the role of SF
agglomeration and consequent creation of additional pore space can be explained as
follows: during early periods, the created pore space allows more hydration product
formation (e.g. ettringite formation (Bentz *et al*., 2001b, Bentz and Peltz, 2008)) without
causing high early expansion (see **Fig. 4-5**). Hence, SRA mixtures with w/c=0.22 showed
lower expansion compared to that of SRA mixtures with w/c=0.25, and thus higher
autogenous strain. At later ages, the effect of SRA on the surface tension of the pore
solution started to be the major mechanism controlling autogenous strain development.

Hence, similar autogenous shrinkage strain rate was exhibited by both w/c=0.22 and 0.25 mixtures as shown in **Fig. 4-6(a)**. Therefore, SF agglomeration can adversely affect SRA mixtures during early-age. SAP mixtures exhibited similar trend to that of the control mixtures as shown in **Fig. 4-6(b)**. However, it is difficult at that point to evaluate the effect of SF agglomeration on autogenous strain with respect to that of SAP. Further research is needed to capture the effect of SAP mixtures without SF at similar level of w/c.
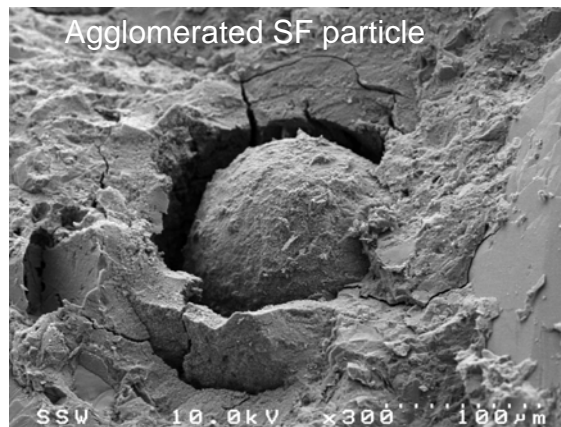
Figure 4-5: Scanning electron micrograph for agglomerated silica fume in SRA mixture with w/c=0.22.

(a)

(b)
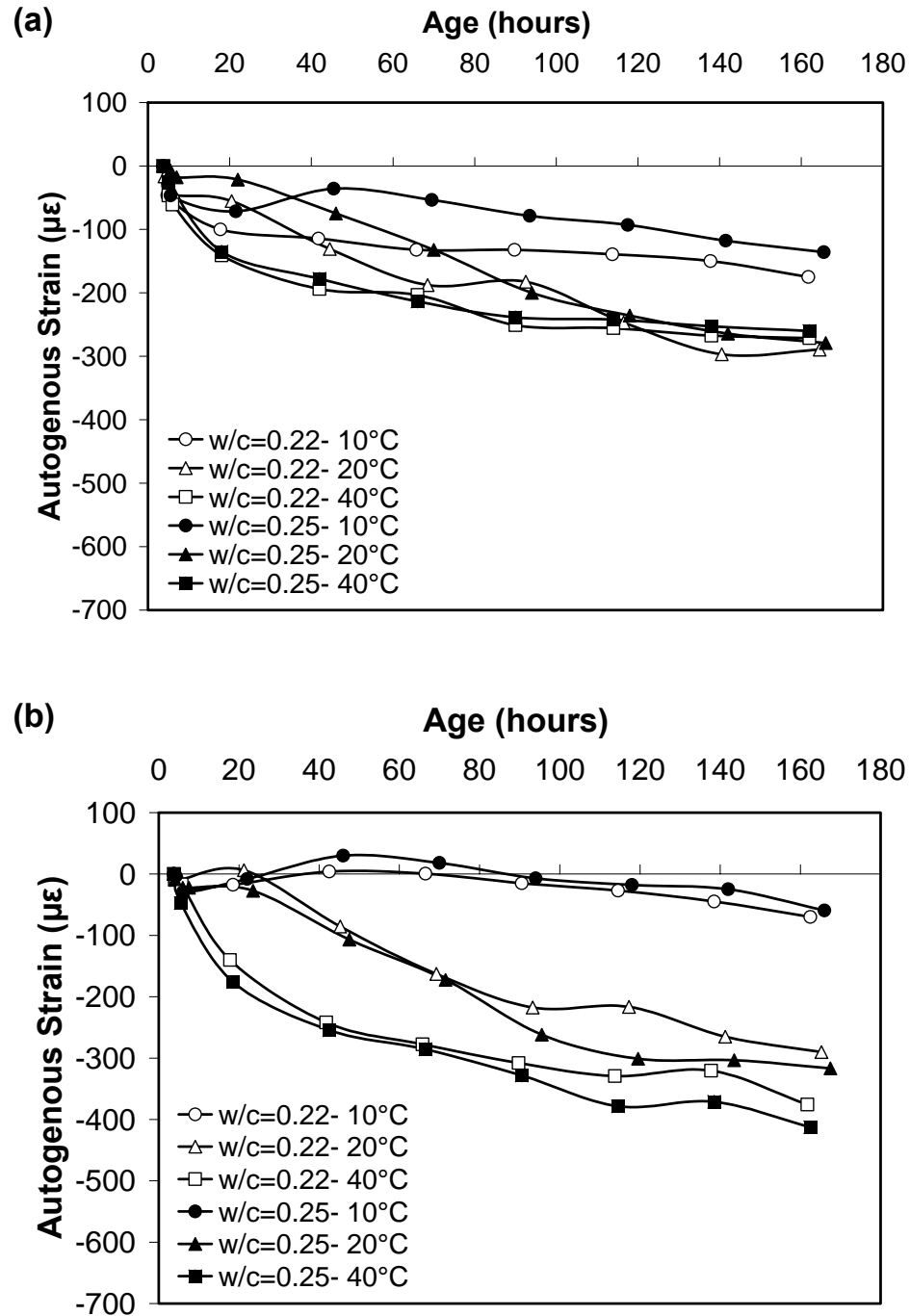
Figure 4-6: Autogenous strains for mixtures with w/c=0.22 and 0.25 at different temperatures a) SRA and b) SAP mixtures.

4.5.4.   Degree of Hydration

4.5.4.1   *Under Sealed Condition*

SRA retarded the hydration reactions at 10 and 40°C, as shown in **Fig. 4-7(a).** A slight

retardation in hydration reactions was observed at 20°C, indicating that the addition of

SRA did not affect the degree of hydration of specimens cured under a sealed condition.

This is consistent with previous results (Bentz *et al.*, 2001a, Bentz, 2006)

SAP mixtures had a relatively higher water content (about 18% of w/c), thus

achieving a higher degree of hydration (Jensen and Hansen, 2002, Jensen and Hansen,

2001), as shown in **Fig. 4-7(b)**. The increase in hydration rate was more pronounced at

40°C, which can be attributed to the thermo-activated characteristics of the hydration

process (Mounanga *et al.*, 2004).
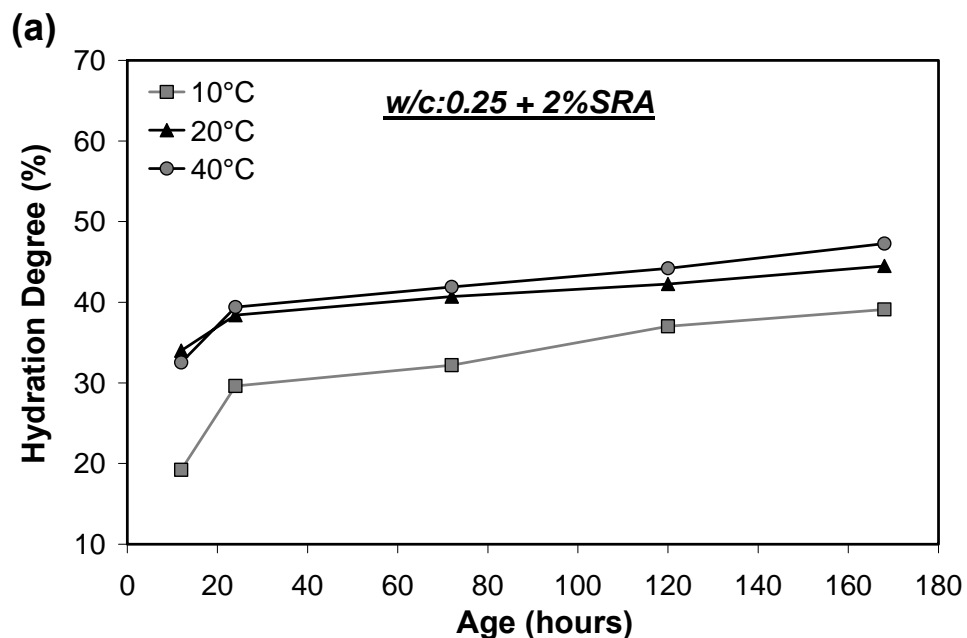
Figure 4-7: Evaluation of degree of hydration Vs. age for a) w/c=0.25 + 2% SRA,
and b) w/c=0.25 + 0.6% SAP UHPC mixtures cured at 10, 20 and 40°C.

(b)
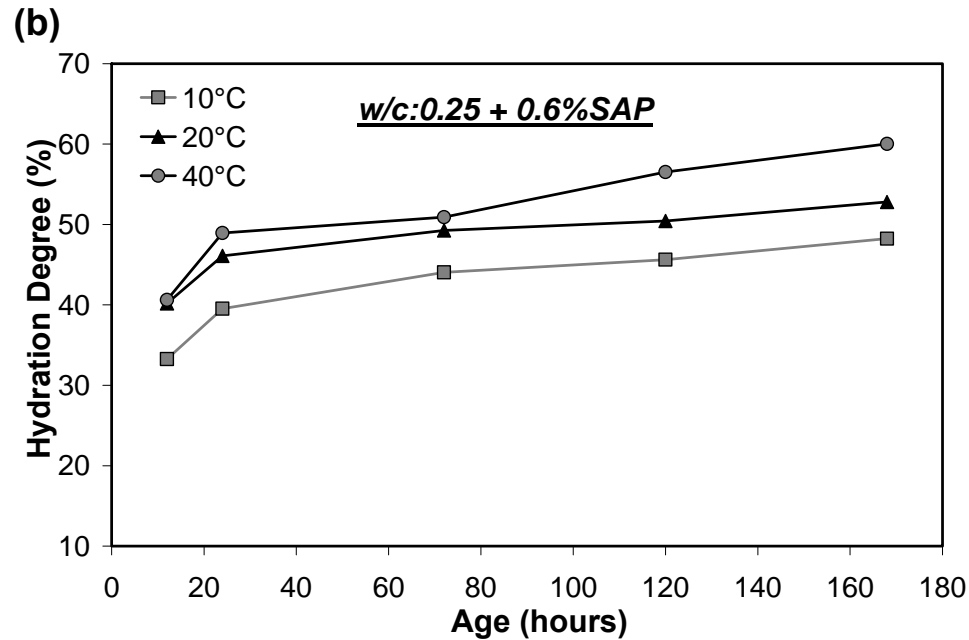
Figure 4-7 Contd': Evaluation of degree of hydration Vs. age for a) w/c=0.25 + 2% SRA, and b) w/c=0.25 + 0.6% SAP UHPC mixtures cured at 10, 20 and 40°C.

4.5.4.2   *Under Drying Condition*

4.5.4.2.1 *SRA mixtures*

Figure 4-8 (a,b,c) shows the effect of curing conditions on the BW for mixtures incorporating 2% SRA. At 20°C, specimens cured at RH=40% showed higher BW compared to that of specimens cured at RH=60% during the initial drying period (up to 3 days). After the initial drying period, the situation was reversed and specimens cured at RH=40% showed lower BW. This was likely due to the sharp drying front induced by SRA (Bentz *et al*., 2001a, Bentz, 2006), as shown in **Fig. 4-9**. During early-age, the initial drying of specimens concentrate SRA in the remaining pore solution at the top exposed surface of the specimens, which in turns restrict pulling more water from deeper parts within the specimens (Bentz, 2006). Consequently, higher degree of hydration is

expected at specimen core compared to its surface. The effect of the sharp drying front seemed to become more important as RH decreased. At later ages, some absorption of SRA by cement hydration products could reduce the efficiency of the drying front in eliminating water extraction from the specimen core; leading to a higher rate of evaporation and a lower BW (Bentz, 2006).

At 10 and 40°C, normal trends were observed. As the RH decreased, the rate of evaporation increased; hence a lower BW was measured. However, at 40°C a lower variation in the amount of BW with respect to RH change was observed, as shown in **Fig. 4-8(c)**. This is believed to be due to the lower evaporation rate and the faster development of the drying front due to the increase in SRA concentration at high temperature, as mentioned earlier.
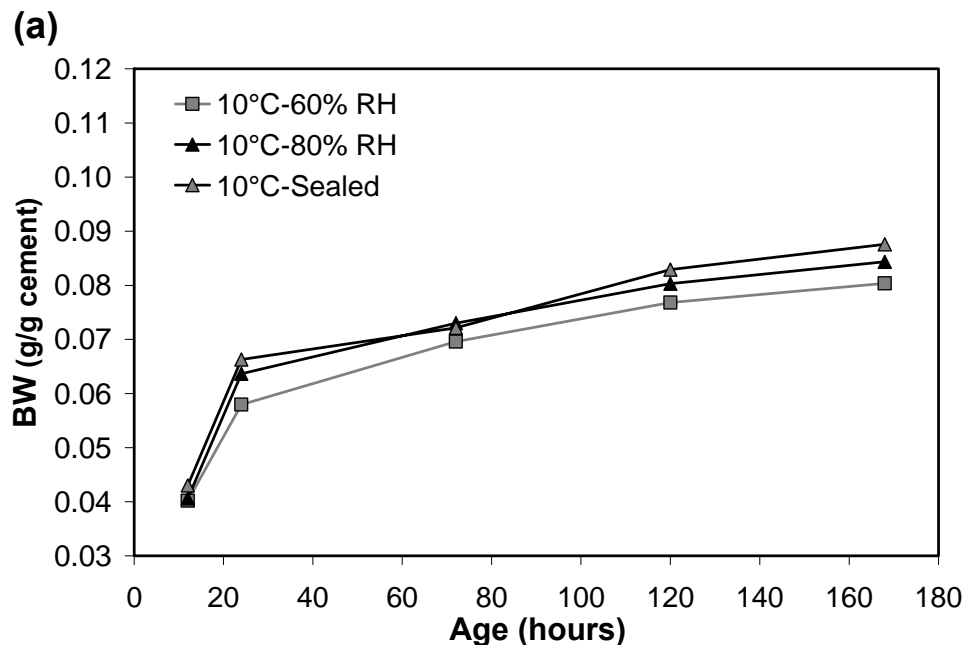
Figure 4-8: Change in BW Vs. ambient humidity for w/c=0.25 + 2% SRA mixture at a) 10°C, b) 20°C, and c) 40°C.

(b)

(c)
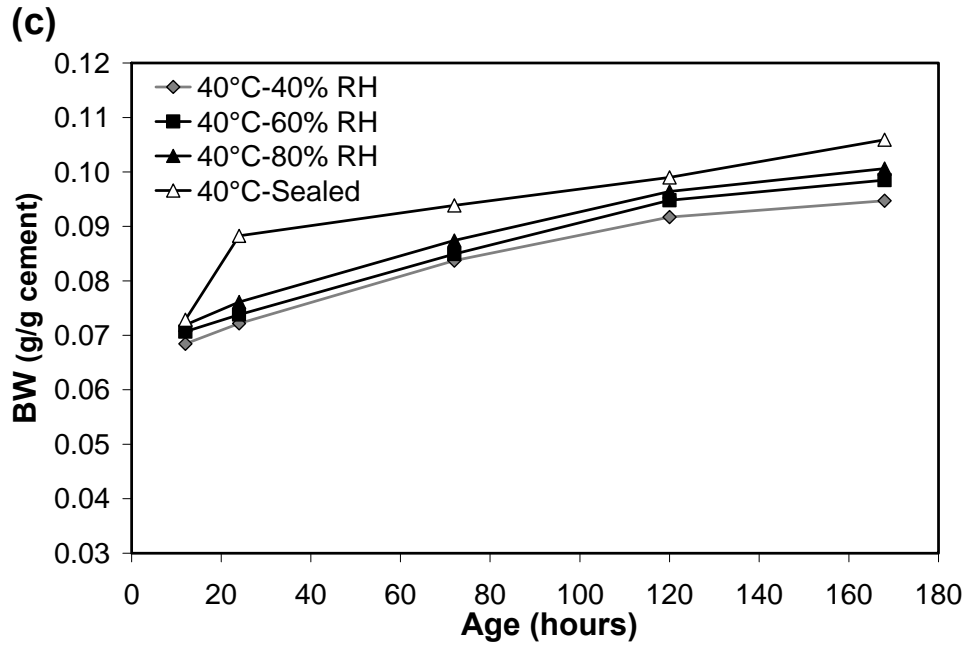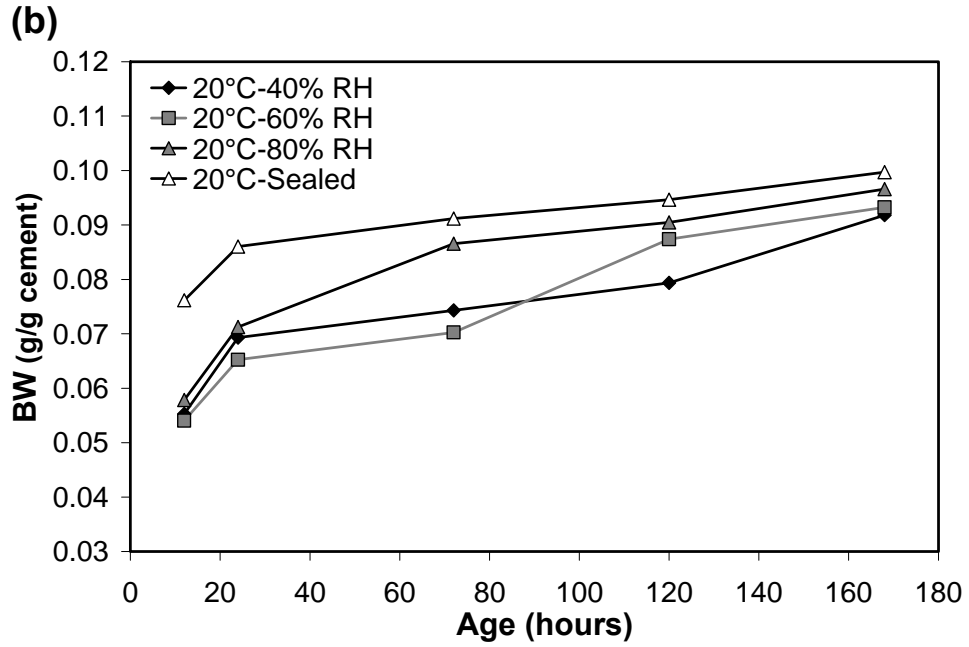
Figure 4-8 Cont'd: Change in BW Vs. ambient humidity for w/c=0.25 +2% SRA

mixture at a) 10°C, b) 20°C, and c) 40°C.

Figure 4-9: Cross section for SRA specimen exposed to drying condition after 7 days.

Figure 4-10 (a,b,c) shows the effect of RH on the mass loss for w/c=0.25 mixture incorporating 2% SRA and cured at 10, 20 and 40°C. Generally, a slight reduction in mass loss compared to that of control mixtures was observed at the different curing temperatures, which is in agreement with (Weiss and Berke, 2003). However, the mass loss of SRA mixtures increased with decreasing RH, similar to that of mixtures without SRA, as previously observed by (Weiss *et al*., 2008).

At 20°C, the specimens cured at RH=40 and 60% showed similar mass loss during the initial period of drying. Subsequently, their results started to deviate until the end of the investigated period, as shown in **Fig. 4-10(b)**. These results agree with earlier discussion of BW results (**Fig. 4- 8(b)**). Furthermore, comparing **Fig. 4- 10(b)** and **4-10(c)**, it can be observed that changing the curing temperature did not cause a significant difference in mass loss. This can also be ascribed to the effect of increasing the curing temperature on the actual SRA concentration.

(a)

(b)
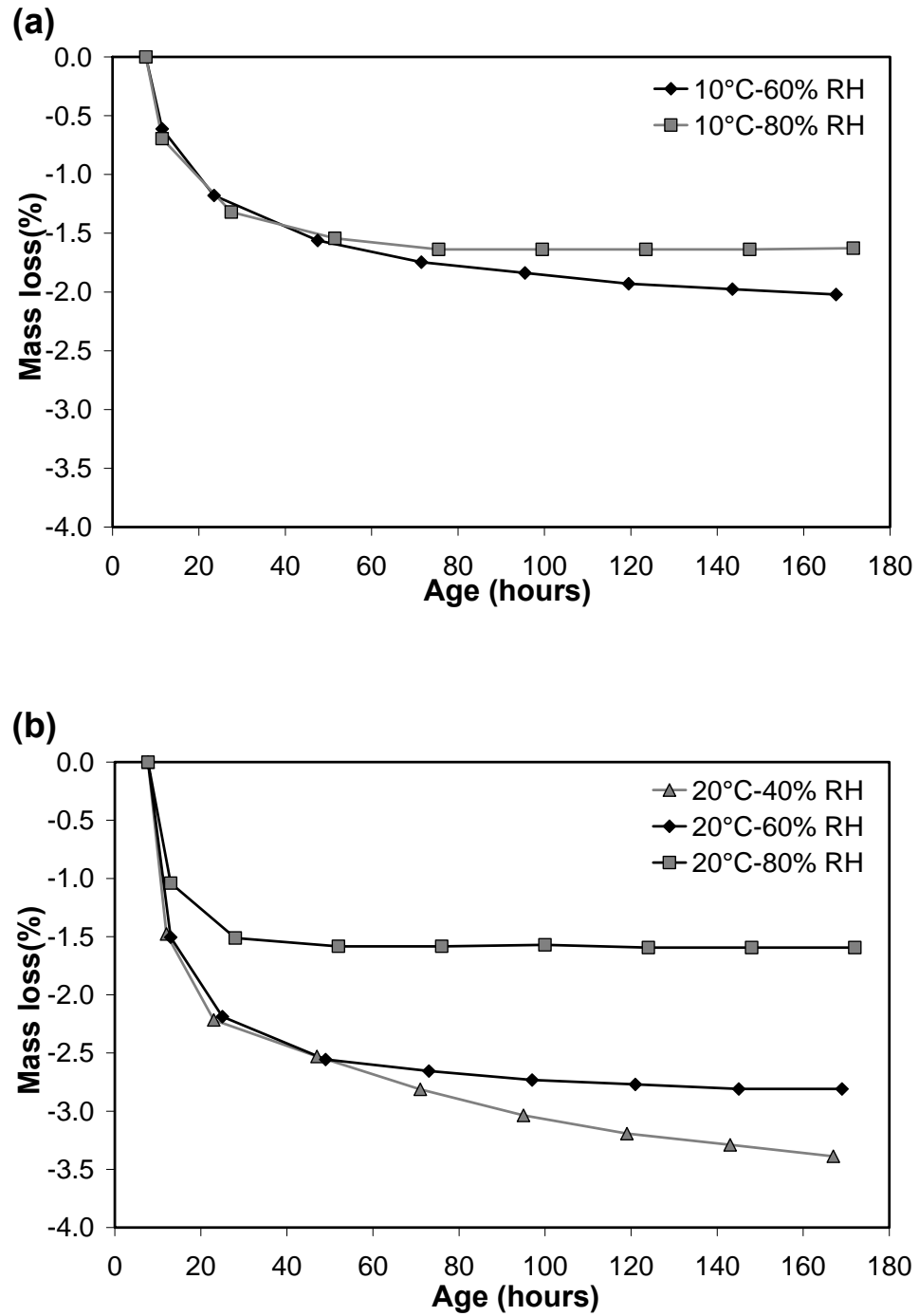
Figure 4-10: Change in mass loss Vs. ambient humidity for w/c=0.25 +2% SRA mixture at a) 10°C, b) 20°C, and c) 40°C.

(c)
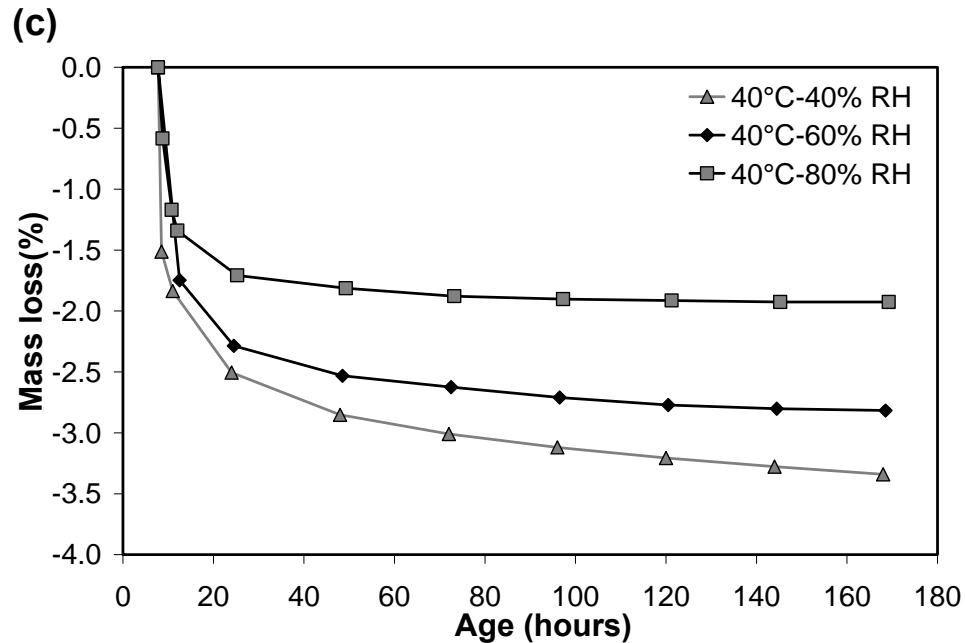
Figure 4-10 Cont'd: Change in mass loss Vs. ambient humidity for w/c=0.25 +2% SRA mixture at a) 10°C, b) 20°C, and c) 40°C.

4.5.4.2.2 SAP Mixtures

Figure 4-11(a,b,c) shows the effect of RH levels on the BW for w/c=0.25 mixtures incorporating 0.6% SAP and cured at 10, 20 and 40°C. Generally, mixtures incorporating SAP showed a higher degree of hydration, as shown by BW results, compared to those of mixture without SAP. However, SAP mixtures were highly affected by the RH level. This was exhibited by higher mass loss when the RH decreased, as shown in **Fig. 4-12(a,b,c).** The higher water content due to the additional entrained water held in SAP particles was likely the main reason for this behaviour. These results are in agreement with previous findings (Kovler, 1996, Mönnig and Lura, 2007).

(a)

(b)
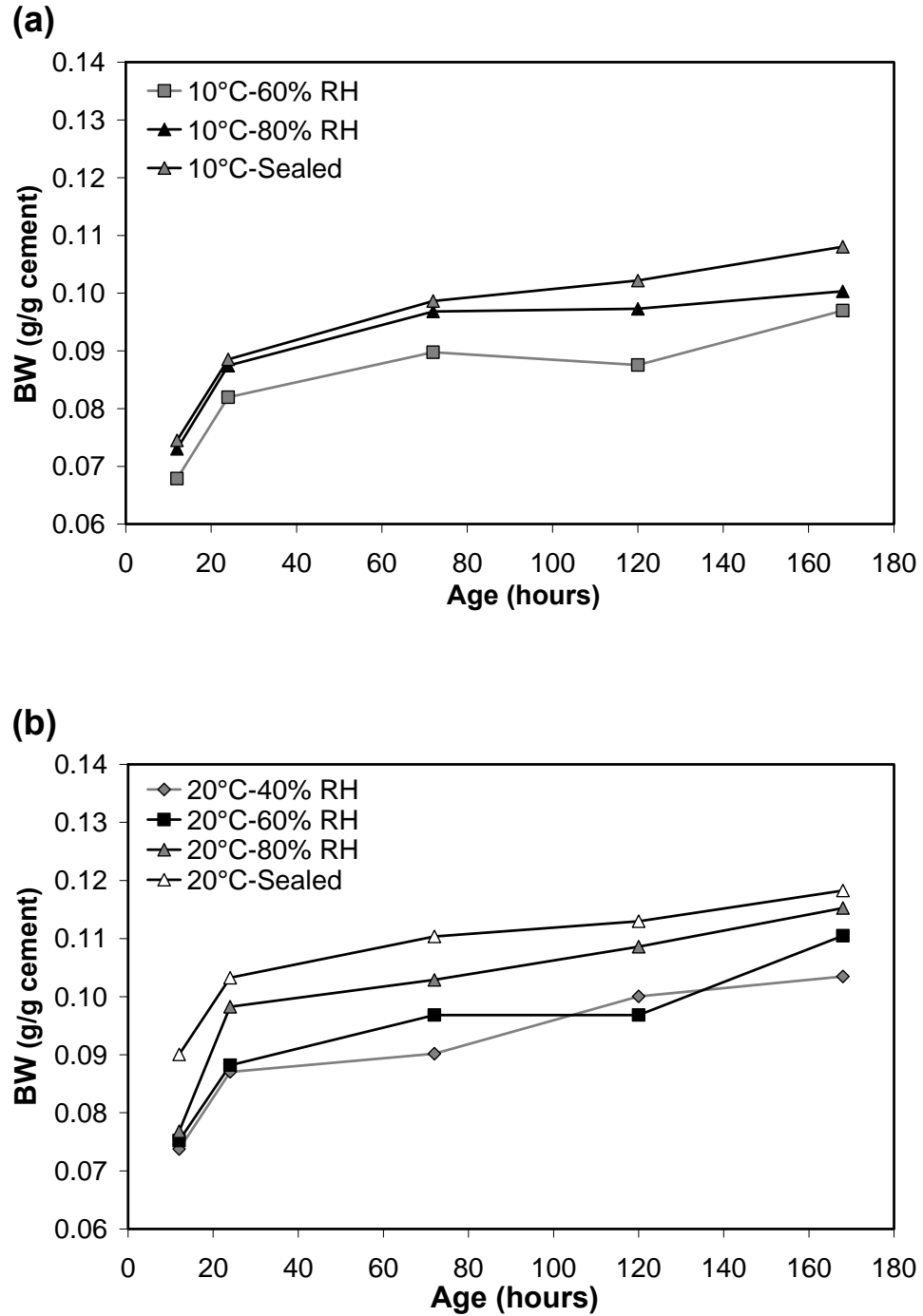
Figure 4-11: Change in BW Vs. ambient humidity for w/c=0.25 +0.6% SAP mixture at a) 10°C, b) 20°C, and c) 40°C.

(c)
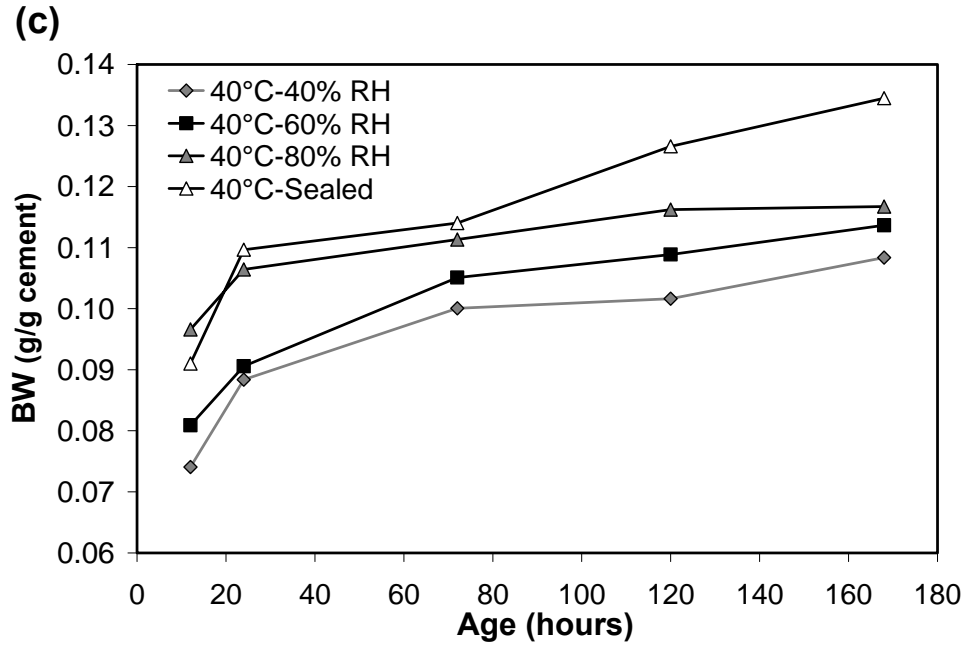
Figure 4-11 Cont'd: Change in BW Vs. ambient humidity for w/c=0.25 +0.6% SAP mixture at a) 10°C, b) 20°C, and c) 40°C.

(a)
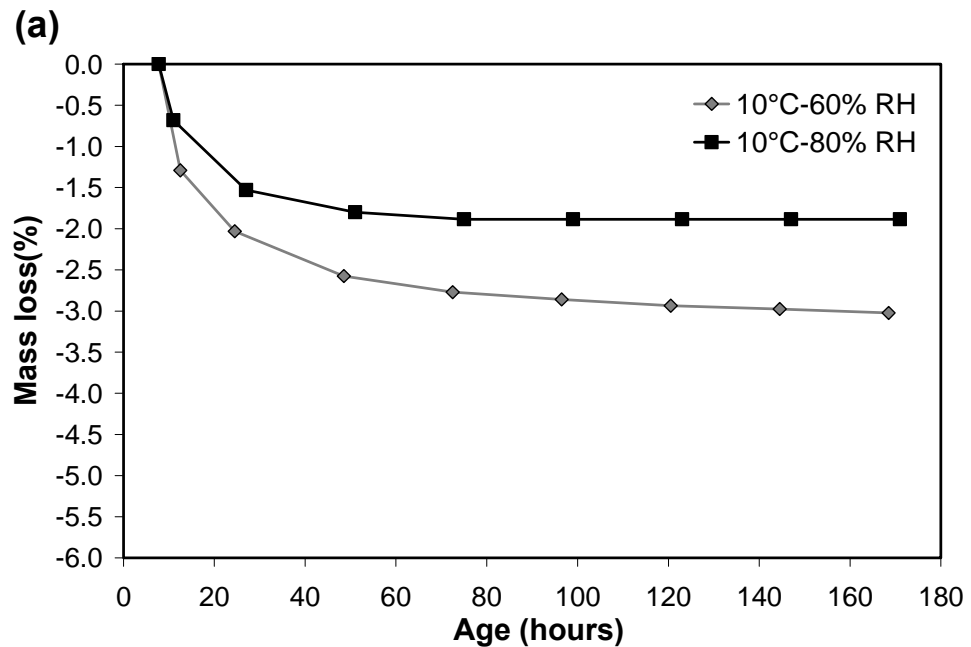
Figure 4-12: Change in mass loss Vs. ambient humidity for w/c=0.25 +0.6% SAP mixture at a) 10°C, b) 20°C, and c) 40°C.

(b)

(c)
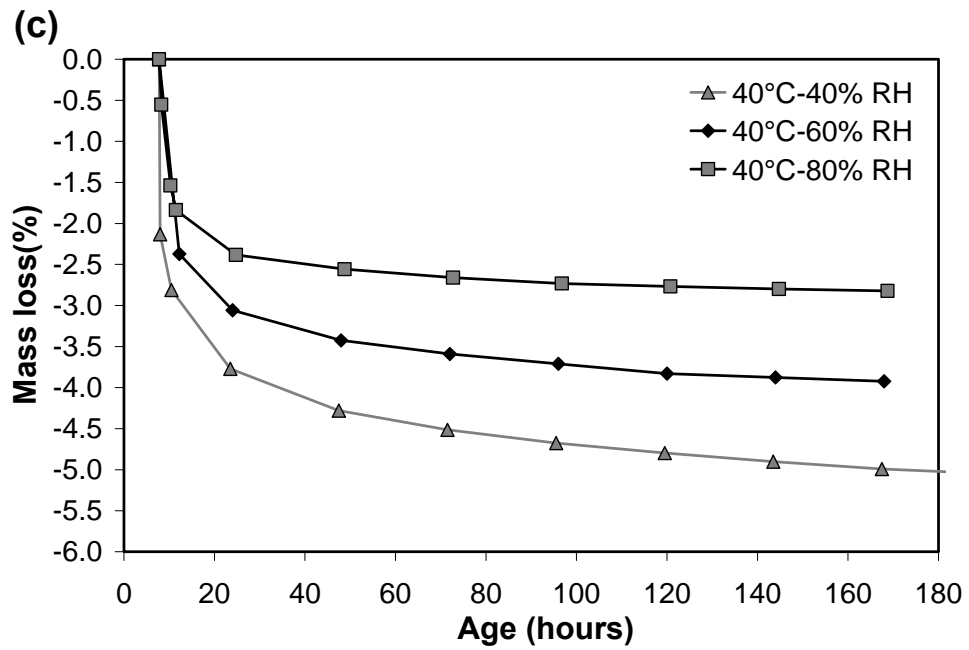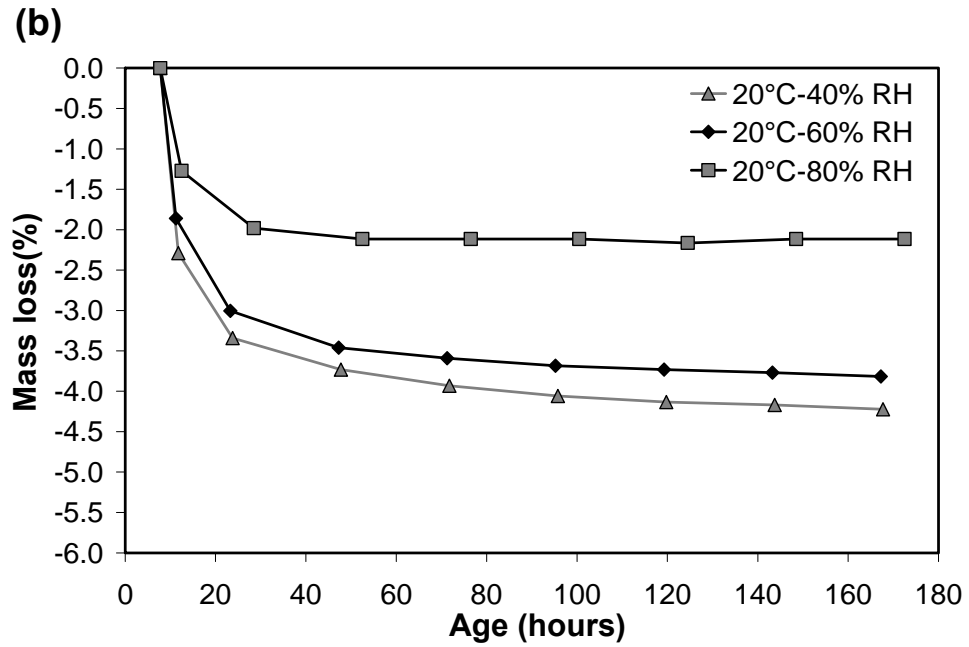
Figure 4-12 Cont'd: Change in mass loss Vs. ambient humidity for w/c=0.25 +0.6% SAP mixture at a) 10°C, b) 20°C, and c) 40°C.

Due to higher ion concentration inside SAP, water flows under the effect of osmosis from the cement matrix to SAP particles (Jensen and Hansen, 2001). As the hydration progresses, more ions dissolve in the pore solution (Lea, 1988). Once the ions concentration in the pore solution becomes higher than that inside SAP particles, water starts to flow in the opposite direction (i.e. from SAP particles to the surrounding cement matrix (Jensen and Hansen, 2001)). Combined with water loss due to evaporation, this resulted in higher ions concentration in the pore solution, which motivates further water flow from the SAP particles. Furthermore, since the rate of hydration and evaporation are functions of the temperature and RH, it is expected that increasing the curing temperature and/or decreasing the RH will result in more extracted water from the SAP particles, thus enhancing evaporation and higher mass loss.

4.5.5.   Correlation between Autogenous Strain and Achieved Degree of Hydration under Sealed Condition

4.5.5.1 SRA Mixtures

Autogenous strains are shown in **Fig. 4-13** as a function of the RBW for mixtures incorporating 2% SRA and cured at 10, 20 and 40°C. A good correlation can be observed between the measured autogenous strains and the RWB for mixtures cured at 10 and 20°C. At 40°C, a different trend was observed. At the same RBW, a higher autogenous strain was achieved at 40°C compared to that at 10 and 20°C. This could be ascribed to the absence of early expansion at 40°C due to the adverse effect of the high curing temperature at early-age on ettringite formation and the acceleration of hydration, leading to higher self-desiccation. Mono-sulphate super-saturation levels and stability (Thomas *et*

al., 2003) will be affected, leading to lower rate of ettringite formation. Moreover, the

higher self-desiccation shrinkage opposes expansion induced by any ettringite formation

(Bentz *et al.*, 2001b, Kaufmann *et al.*, 2004).
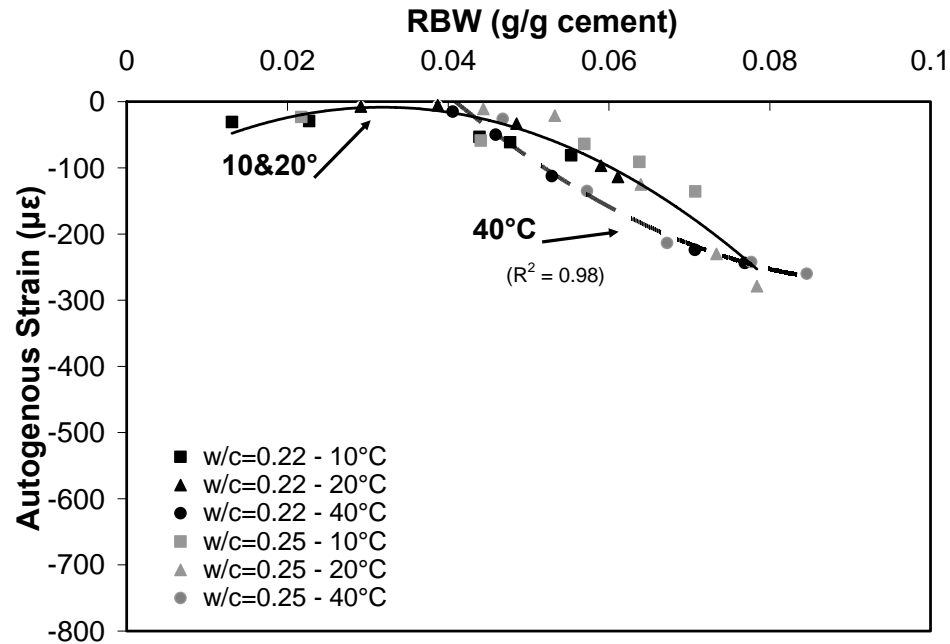
Figure 4- 13: Correlation between autogenous strains and RBW for 2% SRA mixtures cured at 10, 20 and 40°C.

4.5.5.2 SAP Mixtures

For mixtures incorporating 0.6% SAP, experimental results revealed a linear correlation

between the measured autogenous strains and RBW at 20 and 40°C, as shown in **Fig. 4-14**. At 10°C, no correlation was observed, which can be ascribed to the effect of the high

early-age expansion due to a disjoining pressure provided by water released from the

SAP. Such an expansion, depending on its magnitude and rate of development, will act to

offset deformations due to shrinkage. Further research is needed to explore this complex

combination of expansion and autogenous strain. This includes, for instance, the

influence of the rate of dissolution of salts in the pore solution on capillary stresses, the disjoining pressure (Lura, 2003), and the coefficient of super-saturation at low temperature for mixtures incorporating SAP.
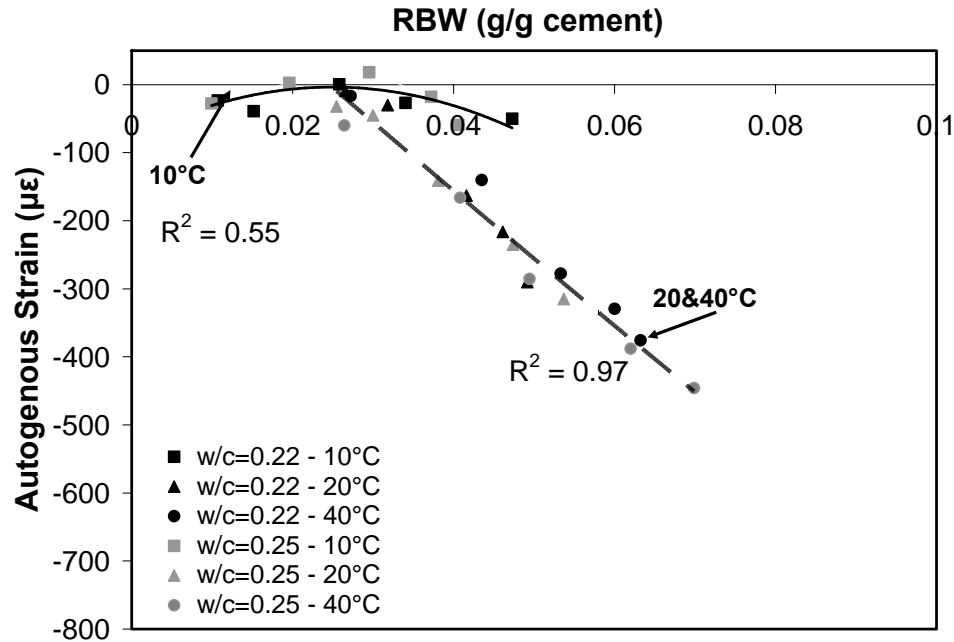
Figure 4- 14: Correlation between autogenous strains and RBW for 0.6% SAP mixtures cured at 10, 20 and 40°C.

4.5.6. Predicting Drying and Autogenous Strains under Different Curing Conditions

To investigate the effect of drying conditions on the role of SRA and SAP, the drying strains were determined based on the superposition principle and the evaluated degree of hydration (described in Chapter 3).

 4.5.6.1 *SRA Mixtures*

Similar to the control mixtures, the contribution of autogenous strains to the total strain under drying conditions for mixtures incorporating 2% SRA, based on the superposition principle, were overestimated when compared with that obtained using the degree of hydration, as shown in **Fig. 4-15**. However, SRA mixtures showed lower variation between the evaluated autogenous strains under different RH and sealed specimens compared to that of the control mixtures (lower overestimation values (**Table 4-1**)). For instance, at 40°C the difference between autogenous strains at RH=40% and sealed specimens was about 50 and 360 $\mu\varepsilon$ for SRA and control mixtures, respectively. This can be ascribed to the role of SRA in maintaining higher internal relative humidity under different drying conditions, which enhanced the hydration process (Bentz *et al.*, 2001a, Weiss *et al.*, 2008). SRA effectively reduced the drying strains for specimens cured under low RH conditions, while reduced autogenous strain slightly. For instance, w/c=0.25 +2% SRA specimens achieved up to 55% reduction in the drying strain at 40°C and RH= 40% compared to only 6% reduction in the autogenous strain at 40°C. Conversely, a higher efficiency of SRA in mitigating autogenous strains was observed at high RH compared to that of the control mixtures, as shown in **Fig. 4-16**. In conclusion, SRA was more effective in reducing drying strains at low RH, where drying dominated the total deformation and autogenous deformation had a minor effect. It can also be argued that SRA can be more effective in reducing autogenous strains for sealed or large cross-section concrete members, where autogenous deformation at the core would be the major cause of deformation.
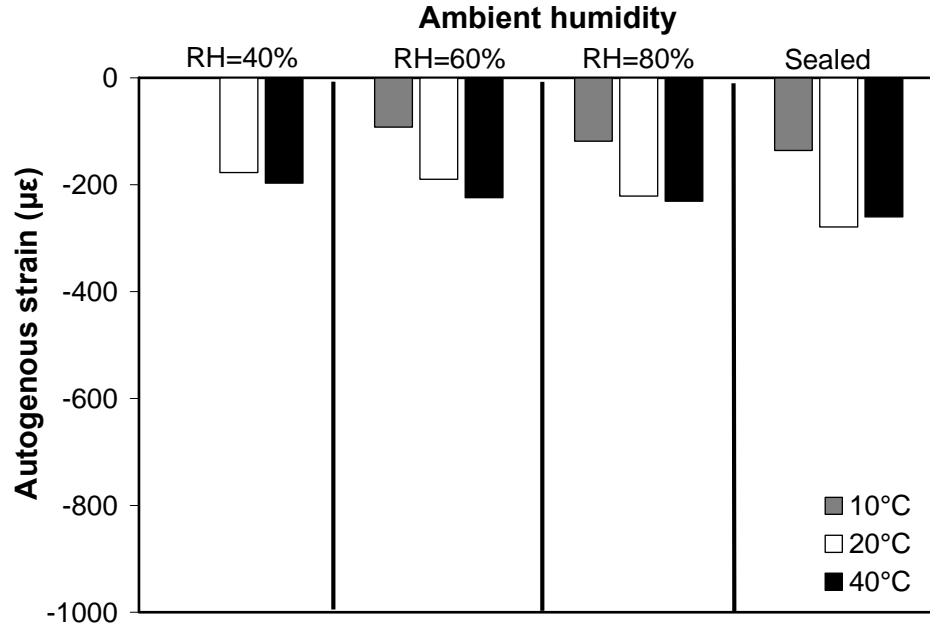
Figure 4-15: Autogenous strains evaluated based on achieved degree of hydration for w/c=0.25 + 2% SRA UHPC mixtures at age 7 days.
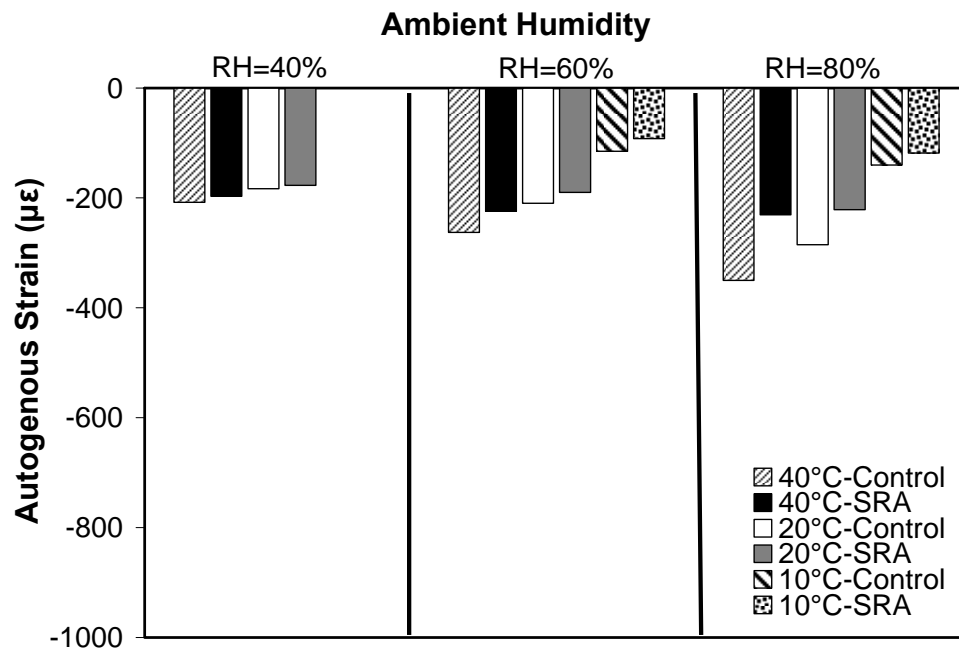
Figure 4-16: Comparison between autogenous strains evaluated based on achieved degree of hydration for w/c=0.25 mixtures at age of 7-days with and without SRA.

Table 4- 1: Overestimation ratios for autogenous strains under different curing conditions for different w/c=0.25 UHPC mixtures

Mixture	Temp.°C/RH%	Overestimation ratio		
		40	60	80
Control	10	----*	0.78	0.46
	20	1.26	0.98	0.45
	40	1.74	1.17	0.63
2% SRA	10	----*	0.47	0.15
	20	0.57	0.46	0.26
	40	0.32	0.16	0.13
0.6% SAP	20	0.98	0.47	0.20
	40	1.13	0.67	0.48

* Condition is not feasible.

4.5.6.2 SAP Mixtures

Figure 4-17 shows autogenous strains evaluated based on the degree of hydration for mixtures incorporating 0.6% SAP under different exposure conditions (except at 10°C, no correlation between the strains and degree of hydration was obtained as discussed earlier). It can be observed that autogenous strains for sealed specimens were significantly higher than that under other exposure conditions as shown by the overestimation ratio in **Table 4-1**. In addition, SAP efficiency in mitigating autogenous strains decreased with lowering the RH. Lowering the RH facilitates water escaping from specimens, which disturbs water storage in the SAP particles as mentioned before. This can affect the role of SAP in mitigating autogenous strains induced by self-desiccation. For instance, the reduction in autogenous strains at 40°C for SAP mixtures

compared to that of control mixtures was about 7 and 21% for RH=40 and 80%, respectively as shown in **Fig. 4-18**. Furthermore, SAP mixtures exhibited higher drying strains compared to that of the control mixtures which is in agreement with mass loss results (see **Fig. 4-12(a,b,c)**).
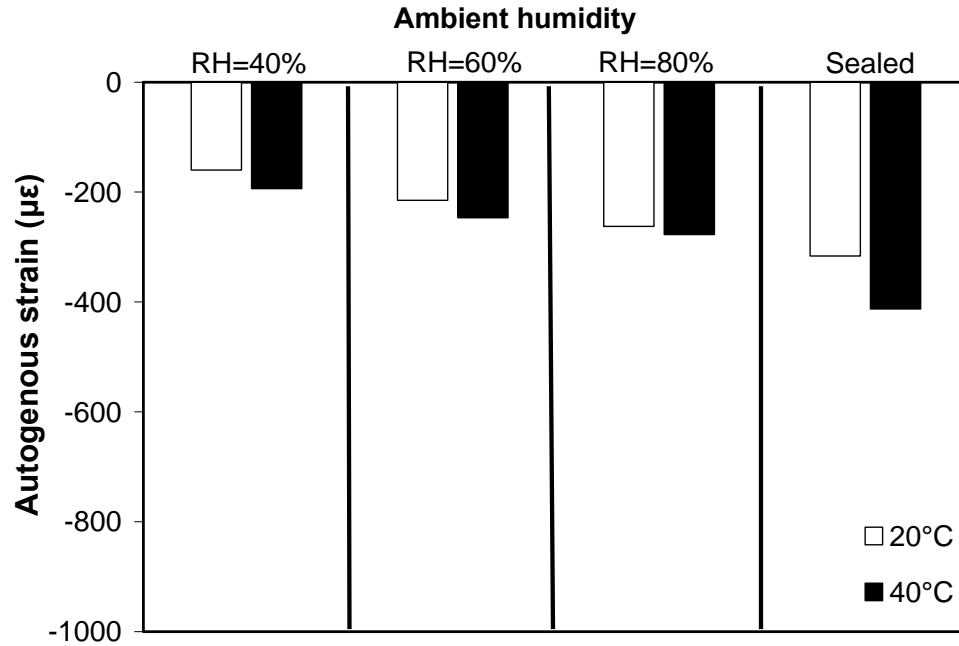
Figure 4-17: Autogenous strains evaluated based on achieved degree of hydration for w/c=0.25 + 0.6% SAP UHPC mixtures at age 7 days.
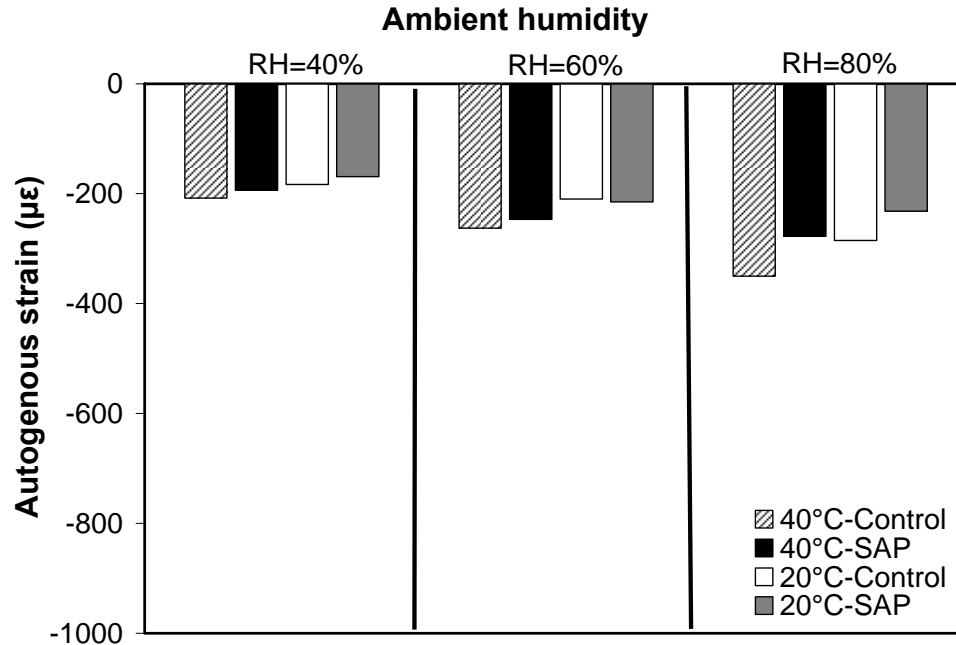
Figure 4-18: Comparison between autogenous strains evaluated based on achieved degree of hydration for w/c=0.25 mixtures at age of 7-days with and without SAP.

4.6. CONCLUSIONS

Using the amount of chemically bound water to assess autogenous and drying strains in ultra high-performance concrete specimens was explored in this study including the effects of a shrinkage reducing admixture and superabsorbent polymer. The following conclusions can be drawn from the experimental results:

1) The reduction in UHPC compressive strength induced by the addition of SRA and SAP should be considered in evaluating the overall field performance.

2) Effect of different shrinkage mitigation techniques on development of autogenous and drying strains are dependent; therefore their behaviour under sealed conditions will differ from that under drying conditions.

3) Applying the superposition principle without considering the effect of drying conditions on the shrinkage mitigation mechanisms will result in overestimating autogenous strains, and consequently an unrealistic evaluation for the efficiency of the applied shrinkage mitigation technique.

4) For thin UHPC sections, drying dominates the total deformation and reduces the development of autogenous strains, leading to lower autogenous contribution to the total deformation.

5) Adding SRA effectively reduced drying strains, which are the dominant strains in UHPC specimens under low RH conditions. At higher RH conditions, SRA reduced autogenous strains, which in turn are the dominant strains at high RH.

6) In sealed UHPC specimens, early-age expansion of SAP mixtures had a significant effect in reducing the net strains.

7) In UHPC specimens under drying conditions, adding SAP resulted in higher drying strains, which disturbed the curing process and diminished the effect of SAP as a shrinkage mitigating method.

8) Adequate external curing is essential to mitigate early-age deformation in UHPC even when internal curing mechanisms are provided, since it guarantees a suitable environment for shrinkage mitigation methods to work properly.

4.7.   REFERENCES

Bao-guo, M., Xiao-dong, W., Ming-yuan, W., Jia-jia, Y. and Gao, X-j., (2007), "Drying Shrinkage of Cement-Based Materials Under Conditions of Constant Temperature and Varying Humidity," *Journal of China Univiversity for Mining and Technology*, Vol. 17, No. 3, pp. 428-431.

Baroghel-Bouny, V., Mounanga, P., Khelidj, A., Loukili, A. and Rafai, N., (2006), "Autogenous deformations of cement pastes: Part II. W/C effects, micro–macro correlations, and threshold values," *Cement and Concrete Research*, Vol. 36, No. 1, pp. 123-136.

Bentz, D.P., (2006), "Influence of Shrinkage-Reducing Admixtures on Early-Age Properties of Cement Pastes," Journal *of Advanced Concrete Technology*, Vol. 4, No. 3, 423-429.

Bentz, D.P., Geiker, M.R. and Hansen, K.K., (2001a), "Shrinkage-reducing admixtures and early-age desiccation in cement pastes and mortars," *Cement and Concrete Research*, Vol. 31, No. 7, pp. 1075-1085.

Bentz, D.P., Jensen, O.M., Hansen, K.K., Olesen, J.F., Stang, H. and Haecker, C-J., (2001b), "Influence of cement particle-size distribution on early age autogenous strains and stresses in cement-based materials," *Journal of American Ceramic Society*, Vol. 84, No. 1, pp. 129-135.

Bentz, D.P. and Peltz, M.A., (2008), "Reducing Thermal and autogenous shrinkage contributions to early-age cracking," *ACI Materials Journal*, Vol. 105, No. 4, pp. 414-420.

Cusson, D. and Hoogeveen, T.J., (2007), "An experimental approach for the analysis of early-age behaviour of high-performance concrete structures under restrained shrinkage," *Cement and Concrete Research*, Vol. 37, No. 2, pp. 200-209.

D'Ambrosia, M., (2002), "Early-age Tensile Creep and Shrinkage of Concrete with Shrinkage Reducing Admixtures," Master Thesis, University of Illinois at Urbana-Champaign, United States.

Jensen, O.M. and Hansen, P.F., (2001), "Water-entrained cement-based materials: I. Principles and theoretical background," *Cement and Concrete Research,* Vol. 31, No. 4, pp. 647-654.

Jensen, O.M. and Hansen, P.F., (2002), "Water-entrained cement-based materials: II. Experimental observations," *Cement and Concrete Research,* Vol. 32, No. 6, pp. 973-978.

Kamen, A., Denarié, E., Sadouki, H. and Brühwiler, E., (2008), "Thermo-mechanical response of UHPFRC at early age - Experimental study and numerical simulation," *Cement and Concrete Research*, Vol. 38, No. 6, pp. 822-831.

Kaufmann, J., Winnefeld, F. and Hesselbarth, D., (2004), "Effect of the addition of ultrafine cement and short fiber reinforcement on shrinkage, rheological and mechanical properties of Portland cement pastes," *Cement and Concrete Composites*, Vol. 26, No. 5, pp. 541-549.

Kovler, K., (1996), "Why Sealed Concrete Swells," *ACI Materials Journal,* Vol. 93, No. 4, pp. 334-340.

Lam, H., (2005), "Effects of internal curing methods on restrained shrinkage and permeability," Master Thesis., University of Toronto

Lea, F.M., (1988). Lea's Chemistry of Cement and Concrete, 4th Edition., J. Wiley, New York.

Loser, R. and Leemann, A., (2009), "Shrinkage and restrained shrinkage cracking of self-compacting concrete compared to conventionally vibrated concrete," *Materials and Structures*, Vol. 42, No. 1, pp. 71-82.

Lura, P., (2003), "Autogenous deformation and internal curing of concrete," PhD. Thesis, Technical University Delft, Netherlands.

Lura, P. and Jensen, O.M., (2007), "Measuring techniques for autogenous strain of cement paste," *Materials and Structures*, Vol. 40, No. 4, pp. 431-440.

Mikhail, R.S., Abo-El-Enein, S.A. and Gabr, N.A., (1977), "Hardened slag-cement pastes of various porosities I. Compressive strength, degree of hydration and total porosity," *Journal of Applied Chemistry and Biotechnology*, Vol. 24, No. 12, pp. 735-743.

Mönnig, S. and Lura, P., (2007), "Superabsorbent Polymers - An Additive to Increase the Freeze-Thaw Resistance of High Strength Concrete," In: *Advances in Construction Materials*, Part V, Springer Berlin Heidelberg, pp. 351-358.

Mounanga, P., Khelidj, A., Loukili, A. and Baroghel-Bouny, V., (2004), "Predicting $Ca(OH)_2$ content and chemical shrinkage of hydrating cement pastes using analytical approach," *Cement and Concrete Research*, Vol. 34, No. 2, pp.255-265.

Odler, I. and Rößler, M., (1985), "Investigations on the relationship between porosity, structure and strength of hydrated Portland cement pastes: II. Effect of pore structure and of degree of hydration," *Cement and Concrete Research*, Vol. 15, No. 3, pp. 401-410.

Rajabipour, F., Sant, G. and Weiss, J., (2008), "Interactions between shrinkage reducing admixtures (SRA) and cement paste's pore solution," *Cement and Concrete Research*, Vol. 38, No. 5, pp. 606-615.

Thomas, J.J., Rothstein. D., Jennings, H.M. and Christensen, B.J., (2003), "Effect of hydration temperature on the solubility behavior of Ca-, S-, Al-, and Si-bearing solid phases in Portland cement pastes," *Cement and Concrete Research*, Vol. 33, No. 12, pp. 2037-2047.

Wang, F., Zhou, Y., Peng, B., Liu, Z. and Hu, S., (2009), "Autogenous shrinkage of concrete with super-absorbent polymer," *ACI Materials Journal*, Vol. 106, No. 2, pp. 123-127.

Weiss, J. and Berke, N., (2003), "Admixtures for reduction of shrinkage and cracking," In: *Early Age Cracking in Cementitious Systems: Report of RILEM Technical Committee 181-EAS*, Bentur A; (ed.), pp. 323-335.

Weiss, J., Lura, P., Rajabipour F. and Sant. G., (2008), "Performance of shrinkage-reducing admixtures at different humidities and at early ages," *ACI Materials Journal*, Vol. 105, No. 5, pp. 478-486.

Yuasa, N., Kasai, Y., Matsui, I., (1999), "Inhomogeneous distribution of the moisture content and porosity in concrete," In: *Proceedings of the International Conference*, R.K. Dhir and M.J. McCarthy, Editors, the University of Dundee, Scotland, United Kingdom, Thomas Telford Publ., pp. 93-101.

<div align="right">**CHAPTER FIVE**</div>

EARLY-AGE SHRINKAGE OF UHPC UNDER DRYING/WETTING CYCLES AND SUBMERGED CONDITIONS*

In the previous chapters (3 and 4), the influence of coupling a wide range of temperatures and relative humidities on drying and autogenous shrinkage behaviour, and their interaction mechanisms was investigated. Moreover, the role of shrinkage reducing admixture (SRA) and superabsorbent polymer (SAP), as shrinkage mitigation techniques, and their efficiency were also explored under similar conditions. However, such tests still not capturing the effect of other factors existing in field conditions, which may modify the early-age shrinkage behaviour of UHPC and its interaction with surrounding environment. Therefore, the present chapter examines the early-age shrinkage behaviour of UHPC mixtures, with and without shrinkage mitigation techniques, along with considering environmental loads (including the application of drying/wetting cycles and/or full immersion). This shall initiate the idea for developing a comprehensive integrated early-age shrinkage testing approach.

5.1.   INTRODUCTION

Concrete is usually subjected to early-age variation in temperature, relative humidity, wind and other environmental loading that can alter its behaviour. Considering in-situ conditions and environmental loading in testing protocols should allow gaining a better

understanding of the early-age behaviour and developing suitable performance specifications. This seems to be more important for new generations of concrete (i.e. UHPC) before being implemented in wide full-scale field constructions.

During early-age curing, before depercolation of capillary pores, concrete can imbibe water from its environment. Hence, self-desiccation shrinkage can be delayed and cracking may be avoided (Bentz and Jensen, 2004). In addition, early curing minimizes early-age moisture loss and maximizes the degree of hydration achieved by the cement, potentially leading to stronger and more durable concrete. Based on the quality of the curing regime, UHPC can be subjected to cyclic drying (intervals between exposures to moisture) and wetting (during moisture exposure). Besides the curing regime, concrete is usually exposed in the field to various environmental conditions. These may include: the drying action of the sun and wind; rain-water containing dissolved chemicals; bridge-deck run-off or road spray contaminated with chlorides from de-icing salts; tidal and wave action in offshore or water-front marine structures, etc. Hence, it can be expected that the quality of the curing regime and the effects of the surrounding environment may be responsible for considerable dimensional instability due to moisture changes, and can thus have major consequences on the long-term performance of concrete.

Therefore, the present chapter explores the shrinkage behaviour of UHPC under different environmental loads. These loads include drying/wetting (*DW*) cycles, which used as an accelerated test method to simulate outdoor environmental conditions in which structures are subjected to moisture cycles, and submerged (*SM*) condition to simulate the submerged part of marine and offshore structures.

5.2.   RESEARCH SIGNIFICANCE

Several studies have been conducted to quantify the shrinkage behaviour of UHPC using a conventional testing approach under controlled environment. However, achieving a proper understanding for the effect of field exposure conditions on such shrinkage a more integrated testing approach is still needed. Hence, this study introduces a simple integrated testing method through considering the effect of environmental load on shrinkage behaviour and the efficiency of shrinkage mitigation methods. Results should have important implications in understanding the evolution of early-age deformations in UHPC and the role of mitigation methods under field-like conditions. In addition, it paves the way for developing a multi-factor integrated testing approach for early-age shrinkage behaviour that can capture different field scenarios.

5.3.   EXPERIMENTAL PROCEDURE

5.3.1.   Materials and Mixture Proportions

The materials, UHPC mixtures and ID coding used in this chapter were similar to that used in Chapter 4 (refer to Section 4.4.1). A new UHPC mixture incorporating 2% SRA and 0.6% SAP was tested in order to investigate the synergetic effect of both mitigation techniques. The chemical and physical properties of the used binders have been given in Chapter 3 (**Tables 3-1**).

5.3.2.   Environmental Conditions

Four exposure conditions were simulated, namely; drying, sealed, *SM* and *DW* cycles. The drying condition was simulated inside a walk-in environmental room, where

temperature and relative humidity (RH) were kept constant (20 ±1°C and RH= 40 ± 5%). Submerged specimens were stored in a temperature controlled water bath at 20 ±2°C. During the *DW*, specimens were allowed to dry inside the walk-in environmental room at 20 ±1°C and RH= 40% for 12 hours, then submerged in a temperature controlled water bath at 20 ± 2°C for 6 hours. Controlling the temperature of specimens insures a similar temperature history; hence, the temperature effects on the developed autogenous shrinkage strains are minimized during the various exposure regimes (Turcry *et al.*, 2002).

5.3.3. Preparation of Test Specimens and Testing Procedures

Prismatic specimens (75×75×280 mm) were used for all conducted tests in order to dispel size effects on the results. All UHPC specimens were taken from a single batch of the tested mixture. Before casting, the moulds were lined with a layer of thin Teflon sheets to minimize friction between the concrete and moulds. Specimens were cast in three layers and compacted on a vibrating table. UHPC was cast in metallic molds with 5-mm thick copper walls. Silicone sealant was used to seal the molds' sides and prevent any water diffusion from the bath. The surface of each specimen was covered with a wide polyethylene sheet which was bent down on both sides of the mold and fixed with a silicone sealant. The temperature of each specimen was controlled using a temperature controlled water bath surrounding the specimens' sides. The top surface temperature was controlled using a wet sponge. The sponge was submerged in the water bath regularly every 15 minutes until the demolding time. At around 5-7 hours from first contact between cement and water, molds were removed from the water bath. The silicon sealant and wall-base attaching screws were removed, then specimens were taken off and moved

to the specific curing conditions. The specimens were installed over roller supports that can rise up the specimens allowing: i) drying from all specimens' faces, and ii) specimens to shrink freely without friction effects. In the remainder of this text, strains will be used to account for both shrinkage and expansion deformations.

5.3.3.1 Chemically Bound Water and Degree of Hydration

Thermo-gravimetric (TGA) combined with derivative thermo-gravimetric (DTG) analysis was previously explained in Chapter 3 (refer to section 3.4.3.1)

5.3.3.2 Strain Measurements

The strain measurements on UHPC specimens were carried out using electrical-resistance strain gauges according to a common procedure (RILEM, 2003, Tazawa, 1999) in which an embedded steel bar, with strain gauges installed on it, is used to measure strain inside the tested specimen. Fresh UHPC mixtures were cast in metallic formwork with steel reinforcing bars (6 mm in diameter, and 280 mm in length). On each steel bar, four strain gauges were installed to form a full bridge circuit, as shown in **Fig. 5-1**. Two strain gauges were installed opposite to each other along a fabricated 20 mm smooth length at the middle of the bar to eliminate the bending effect on the measured strains (Hannah and Reed, 1992, Sule and Van Breugel, 2001). The other two strain gauges were installed in the transverse direction to minimize the temperature effect on the measured strains (RILEM, 2003, Hannah and Reed, 1992). In addition, two metallic plates were added at the ends of the bar to capture any expansion deformation. The measured strains were corrected to account for the local restraint induced by the embedded bar due to the difference between the stiffness of concrete and that of the embedded steel bar as follows (RILEM, 2003):

$$\varepsilon_t = \varepsilon_m \left[1 + \frac{E_s A_s}{E_c A_c} \right] + \alpha_s \Delta T \qquad\qquad \textbf{Eq. 5-1}$$

Where ε_t is the total concrete strain after correction, ε_m is the measured strain after deducting the temperature effect on the measurements, E_s, A_s and E_c, A_c are the modulus of elasticity and cross-section area of the embedded steel bar and tested UHPC specimens, respectively, α_s is the coefficient of thermal expansion of the embedded steel bar, and ΔT is the change in temperature from the onset of the test. The calculated value $(E_s A_s / E_c A_c)$ was much lower than 1, which indicates a very low restraint induced by the steel bar against shrinkage.
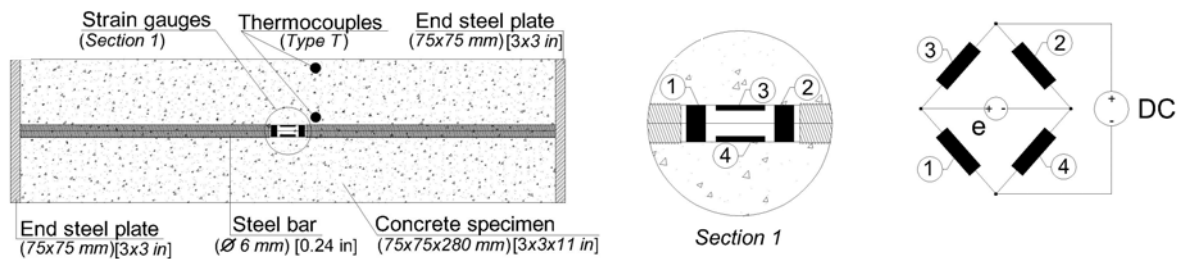
Figure 5-1 : (a) Strain measurement specimen, and (b) strain gauges arrangement to form full bridge circuit.

For each UHPC mixture, three replicate specimens per curing condition were made. Immediately after demolding, specimens for autogenous strain measurements were wrapped with four layers of polyethylene sheets and a layer of paraffin wax membrane to prevent moisture loss. Specimens for drying and drying/wetting strain measurements were exposed to the drying condition inside the walk-in environmental room. Submerged specimens were moved to the controlled water bath. Moreover, two type-T

thermocouples were inserted in the specimens to monitor concrete temperature changes from the onset of testing.

5.3.3.3 Moisture Loss

Three identical prisms (75×75×280 mm) were made for each mixture and demolded at the time of starting strain measurements. The prisms were transferred to the different exposure conditions after measuring the initial mass of each prism using a balance with an accuracy of 0.01 g. The mass measurements were started along with measurements of total strains.

5.3.3.4 Mercury Intrusion Porosimetry (MIP):

UHPC fragments were taken from tested specimens and immediately plunged in an isopropanol solvent to stop hydration and subsequently dried inside a desiccator until a constant mass was achieved. The pore size distribution for each specimen was determined automatically using a Micromeritics AutoPore IV 9500 Series porosimeter allowing a range of pressures from 0 to 414 MPa. The assumed surface tension of mercury was about 0.484 N/m at 25°C according to ASTM D 4404-84 (Standard Test Method for Determination of Pore Volume and Pore Volume Distribution of Soil and Rock by Mercury Intrusion Porosimetry). The density of the mercury was 13.546 g/ml and the assumed contact angle was 140°.

5.3.3.5 Chemical Oxygen Demand (COD)

Chemical Oxygen Demand (COD) test determines the oxygen requirement equivalent of organic matter that is susceptible to oxidation with the help of a strong chemical oxidant. In the COD method, the water sample is oxidized by digesting in a sealed reaction tube

with sulphuric acid and potassium dichromate in the presence of a silver sulphate catalyst. The amount of dichromate reduced is proportional to the COD. A reagent blank is prepared for each batch of tubes in order to compensate for the oxygen demand of the reagent itself. Over the range of the test a series of colours from yellow through green to blue are produced. The colour is indicative of the chemical oxygen demand and is measured using a Photometer. The results are expressed as milligrams of oxygen consumed per litre of sample.

5.4. RESULTS AND DISCUSSION

5.4.1. Mass Change

The mass change of the control UHPC specimens due to the ingress/absorption of moisture is illustrated in **Fig. 5-2**. Under the drying condition, specimens showed a continuous mass loss over the investigated period. Conversely, specimens subjected to *DW* cycles showed fluctuation of mass change while switching between the drying and wetting periods. On the other hand, submerged specimens gained mass rapidly during the first 24 hours, and then their mass became nearly constant. This can be attributed to the higher ability for imbibing water during the early period before depercolation of capillary porosity (Bentz and Garboczi, 1991). However, control specimens with w/c=0.22 exhibited a lower mass change of about 25% and 58% under the drying and submerged conditions, respectively, compared to that of control specimens with w/c=0.25. This can be ascribed to the reduction in porosity as a result of reducing the w/c. Reducing the w/c generally leads to lower capillary suction of water and reduced diffusion coefficient due to the development of a denser pore structure (Lea and Hewlett, 1998, Martys and

Ferraris, 1997, Teichmann and Schmidt, 2004). Moreover, the w/c=0.22 control mixture had a lower content of evaporable water compared to that of the w/c=0.25 control mixture due to its lower water content and higher consumption of evaporable water in the hydration process (i.e. self-desiccation) (Dhir and McCarthy, 1999).

(a)

(b)
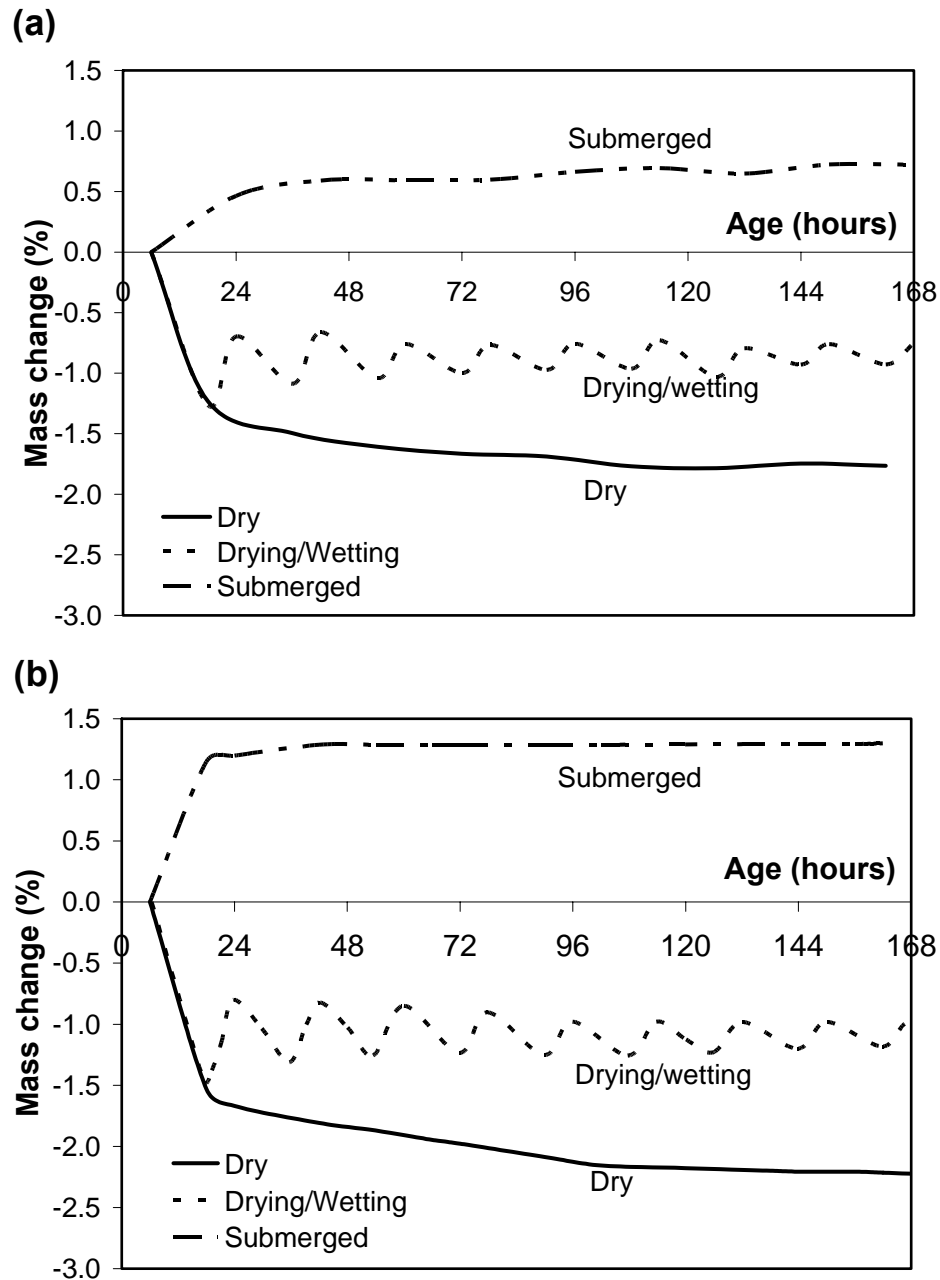
Figure 5-2: Mass change of control mixtures a) w/c=0.22 and b) w/c=0.25 under different exposure conditions.

Similar trends were observed for UHPC mixtures incorporating SRA and SAP (**Fig. 5-3**). Compared with control mixtures, the SRA mixtures did not exhibit a significant mass change under drying and *DW* conditions. Conversely, the SAP mixtures showed a higher mass loss. Under the *SM* condition, SRA and SAP mixtures behaved differently when the w/c changed. SRA and SAP mixtures with w/c=0.25 showed a lower mass gain compared to that of the w/c=0.25 control mixture. This can be ascribed to the effect of SRA and SAP on the capillary suction, which is considered the driving force for water diffusion into the porous material (Lstiburek and Carmody, 1994). Using SRA is believed to reduce the capillary suction since it reduces the pore fluid surface tension (Ribeiro *et al.*, 2006). The SAP mixture had a higher water content leading to lower capillary suction (Lstiburek and Carmody, 1994). On the other hand, SRA and SAP mixtures with a w/c=0.22 showed similar mass gain compared to that of the w/c=0.22 control mixture (see **Fig. 5-3**), which indicates that the water diffusion and consequently mass change at such a low w/c is dominated by the development and depercolation rate of the pore structure leading to lower diffusion characteristics (Lea and Hewlett, 1998).

(a)

(b)
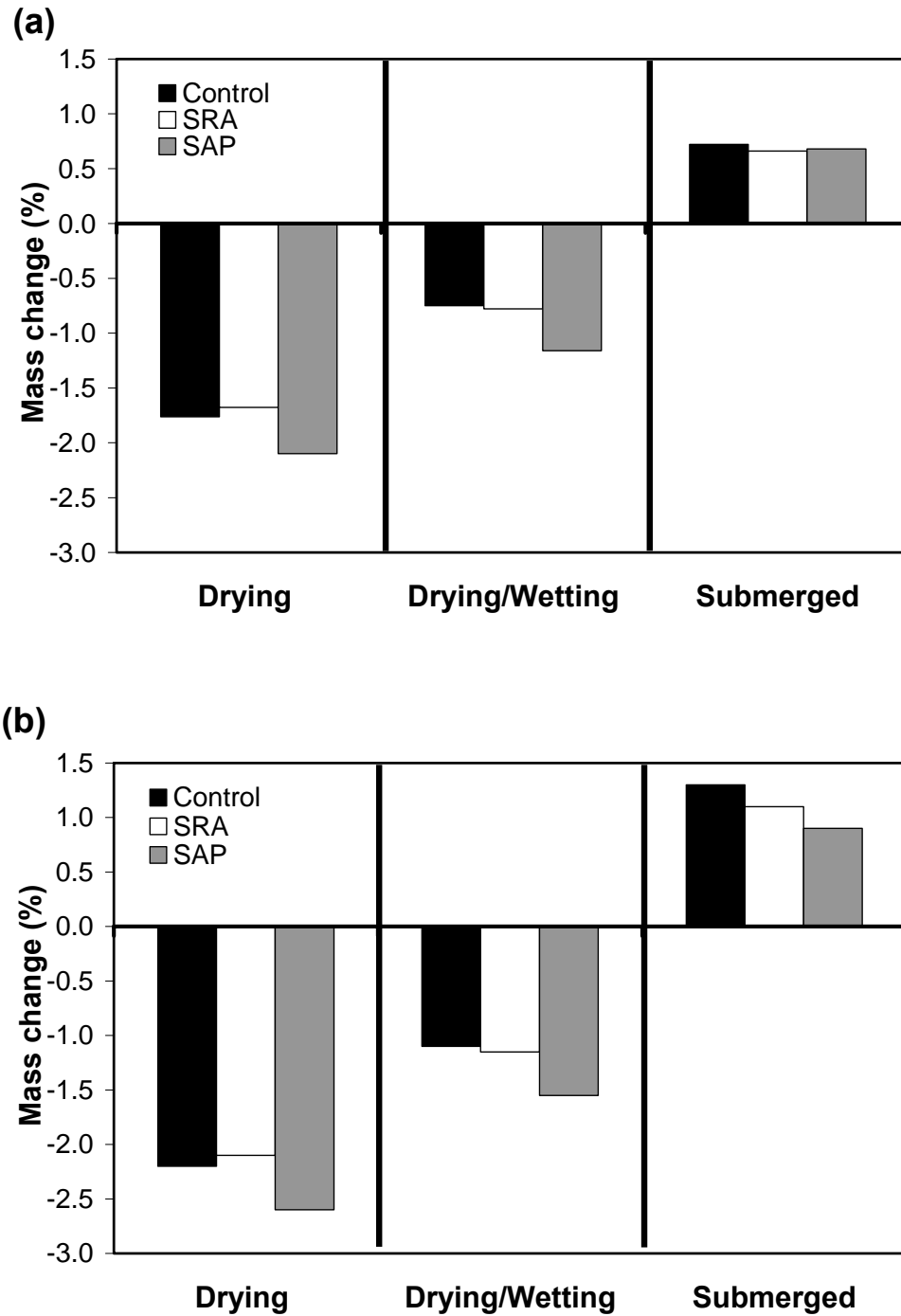
Figure 5-3: Mass change for a) w/c=0.22 and b) w/c= 0.25 mixtures incorporating 2% SRA or 0.6% SAP under different exposure conditions.

5.4.2.   Shrinkage Strain under Different Environmental Exposure Conditions

5.4.2.1 Control Mixture

UHPC specimens exposed to the drying and sealed conditions showed significant shrinkage strain. *DW* cycles seemed to be somewhat effective in counteracting shrinkage strain. The final shrinkage strains after *DW* cycles were reduced by about 21% and 37% compared to that under the drying condition for mixtures with w/c=0.22 and 0.25, respectively. **Figure 5-4** shows the strain development for the w/c=0.25 control mixture under different curing conditions.
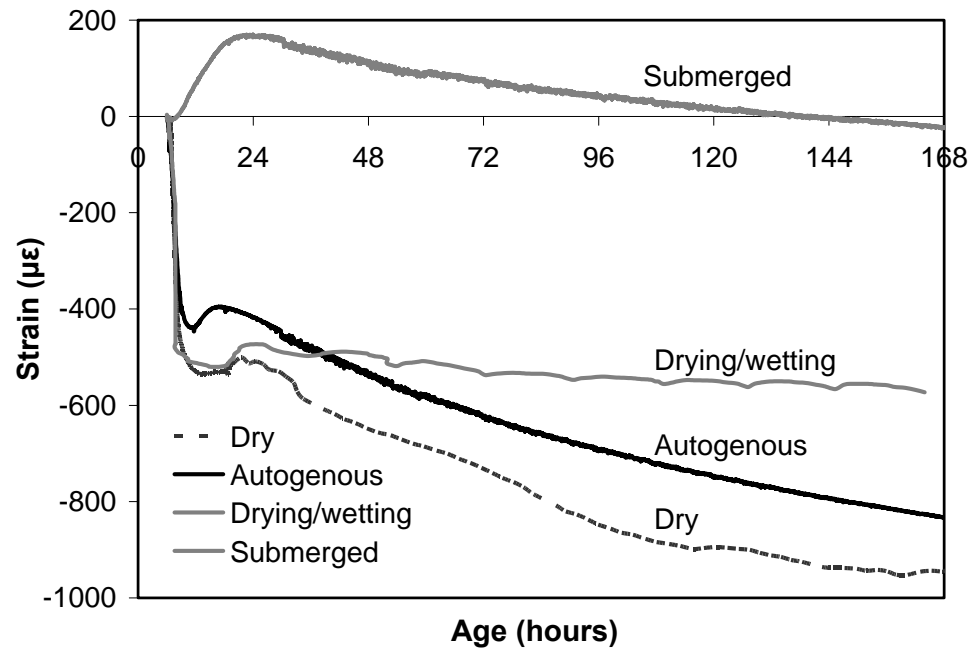
Figure 5-4: Measured strain for w/c=0.25 control specimens under different exposure conditions.

It can be seen that during the wetting period in *DW* cycles (**Fig. 5-5**), specimens expanded as a result of water absorption. Conversely, during the drying period, it started to shrink due to the loss of moisture, along with thermal deformation caused by

evaporative cooling due to the removal of free water (Kovler, 1996). These thermal deformations (which ranged from 20 to 35 $\mu\varepsilon$) were eliminated from strain measurements based on the measured specimens' temperature and coefficient of thermal expansion, which was evaluated using a similar procedure to that proposed by (Cusson and Hoogeveen, 2006, Cusson and Hoogeveen, 2007).
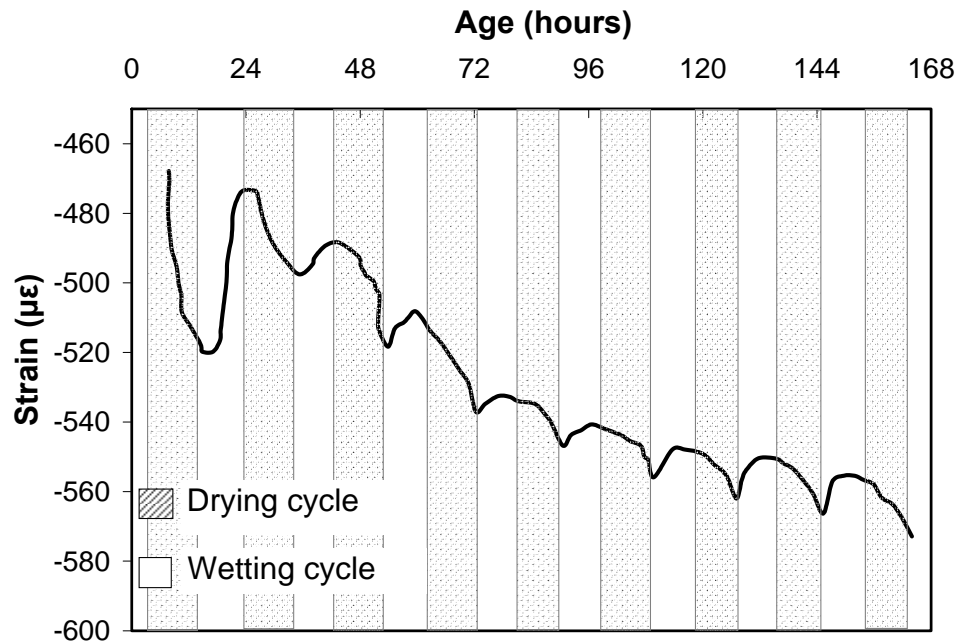
Figure 5-5: Measured strain for w/c=0.25 control specimens under drying/ wetting cycles.

Moreover, the amount and rate of strain development during either the drying or wetting period was found to decrease with time. This can be explained as follows: the higher the pore volume of the specimen, the deeper was the level of internal free water that can evaporate and be exchanged with the surrounding environment (Aïtcin, 1998), the so-called moisture influential depth (Chunqiu *et al.*, 2008). As the hydration process progresses, especially for UHPC, hydration products start filling voids and pores, thus

leading to denser internal microstructure (Loukili *et al.*, 1999, Lstiburek and Carmody, 1994). This will limit the exchange of water with the external surface layer of the specimen. **Figure 5-6(a,b)** illustrate the progress of the degree of hydration and pore volume for the surface layers and cores of UHPC specimens with w/c=0.25 subjected to *DW* cycles. It can be observed that the cores of specimens have higher degree of hydration and denser pore structure compared to that of the external layer.
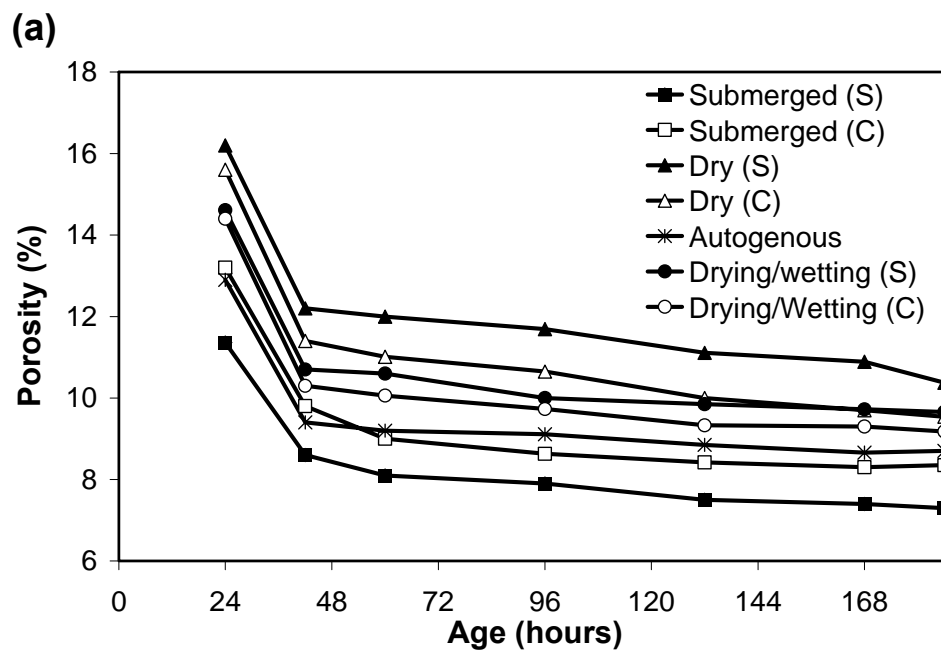
Figure 5-6: Measured (a) porosity and (b) degree of hydration for w/c=0.25 control specimens surface (S) and core (C) under different exposure conditions.

(b)
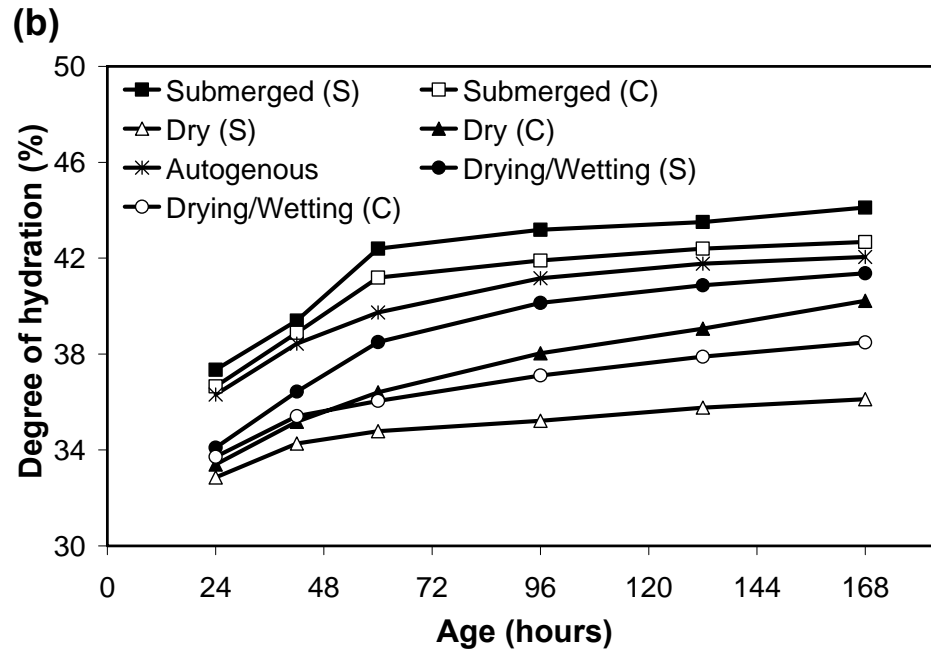
Figure 5-6 Contd': Measured (a) porosity and (b) degree of hydration for w/c=0.25 control specimens surface (S) and core (C) under different exposure conditions.

Under *SM* conditions, specimens continued to swell during the first 24 hours. Then, it started to shrink until the end of the investigated period. This high early swelling resulted in a lower net shrinkage compared with that of sealed specimens (about 79% and 98% reduction in the shrinkage strain for mixtures with w/c=0.22 and 0.25, respectively). The swelling of submerged specimens can be ascribed to the continuous supply of water, allowing the cement gel to absorb water and expand (Neville, 1996). The reduction in the swelling strain can be explained by the fact that the progress of the hydration process reduced and depercolated the concrete capillary porosity, which interfered with water imbibing from the surrounding environment to the specimen's core. As a result, higher self-desiccation occurred as water was drained from increasingly finer capillaries, thus leading to higher capillary tension and higher deformations. Unlike the case of *DW*

cycles, the external layers were found to be denser and had higher degree of hydration than that of specimen cores as shown in **Fig. 5-6 (a,b)**.

However a similar behaviour was observed for the w/c=0.22 control mixture, which showed a lower rate and amount of strain during *DW* cycles and under the *SM* condition compared to that of the w/c=0.25 control mixture. For instance, the w/c=0.22 control mixture exhibited an early expansion strain during the first 24 hours of about 21% less than that of the w/c=0.25 control mixture. This behaviour of the w/c=0.22 mixture can be attributed to its denser pore structure, which eliminated the water exchange between the specimens and their surrounding (Tazawa, 1999), whether during drying or wetting periods. **Figure 5-7** illustrates the effects of the w/c and exposure conditions on the surface pore volume distribution after one *DW* cycle. It can be observed that reducing the w/c and applying moist curing resulted in lower total porosity values and movement of the pore width peak to smaller widths in agreement with previous research (Cook and Hover, 1999, Alford and Rahman, 1981).
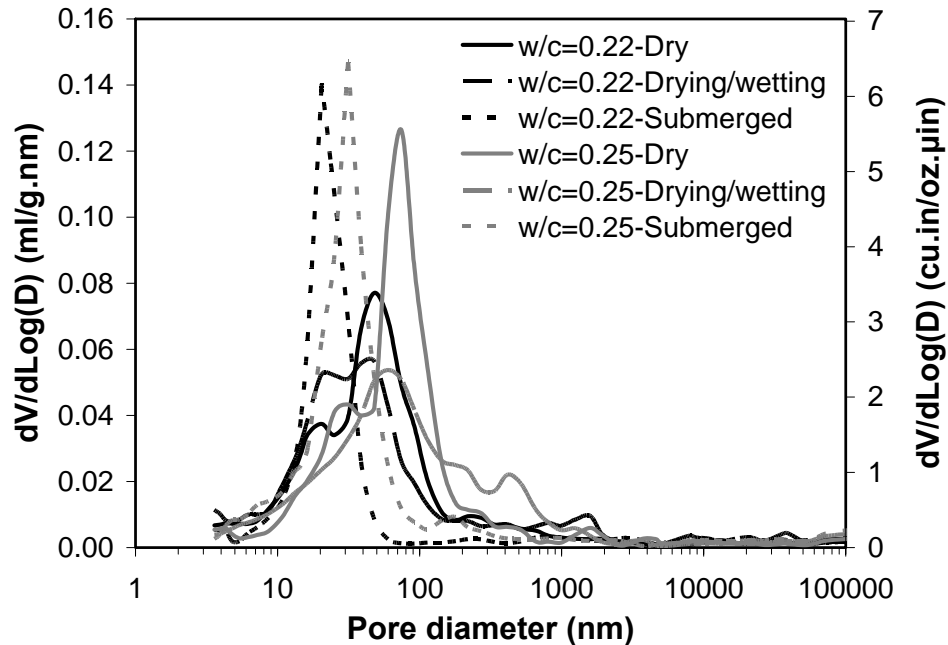
Figure 5-7: Pore size distribution for control specimen's surface under different exposure conditions after the first drying/wetting cycle.

5.4.2.2 Effect of SRA

Figure 5-8 illustrates the shrinkage strain for w/c=0.25 specimens incorporating SRA under different curing conditions. Incorporating SRA led to a significant reduction in both the drying and autogenous strains by about 24 and 38% for w/c=0.22 mixtures and about 18% and 25% for w/c= 0.25 mixtures, respectively, compared to that of corresponding control specimens with no SRA. This is attributed to the effect of SRA in reducing the surface tension of the pore fluid, leading to a reduction in the developed capillary stress and drying shrinkage strains (Bentz, 2006, Weiss *et al.*, 2008). Moreover, SRA is believed to mitigate the drop in internal relative humidity of specimens, leading to lower self-desiccation and autogenous shrinkage (Bentz *et al.*, 2001).
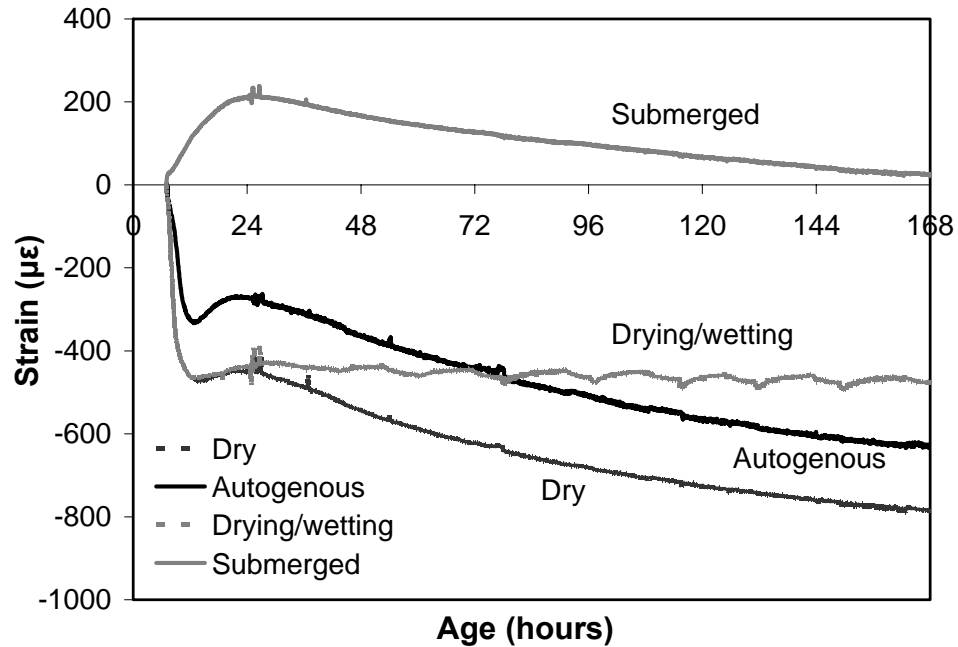
Figure 5-8: Measured strain for w/c=0.25 UHPC specimens incorporating 2% SRA under different exposure conditions.

Figure 5-9 illustrates changes in the drying strain rate during *DW* cycles for the control and SRA mixtures. Two interesting features can be observed. First, a steep reduction in the drying strain rate after about 1 and 3 *DW* cycles is observed for w/c=0.22 and 0.25 mixtures, respectively. As hydration proceeds, hydration products fill the pore space, thus diminishing the size and connectivity of pores (Cook and Hover, 1999). The resulting lower water exchange with the surrounding environment causes a steep reduction in the drying strain rate. The lower the w/c, the lower was the pore space to be filled, leading to earlier reduction in the rate of water exchange (Loukili *et al.,* 1999, Lstiburek and Carmody, 1994).
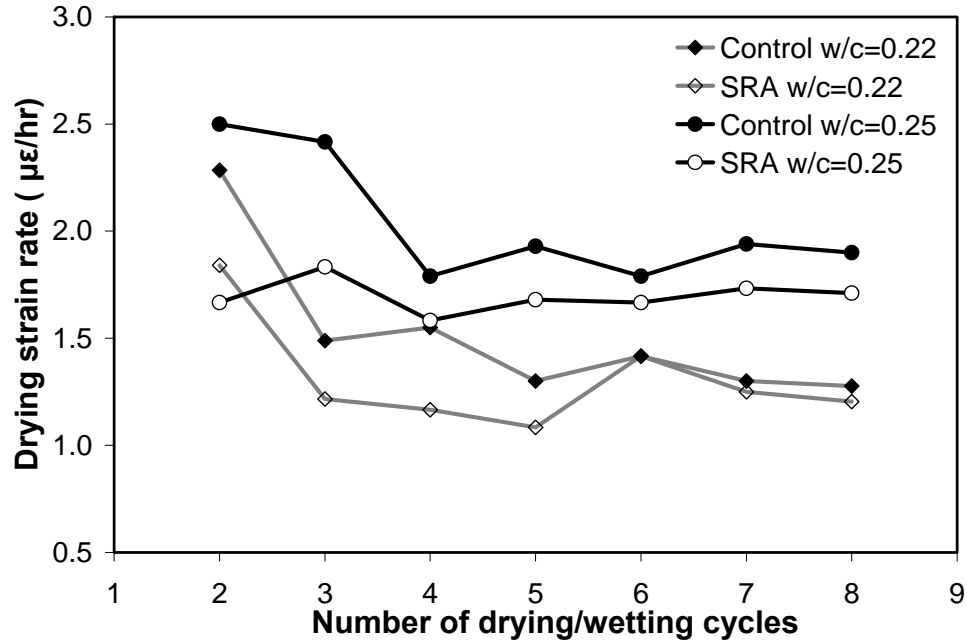
Figure 5-9: Drying strain rate during drying/wetting cycles for control and SRA UHPC specimens.

Secondly, mixtures incorporating SRA had higher efficiency in reducing the drying strain rate during the early period compared to that of control mixtures, but had a lower efficiency at later stage. Furthermore, UHPC specimens incorporating SRA exhibited about 36 and 14% reduction in the developed strain during the initial drying period compared to that of the w/c=0.22 and 0.25 control specimens, respectively. This strain reduction due to incorporating SRA continued to decrease with the application of *DW* cycles. Moreover, submerged specimens incorporating SRA showed similar shrinkage strain to that of the submerged control specimens with no SRA. **Figure 5-10** shows the measured shrinkage strain after fixing the strain to zero at the end of the expansion period. Therefore, it is hypothesized that SRA is washed out with migrating water since SRA is a chemical that reduces the pore fluid surface tension but does not

chemically combine with other hydration products (Rodden and Lange, 2004). To validate this hypothesis, chemical oxygen demand (COD) tests were conducted on water samples taken from the submersion tanks. The COD test is based on the fact that nearly all organic compounds can be oxidized by strong oxidizing agents (Sawyer *et al.*, 2003). Specifically, the COD test measures the total amount of oxygen required to oxidize the organic matter in a water sample, regardless of the biodegradability of the organic substances. Hence, it is widely used for measuring water quality.
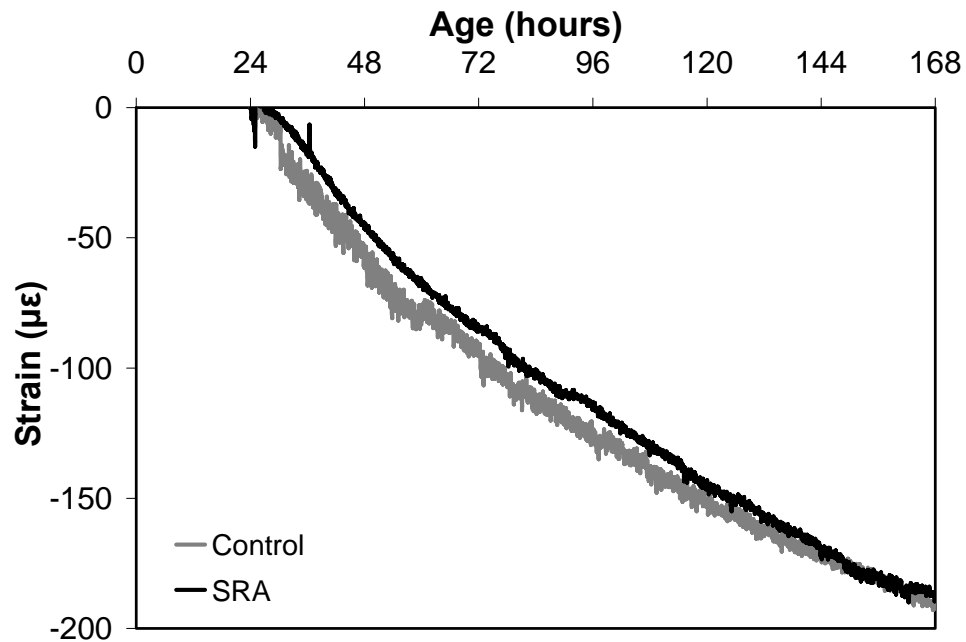
Figure 5-10: Measured strain after the early expansion period under submerged condition.

Figure 5-11 (a,b) show the COD values for the control and SRA mixtures. The results confirm the existence of SRA in the submerging water. The cumulative SRA percentage increased with time, which indicates continuous washout of SRA. However,

the w/c=0.22 mixture incorporating SRA showed lower COD values compared to that of the w/c=0.25 mixture with SRA, which indicates a reduction in the amount of washed out SRA. Based on the COD value for organic SRA, about 17% and 22% of the SRA was washed out from the w/c=0.22 and 0.25 mixtures by the end of the investigated period, respectively. In the case of *DW* cycles, COD values decreased simultaneously with *DW* cycle repetition, especially for the w/c=0.22 mixture, which showed a significant reduction in the COD values after the first cycle, as shown in **Fig. 5-11(b)** This can be attributed to the reduction and depercolation of capillary pores by hydration products as mentioned before. In addition, the ability of SRA to migrate to the curing water decreased as the SRA concentration in the specimens decreased with time due to SRA leaching.

(a)
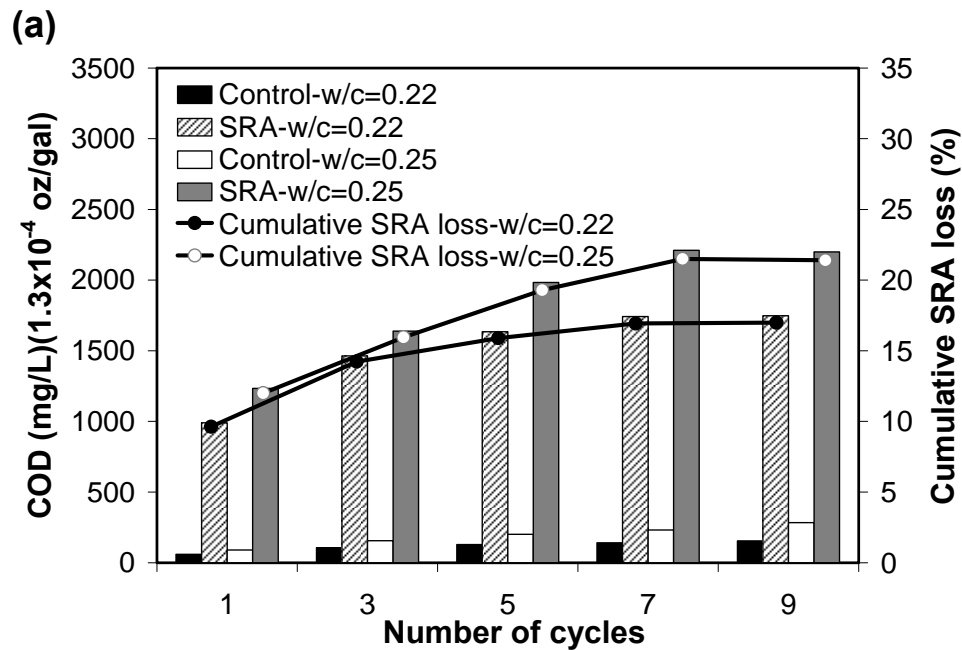
Figure 5-11: COD values for control and SRA UHPC specimens under a) submerged condition and b) drying/wetting cycles.

(b)
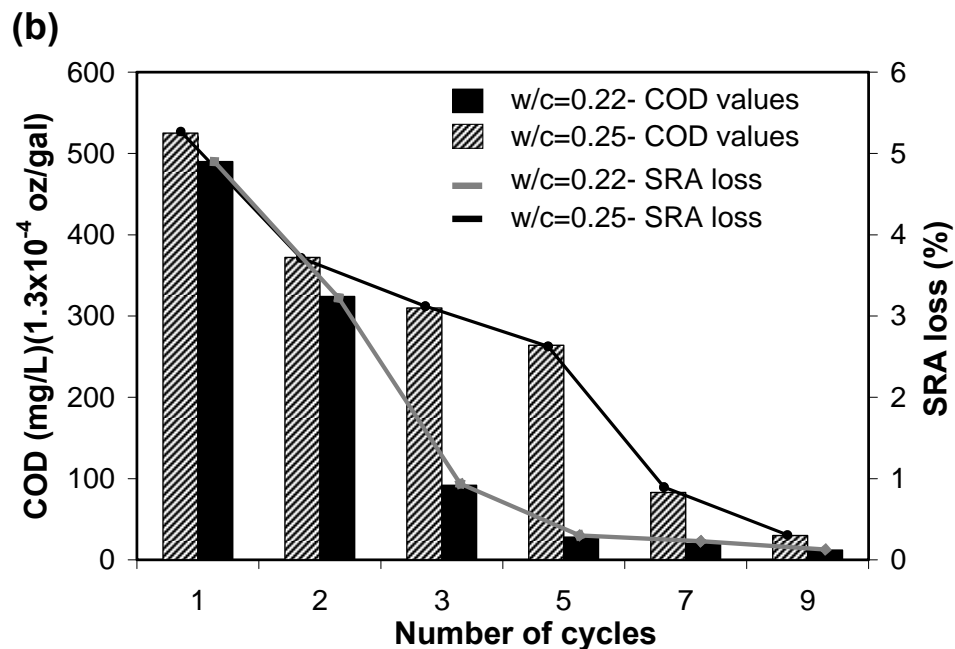
Figure 5-11 Cont'd: COD values for control and SRA UHPC specimens under a) submerged condition and b) drying/wetting cycles.

5.4.2.3 Effect of SAP

Figure 5-12 illustrates the shrinkage strain development for w/c=0.25 UHPC specimens incorporating SAP under different curing conditions. Regardless of the w/c, UHPC specimens incorporating SAP showed higher mass loss during drying than that of the control mixtures, yet showed a significantly lower total shrinkage. This can be ascribed to the effect of the pore size distribution and developed capillary tensile stress (Wittmann, 1982). According to the Laplace law (**Eq. 5-2**), this capillary stress is highly affected by the radius of the pore (r_s) in which the meniscus forms. Therefore, water loss from smaller pores will probably induce higher capillary tensile forces, leading to higher shrinkage (Aly and Sanjayan, 2009, Collins and Sanjayan, 2000).

$$\sigma_c = -\frac{2\gamma \cdot \cos\theta}{r_s}$$ **Eq. 5-2**

Where σ_c is the capillary stress, γ is the surface tension of the pore solution, θ is the contact angle between the pore solution and the solid (often assumed to be 0°), and r_s is the average radius of meniscus curvature.
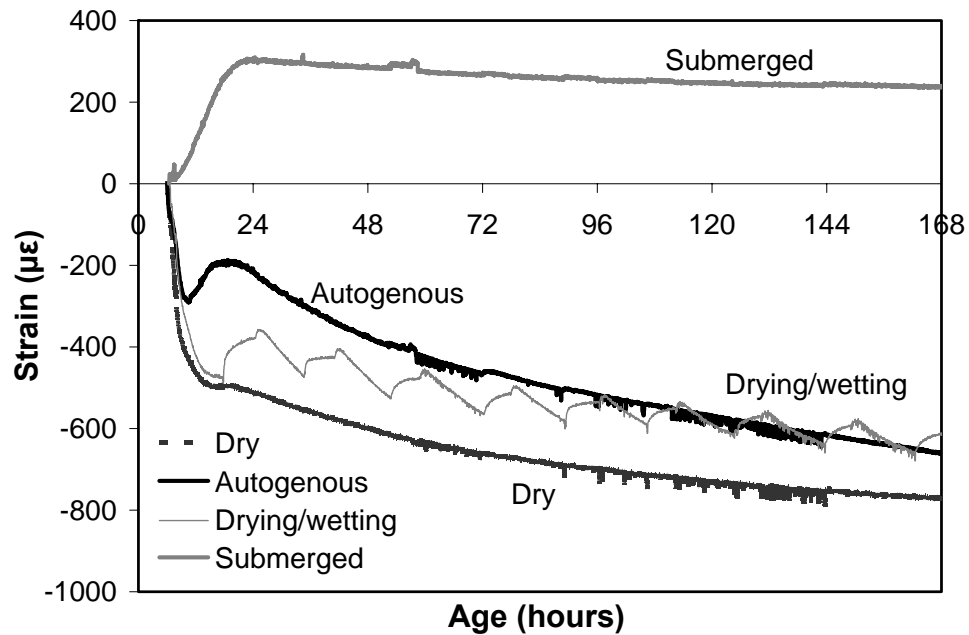
Figure 5-12: Measured strain for w/c=0.25 UHPC specimens incorporating 0.6% SAP under different exposure conditions.

Analysis of the incremental pore size distribution data from MIP tests showed that SAP specimens had a proportion of finer pore size similar to that of the control specimens as shown in **Fig. 5-13**. The different pore sizes were classified according to the International Union of Pure and Applied Chemistry system (IUPAC) (IUPAC, 1972). The calculated (r_s) values were higher for SAP specimens than that for the control

specimens with no SAP, as shown in **Table 5-1**. This is expected to result in lower capillary stress, leading to lower shrinkage regardless the mass loss. The parameter (r_s) was calculated following the same procedure reported by (Aly and Sanjayan, 2009, Collins and Sanjayan, 2000). Furthermore, since the UHPC tested had a very low w/c (i.e. w/c=0.22 and 0.25), the contribution of autogenous shrinkage to the total shrinkage cannot be ignored. Therefore, a percentage of the total shrinkage reduction can be ascribed to a reduction in the autogenous shrinkage induced by SAP in drying specimens (Jensen and Hansen, 2002).
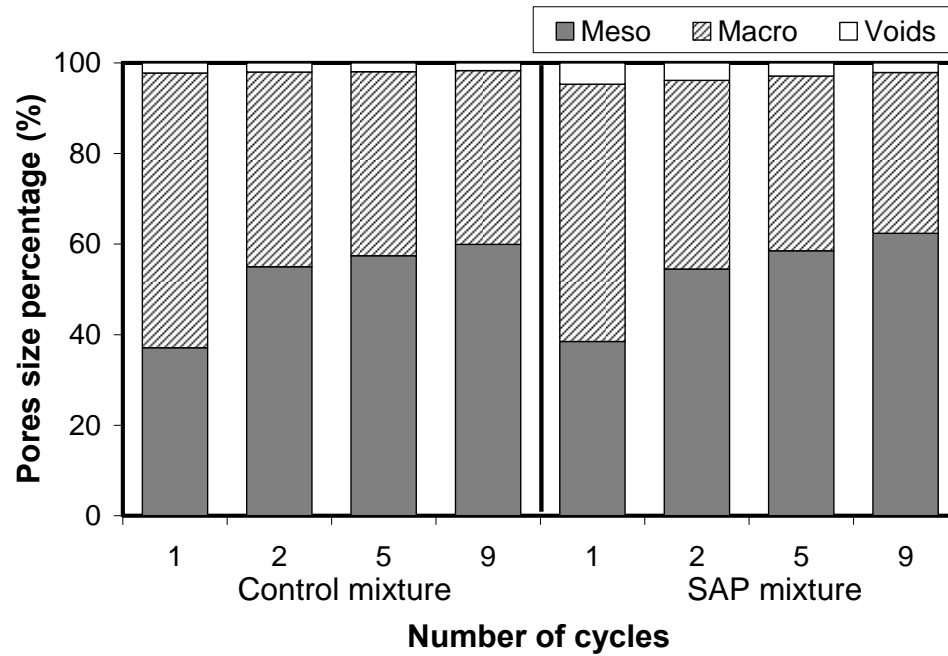
Figure 5-13: Pore size percentage for w/c=0.25 control and SAP UHPC specimens under drying conditions.

Table 5-1: Computation of (r_s) for control and SAP mixtures under drying conditions and drying/wetting cycles

	Control			SAP		
	Drying conditions					
Number of cycles	1	5	9	1	5	9
% Moisture loss from	1.50	2.00	2.20	1.68	2.43	2.55
Volume of water dried	3.10	4.20	4.60	3.55	5.18	5.51
Total porosity (from MIP)	14.8	11.1	9.66	14.51	11.4	10.6
r_s (nm)	70.0	46.0	16.00	90.00	65.0	22.0
	DW cycles					
Number of cycles	3	5	9	3	5	9
% Moisture loss from	1.19	1.42	1.13	1.27	1.33	1.22
Volume of water dried	2.54	3.04	2.48	2.72	2.89	2.59
Total porosity (from MIP)	12.5	10.2	9.56	13.83	9.69	8.57
r_s (nm)	65.0	38.0	12.00	36.00	20.0	8.00

On the other hand, SAP specimens showed mass loss and net shrinkage under *DW* cycles higher than those of the control specimens at different w/c ratios. Moreover, the shrinkage rate was much higher than that of the control specimens. Analysis of the TGA and MIP results for UHPC specimens incorporating SAP under *DW* cycles indicates that such specimens had higher degree of hydration and lower value of the parameter (r_s) compared to that of the control specimens subjected to *DW* cycles as shown in **Fig. 5-14** and **Table 5-1**. SAP particles have a high tendency to absorb water and expand (Jensen and Hansen, 2001). Hence, it is expected that SAP will absorb water during the wetting period, leading to higher expansion as a result of SAP particles swelling. During the drying period, SAP particles release water and occupy smaller volume (Wang *et al.*, 2009), thus leading to an additional shrinkage strain along with drying and autogenous strains. Furthermore, SAP enhances the hydration process leading to a higher degree of

hydration and smaller capillary pores. The smaller the capillary pores (i.e. parameter

(r_s)), the higher the capillary stress induced by water loss during the drying period, thus

resulting in higher shrinkage.
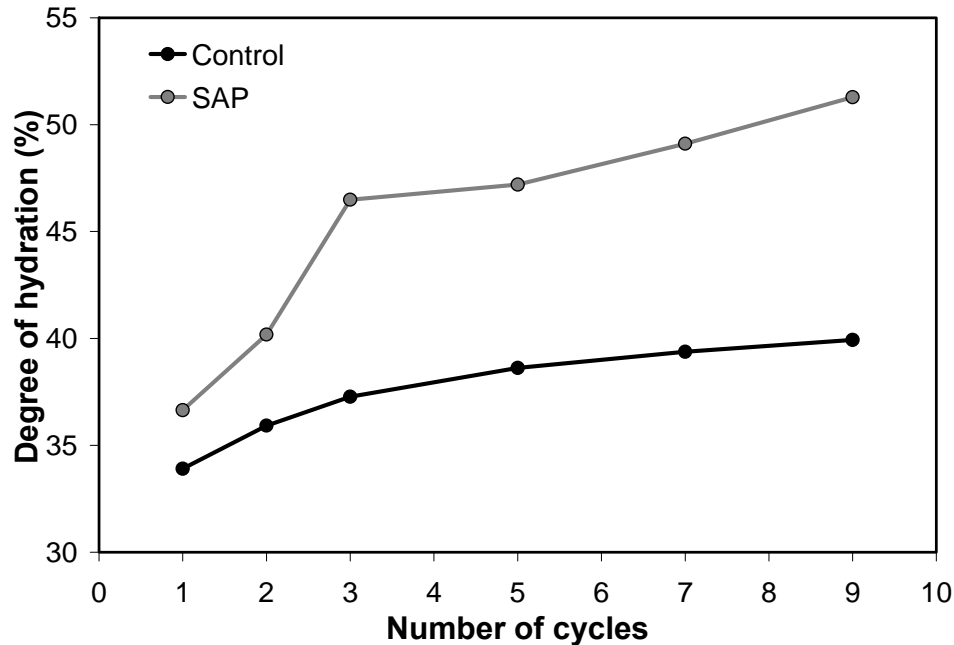
**Figure 5-14: Degree of hydration for w/c=0.25 control and SAP UHPC specimens
under drying/wetting cycles.**

However, UHPC specimens incorporating SAP gained less mass under *SM*

conditions, but exhibited higher early expansion compared to that of the control

specimens. For instance, after 24 hours specimens incorporating SAP exhibited about

70% and 81% higher expansion strains compared to that of the control specimens with

w/c=0.22 and 0.25, respectively. Moreover, SAP specimens showed a significant

reduction in the developed shrinkage after the initial swelling compared to that of the

control and SRA specimens. As a result, the net strain at the end of the investigation

period was an expansion (about 122 and 237 με for mixtures with w/c=0.22 and 0.25, respectively). During the early period, submerged specimens absorb water leading to mass increase and swelling, as can be observed in **Figs. 5-3** and **5-12**. On the other hand, sealed specimens showed a high autogenous shrinkage (**Fig. 5-12**), which is likely attributed to self-desiccation (Ma *et al.*, 2004). Therefore, it can be expected that the imbibed water effectively mitigates self-desiccation during the early period rather than the SAP itself. Once depercolation of capillary pores occurred, water stored inside SAP particles started its role in mitigating self-desiccation. This would explain the relatively lower shrinkage rate after the initial swelling for submerged SAP specimens compared to that of the control specimens. **Figure 5-15** captures this behaviour in which the strain curves for the *SM* condition were initiated to zero at the end of the swelling. The reduction in shrinkage strains after the early expansion was about 52% and 66 % for mixtures incorporating SAP compared to that of the control mixtures with w/c=0.22 and 0.25, respectively.
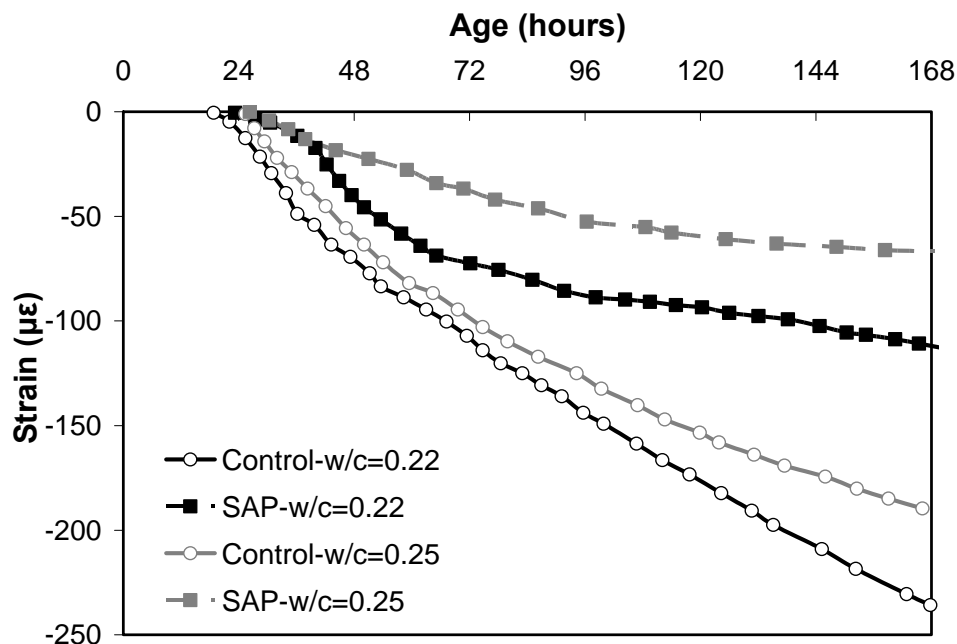
Figure 5-15: Measured strain for control and SAP UHPC specimens under SM condition after early expansion

5.4.2.4 Synergistic Effect of SRA and SAP

To investigate a possible synergistic effect of SRA and SAP, an additional mixture with w/c=0.25 and incorporating both 2% SRA and 0.6% SAP was tested. This mixture (noted MSS) achieved higher efficiency in reducing shrinkage strains under different exposure conditions. **Table 5-2** shows the percentages of shrinkage strain reduction of MSS compared to those of the other mixtures. Under *SM* conditions, MSS specimens showed high expansion during early-age, similar to that of UHPC specimens incorporating SAP, resulting in a net shrinkage strain reduction of about 70% and 71% compared to that of the control and SRA specimens. Moreover, the measured COD for MSS specimens indicated only 5% reduction in SRA loss compared to that of the SRA specimens. Hence, SAP can be considered to have the dominant effect under *SM* conditions.

Under *DW* cycles, MSS specimens showed a significant reduction in shrinkage strains compared to that of the other mixtures as shown in **Table 5-2**. Moreover, COD results indicated a significant reduction in SRA loss during *DW* cycles. After the first *DW* cycle, the net measured COD value for the MSS mixture was about 525 mg/L, which is similar to that of the SRA mixture. At the end of the second cycle, the net measured COD value was about 129 mg/L compared to 372 mg/L for the SRA mixture (about 65% reduction). On the other hand, MSS specimens showed lower mass loss and shrinkage strains compared to that of the SAP mixture specimens. This can be explained as follows: SAP supplies water for further hydration and consequently a denser pore structure is developed. This, in turn leads to a smaller meniscus radius which results in higher capillary stresses. However, the developed denser pore structure also reduces the amount of washed out SRA, which decreases the surface tension of the pore water, leading to lower mass loss and capillary stresses. Hence, the synergistic effect of SRA and SAP optimizes the mutual benefits of these shrinkage mitigation methods and could overcome their individual deficiencies in the various exposure conditions. However, further research is needed to investigate this synergistic mechanism in order to possibly develop a new generation of high- performance shrinkage mitigation admixtures.

Table 5-2: Percentage of reduction in shrinkage strain for each exposure condition due to incorporating both SRA and SAP compared to reference mixtures.

Reference mixtures	% Reduction in strain due incorporating both SRA and SAP			
	Exposure conditions			
	Sealed	Drying	*Drying/Wetting*	*Submerged*
Control	50.0%	52.0%	44.0%	70.0%
SAP	39.0%	40.0%	49.0%	16.0%
SRA	35.0%	42.0%	32.0%	71.0%

5.5. CONCLUSIONS

In this study, UHPC mixtures with different w/c and with or without SRA and SAP were tested under sealed, *SM* and *DW* cycles conditions. Based on this work, the following conclusions can be drawn:

1) Environmental exposure conditions alter the shrinkage behaviour of UHPC with and without shrinkage mitigation methods.

2) Initial high early swelling of submerged specimens results in very low net shrinkage strain.

3) The washout of SRA during *SM* and/or *DW* cycles can dismiss its effectiveness in mitigating shrinkage strains.

4) Using SAP under *DW* cycles can result in higher shrinkage strains of UHPC since it stimulates a higher degree of hydration (i.e. smaller capillary pores) leading to higher capillary tensile stress.

5) Using SAP under submerging condition is very effective in reducing the developed shrinkage strain.

6) Using a combination of SRA and SAP creates a synergistic effect whereby the benefits of these shrinkage mitigation methods are optimized. This allows overcoming their individual deficiencies under different exposure conditions, which is promising for developing a new generation of high-performance shrinkage mitigation admixture with dual effect.

5.6.   REFERENCES

Acker, P. and Behloul, M., (2004), "Ductal ® technology: A large spectrum of properties, a wide range of applications" In: *Proceedings of the International Symposium on UHPC*, Kassel, Germany, pp. 11-23.

Aïtcin, P.C., (1998). High-Performance Concrete, 4th Edition, Taylor & Francis, London, 591 p.

Alford, N.N. and Rahman, A.A., (1981), "An assessment of porosity and pore sizes in hardened cement pastes," *Journal of Materials Science*, Vol. 16, No. 11, pp. 3105-3114.

Aly, T. and Sanjayan, J.G., (2009), "Mechanism of early age shrinkage of concretes," *Materials and Structures*, Vol. 42, No. 4, pp. 461-468.

Bentz, D.P. and Garboczi, E.J., (1991), "Percolation of phases in a three-dimensional cement paste microstructural model," *Cement and Concrete Research*, Vol. 21, No. 2-3, pp. 325-344.

Bentz, D.P., Geiker, M.R. and Hansen, K.K., (2001), "Shrinkage-reducing admixtures and early-age desiccation in cement pastes and mortars," *Cement and Concrete Research*, Vol. 31, No. 7, pp. 1075-1085.

Bentz, D.P. and Jensen, O.M., (2004), "Mitigation strategies for autogenous shrinkage cracking," *Cement and Concrete Composites*, Vol. 26, No. 6, pp. 677-685.

Bentz, D.P., (2006), "Influence of shrinkage-reducing admixtures on early-age properties of cement pastes," *Journal of Advanced Concrete Technology*, Vol. 4, No. 3, pp. 423-429.

Cheyrezy, M., Maret, V. and Frouin, L., (1995), "Microstructural analysis of RPC (Reactive Powder Concrete)," *Cement and Concrete Research*, Vol. 25, No. 7, pp. 1491-1500.

Chunqiu, L., Kefei, L. and Zhaoyuan, C, (2008), "Numerical analysis of moisture influential depth in concrete during drying-wetting cycles," *Tsinghua Science and Technology*, Vol. 13, No. 5, pp. 696-701.

Collins, F. and Sanjayan, J.G., (2000), "Effect of pore size distribution on drying shrinking of alkali-activated slag concrete," *Cement and Concrete Research*, Vol. 30, No. 9, pp. 1401-1406.

Cook, R.A. and Hover, K.C., (1999), "Mercury porosimetry of hardened cement pastes," *Cement and Concrete Research*, Vol. 29, No. 6, pp. 933-943.

Cusson, D. and Hoogeveen, T.J., (2006), "Measuring early-age coefficient of thermal expansion in high-performance concrete," *International RILEM Conference on*

Volume Changes of Hardening Concrete: Testing and Mitigation, Lyngby, Denmark RILEM Publications SARL, pp. 321-330.

Cusson, D. and Hoogeveen, T.J., (2007), "An experimental approach for the analysis of early-age behaviour of high-performance concrete structures under restrained shrinkage," *Cement and Concrete Research*, Vol. 37, No. 2, pp. 200-209.

Dhir, R.K. and McCarthy, M.J., (1999), "Concrete Durability and Repair Technology." Proceedings of International Conference : Creating with Concrete, Dyer T.D., Henderson, N.A, and Jones R.M (ed.), Thomas Telford, Scotland, U.K., 794 p.

Garas, V.Y., Kahn, L.F. and Kurtis, K.E., (2009), "Short-term tensile creep and shrinkage of ultra-high performance concrete," *Cement and Concrete Composites*, Vol. 31, No. 3, pp. 147-152.

Hannah, R.L. and Reed S.E., (1992). Strain Gage Users' Handbook, 1st Edition, Springer, New York, 496 p.

Holschemacher; K., Weiße, D. and Klotz, S., (2004), "Bond of Reinforcement in Ultra High Strength Concrete", *Proceedings of the International Symposium on UHPC*, Kassel, Germany, pp. 375-388.

Holschemacher, K. and Weiße, D., (2005), "Economic mix design of ultra high strength concrete" *Proceedings of the 7th International Symposium on Utilization of High-Strength/ High-Performance Concrete*, Washington D.C., Vol. 2, pp.1133-1144.

Ichinomiya, T., Hishiki, Y., Ohno, T., Morita, Y. and Takada, K., (2005), "Experimental study on mechanical properties of ultra-high-strength concrete with low-autogenous-shrinkage," *ACI Materials Journal*, Vol. 228, pp. 1341-1352.

IUPAC, (1972). Manual of Symbols and Terminology, Appendix 2, Part 1. In: Colloid and Surface Chemistry, *Pure Applied Chemistry*, Vol. 31, 578 p.

Jensen, O.M. and Hansen, P.F., (2001), "Water-entrained cement-based materials: I. Principles and theoretical background," *Cement and Concrete Research*, Vol. 31, No. 4, pp. 647-654.

Jensen, O.M. and Hansen, P.F., (2002), "Water-entrained cement-based materials: II. Experimental observations," *Cement and Concrete Research*, Vol. 32, No. 6, pp. 973-978.

Kovler, K., (1996), "Why sealed concrete swells," *ACI Materials Journal*, Vol. 93, No. 4, pp. 334-340.

Lea, F.M. and Hewlett, P.C., (1998). Lea's Chemistry of Cement and Concrete, 4th Edition, John Wiley & Sons, New York, 1057 p.

Loukili, A., Khelidj, A. and Richard, P., (1999), "Hydration kinetics, change of relative humidity, and autogenous shrinkage of ultra-high-strength concrete," *Cement and Concrete Research*, Vol. 29, No. 4, pp. 577-584.

Lstiburek, J. and Carmody, J., (1994). Moisture Control Handbook: Principles and Practices for Residential and Small Commercial Buildings, 2nd Edition, John Wiley & Sons, New York, 232 p.

Ma, J., Dehn, F., Tue, N.V., Orgass, M. and Schmidt, D., (2004), "Comparative investigation on ultra-high performance concrete with and without coarse aggregate," *Proceedings of the International Symposium on UHPC*, Kassel, Germany, pp. 206-212.

Martys, N.S. and Ferraris, C.F., (1997), "Capillary transport in mortars and concrete," *Cement and Concrete Research*, Vol. 27, No. 5, pp. 747-760.

Neville, A.M., (1996). Properties of Concrete, 4th Edition, John Wiley &Sons, New York, 797 p.

Ribeiro, A.B., Gonçalves, A. and Carrajola, A., (2006), "Effect of shrinkage reducing admixtures on the pore structure properties of mortars," *Materials and Structures*, Vol. 39, No. 2, pp. 179-187.

RILEM Report 25, (2003), "Early-age Cracking in Cementitious Systems," In: *RILEM Technical Committee 181-EAS: Early-age Shrinkage Induced Stresses and Cracking in Cementitious Systems*, A. Bentur (ed.), 335 p.

Rodden, R.A. and Lange, D.A., (2004), "Feasibility of shrinkage reducing admixtures for concrete runway pavements," Technical note No. 4, *The Center of Excellence for Airport Technology (CEAT)*, 6 p.

Sawyer, C.N., McCarty, P.L. and Parkin, G.F., (2003). Chemistry for Environmental Engineering and Science, 5th Edition, McGraw-Hill Professional, New York, 752 p.

Schmidt, M. and Fehling, E., (2005), "Ultra-high-performance concrete: research, development and application in Europe" *Proceedings of the 7th International Symposium on Utilization of High-Strength/High-Performance Concrete*, Washington D.C., Vol. 1, pp. 51-77.

Sule, M. and Van Breugel, K., (2001), "Cracking behavior of reinforced concrete subjected to early-age shrinkage," *Materials and Structures*, Vol. 34, No. 5, pp. 284-292.

Tazawa, E., (1999), "Autogenous Shrinkage of Concrete," *Proceedings of the International Workshop organized by the Japan Concrete Institute*, Hiroshima, Japan, Routledge, Taylor & Francis, New York, 411 p.

Teichmann, T. and Schmidt, M., (2004), "Influence of packing density of fine particles on structure, strength and durability," *Proceedings of the International Symposium on UHPC*, Kassel, Germany, pp. 227-237.

Turcry, P., Loukili, A., Barcelo, L. and Casabonne, J.M., (2002), "Can the maturity concept be used to separate the autogenous shrinkage and thermal deformation of a cement paste at early age?," *Cement and Concrete Research*, Vol. 32, No. 9, pp. 1443-1450.

Wang, F., Zhou, Y., Peng, B., Liu, Z. and Hu, S., (2009), "Autogenous Shrinkage of Concrete with Super-Absorbent Polymer," *ACI Materials Journal*, Vol. 106, No. 2, pp. 123-127.

Weiss, J., Lura, P., Rajabipour, F. and Sant, G., (2008), "Performance of shrinkage-reducing admixtures at different humidities and at early ages," *ACI Materials Journal*, Vol. 105, No. 5, pp. 478-486.

Wittmann, F.H., (1982), "Creep and shrinkage mechanisms," In: *Creep and Shrinkage in Concrete Structures*, Bazant, Z.P. and Wittmann, F.H. (ed.), Wiley, Chichester, pp. 129-161.

Yazici, H., (2007), "The effect of curing conditions on compressive strength of ultra high strength concrete with high volume mineral admixtures," *Building and Environment*, Vol. 42, No. 5, pp. 2083-2089.

CHAPTER SIX

SELF-RESTRAINING SHRINKAGE CONCRETE: MECHANISMS AND EVIDENCE *

In the previous chapters, the effect of environmental conditions (i.e. field-like conditions) and active shrinkage mitigation techniques on the early-age shrinkage behaviour of UHPC was investigated. It was proven that the addition of shrinkage reducing admixture and/or superabsorbent polymer can significantly reduce shrinkage under different exposure conditions. However, a number of disadvantages including, reduction in mechanical properties, retarding hydration process, higher water loss, higher porosity, washing out effect and cost, are still limiting these materials applications. Further, these shrinkage mitigation techniques do not provide a reduction in the environmental impact of concrete production. In this chapter, a passive shrinkage mitigation technique is introduced as a solution that provides adequate benefits for both facets.

6.1.   INTRODUCTION

Once water comes in contact with cement, exothermic chemical reactions (so-called hydration reactions) initiate, leading to the formation of hydration products (Neville, 1996). These hydration products connect un-hydrated cement particles and other concrete constituents together to form the internal microstructure of concrete (Struble *et al.*, 1980). As hydration reactions progress with time, the concrete microstructure gains rigidity and increased ability to resist different stresses (Roy and Idorn, 1993).

---

*Some parts of this chapter (Part 1) were accepted by the ACI Materials Journal. Other parts (Part 2) have been submitted for review to Cement and Concrete Research.

On the other hand, the volume occupied by hydration products will be less than that occupied by its reactants before hydration, leading to a volume contraction. This internal deformation is known as chemical shrinkage (Le Chatelier contractions) (Mehta and Monteiro,2006). Under sealed conditions, the progress of hydration reactions and associated chemical shrinkage will result in an external bulk deformation, which is referred to as autogenous deformation (Kovler and Zhutovsky, 2006, Hansen, 2011). Hence, chemical shrinkage can be considered as the main driving force behind autogenous deformation (Barcelo *et al*., 2001). Such an early-age shrinkage of concrete is a complex physico-chemical phenomenon, which is related to the hydration reactions and progressive hardening of the concrete skeleton.

This chapter describes a new concept for reducing early-age shrinkage in hydrating cement-based materials through the addition of partially hydrated cementitious materials (PHCM) as a concrete admixture. During the mixing of concrete, the added PHCM will form restraining clusters, which essentially consist of a hydrated cement paste structure and micro-crystals of hydration products. Conceptually, this is similar to the role played by un-hydrated cement particles and aggregates, which impart a passive internal restraint within concrete (Bentz and Jensen, 2004). The PHCM technique creates deformation resistance as early as the cementitious materials are mixed through developing a connected strength-gaining skeleton at the fresh stage. An explanation of the mechanism and rationale of the PHCM technique is given below; validity and benefits are also discussed below.

6.2. EARLY-AGE PHASES AND AUTOGENOUS SHRINKAGE IN CEMENTITIOUS MATERIALS

Early-age shrinkage is defined as a volume change occurring immediately after placing concrete up to the age of about 24 hours (Holt, 2001). During this time the structural development in concrete can be categorized into three stages (Esping, 2007) (i) liquid stage when concrete is plastic, workable, and having a visco-elastic behaviour, (ii) skeleton formation stage (semi-plastic) when concrete undergoes early stiffening and a transition from fluidity to rigidity through the progressive forming a self-supporting skeleton which usually begins after the initial setting), and (iii) hardened (rigid) stage which starts at the point of final setting when the concrete starts developing mechanical strength as a result of continuing hydration reactions.

At the liquid stage, when no significant skeleton that restrains deformation exists, autogenous shrinkage is considered to be equal to chemical shrinkage (Barcelo *et al.*, 2001, Holt, 2001). Once concrete enters the skeleton formation stage, a self-supporting skeleton starts to form; hence, autogenous shrinkage will diverge from chemical shrinkage since the rigidity of the paste restrains volume changes (Mehta and Monteiro,2006). At this stage, the rate of autogenous shrinkage will decrease to about (1/10) of the rate of chemical shrinkage (Hammer, 1999a). In conclusion, autogenous shrinkage initially originates from the chemical shrinkage, once the concrete set the development of a contracting capillary pore pressure will control the subsequent deformations (Hansen, 2011).

Autogenous and chemical shrinkage are influenced by several factors. However, these factors can have similar or conflicting effects on autogenous and chemical shrinkage. Indeed, factors that increase chemical shrinkage may reduce autogenous shrinkage, for instance when they reduce the setting time and/or generate a more rigid restraining structure (Esping, 2007).

6.3. EARLY-AGE SHRINKAGE MITIGATION TECHNIQUES

Early-age shrinkage can be more likely to cause cracking than long-term shrinkage since it develops more rapidly and occurs when the cement-based material still has low mechanical properties (Holt and Leivo, 2004). When formed, cracks may reduce strength, jeopardize durability, cause loss of pre-stress, etc. Therefore, different strategies for mitigating early-age shrinkage cracking have been proposed.

Understanding the relationships amongst forces existing in a cement paste during various early-age phases, their sources and how they affect the overall behaviour is key to tailoring effective shrinkage mitigation strategies. According to the Laplace equation (**Eq. 6-1**), at the maximum capillary pore radius filled with water, water is under tensile stresses:

$$P_{ca} = \frac{-2 \cdot \sigma \cdot \cos(\theta)}{r}$$

Eq. **6-1**

Where P_{ca} is the tensile stress in the pore solution, σ is the surface tension of the pore solution, θ is the wetting angle of the solid with pore solution, and r is the radius of the meniscus curvature. The tensile stresses developed in the capillary water must be

balanced by compression stresses on the surrounding solid (Kovler and Zhutovsky, 2006). During the liquid phase, the induced capillary stresses are greater than the bonding strength among cement paste particles; hence, the particles will be rearranged in the water. At that time, autogenous shrinkage is considered to be equal to chemical shrinkage (Barcelo *et al*., 2001, Tazawa, 1999). Once a solid path within the material is developed, the material rigidity gradually increases due to increasing connectivity of the solid particles; the bond strength among particles becomes greater than capillary stresses. This moment is known as the mineral percolation threshold (Barcelo *et al*., 2001).

Consequently, the developed skeleton starts restraining particle displacements; however, it does not yet have sufficient strength to resist compressive stresses, which results in a volume decrease (i.e. bulk shrinkage). Meanwhile, water will move within the paste without particle displacements. Hence, autogenous shrinkage starts to diverge from chemical shrinkage (Justens *et al*., 1996, Hammer, 1999b). As hydration reactions progress, the paste skeleton gains increased strength to resist further three-dimensional deformation and air voids develop within capillary pores, leading to self-desiccation (Barcelo *et al*., 2001). Once the breakthrough pressure has been reached, the water meniscus cannot find a stable position due to discontinuity of the water system. Hence, a collapse of capillary pressure takes place (Wittmann, 1976). Therefore, early-age shrinkage of cementitious materials is mainly related to the development of capillary stresses, internal self-desiccation, and the strength of the restraining skeleton. **Figure 6-1** illustrates a correlation between cement paste structure development and volume change during different early-age stages.

| Initial Vol. | Vol. after particles rearrangement | Vol. after Initial setting | Vol. after hardening |
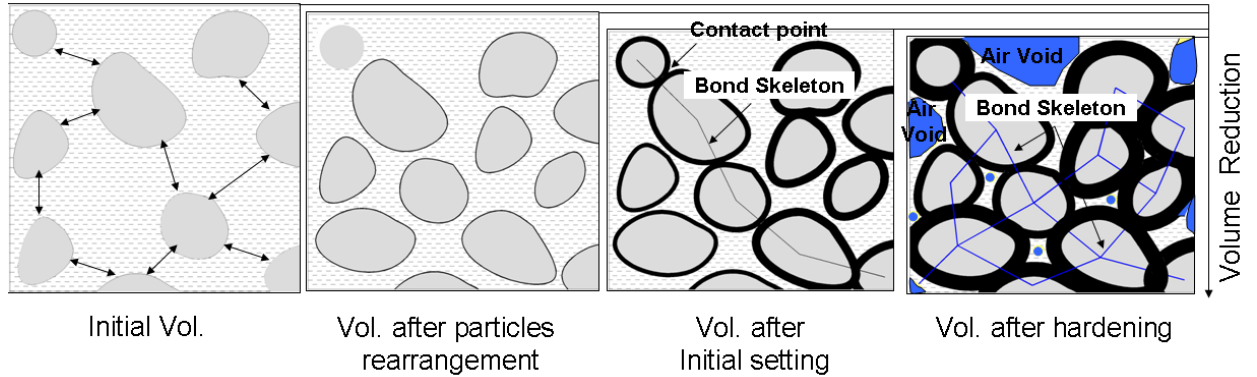
Figure 6-1: Structure development and volume change during different early-age stages.

Considering the various mechanisms discussed above, several concrete shrinkage mitigation techniques have been proposed. The first mitigation strategy deals with the surface tension of the pore solution. The latter is indeed a critical parameter for autogenous shrinkage as it directly affects capillary stress based on Laplace's equation (**Eq. 6-1**). The most commonly used material in this category is shrinkage-reducing admixtures (SRA). SRA decrease the surface tension of the pore solution, hence, it is considered as a direct method for reducing autogenous shrinkage (Tazawa and Miyazawaa, 1995a). However, possible disadvantages of SRA include a reduction of its effectiveness over time due to absorption of SRA by hydration products, destabilization of the entrained air void system (Schemmel *et al*., 1999), delaying the setting time and retardation of hydration reactions, thus leading to reduced mechanical strength (Bentz, 2006). Moreover, the surface tension is also influenced by temperature, which may result in dosage variations to achieve optimum behaviour (Jensen and Hansen, 1999). In addition, washing out effect of SRA can significantly reduce it shrinkage mitigation efficiency as illustrated in chapter 5.

The second shrinkage mitigation strategy deals with both the radius of the water meniscus of the largest water-filled pore within the microstructure and the availability of water for hydration. These two parameters have a significant effect on capillary stresses and the internal self-desiccation process. In this strategy, internal curing techniques have been proposed, including the use of saturated lightweight aggregate particles with coarser pores (i.e. larger radius) (Bentur *et al*., 2001). This results in the development of lower capillary stress since the formation of empty pores due to chemical shrinkage first takes place in such coarser pores (in the aggregate) and does not involve relatively finer pores in the cement paste (Henkensiefken *et al*., 2010). In addition, the water contained within the saturated aggregate pores provides internal curing for the hydrating cement paste. Nevertheless, difficulties in controlling the consistency of the rheological properties of concrete incorporating such aggregates, along with potential reductions in its mechanical strength and elastic modulus constitute limitations of this technique. More recently, based on a similar principle to that of saturated lightweight aggregate particles, superabsorbent polymer particles (SAP) have been proposed as a shrinkage mitigation admixture for concrete (Jensen and Hansen, 2001). SAP is a more direct technique which produces a better controlled microstructure since it uniformly distributes the curing water.

While significant research has investigated the above shrinkage mitigation strategies, to the best of the authors' knowledge, research dedicated to exploring the effect of a restraining skeleton on shrinkage is rather scarce. Therefore, the present study focuses on the restraining skeleton concept and pioneers a self-restraining shrinkage system to reduce early-age shrinkage of concrete through the addition of partially hydrated cementitious material.

6.4.   SHRINKAGE RESTRAINING SYSTEMS

The concept of a shrinkage restraining system itself is not new. Generally, un-hydrated cement particles and aggregates constitute an internal restraining system (Bentz and Jensen, 2004), which resists autogenous deformation and reduces physical shrinkage (Tazawa and Miyazawaa, 1995b). However, using a higher aggregate content for reducing autogenous shrinkage in modern concretes such as high performance concrete or self-consolidating concrete is not practical. This is because increasing the aggregate content leads to reducing the paste volume, which is detrimental to workability in low w/c systems (Kovler and Zhutovsky, 2006) or where aggregate friction causes blockage of flow.

One of the key parameters in early-age autogenous shrinkage is the time of hardening (Holt, 2001). This corresponds to the time when the cementitious material has sufficient strength to resist shrinkage stresses. The hydrated cement paste in fresh concrete forms a self-restraining system that reduces the absolute volume contraction (Aitcin, 1999). Therefore, accelerating agents and heat curing which cause an earlier setting and structuring of a stiff skeleton will shorten the period during which early-age autogenous shrinkage occurs (Holt, 2001, Kronlöf *et al*., 1995). However, such accelerating methods also accelerate the rate of autogenous shrinkage along with increasing mechanical strength.

At the micro-level, calcium hydroxide (*CH*) crystals act as a passive restraint and reduce the measured physical shrinkage (Jensen and Hansen, 1996). The hypothesis that *CH* micro-crystals provide restraint was proposed by (Bentz and Jensen, 2004) based on results reported in (Carde and Francois, 1997, Powers, 1962) which indicate a significant

effect of leaching of *CH* crystals on deformation properties. The role of *CH* micro-crystals is schematically illustrated in **Fig. 6-2.**
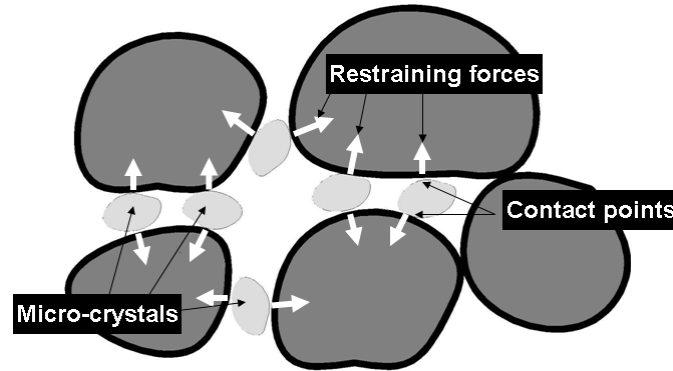
Figure 6-2: Micro-crystals role in restraining deformation.

6.5.   CAN PHCM ADDITION REDUCE CONCRETE SHRINKAGE

The ability of PHCM addition to reduce early-age concrete shrinkage in concrete is affirmative at least for the main reasons below.

First, a cement paste matrix can be divided into two phases, the liquid phase and solid phase (i.e. un-hydrated particles and hydration products). As discussed earlier, emptying of capillary pores in a cementitious material via drying or chemical reactions subjects capillary water to tensile stresses and the solid paste to compressive stresses, which leads to volume reductions (Kovler and Zhutovsky, 2006). The compressive pressure that induces such stresses on the solid paste represents effective pressure transmitted through points of contact between the solid phase particles (Fosså, 2001). This effective pressure can be calculated from **Eq. 6-2**:

$$p' = p - u\left(\frac{A - A_c}{A}\right)$$ **Eq. 6-2**

Where p' is the effective pressure, p is the total pressure, u is the pore water pressure, A is the total area, and A_c is the particle contact area. Increasing contact points between grains increases the resistance to apparent volume changes (Barcelo *et al.*, 2005). During the liquid stage, the bonds and contact areas amongst particles are very small. Hence, the concrete does not resist significant stresses or deformations (Fosså, 2001). As hydration reactions proceed, the contact areas and bond between particles increase, resulting in increased ability to resist deformation. The higher the contact area, the higher is the resistance. Adding PHCM increases the contact areas acting as a load bearing structure for induced compressive stresses. This reduces volume reduction and overall deformation.

Second, the added PHCM provides a sufficient initial amount of hydration product crystals (i.e. calcium silicate hydrate (*CSH*) and *CH*) and induces a hydrated cement paste structure within the original otherwise fresh mixture at the onset of the hydration process. In other words, the PHCM increases the passive internal restraint within the fresh cementitious matrix, which is analogous to the role of un-hydrated cement and aggregate particles. This can be illustrated as follows: in concrete, the hydrated cement paste constitutes a continuous matrix phase; shrinkage can be reduced due to the presence of discrete restraining particles (i.e. un-hydrated cement and aggregates). The volume of the shrinkable paste can be expressed as follows (Hansen, 1987):

$$v_{pc} = v_c - (v_a + v_{uc})$$ **Eq. 6-3**

Where v_{pc} is the volume of paste in concrete, v_c is the volume of concrete, v_a is the volume of aggregate, and v_{un} is the volume of un-hydrated cement. Aggregates and un-hydrated cement particles are assumed to be the sole shrinkage restraining agents. However, concrete contains partially hydrated cement. Thus, the volume of un-hydrated cement should be expressed as follows (Hansen, 1987):

$$v_{un} = v_{co}(1 - \alpha)$$ **Eq. 6-4**

Where v_{co} is the volume of cement added originally and α is the relative degree of hydration, which varies between 0 and 1. Substituting **Eq. 6-4** into **Eq. 6-3**, one obtains the following equation:

$$v_{pc} = v_c - \left[v_a + v_{co}(1 - \alpha) \right]$$ **Eq. 6-5**

Therefore, the relative shrinkage restraining volume (V_d) can be defined as follows (Hansen, 1987):

$$V_d = \frac{v_a + (v_{co}(1 - \alpha))}{v_c}$$ **Eq. 6-6**

For mixtures incorporating PHCM, the added PHCM can be considered as an additional internal shrinkage restraining material, the volume of shrinkage paste can be modified to the following:

$$v_{pc} = \underbrace{\left[v_c - (v_a + v_{co}(1-\alpha_2))\right] \cdot (1-\eta)}_{Part\ 1} + \underbrace{\left[v_c - (v_a + v_{co}(1-\alpha_1)(1-\alpha_2) + v_{co}\alpha_1\right] \cdot \eta}_{Part\ 2}$$

Eq. 6-7

Where *Part 1* represents the volume of paste in the mixture batch before adding PHCM, while *Part 2* represents the volume of paste in the added PHCM; α_1 is the relative degree of hydration of the paste in the added PHCM, η is the percentage of the added PHCM; α_2 is the relative degree of hydration of the paste without PHCM addition. By rearranging **Eq. 6-7**, it can be reduced to the follow:

$$v_{pc} = v_c - \left[v_a + v_{co}(1-\alpha_2 + \eta \cdot \alpha_1 \cdot \alpha_2)\right] = v_c - \left[v_a + v_{co}(1-\alpha_2) + v_{co} \cdot \eta \cdot \alpha_1 \cdot \alpha_2)\right] \quad \textbf{Eq. 6-8}$$

Hence, the relative restraining volume (V_d) can be reformulated to include the effect of the PHCM as follow:

$$V_d = \frac{v_a + v_{co}(1-\alpha_2)}{v_c} + \frac{v_{co} \cdot \eta \cdot \alpha_1 \cdot \alpha_2}{v_c}$$

Eq. 6-9

Comparing the **Eq. 6-6** and **Eq. 6-9**, a new term (i.e. $\frac{v_{co} \cdot \eta \cdot \alpha_1 \cdot \alpha_2}{v_c}$), representing the relative shrinkage resistance induced by the addition of PHCM, is added. Therefore, mixtures incorporating PHCM can possess a higher relative deformation restraining volume compared to that in normal mixtures. According to (Hansen, 1987), the volumetric shrinkage of concrete ($(\Delta v/v)_c$ can be expressed as follows:

$$\left(\frac{\Delta v}{v}\right)_c = \frac{P_{pc}}{K_p}(1-V_d)$$

Eq. 6-10

Where P_{pc} is the total hydrostatic shrinkage stress within the paste in concrete, and K_p is the bulk modulus of the paste. It can be deduced from **Eq. 6-10** that the volumetric

shrinkage of concrete decreases as V_d increases. Hence, it is expected that mixtures incorporating PHCM can exhibit lower shrinkage compared to that in similar mixtures without PHCM.

Third, previous work (Lobo *et al*., 1995) indicated that reused concrete can induce acceleration effect. Hence, this acceleration will increase the very early-age strength (Kronlöf *et al*., 1995) and structure a strong and stiff skeleton frame which withstand forces and limit shrinkage within fresh concrete (higher passive internal restraining system). This is consistent with **Eq. 6-10** which shows that the volumetric shrinkage of concrete is indirectly proportional to the bulk modulus of the paste. Since PHCM addition accelerates the hydration process, resulting in a higher paste bulk modulus, a reduction in volumetric shrinkage can be expected. The main difference between PHCM addition and conventional acceleration techniques is that PHCM accelerates hydration reactions along with inducing a pre-existing passive internal restraint system, which in turn reduces the amount of deformation developed.

6.6.   SOURCES OF PHCM

It is estimated that an annual average of 17.5 million cubic meters of ready mixed concrete produced in the USA is returned to concrete batch plants (Obla *et al*., 2007). The disposal of this returned concrete has serious environmental and economical implications. However, such a returned material can be used as a source of PHCM after some treatment. This treatment may include the use of stabilizing admixtures (Lobo *et al*., 1995) to control the degree of hydration of the *PHCM* before adding to a newly mixed concrete.

6.7.   PARTIALLY HYDRATED CEMENTITIOUS MATERIALS METHODOLOGY

The main idea behind the PHCM technique is to provide a sufficient initial amount of calcium silicate hydrate (CSH) and calcium hydroxide (CH) through adding PHCM to the original mixture at the onset of the hydration process. This can be achieved through mixing the concrete batch in two stages. In the first, a portion of the mixture batch is mixed and stored under adequate curing conditions to avoid altering the quality of the hydrated material due to drying. The second step includes conventional mixing of the remaining portion of the batch with the pre-mixed portion from the first stage. During the elapsed time between the two mixing steps, hydration reactions progress and hydration products are formed within the mixed portion before remixing. The longer the elapsed time and/or the greater the portion mixed in the first step, the higher is the hydration product formation, which enhances the efficiency of the added PHCM as passive internal restraint system.

6.8.   EXPERIMENTAL PROCEDURE

This experimental program aims to gain an understanding of the mechanisms involved in using PHCM. This is of primary importance in order to enable the production of self-restraining concrete. In this study, monitoring of the hydration process and characterization of the cement paste microstructure has been carried out on concrete mixtures incorporating PHCM. The experimental includes two parts. Part I was devoted to validating the addition of PHCM as shrinkage mitigation technique and to evaluate its effect on other early-age properties. The second part focuses on explaining the mechanism of the PHCM technique.

6.8.1. Materials and Mixture Proportions

The materials used in this chapter were similar to that used in Chapter 3 (refer to Section 3.4.1). The chemical and physical properties of the used binders have been given in Chapter 3 (**Table 3-1**). In addition, **Fig. 6-3** shows the NMR spectra for the anhydrous cement and SF used in this study. The peak of the anhydrous cement (Q^0) and SF (Q^4) occur at -71 and -110 ppm, respectively. Three PHCM proportions, namely, 25, 33 and 50% of the batch weight were used to investigate the effect of the PHCM portion on the early-age behaviour. The elapsed time between the two mixing steps was taken equal to 6 hrs according to previous hydration kinetics studies (Odler and Dörr, 1979). The selected composition and proportions for the control and PHCM mixtures, and the characteristics of the tested mixtures are shown in **Tables 6-1** and **6-2**, respectively.

Table 6-1: Composition of control and PHCM mixtures.

Material	Mixture (mass/ cement mass)							
	Control		PHCM 25%		PHCM 33%		PHCM 50%	
	Mixing Stage							
	1	2	1	2	1	2	1	2
Cement	----	1.0000	0.2500	0.7500	0.3300	0.6700	0.5000	0.5000
Silica fume	----	0.3000	0.0750	0.2250	0.0990	0.2010	0.1500	0.1500
Quartz powder	----	0.4300	0.1075	0.3225	0.1419	0.2881	0.2150	0.2150
Quartz sand	----	1.5300	0.3825	1.1475	0.5049	1.0251	0.7650	0.7650
Water	----	0.2500	0.0625	0.1875	0.0825	0.1675	0.1250	0.1250
HRWRA	----	0.0300	0.0075	0.0225	0.0099	0.0201	0.0150	0.0150

Table 6-2: Tested mixtures

Mixture	PHCM (% of the batch weight)
C	0.0
H1	25.0
H2	33.0
H3	50.0
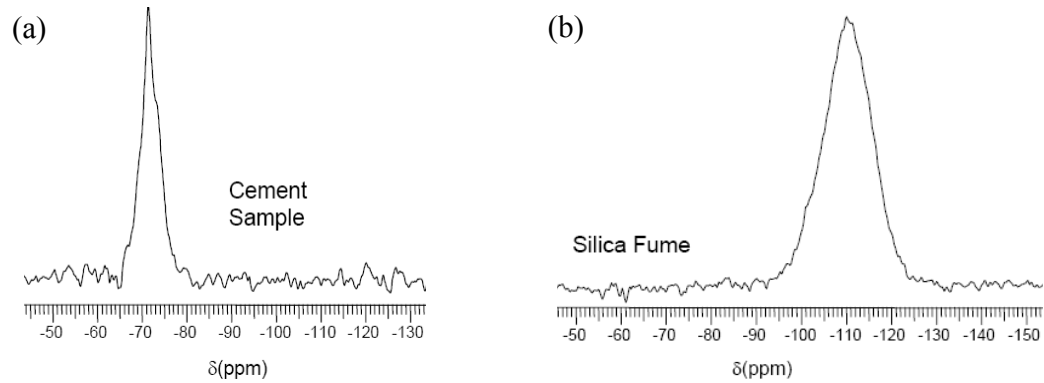
Figure 6-3: NMR spectra for anhydrous a) Portland cement, and b) Silica fume.

6.8.2.   Preparation of Test Specimens and Testing Procedures

The experimental methods used in this chapter are the cubic compressive strength test, Semi-adiabatic calorimetry, TGA, Differential scanning calorimetry (DSC), measurements of total free shrinkage, setting time, the corrugated tube protocol for measuring autogenous shrinkage, and solid-state ^{29}Si MAS-NMR. The cubic compressive strength test, Semi-adiabatic calorimetry, TGA, and measurements of total free shrinkage method were previously explained in chapter 3. The setting time, Differential scanning calorimetry (DSC), the corrugated tube protocol for measuring autogenous shrinkage, and solid-state ^{29}Si MAS-NMR are explained in the following sections.

The time of setting was measured on three replicate paste specimens using a Vicat needle according to ASTM C191 (Standard Test Method for Time of Setting of Hydraulic Cement by Vicat Needle).

The decomposition of different hydration phases (e.g. calcium hydroxide (CH)) can be calculated from DTG results. However, DSC tests were performed as it requires much less time, allowing testing every 2 hrs. The UHPC samples, around 30 to 60 mg,

were heated in a helium atmosphere at a constant rate of 10°C per minute up to 550°C. The DSC data analysis was done using TA Instruments thermal analysis software. The CH content was equivalent to the area (enthalpy) under the respective endothermic peaks. The endothermic peak for CH was observed at around 440°C. The area under the curve was related to the quantity of the material in the sample using the regression equation obtained from the calibration graphs for the used TA Instruments machine. At least two DSC analyses were performed on identical specimens for each mixture at each age to ensure repeatability of results.

Autogenous shrinkage was assessed using a special measuring technique developed by (Jensen and Hansen, 1995), where the concrete is encapsulated in thin, corrugated polyethylene moulds. The dilatometer was equipped with automatic data-logging and high accuracy electronic linear displacement transducers (0.001mm). Moreover, the dilatometer was fabricated with a built-in temperature-controlled light paraffin oil bath at 20 ± 1°C to ensure isothermal conditions during measurements, where three replicate specimens were evaluated concurrently while being submerged in the light paraffin oil bath (see **Fig. 6-4**). Autogenous deformation measurements were zeroed at the final setting times (Bentz and Peltz, 2008).

High-resolution solid-state ^{29}Si MAS-NMR experiments were performed in the Biomolecular NMR facility at the University of Western Ontario using a Varian Infinity Plus 400 spectrometer operating at 79.4 MHz with a triple-resonance Varian T3 HXY MAS probe having 7.5 mm ZrO_2 rotors rotating at 6.0 kHz. The ^{29}Si NMR spectra were obtained using a single-pulse experiment with a 2.5 μs pulse roughly corresponding to a 40-degree tip-angle ($\pi/2$-pulse = 5.5 μs). The chemical shifts were all relative to

tetramethylsilane (TMS). The free induction decays (*FIDs*) were apodized with 100 Hz line-broadening and zero-filled two times before Fourier transform. The experimental error in peak position values was estimated as ±0.1 ppm. At testing age, NMR samples hydration were stopped using freeze-drying method.
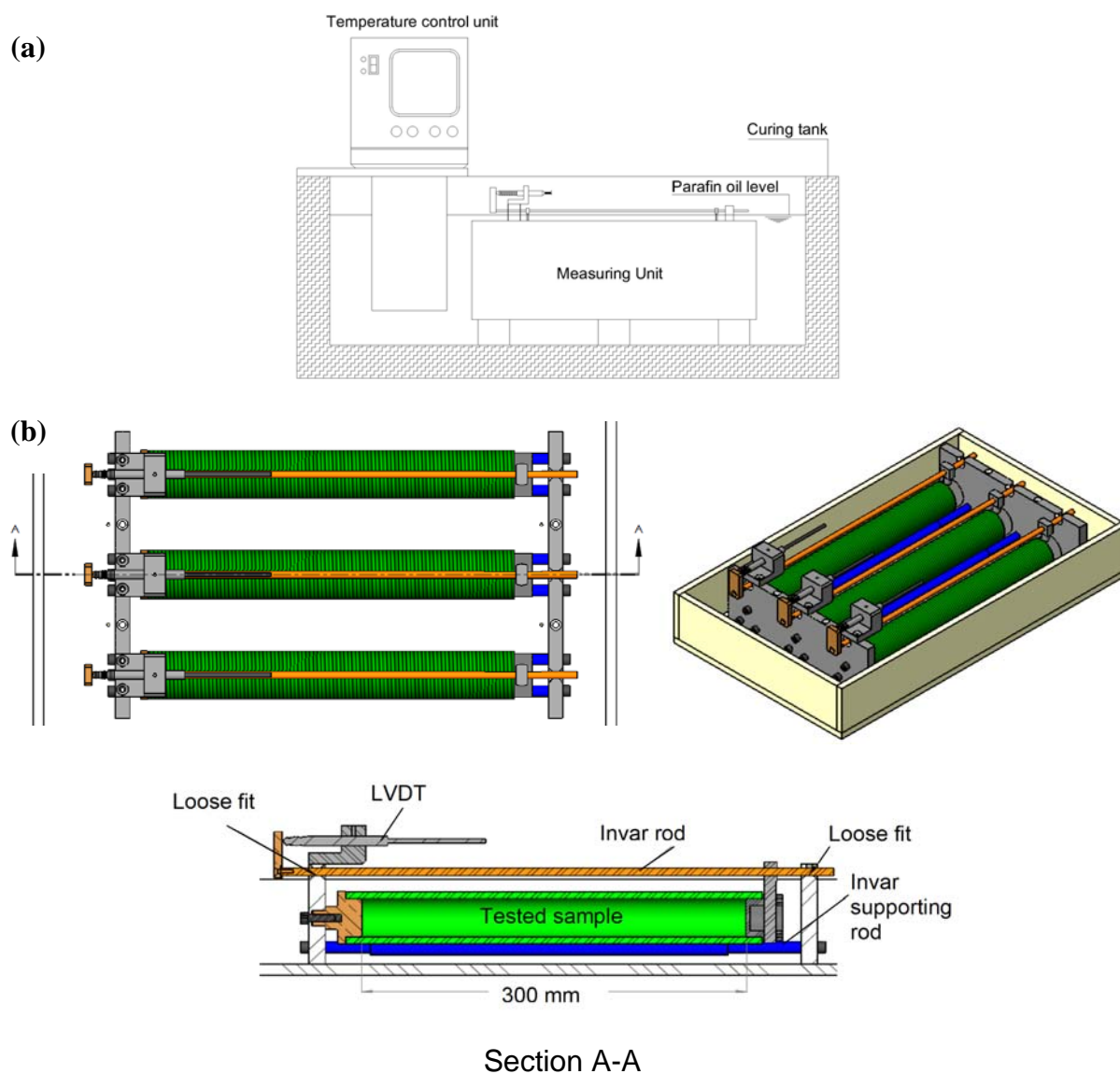
Figure 6-4: The corrugated tube protocol a) test setup, and b) measuring unit.

6.9. RESULTS AND DISCUSSION

6.9.1. Setting Time and Compressive Strength

Regardless of the added amount of PHCM, the PHCM technique significantly enhanced the development of early-age compressive strength. All PHCM mixtures consistently produced higher early-age compressive strengths compared to that of the control mixture (*C*) cured at 10 and 20°C, as shown in **Fig. 6-5(a,b)**. The increase in compressive strength compared to that of the *C* was directly proportional to the added amount of PHCM. For instance, the 24 hrs compressive strength at 10 and 20°C increased by 70% and 30% for *H1*, 85% and 40% for *H2* and by 140% and 45% for *H3* of their respective *C* values. At 10°C, higher increase in compressive strength with PHCM addition was achieved compared to that at 20°C. This is likely due to the influence of the added PHCM on accelerating hydration reactions. Hence, the slow rate of hydration and strength development at the low temperature of 10°C were compensated for, leading to more hydration products and stronger microstructure (ACI committee 701, 2001).
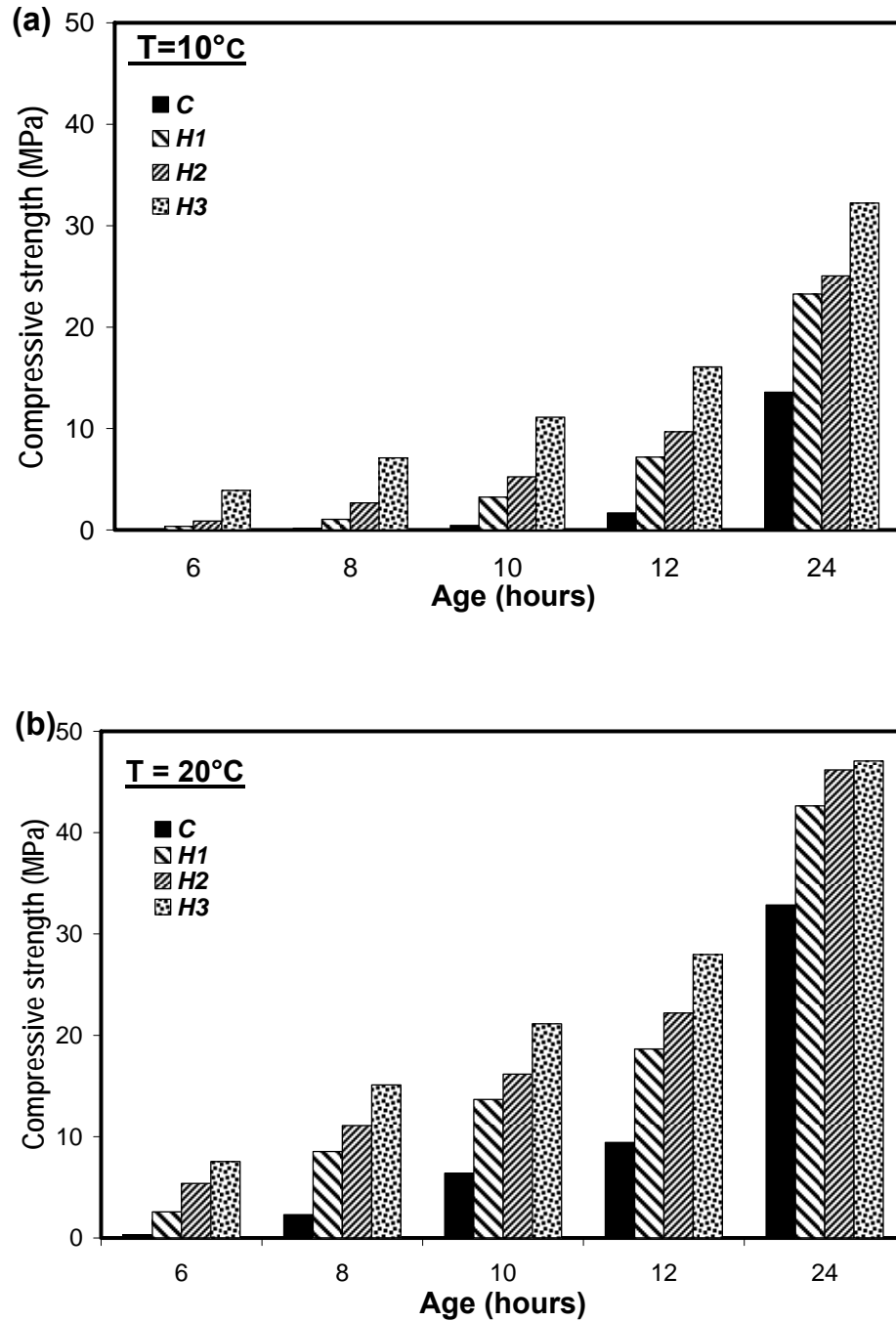
Figure 6-5: Early-age compressive strength of UHPC mixtures incorporating PHCM cured at a) 10°C and b) 20°C. [Maximum COV (10°C, 20°C): *C* (0.9%, 2.0%), *H1* (1.9%, 4.8%), *H2* (2.3%, 5.6%), *H3* (2.7%, 2.2%)].

Compared with the control mixture setting time, the PHCM technique also reduced the setting time significantly as shown in **Table 6-3**. These results demonstrate that the PHCM technique can be considered as an effective setting and hardening accelerating method.

Table 6-3: Initial and final setting times for different mixtures.

Mixture	Temperature			
	10°C		20°C	
	Setting time (min)			
	Initial	Final	Initial	Final
C	510	715	460	520
H1	450	495	340	420
H2	405	465	220	270
H3	245	280	170	210

The improvement in early-age compressive strength and reduction in setting time induced by PHCM addition can not be attributed to addition of older material. For instance, mixture **H3** after 6 hours curing at 10°C, 50% of the mixed cementitious material is 6 hours older. Hence, 50% of the cementitious material has an age of 12 hours, while the other 50% has an age of 6 hours. Summing up 50% of the **C** compressive strength at age 6 hours (0.0 MPa) and 12 hours (1.68 MPa) results in a compressive strength about (0.84 MPa) which is much lower than that of **H3** at 6 hours (3.90 MPa). On the other hand, setting time of normal paste starts to set at about 510 min at 10°C, hence, adding 50% of 6-hour older paste material should theoretically reduce the setting to about 150 min. However, the setting time was only reduced to about 245 min (which represents about 52% reduction with respect **C** value). The longer setting time achieved by **H3** than the theoretical one (150 min) can be attributed to the effect of

remixing on the developed microstructure. Remixing break down the formed connection between hydration products (Lea, 1988), hence, the **H3** paste will initially have a lower stiffness than that of paste mixed 6 hours earlier.

Figure 6-6 shows the compressive strength results for different mixtures at age 28 days. Generally, all mixtures exhibited comparable 28 days compressive strength compared to that of the control mixture regardless the curing temperature. For instance, the difference in 28 days compressive strength between control mixture and PHCM mixtures at 10°C and 20°C, ranged from -1% to +6.5% and from -4% to +0.85% with respect to the control mixture values, respectively. This slight variation in the 28 days compressive strength can be attributed to the fact that at low w/c ratio, hydration progress is mainly controlled by the availability of sufficient space for hydration products to form (Lea, 1988).
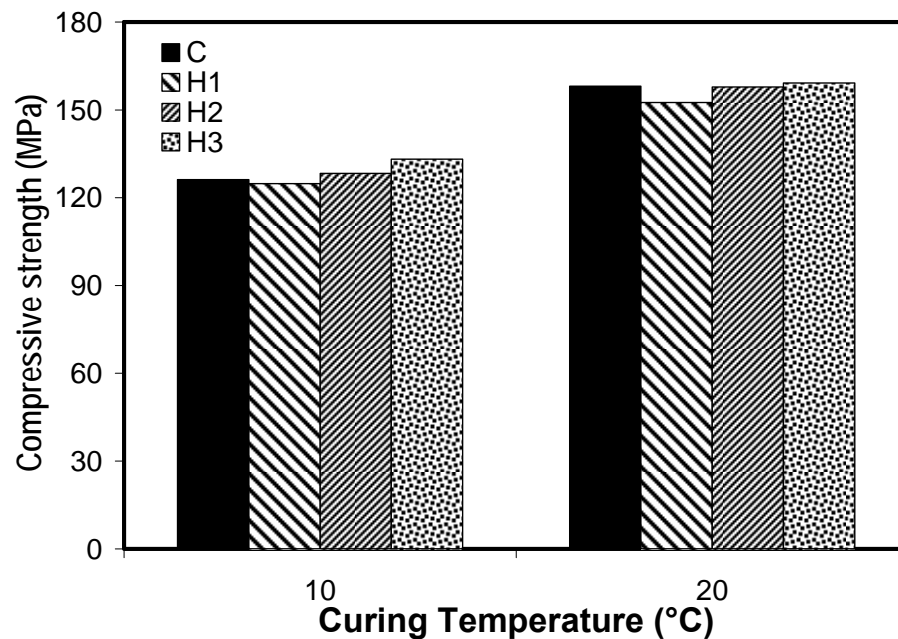
Figure 6-6: 28 days compressive strength of UHPC mixtures incorporating PHCM cured at 10°C and 20°C.

6.9.2. Degree of Hydration

Early-age strength development of concrete mixtures highly relies on the degree of hydration achieved (Xiao and Li, 2008). The correlation between the compressive strength and degree of hydration (represented by the amount of BW) is plotted in **Fig. 6-7**. It can be observed that the relationship exhibits a linear trend for PHCM mixtures (with $R^2 = 0.97$). This linear relationship between compressive strength and degree of hydration indicates a proportional relationship between the added dosages of PHCM and the development of hydration and strength.
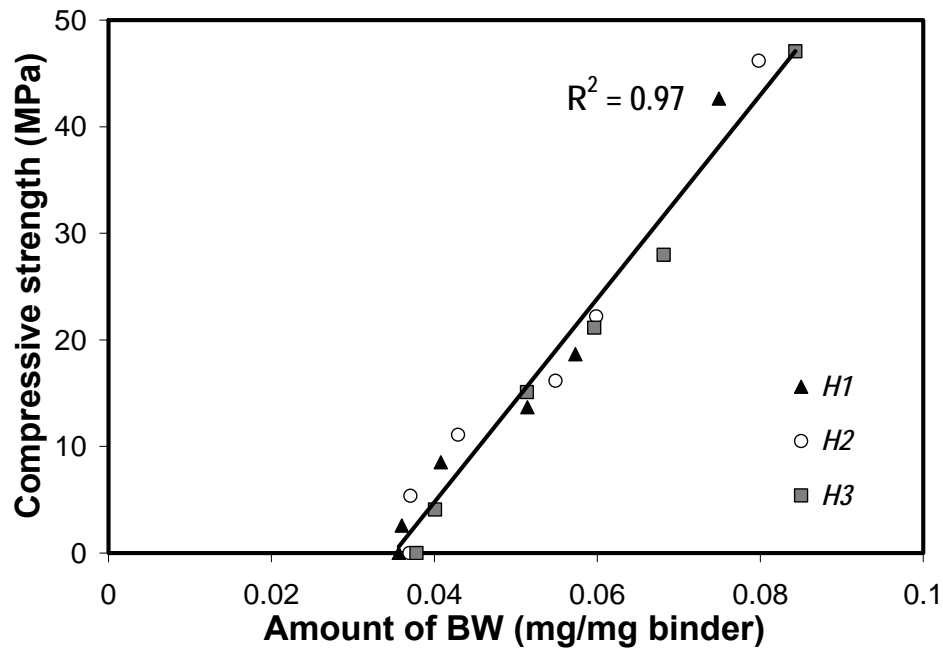
Figure 6-7: Relation between degree of hydration (amount of BW) and compressive strength development for the PHCM mixtures.

6.9.3. Heat of Hydration

A key characteristic of cementitious materials is the heat generated due to the exothermic hydration reactions of cement. This heat is translated into a temperature increase from

which the heat quantity developed can be evaluated (Chikh *et al*., 2008) in the present study. Test results were presented graphically in terms of semi-adiabatic temperature evolution versus time.

Mixtures incorporating PHCM had similar temperature evolution curves that differed from that of the control mixture, as shown in **Fig. 6-8**, indicating a variation in the hydration kinetics. Initially, the temperature for PHCM mixtures rose rapidly after casting the specimen in the semi-adiabatic cell (20 min from water addition) and did not exhibit an induction period (period in which the rate of hydration reactions slows down significantly (Ramachandran *et al*., 2002)). Temperature rised up until reaching a peak of about 42°C after about 7.5 hrs for *H3*, 38°C and 39°C after about 8 hrs for *H1* and *H2*, respectively. On the other hand, *C* hydration exhibited induction and acceleration periods as shown in **Fig. 6-8**. The acceleration period for *C* was initiated at about 6 hrs later than that of PHCM mixtures and had a temperature peak of about 36°C at around 12 hrs from water addition. Hence, the PHCM technique effectively diminished the induction period, leading to a continuous progress of hydration reactions and consequently shorter setting time and higher early-age compressive strength as discussed earlier.
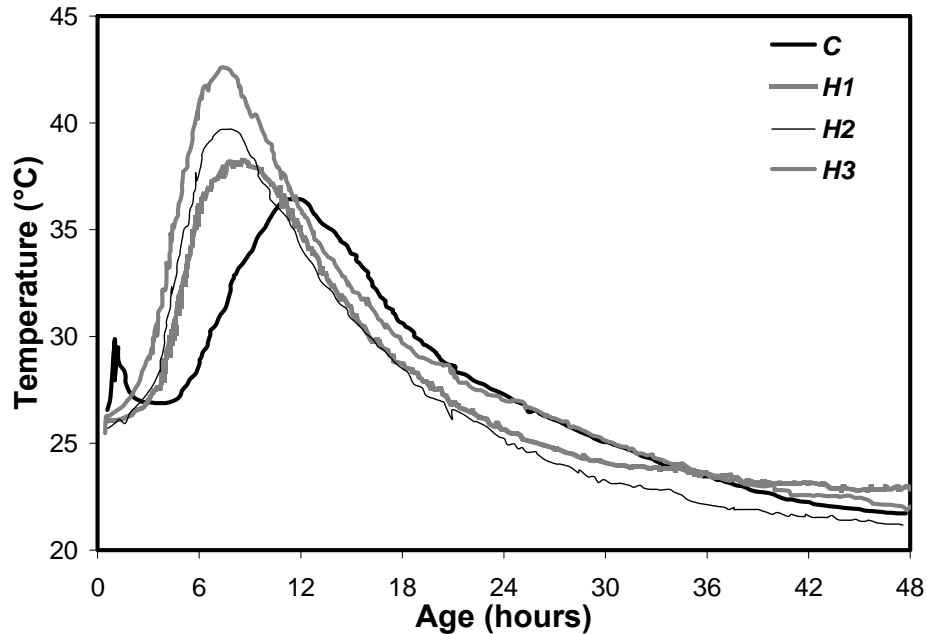
Figure 6-8: Heat of hydration for UHPC mixtures incorporating PHCM.

6.9.4. Shrinkage

Shrinkage results for mixtures incorporating different contents of PHCM are shown in **Fig. 6-9**. PHCM mixtures showed lower shrinkage and mass loss compared to that of the control mixture (**Figs. 9** and **10**). This can be attributed to the fact that the measured shrinkage includes drying and autogenous shrinkage (thermal deformation can be ignored due to the small cross-section of the samples (Baroghel-Bouny *et al.*, 2006)). Autogenous shrinkage is strongly related to hydration reactions in which water is consumed, leading to internal self-desiccation (without external water loss) (Power and Brownyard, 1947). For low w/c mixtures, the amount of autogenous shrinkage can be comparable to that of drying shrinkage (Tazawa and Miyazawa, 1999). Generally, accelerating the rate of hydration increases the internal self-desiccation, and consequently increases the autogenous shrinkage contribution to the measured shrinkage.
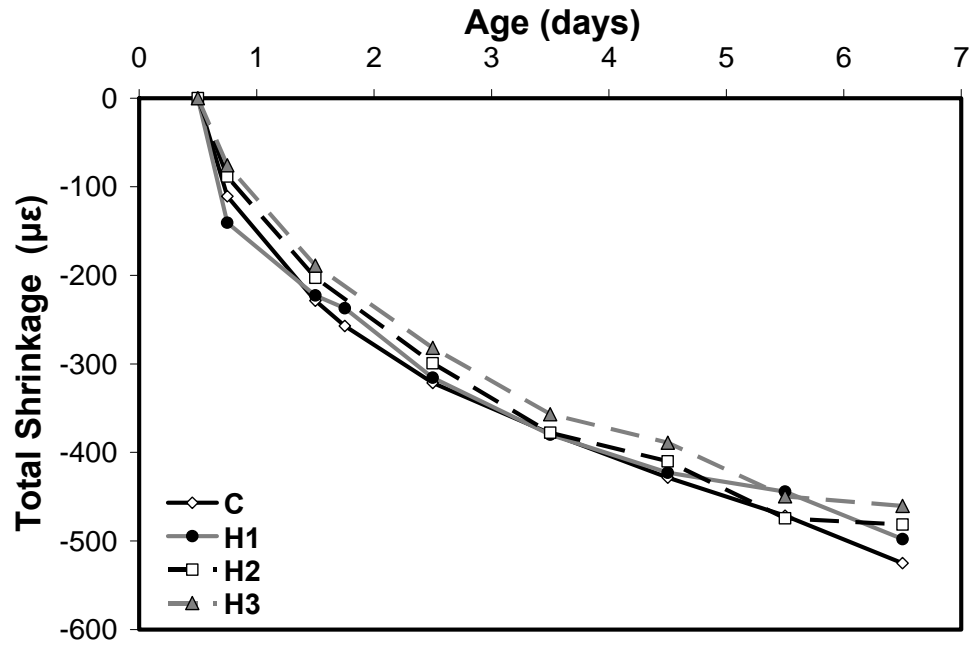
Figure 6-9: Total shrinkage for PHCM mixtures

[Maximum **COV**: *C* (4.5%), *H1* (3.1%), *H2* (1.5%), *H3* (4.6%)].
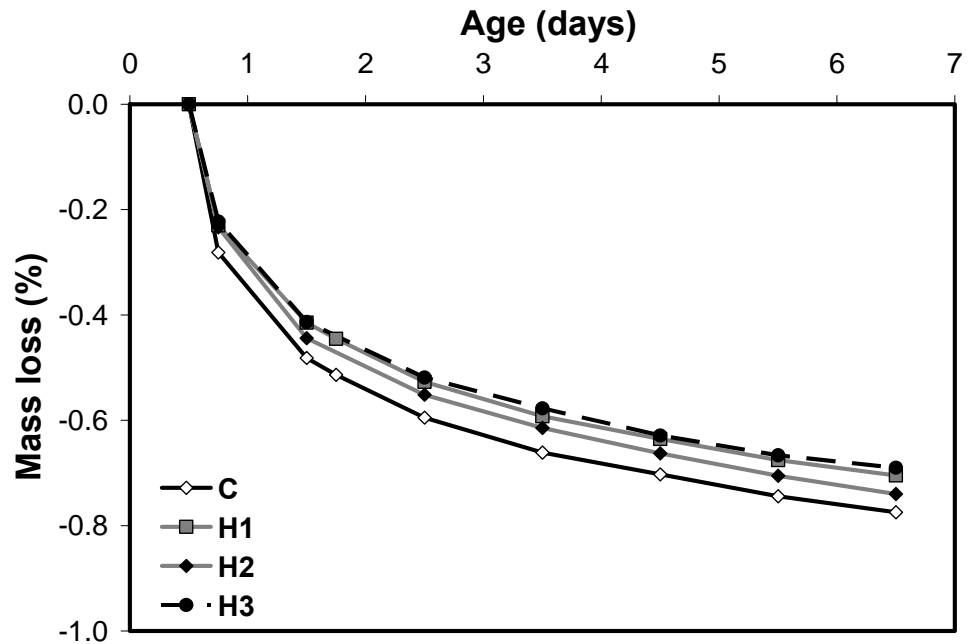
Figure 6-10: Mass loss for PHCM mixtures.

However, the added PHCM will act as a passive internal restraint, thus reducing the amount of deformation developed along with accelerating the hydration reactions. At the micro-level, the added PHCM provides CH crystals that can act as a passive restraint and reduce the measured physical shrinkage (Jensen and Hansen, 1996). This explanation is consistent with autogenous shrinkage results shown in **Fig. 6-11**, and with DSC results presented below. Increasing the amount of added PHCM increased the passive internal restrain and consequently reduced the amount of autogenous shrinkage.
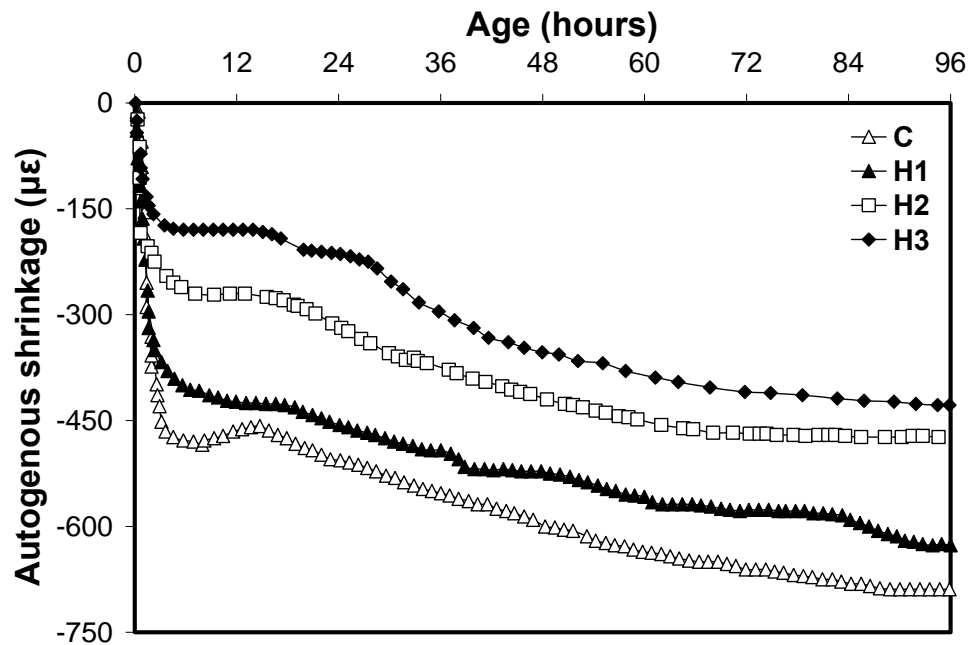
Figure 6-11: Autogenous shrinkage for PHCM mixtures.

Furthermore, the evaporable water content in PHCM mixtures is probably less than that in the control mixture at the onset of drying. This can be explained as follows: all mixtures initially have the same amount of mixing water, however, the added mixing water before casting the specimens for PHCM mixtures (i.e. mixing water at the second

stage) is less than that of the ordinary mixture. For instance, for the mixture *H3*, half of the mixing water is added in the first mixing stage, while the other half is added at the second stage before casting the shrinkage specimens. Hence, PHCM mixtures possess lower evaporable water and consequently exhibited lower mass loss as shown in **Fig. 6-10**.

6.10.   MECHANISM OF PHCM ACTION

The results above demonstrate that the PHCM technique does accelerate the setting and hardening processes. Consequently, it accelerates the rigid skeleton formation and development of restraining system within the microstructure. The subsequent part of this study focuses on explaining PHCM mechanisms. The *H2* mixture containing a moderate dosage of PHCM will be used in this discussion.

The modification in the hydration kinetics of PHCM mixtures compared to that of the control mixture can be ascribed to a number of effects. Adding pre-hydrated C_3S provides CH and CSH acts as nuclei for further CSH formation or for the conversion of the 'first-stage' CSH (water impermeable product formed within the first few minutes of hydration), into a 'second-stage' CSH (better permeable hydrate). Hence, this way accelerates the hydration reactions, leading to abolishing the induction period. This was found to be consistent with NMR results. Sets of NMR spectra for control and *H2* samples at ages of 8, 10, 12 and 24 hours are shown in **Fig**. **6-12.** The peaks corresponding to CSH (Q^1 and Q^2) occur at about -79 and -84 ppm, respectively, similar to previous findings (Fernandez *et al*., 2008, Al-Dulaijan *et al*., 1995, Cong and Kirkpatrick, 1996). During the first hours of hydration, CSH formed with a

predominantly protonated Q^1 species, which represents the onset of SiO_4 polymerization (Johansson *et al.*, 1999). As hydration progressed, increased amount of protonated Q^2 species also became detectable in addition to Q^1 (Lea, 1988). Comparing the NMR spectra for control and **H2**, Q^1 and Q^2 had appeared, as early as 8 and 10 hrs for the **H2** mixture and at 12 hrs for control mixture, respectively. This indicates an earlier onset of polymerization and conversion of CSH from the first to the second stage for **H2** compared to **C**, as shown in **Fig. 6-12**. These results are consistent with the early-age heat evolution and compressive strength measurements.
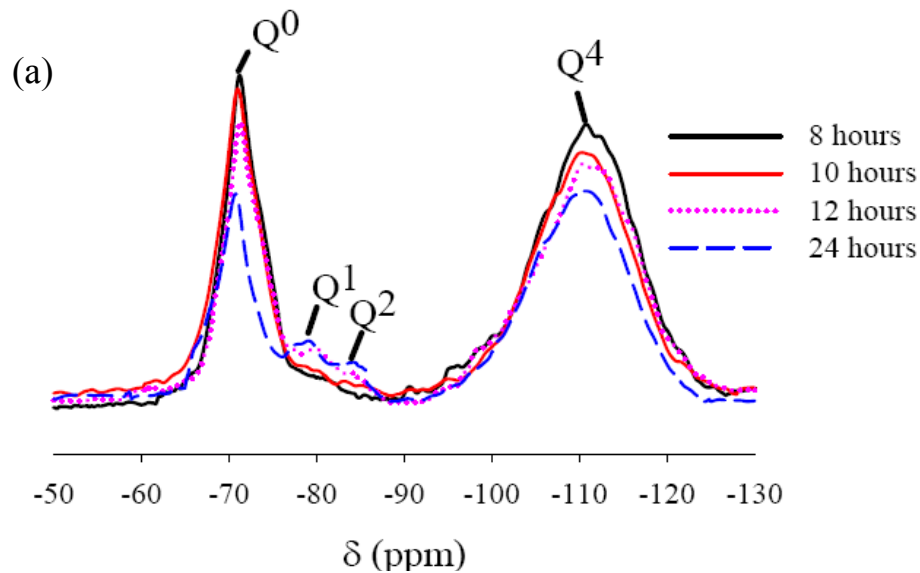
Figure 6-12: NMR spectra for a) *C* and b) *H2* samples at different ages.
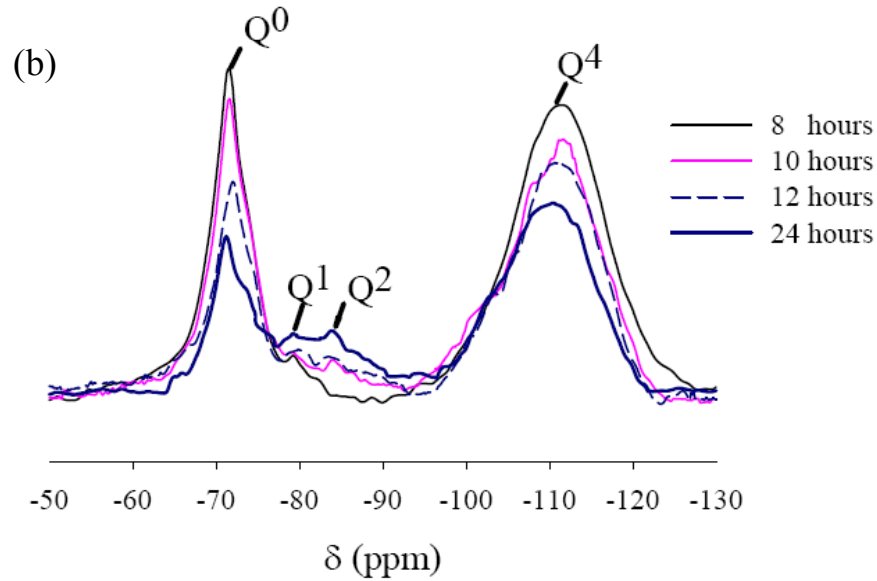
Figure 6-12 Contd': NMR spectra for a) *C* and b) *H2* samples at different ages.

Moreover, added crystalline *CH*, besides acting as a passive internal restraint, it enables further dissolution of C_3S, renewed *CSH* formation (Tadros *et al*., 1976, Kondo and Daimon, 1969). Furthermore, this reduction in the calcium and silicate ions in the solution can result in the breakdown of the electrical double layer of calcium and silicate ions formed on C_3S during its initially dissolution, as indicated by the electrical double layer theory. This can also lead to renewed acceleration of the hydration process (Lea, 1988, Tadros *et al*., 1976, Kondo and Daimon, 1969, Young *et al*., 1977). This is depicted by the DSC results in **Fig. 6-13**, where enthalpies of CH (440°C) for the *H2* were significantly higher than that of the *C* over the investigated period.
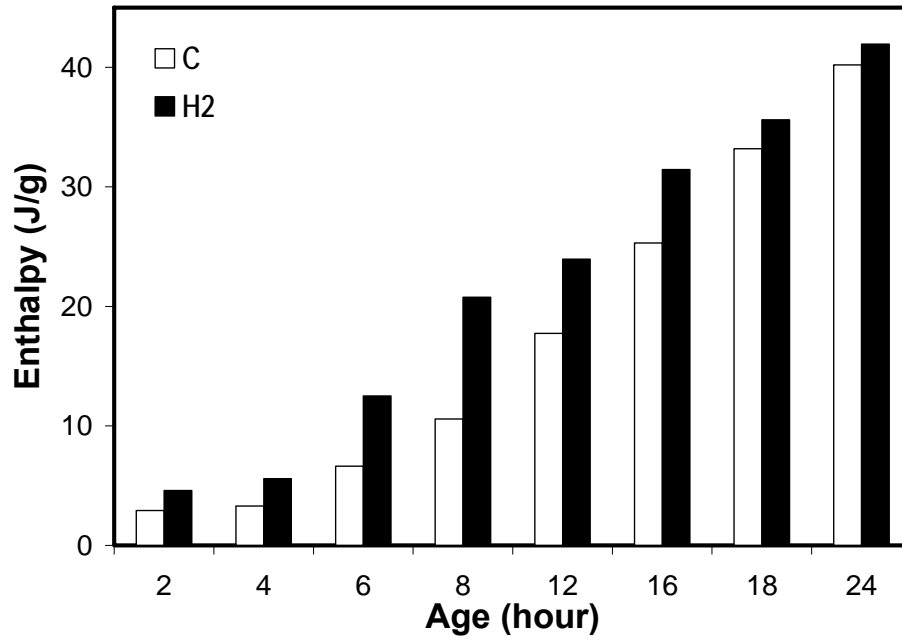
Figure 6-13: **Enthalpy values for *C* and *H2* mixtures during the first 24 hours.**

Another mechanism emanates from the principle that silica fume (amorphous silica) affects the rate of hydration during the early-age. Silica fume provides large amounts of reactive siliceous surface, serving as a site for the early CSH precipitation. Accordingly, the initial CSH layer will be formed mostly on silica surface rather than developing a protective layer on the surface of the most reactive phases (i.e. C_3S), thus preventing a hydration delay (Korpa *et al*., 2008). Microstructure analysis confirms this hypothesis as explained below. Furthermore, the pozzolanic reaction of silica fume with CH (provided by PHCM) leads to an increase in the amount of developed CSH (less protective than the initially formed CSH (McCurdy and Erno, 1970)) and the Q^2 signal which indicates a growth in the mean chain length of CSH phases (i.e. degree of polymerization) (Schachinger *et al*., 2008). This is confirmed by the consumption of

silica fume during the hydration period as detected by NMR results. **Figure 6-12(b)** shows the gradual reduction in the silica fume NMR peak with time. Also, this early pozzolanic reaction can be considered the reason for the high early-age compressive strength (Al-Dulaijan *et al*., 1995).

The microstructure of *H2* specimens was found to be uniformly developed in the inter-granular space, as shown in **Fig. 6-14(a)**. More anhydrous silica fume clusters and large plate-like formations of CH can be observed clearly within the *H2* matrix during early-age (about 8 hours) compared to that at later ages (after 24 hours). This observation emphasizes the role of PHCM in providing crystalline CH during early hydration as mentioned before. In addition, the thin rim of CSH was not detected at that early-age. Conversely, the *H2* matrix at 24 hrs was found to be rich in dark CSH with a Ca/Si ratio of about 0.86, as shown in **Fig. 14(b)**. This reveals the effect of the pozzolanic reactions of silica fume, which consumed the CH, producing less protective dark CSH (Scrivener, 2004) with low Ca/Si ratio range (0.83-1.5) (Lea, 1988), which allows more hydration reactions to occur.
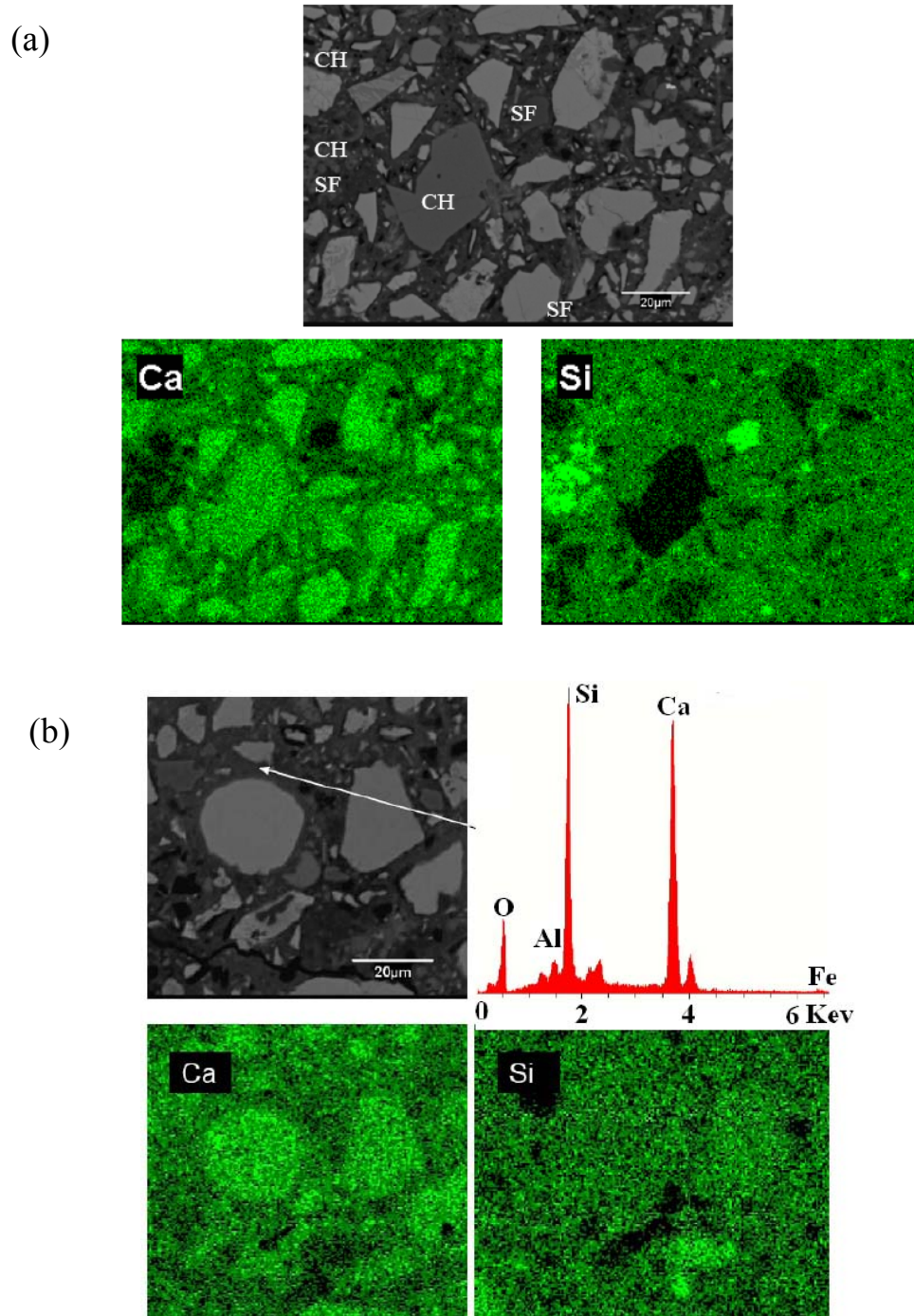
Figure 6- 14: Microstructure of *H2* mixtures after a) 8, and b) 24 hrs as in backscattered electron microscopy, and energy dispersive X-ray element analysis.

6.11.   CONCLUSIONS

The main conclusions that can be drawn from this experimental investigation are the following:

1) The addition of PHCM had a strong acceleration effect on the development of the internal microstructure leading to early setting and hardening process.

2) PHCM technique showed a high potential for reducing early-age shrinkage.

3) Addition of PHCM increases contact points and acts as load bearing structure providing an internal passive restraining system.

4) The higher the added PHCM, The higher was the restraining effect.

5) The PHCM technique initiates the concept of self-restraining concrete.

6) Concrete sustainability enhanced through using left-over and returned concrete in produce self-accelerated concrete, thus preventing waste and disposal.

7) Mixtures incorporating PHCM achieved a high potential for reducing autogenous shrinkage through providing internal passive restrains.

8) The PHCM showed an acceleration effect, which has a paramount potential, particularly in the pre-cast industry. It resolves the two major drawbacks associated with chloride accelerator; corrosion related to chlorides and increased shrinkage. (A Comparison between PHCM and conventional chloride and non chloride accelerators are shown in **Appendix B**).

6.12.   REFERENCES

ACI Committee E-701, (2001). Cementitious Materials for Concrete, ACI Education Bulletin E3-01, American Concrete Institute, Farmington Hills, Michigan, 25 p.

Al-Dulaijan, S.U., Al-Tayyib, A-H.J., Al-Zahrani, M.M., Parry-Jones, G. and Al-Mana, A.I., (1995), "^{29}Si MAS-NMR study of hydrated cement paste and mortar made with and without silica fume," *Journal of the American Ceramic Society*, Vol. 78, No. 2, pp. 342-346.

Aitcin, P.C., (1999), "Demystifying autogenous shrinkage," *Concrete International*, Vol. 21, No. 11, pp. 54-56.

Barcelo, L., Boivin, S., Acker, P., Toupin, J. and Clavaud, B., (2001), "Early age shrinkage of concrete: back to physical mechanisms," *Concrete Sciences and Engineering*, Vol. 3, No. 10, 2001, pp. 85-91.

Barcelo, L., Moranville, M. and Clavaud, B., (2005), "Autogenous shrinkage of concrete: a balance between autogenous swelling and self-desiccation," *Cement and Concrete Research*, Vol. 35, No. 1, 2005, pp. 177-183.

Baroghel-Bouny, V., Mounanga, P., Khelidj, A., Loukili, A. and Rafaï, N., (2006), "Autogenous deformations of cement pastes: Part II. W/C effects, micro–macro correlations, and threshold values," *Cement and Concrete Research*, Vol. 36, No. 1, pp. 123-136.

Bentur, A., Igarashi, S. and Kovler, K., (2001), "Prevention of autogenous shrinkage in high strength concrete by internal curing using wet lightweight aggregates," *Cement and Concrete Research*, Vol. 31, No. 11, pp. 1587-1591.

Bentz, D.P., (2006), "Influence of shrinkage-reducing admixtures on early-age properties of cement pastes," *Journal of Advanced Concrete Technology*, Vol. 4, No. 3, pp. 423-429.

Bentz, D.P. and Jensen, O.M., (2004), "Mitigation strategies for autogenous shrinkage cracking," *Cement and Concrete Composites*, Vol. 26, No. 6, pp. 677-685.

Bentz, D.P. and Peltz, M.A., (2008), "Reducing thermal and autogenous shrinkage contributions to early-age cracking," *ACI Materials Journal*, Vol. 105, No. 4, pp. 414-420.

Carde, C. and Francois, F., (1997), "Effect of the leaching of calcium hydroxide from cement paste on mechanical and physical properties," *Cement and Concrete Research*, Vol. 27, No. 4, pp. 539-550.

Chikh, N., Cheikh-Zouaoui, M., Aggoun, S. and Duval, R., (2008), "Effects of calcium nitrate and triisopropanolamine on the setting and strength evolution of Portland cement pastes," *Materials and Structures*, Vol. 41, No. 1, pp. 31-36.

Cong, X. and Kirkpatrick, R.-J., (1996), "^{29}Si MAS NMR study of the structure of calcium silicate hydrate," *Advanced Cement Based Materials*, Vol. 3, No. 3-4, pp. 144-156.

Esping, O., (2007), "Early-age properties of self-compacting concrete - Effects of fine aggregate and limestone filler," PhD Thesis, Department of Civil and Environmental Engineering, Chalmers University of Technology, Sweden.

Fernandez, L., Alonso, C., Andrade, C. and Hidalgo, A., (2008), "The interaction of magnesium in hydration of C_3S and CSH formation using ^{29}Si MAS-NMR," *Journal of Materials Science*, Vol. 43, No. 17, pp. 5772-5783.

Fosså, K.T., (2001), "Slipforming of vertical concrete structures: Friction between concrete and slipform panel," PhD Thesis, the Norwegian University of Science and Technology, Trondheim, Norway.

Hansen, W., (1987), "Constitutive model for predicting ultimate drying shrinkage of concrete," *Journal of American Ceramic Society*, Vol. 70, No. 5, pp. 329-332.

Hansen, W., (2011), "Report on early-Age cracking: A summary of the latest document from ACI Committee 231," *Concrete International*, Vol. 33, No. 3, pp. 48-51.

Hammer, T.A., (1999a), "Early age chemical shrinkage and autogenous deformation of cement paste," In: *Proceedings of the International Seminar on Self-desiccation and its importance in concrete technology*, Lund, pp. 27-33.

Hammer, T.A., (1999b), "Test methods for linear measurements of autogenous shrinkage before setting," *Proceedings of the International Workshop "Autogenous Shrinkage of Concrete"*, Taylor, New York, pp. 143-154.

Henkensiefken, R., Briatka, P., Bentz, D.P., Nantung, T. and Weiss, J., (2010), "Plastic shrinkage cracking in internally cured mixtures," *Concrete International*, Vol. 32, No. 2, pp. 49-54.

Holschemacher, K., Dehn, F., Klotz, S. and Weiße, D., (2005), "Experimental investigation on ultra high-strength concrete under concentrated loading," In: *Proceedings of the Seventh International Symposium on Utilization of high-strength/ high performance concrete*, Washington D.C., USA, Vol. 2, pp. 1145-1158.

Holt, E.E., (2001), "Early-age autogenous shrinkage of concrete," PhD Thesis, University of Washington, United States.

Holt, E. and Leivo, M., (2004), "Cracking risks associated with early age shrinkage," *Cement and Concrete Composites*, Vol. 26, No. 5, pp. 521-530.

Jensen, O.M. and Hansen, P.F., (1995), "A dilatometer for measuring autogenous deformation in hardening Portland cement paste," *Materials and Structures*, Vol. 28, No. 181, pp. 406-409.

Jensen, O.M. and Hansen, P.F., (1996), "Autogenous deformation and change of relative humidity in silica fume modified cement paste," *ACI Materials Journal*, Vol. 93, No. 6, pp. 539-543.

Jensen, O.M. and Hansen, P. F., (1999), "Influence of temperature on autogenous deformation and relative humidity change in hardening cement paste," *Cement and Concrete Research*, Vol. 29, No. 4, pp. 567-575.

Jensen, O.M. and Hansen, P.F., (2001), "Water-entrained cement-based materials: I. Principles and theoretical background," *Cement and Concrete Research*, Vol. 31, No. 4, pp. 647-654.

Johansson, K., Larsson, C., Antzutkin, O.N., Forsling, W., Kota, H.R. and Ronin, V., (1999), "Kinetics of the hydration reactions in the cement paste with mechanochemically modified cement ^{29}Si magic-angle-spinning NMR study," *Cement and Concrete Research*, Vol. 29, No. 10, pp. 1575-1581.

Justens, H., Van Gemart, A., Verboven, F. and Sellevold, E.J., (1996), "Total and external chemical shrinkage of low w/c ratio cement pastes," *Advances in Cement Research*, Vol. 8, No. 31, pp. 121-126.

Kondo, R. and Daimon, M., (1969), "Early hydration of tricalcium silicate: a solid reaction with induction and acceleration periods," *Journal of the American Ceramic Society*, Vol. 52, No. 9, pp. 503-508.

Korpa, A., Kowald, T. and Trettin, R., (2008), "Hydration behaviour, structure and morphology of hydration phases in advanced cement-based systems containing micro and nanoscale pozzolanic additives," *Cement and Concrete Research*, Vol. 38, No. 7, pp. 955-962.

Kovler, K. and Zhutovsky, S., (2006), "Overview and future trends of shrinkage research," *Materials and Structures*, Vol. 39, No. 9, pp. 827-847.

Kronlöf, A., Leivo, M. and Sipari, P., (1995), "Experimental study on the basic phenomena of shrinkage and cracking of fresh mortar," *Cement and Concrete Research*, Vol. 25, No. 8, pp. 1747-1754.

Lea, F.M., (1988). Lea's Chemistry of Cement and Concrete, 4th Edition, (ed.) P.C. Hewlett, J. Wiley, New York, 1053 p.

Lobo, C., Guthrie, W.F. and Kacker, R., (1995), "A study of the reuse of plastic concrete using extended set-retarding admixtures," *Journal of Research of National Institute of Standards and Technology*, Vol. 100, No. 5, pp. 575-589.

Ma, J., Orgass, M., Dehn, F., Schmidt, D and Tue, N.V., (2004), "Comparative investigations on ultra-high performance concrete with and without coarse aggregates," *Proceedings of the International Symposium on Ultra High Performance Concrete*, Germany, pp. 205-212.

McCurdy, K.G. and Erno, B.P., (1970), "The kinetics of hydration of tricalcium silicate," *Canadian Journal of Chemistry*, Vol. 48, No. 21, pp. 3291-3299.

Mehta, P.K. and Monteiro, P.J.M., (2006). Concrete: Microstructure, Properties, and Materials. 3rd Edition, McGraw-Hill, New York, 659 p.

Neville, A.M., (1996). Properties of Concrete. 4th Edition, Wiley, New York, 844 p.

Obla, K., Kim, H. and Lobo, C., (2007), "Crushed returned concrete as aggregates for new concrete: Final report," *The RMC Research & Education Foundation*, Project 05-13, 51 p.

Odler, I. and Dörr, H., (1979), "Early hydration of tricalcium silicate I : Kinetics of the hydration process and the stoichiometry of the hydration products," *Cement and Concrete Research*, Vol. 9, No. 2, pp. 239-248.

Powers, T.C., (1962), "A hypothesis on carbonation shrinkage," *Journal of the Portland Cement Association Research & Development Laboratories*, Vol. 4, No. 2, pp. 40-50.

Powers, T.C. and Brownyard, T.L., (1947), "Studies of the physical properties of hardened portland cement paste," *Bulletin No. 22*, 1948, Research Laboratories of the Portland Cement Association. Reprinted from Journal of the American Concrete Institute, October 1946–April 1947, Proceedings 43, Detroit, pp. 971-992.

Ramachandran, V.S., Haber, R.M., Beaudoin, J.J. and Delgado, A.H., (2002). Handbook of Thermal Analysis of Construction Materials, Noyes & William Andrew Publishing, Norwich, 655 p.

Roy, D.M. and Idorn, G.M., (1993). Concrete Microstructure. SHRP-C340, Strategic Highway Research Program, 179 p.

Scrivener, K.L., (2004), "Backscattered electron imaging of cementitious microstructures: under- standing and quantification," *Cement and Concrete Composites*, Vol. 26, No. 8, pp. 935-945.

Schachinger, I., Hilbig, H. and Stengel, T., (2008), "Effect of curing temperature at an early age on the long-term strength development of UHPC," In: *Proceedings of the Second International Symposium on Ultra High-Performance Concrete*, Kassel, Germany, pp. 205-212.

Schemmel, J.J., Ray, J.C. and Kuss, M.L., (1999), "Impact of shrinkage reducing admixture on properties and performance of bridge deck concrete, high-performance concrete research to practice," *ACI*, Special Publication, SP-189, pp. 367-386.

Struble, L., Skalny, J. and Mindess, S., (1980), "A review of the cement-aggregate bond," *Cement and Concrete Research*, Vol. 10, No. 2, pp. 277-286.

Tadros, M.E., Skalny, J. and Kalyoncu, R.S., (1976), "Early hydration of tricalcium silicate," *Journal of the American Ceramic Society*, Vol. 59, No. 7-8, pp. 344-347.

Tazawa, E., (1999). Autogenous Shrinkage of Concrete. In: *Proceedings of the International Workshop organized by the Japan Concrete Institute,* Taylor, New York.

Tazawaa, E. and Miyazawaa, S., (1995a), "Influence of cement and admixture on autogenous shrinkage of cement paste," *Cement and Concrete Research*, Vol. 25, No. 2, pp. 281-287.

Tazawa, E. and Miyazawa, S., (1995b), "Experimental study on mechanism of autogenous shrinkage of concrete," *Cement and Concrete Research*, Vol. 25, No. 8, pp. 1633-1638.

Tazawa, E. and Miyazawa, S., (1999), "Effect of constituents and curing condition on autogenous shrinkage of concrete," In: *Autogenous Shrinkage of Concrete: Proceedings of the International Workshop*, Eiichi Tazawa (ed.), Taylor & Francis, pp. 269-280.

Wittmann, F.H., (1976), "On the action of capillary pressure in fresh concrete," *Cement and Concrete Research*, Vol. 6, No. 1, pp. 49-56.

Xiao, L. and Li, Z., (2008), "Early-age hydration of fresh concrete monitored by non-contact electrical resistivity measurement," *Cement and Concrete Research*, Vol. 38, No. 3, pp. 312-319.

Young, J.F., Tong, H.S. and Berger, R.L., (1977), "Compositions of solutions in contact with hydrating tricalcium silicate pastes," *Journal of the American Ceramic Society*, V. 60, No. 5-6, pp. 193-198.

CHAPTER SEVEN

EVALUATION OF SELF-RESTRAINING SHRINKAGE TECHNIQUE COMPARED TO CONVENTIONAL METHODS IN UHPC: INDIVIDUALLY AND COMBINED*

In the previous chapter (Chapter 6), the concept of developing self-restraining concrete was introduced. Using partially hydrated cementitious materials (PHCM) had shown a high potential to improve the early-age properties of UHPC. In addition, it provides an environmental and economic technique for producing precast and cast in place self-restraining shrinkage concrete, through inducing internal passive restraint within fresh concrete. In this chapter, the efficiency of PHCM as a shrinkage mitigation method was evaluated in comparison to conventional techniques including, shrinkage-reducing admixture (SRA) and/or a superabsorbent polymer (SAP). In addition, the combined effects of PHCM, SRA and SAP techniques in reducing early-age shrinkage were investigated.

7.1.   INTRODUCTION

General literature about UHPC characterizations, potential applications, shrinkage problems and different mitigation strategies has been given in proceeding chapters 3 and 4. It has been outlined that the ultimate mechanical properties and enhanced durability make it a promising material for many construction applications. However, its high self-desiccation shrinkage and potential of early-age cracking may defeat its purposes. Hence,

---

several shrinkage mitigation methods were proposed. Among these methods, SRA is the most commonly used method, while SAP represents an enhanced version of internal curing technique.

In addition to the shrinkage mitigation strategies described above, various concrete components can provide passive internal restraint that resists autogenous shrinkage and reduces the measured physical deformations (Bentz and Jensen, 2004). Chief amongst these are aggregate particles (Hobbs, 1974, Hansen and Nielsen, 1965). At the micro-level, a passive restraint can be provided by several components including un-hydrated cement particles, hydrated cement paste skeleton (Aitcin, 1999) and other hydration products (e.g. calcium hydroxide (CH) micro-crystals) (Jensen and Hansen, 1996).

Therefore, it was proven in Chapter 6 that adding PHCM can provide an internal restraint system which varies in size from as small as CH micro-crystals up to networks of hydration products and clusters. These clusters can provide load-bearing mechanisms at the micro-structural level to resist contracting forces in fresh concrete. Besides, using PHCM has two major positive environmental and economical benefits through eliminating, or greatly reducing wastage of concrete, which consequently can lead to cost reduction. Hence, the focus of this chapter is to investigate the effectiveness of PHCM as a passive internal restraint system to reduce early-age shrinkage strains in comparison to SRA and SAP.

7.2.   RESEARCH SIGNIFICANCE

Early-age shrinkage cracking is a considerable problem for concrete structures. Several shrinkage mitigation techniques have been proposed to reduce shrinkage and to avoid crack formation. However, such mitigation methods can adversely affect other key properties of concrete inducing difficulties in controlling consistency, retardation of hydration reactions, reduction in mechanical properties, etc. Adding partially hydrated cementitious materials (PHCM) to the fresh concrete during mixing had shown a high potential to reduce early-age shrinkage. This chapter confirms the efficacy of PHCM as a new environmental-friendly shrinkage mitigation technique compared to SRA and SAP. PHCM mitigates undesirable behaviour induced by SRA and/or SAP, including setting time delays and reduction in mechanical properties. Hence, unused/returned concrete can be recycled in new mixtures, individually or combined with other shrinkage mitigation techniques, to enhance mechanical strength and resistance to shrinkage, and to mitigate set retardation effects.

7.3.   EXPERIMENTAL PROGRAM

The experimental program aims at gaining an understanding of the mechanisms involved in using PHCM. This is of primary importance in order to enable the production of shrinkage self-restraining concrete. In this study, monitoring the hydration process (degree of hydration, heat of hydration, Vicat setting time) and characterization of the shrinkage behaviour have been carried out on concrete mixtures incorporating PHCM, SRA and SAP. The chapter consists of two parts. Part I was devoted to investigating the effects of PHCM addition on the early-age properties of control mixtures with and without SRA and/or SAP. The second part focused on validating the addition of PHCM

as a shrinkage mitigation technique and evaluating its efficiency compared to that of SRA
and SAP. Combined effects of the tested shrinkage mitigation techniques including
PHCM, SRA, and SAP were also investigated. Mixtures containing a moderate dosage of
PHCM (i.e. 33%) were selected for comparison in this second part.   All tests were
conducted on UHPC specimens without heat curing in order to explore realistic effects
that govern UHPC shrinkage in structural elements cast in situ.

7.3.1.   Materials and Mixture Proportions

The materials used in this chapter were similar to that used in Chapter 4 (refer to Section
4.4.1). The chemical and physical properties of the used binders have been given in
Chapter 3 (**Table 3-1**). The selected composition of the control and PHCM mixture are
shown in Chapter 6 (refer to **Table 6-1**). The characteristics of the tested mixtures are
shown in **Table 7-1**.

Table 7-1: Tested mixtures.

Mixture	PHCM(%)*	SRA (%)**	SAP (%)**
C	----	----	----
H1	25.0	----	----
H2	33.0	----	----
H3	50.0	----	----
CR2	----	2.0	----
CS	----	----	0.6
CR2S	----	2.0	0.6
H2R2	33.0	2.0	----
H2S	33.0	----	0.6
H2R2S	33.0	2.0	0.6

*Added as % of the batch weight
** Added as % by mass of cement

7.3.2.   Preparation of Test Specimens and Testing Procedures

The experimental methods used in this chapter are the cubic compressive strength test, Semi-adiabatic calorimetry, TGA, measurements of total free shrinkage, setting time and the corrugated tube protocol for measuring autogenous shrinkage. All experimental methods were previously explained in chapters 3 and 6.

7.4.   RESULTS AND DISCUSSION

7.4.1.   Setting Time and Early-Age Compressive Strength

Regardless of the added amount of PHCM, the PHCM technique significantly affected the development of early-age compressive strength. All UHPC mixtures incorporating PHCM consistently produced higher early-age compressive strength compared to that of the control mixture as discussed in chapter 6 (see **Fig. 6-5(b)**).

On the other hand, the mixture incorporating 2% SRA (*CR2*) achieved a lower early-age compressive strength compared to that of the *C* (**Fig. 7-1(a)**). This can be attributed to the retardation effect induced by SRA, in agreement with previous work (He *et al.*, 2006). The mixture incorporating PHCM and SRA (*H2R2)* achieved higher compressive strength than that of the *CR2* mixture, indicating that the accelerated hydration induced by PHCM addition offset the early-age compressive strength reduction induced by SRA. For instance, *H2R2* exhibited a compressive strength of about 1.1 MPa at the age of 6 hours, while *CR2* did not exhibit any strength at that age (**Fig. 7-1(a,b)**).

The early-age compressive strength of the mixture incorporating SAP (*CS*) was lower than that of the *C* (**Fig. 7-1(a)**). This can be ascribed to the higher water content of

the *CS* mixture, leading to higher porosity and consequently lower strength (Jensen and Hansen, 2002). Adding PHCM to the *CS* mixture improved its early-age compressive strength. This can be explained as follows: the higher water content imparted by SAP provided enhanced conditions for hydration reactions to progress. SAP particles release their entrained water and occupy a lower volume (Wang *et al.*, 2009), leading to more space for hydration products to form. At such a very low w/c, the availability of space for hydration products to form is a main restriction on hydration development (Acker, 2004). Hence, enhanced curing conditions and availability of space along with accelerated hydration reactions induced by PHCM addition produced a well developed microstructure and consequently higher early-age strength was achieved.

The mixture incorporating both SRA and SAP (*CR2S*) exhibited a lower early-age compressive strength than that of the *CS*; reflecting the set retarding effect induced by SRA. However, the *CR2S* mixture exhibited higher early-age strength compared to that of the *CR2*. This can be ascribed to the lower SRA concentration in *CR2S* as a result of the higher water content (Rajabipour *et al.*, 2008) and the ability of SAP particles to absorb SRA (Bentz, 2005). Adding PHCM to the *CR2S* mixture enhanced its early-age compressive strength by about 26% at 24 hours (**Fig. 7-1(b)**). This improvement exhibits the resultant of conflicting effects of SRA, SAP and PHCM on the early-age strength developments.
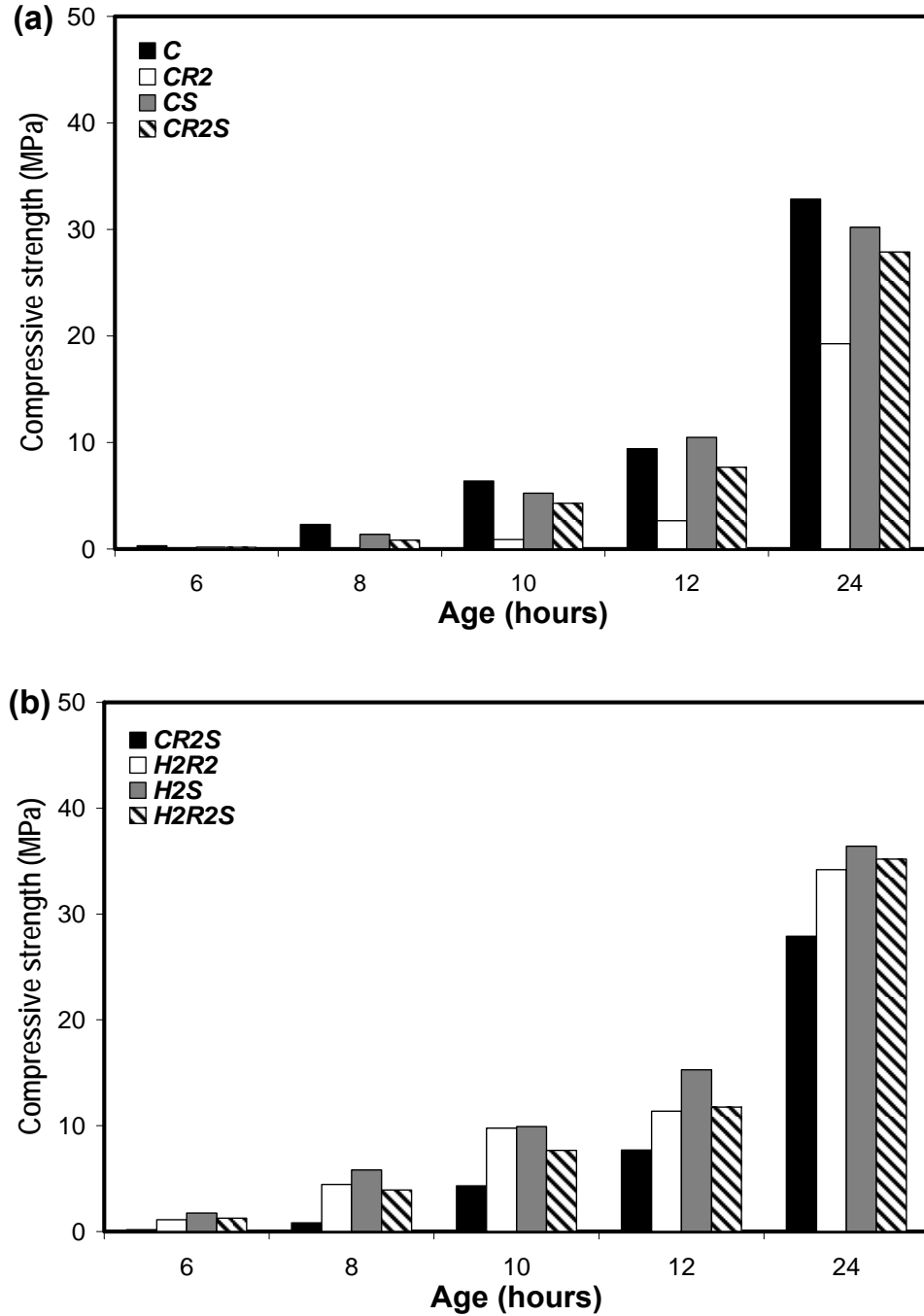
Figure 7-1 : Early-age compressive strength development for mixtures incorporating a) SRA and/or SAP and b) combined shrinkage mitigation techniques.

Adding SRA tends to prolong the setting time compared to that of the control mixture, while adding SAP tends to shorten it slightly owing to the better curing condition offered by the SAP entrained water and consequently the better progress of hydration reactions. Adding PHCM shortened the setting time significantly compared to that of the *C* mixture as shown in **Table 7-2**. The higher the PHCM addition, the shorter was the measured setting time. These results confirm the acceleration of hydration reactions imparted by the PHCM technique. This acceleration effect offsets the undesirable behaviour induced by SRA and/or SAP. For instance, it mitigates the retardation effect induced by SRA addition, leading to enhanced early-age compressive strength (**Fig. 7-1(b)**).

Table 7-2 : Setting time results for the tested mixtures.

| Mixture | Setting Time | | | |
| | Initial | | Final | |
	Hours	Minutes	Hours	Minutes
C	5	25	6	10
H1	4	45	5	10
H2	3	05	4	00
H3	2	35	3	20
CR2	6	17	7	10
CS	5	08	5	50
CR2S	5	55	6	35
H2R2	5	35	6	15
H2S	4	45	5	30
H2R2S	5	00	5	53

7.4.2. Degree of Hydration

The early-age compressive strength development of concrete mixtures greatly depends on the degree of hydration achieved (Xiao and Li, 2008). Shrinkage mitigation techniques

usually affect the rate of hydration reactions. Accordingly, the degree of hydration and amount of BW will be changed (Bentz *et al.*, 2001a). TGA was used to investigate the hydration evolution. The measured degree of hydration (represented by the relative BW) versus age is shown in **Fig. 7-2(a,b)**.

Adding PHCM accelerated the rate of hydration reactions, leading to a higher degree of hydration. The higher the added dosage of PHCM, the higher was the degree of hydration achieved as shown in **Fig. 7-2(a)**. This is in agreement with previous early-age compressive strength results (see **Fig. 6-5(b)**). Adding SRA retarded the hydration reactions leading to a lower degree of hydration compared to that of the *C* mixture (**Fig. 7-2(a)**). Conversely, the *CS* mixture had relatively higher water content, thus achieving a higher degree of hydration compared to that of the *C* mixture (Jensen and Hansen, 2001, Jensen and Hansen, 2002). Despite its higher degree of hydration, the *CS* mixture exhibited a lower early-age compressive strength compared to that of the *C* mixture (**Fig. 7-1(a)**) as a result of its higher porosity. Analysis of the incremental pore size distribution data from MIP tests at age 24 hrs showed that SAP specimens had a higher proportion of voids compared to that of the control specimens. The percentage of voids, classified according to the International Union of Pure and Applied Chemistry system (IUPAC) (IUPAC, 1972) was about 4.7% and 2.2% for mixtures *CS* and *C*, respectively. This can be explained as follows: in the mixture without SAP, a lower amount of hydration is required to gain strength since the space between solid particles and the porosity to be filled by hydration products are relatively lower than that of the SAP mixture. Conversely, in the SAP mixture, a higher degree of hydration is achieved while the volume of pores to be filled increases, resulting in a higher net porosity. This is consistent

with previous findings which indicate that porosity has a more dominate effect on the achieved strength than that of the degree of hydration (Odler and Rößler, 1985, Mikhail *et al.*, 1977). The mixture incorporating both SRA and SAP (*CR2S*) did not exhibit a significant improvement in degree of hydration; however, its degree of hydration was higher than that of the *CR2* mixture (**Fig. 7-2(a,b)**). Adding PHCM to the *CR2* mixture improved its degree of hydration significantly. After 24 hours, mixture *H2R2* had about 18% higher BW than that of the *CR2* mixture. This is ascribed to the hydration acceleration effect induced by PHCM. On the other hand, adding PHCM to the *CS* mixture resulted in the highest degree of hydration compared to that of the other mixtures, indicating a considerable progress of hydration reactions (**Fig. 7-2(b)**). This can be ascribed to the coupled effects of adequate curing conditions provided by SAP particles and the acceleration effect of PHCM addition. Similar to the trend of *C* and *CS* mixtures, the *H2S* mixture showed lower compressive strength than that of *H2* mixture. Adding SRA to the mixture incorporating PHCM and SAP (*H2S*) led to a reduction in the amount of the BW (i.e. degree of hydration) compared to that of the *H2S* mixture, which is expected due to the retardation effect imparted by SRA.
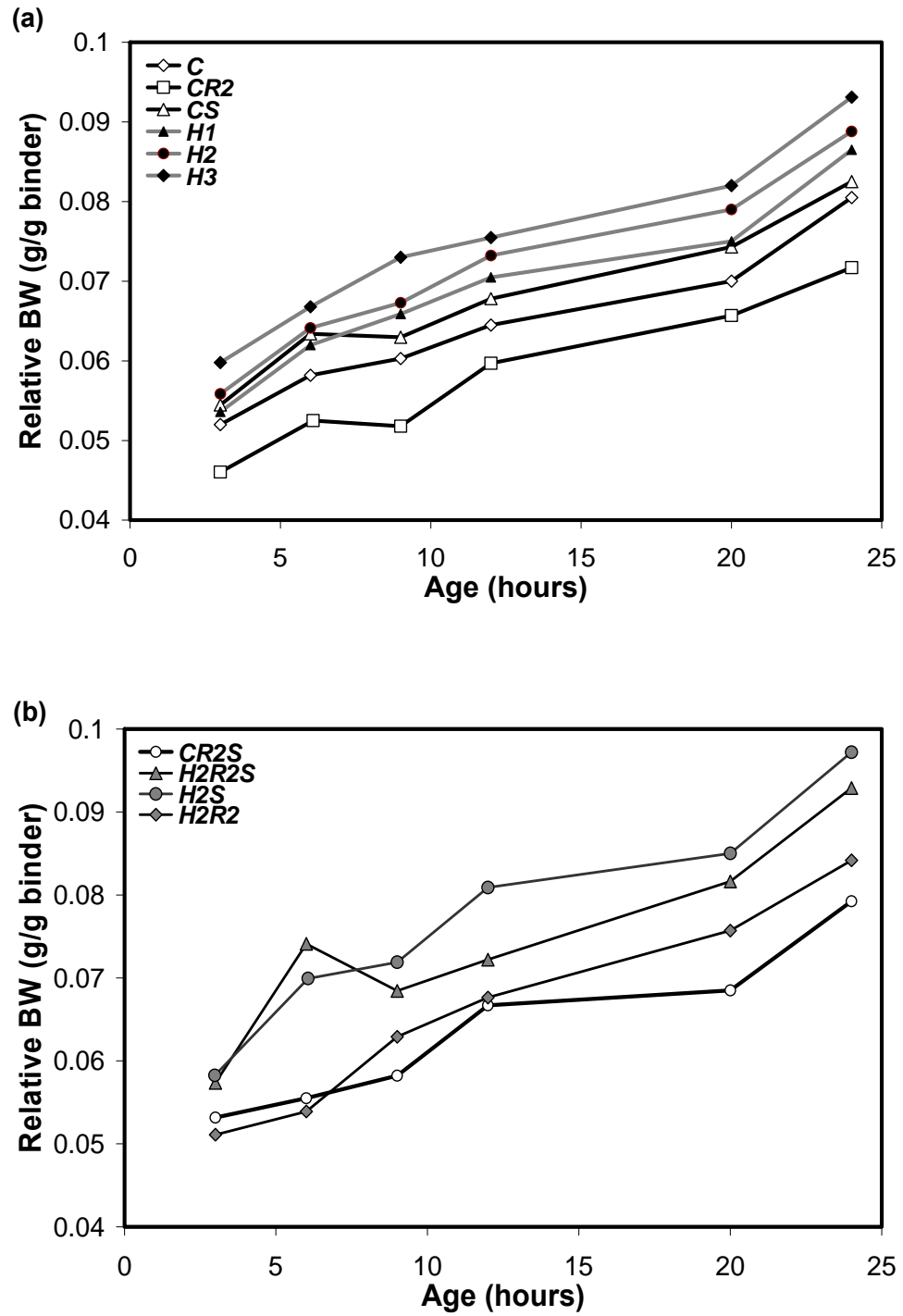
Figure 7-2: Degree of hydration development for mixtures incorporating a) single and b) combined shrinkage mitigation techniques.

7.4.3. Heat of Hydration

The heat of hydration for mixtures incorporating PHCM has been discussed in chapter 6 (see **Fig. 6-8).** Adding PHCM effectively diminished the induction period, leading to a continuous progress of hydration reactions and consequently shorter setting time and more advanced development of microstructure.

It can be noted that adding SRA retarded hydration reactions and reduced the liberated heat compared to that of mixture *C*, as shown in **Fig. 7-3(a)**. This is consistent with previous results (Eberhardt and Kaufmann, 2006). Adding PHCM to the *CR2* mixture resulted in a higher heat of hydration compared to that of the original *CR2* mixture. **Figure 7-3(b)** illustrates the synergetic effect of PHCM and SRA, which represents the net result of two conflicting effects: acceleration and retardation. Adding PHCM accelerated the hydration process and shifted the hydration curve upward and to the left (compared to that of the *CR2* mixture). Concurrently, SRA limited the acceleration effect induced by PHCM addition, resulting in a slightly lower hydration peak at a later time of about 1 hour with respect to that of the *H2* mixture.

The mixture incorporating SAP (*CS*) exhibited a different trend than that of mixture *C*. It initially exhibited a lower temperature peak. This can be ascribed to the high volume fraction of water in the *CS* mixture, which led to higher heat capacity compared to that of the *C* mixture (Bentz, 2008). After about 24 hours, another peak occurred, which indicates further hydration. This can be ascribed to the further hydration reactions between the un-hydrated binder and water released from SAP particles. The mixture incorporating PHCM and SAP (*H2S*) exhibited a higher temperature peak compared to that of the *H2* mixture. Moreover, there was no indication of a second peak

as in the *CS* mixture. This can be ascribed to the early accelerated hydration induced by PHCM, which consumed the majority of the available water (i.e. original mixing water and water entrained by SAP particles) leading to a single temperature peak.

The combined effect of SRA and SAP (mixture *CR2S*) slightly affected the hydration curve with respect to that of the *CR2* and *CS* mixtures. The set retardation effect of SRA shifted the temperature peak downward and to a later time by approximately 1 hour with respect to that of the *CS* mixture. Moreover, similar to the case of the *CS* mixture, a small secondary peak occurred. The mixture incorporating PHCM, SRA and SAP (*H2R2S*) showed a combined trend to that of the *CS*, *CR2S* and *H2* mixtures. The temperature maximum shifted upward and to an earlier time by approximately 3 hours compared to that of the *CR2S* mixture as a result of the hydration acceleration effect induced by PHCM. However, *H2R2S* exhibited a lower temperature peak compared to that of the *H2* mixture, which can be ascribed to the SRA hydration retardation effect and higher heat capacity (as a result of higher water content) (**Fig. 7-3(c)**). Moreover, a secondary temperature peak occurred at about 8 hours earlier than that of the *CS* mixture (**Fig. 7-3(a,b)**). This indicates that SAP released its entrained water earlier, reflecting the higher water demand induced by the accelerated hydration.
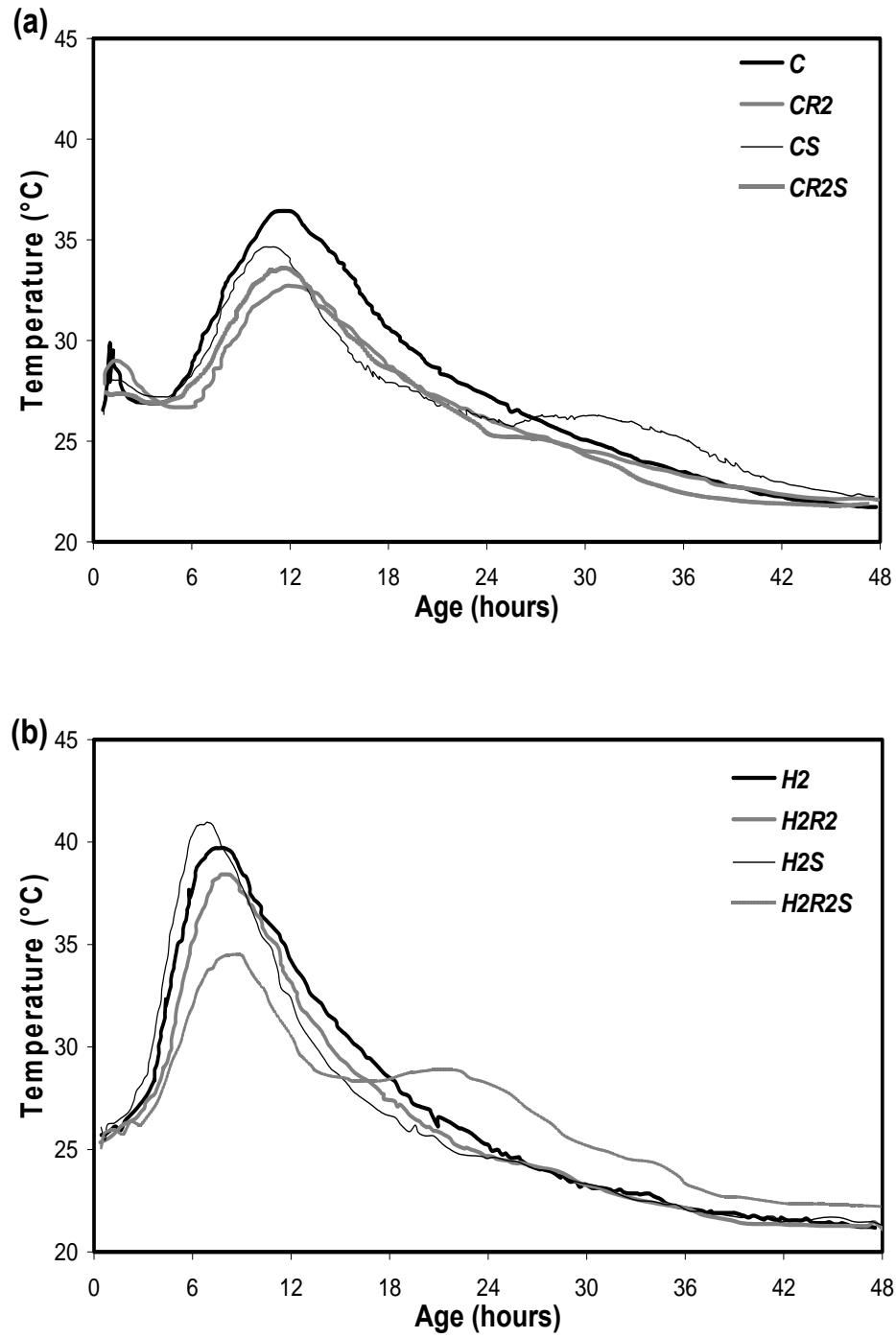
Figure 7-3: Heat of hydration development for mixtures incorporating a) SRA and/or SAP and b) combined shrinkage mitigation techniques.

7.4.4.   Shrinkage and Mass Loss

The mass loss and shrinkage curves of mixtures incorporating SRA, SAP and/or PHCM are shown in **Fig. 7-4 and 7-5**. The measured total shrinkage includes both drying and autogenous shrinkage (thermal deformation can be ignored due to the small cross-section of the samples (Baroghel-Bouny *et al.*, 2006)). For very low w/c (Tazawa and Miyazawa, 1999), the contribution of autogenous shrinkage to the total shrinkage can be comparable to that of drying shrinkage.
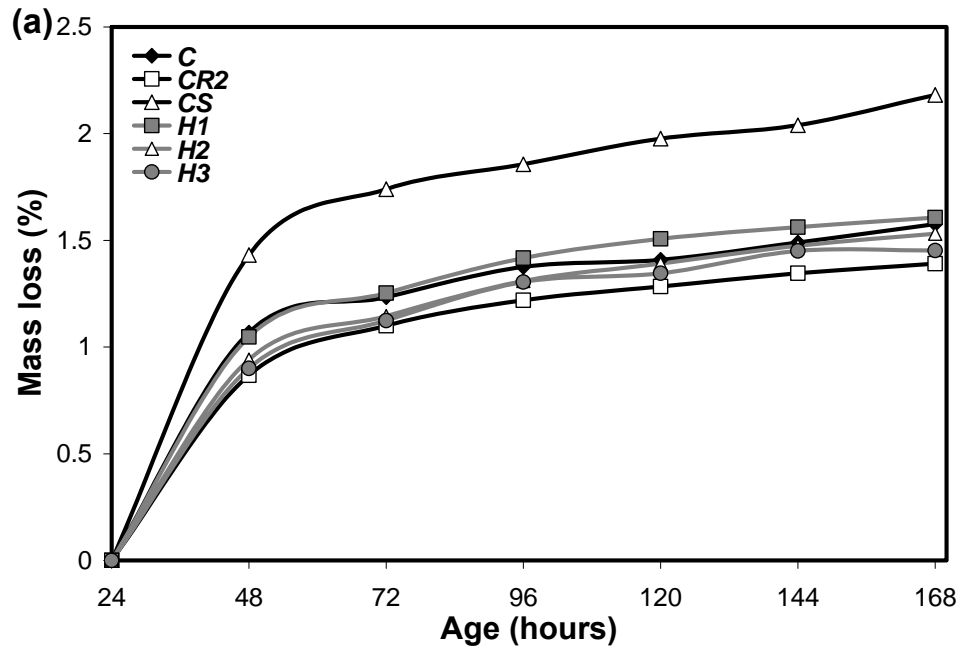
Figure 7-4: Mass loss for mixtures incorporating a) single and b) combined shrinkage mitigation techniques.
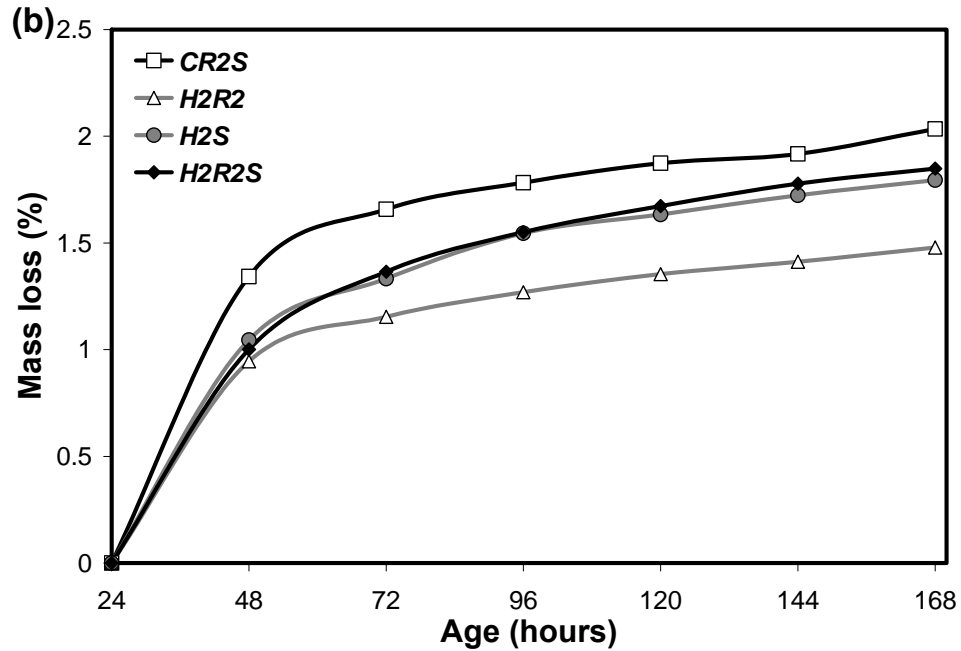
Figure 7-4 Contd': Mass loss for mixtures incorporating a) single and b) combined shrinkage mitigation techniques.
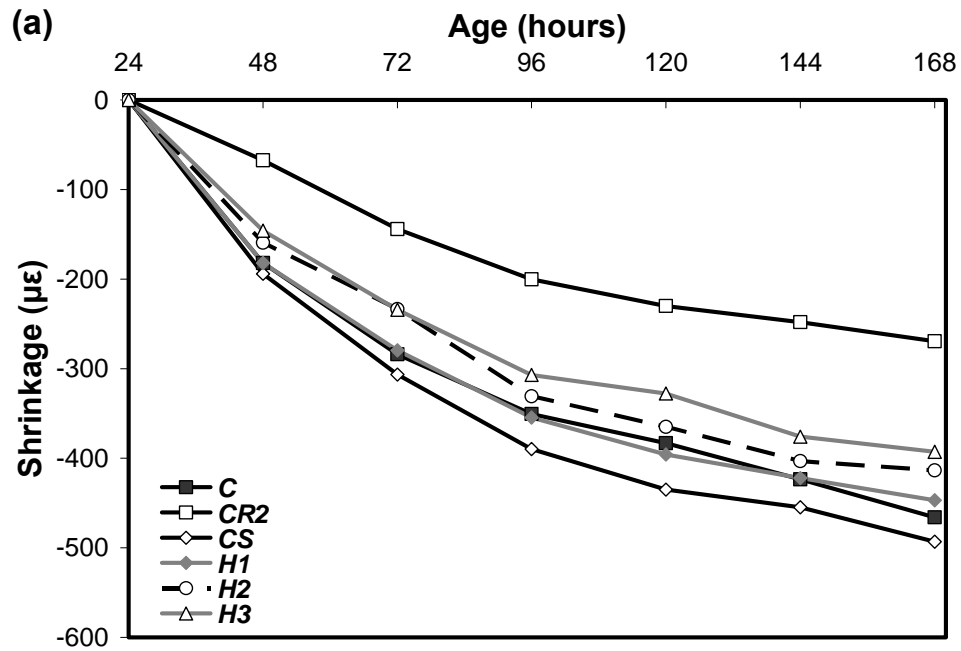
Figure 7-5: Shrinkage development for mixtures incorporating a) single and b) combined shrinkage mitigation techniques.
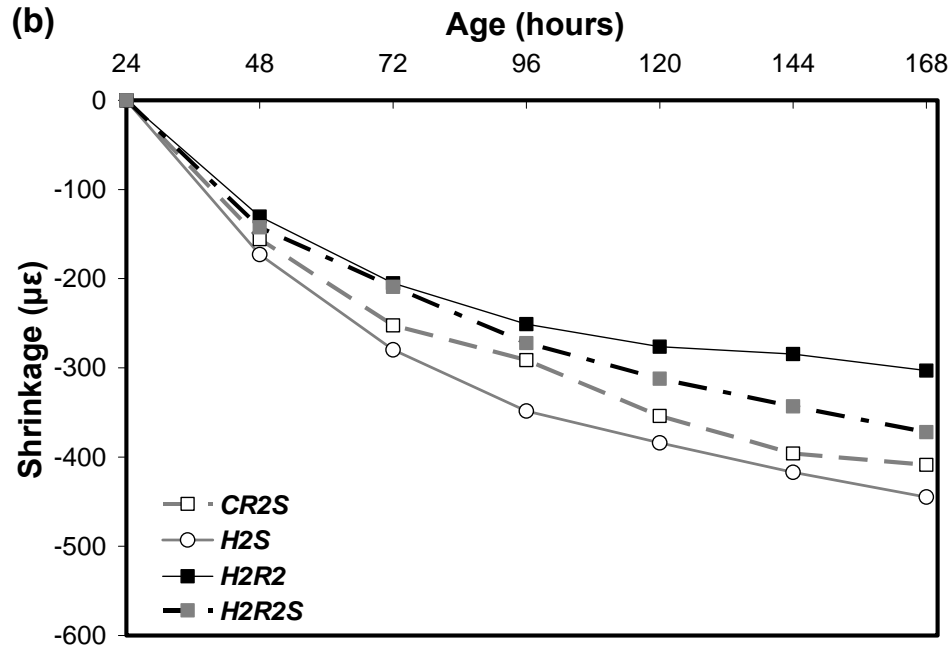
Figure 7-5 Contd': Shrinkage development for mixtures incorporating a) single and b) combined shrinkage mitigation techniques.

Incorporating SRA slightly reduced the mass loss with respect to that of the C mixture, yet it induced a significant reduction in the total shrinkage, in agreement with previous findings (Ichinomiya *et al.*, 2005, Bentz, 2006, He *et al.*, 2006). **Figure 7-6** demonstrates the relationship between a given mass loss and the corresponding shrinkage. The lower slope for the initial linear part and the second part of the mass loss-shrinkage curve for mixture *CR2* compared to that of mixture *C* is consistent with the mechanisms of reduction in surface tension induced by SRA (Kovler and Bentur, 2009). As a result, lower capillary stresses developed, resulting in lower total shrinkage for a given mass loss.

(a)

(b)
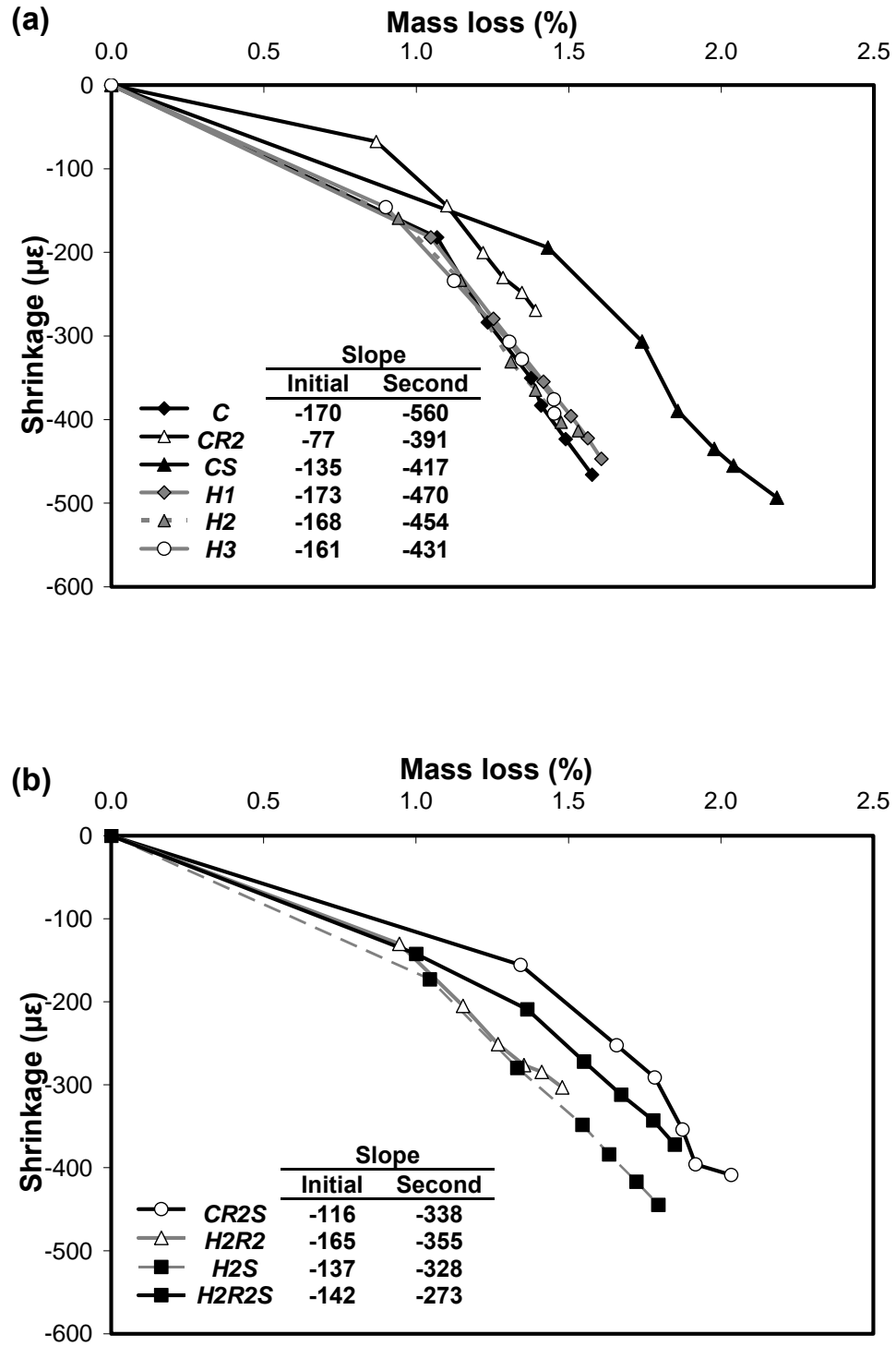
Figure 7-6: Mass loss- shrinkage relationship for mixtures incorporating a) single and b) combined shrinkage mitigation techniques.

This reduction in capillary stresses also explains the lower autogenous shrinkage of mixture **CR2** compared to that of mixture **C** (about 59% reduction at 7 days) as shown in **Fig. 7-7(a)**. Moreover, SRA is believed to reduce the drop in internal relative humidity of specimens, leading to lower self-desiccation and autogenous shrinkage (Bentz *et al.*, 2001b). A few hours after final setting, **CR2** specimens showed an expansion of approximately 85 με compared to only about 21 με for **C** specimens (**Fig. 7-7(a)**). This expansion along with the reduction in autogenous shrinkage induced by SRA resulted in lower net shrinkage compared to that of **C** specimens (Weiss *et al.*, 2008).

Conversely, **CS** specimens exhibited higher mass loss (about 35% at 7 days) compared to that of **C** specimens, while the measured shrinkage at the same age was increased by only 12%. Consequently, the mass loss-shrinkage curve for **CS** mixture (**Fig. 7-6(a)**) exhibited lower slope compared to that of the **C** mixture. This can be explained by the specific shrinkage mitigation mechanism of SAP. The higher water content (due to added entrained water) initially results in higher mass loss (Mönnig and Lura, 2007). Concurrently, SAP particles release water and occupy a smaller volume, leading to additional coarse pores from which water first evaporates, regardless of its location from the drying surface (Bentz *et al.*, 2001a). Such water evaporation results in lower capillary stresses compared to that in the **C** mixture having a finer porosity. In addition, releasing the entrained water from SAP particles likely resulted in expansion (Jensen and Hansen, 2002). Different phenomena are believed to induce this expansion, including swelling of cement gel due to water absorption (Jensen and Hansen, 2002), and capillary distension as a result of capillary vapour pressure increase leading to capillary surface tension relaxation and consequently lower capillary stresses (Kovler, 1996).

Furthermore, autogenous shrinkage and expansion occur simultaneously during early-age, resulting in lower net autogenous shrinkage. This is consistent with the lower autogenous shrinkage exhibited by *CS* specimens compared to that of *C* specimens (22% reduction) (**Fig. 7-7(a)**) and is in agreement with previous findings (Baroghel-Bouny *et al.*, 2006, Kamen *et al.*, 2008)

PHCM mixtures showed a slight reduction in the mass loss and measured total shrinkage compared to that of the *C* mixture (**Figs. 7-4 and 7-5**). For instance, the *H3* mixture had the lowest mass loss among the other PHCM mixtures, which was about 10% lower than that of the *C* mixture. Increasing the amount of added PHCM reduced the measured shrinkage. This can be ascribed to the passive internal restraint system (i.e. hydration micro-crystals (Aitcin, 1999, Jensen and Hansen, 1996)), provided by PHCM addition. The hypothesis that *CH* micro-crystals provide restraint was proposed by (Jensen and Hansen, 1996) based on results reported in (Carde and Francois, 1997, Powers, 1962) which indicated a significant effect of leaching of *CH* micro-crystals on deformation properties. Adding PHCM accelerates the hydration process leading to two conflicting mechanisms: higher rate of autogenous shrinkage and faster structuring of a stiff hydrated skeleton. This internal skeleton can withstand compressive stresses induced by capillary stress due to either drying or self-desiccation (Aitcin, 1999, Acker, 2004, Anna *et al.*, 1995). Consequently, PHCM mixtures had a lower shrinkage, leading to a lower mass loss-shrinkage ratio as shown in **Fig. 7-6(a)**. PHCM mixtures exhibited slope of the initial part of the mass loss-shrinkage curves comparable to that of the *C* mixture, reflecting the similarity of the large pore structure (Kovler and Bentur, 2009), while the

slopes of the second part were lower, indicating that the same water loss resulted in lower shrinkage strain.

The relatively stiffer skeleton and passive internal restraint system induced by PHCM can explain the significant reduction in autogenous shrinkage of PHCM mixtures compared to that of the *C* mixture (**Fig. 7-7(a)**). The reduction in the measured autogenous shrinkage after 24 hours versus that of *C* was about 10% for *H1*, 37% for *H2*, and 57% for *H3*.
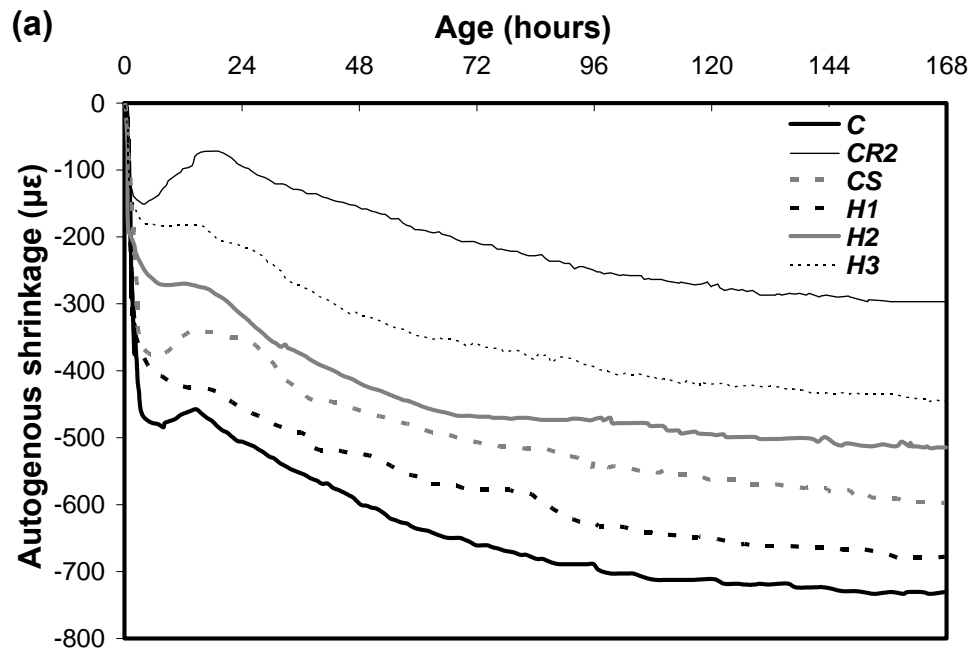
Figure 7-7: Autogenous shrinkage for mixtures incorporating a) single and b) combined shrinkage mitigation techniques.
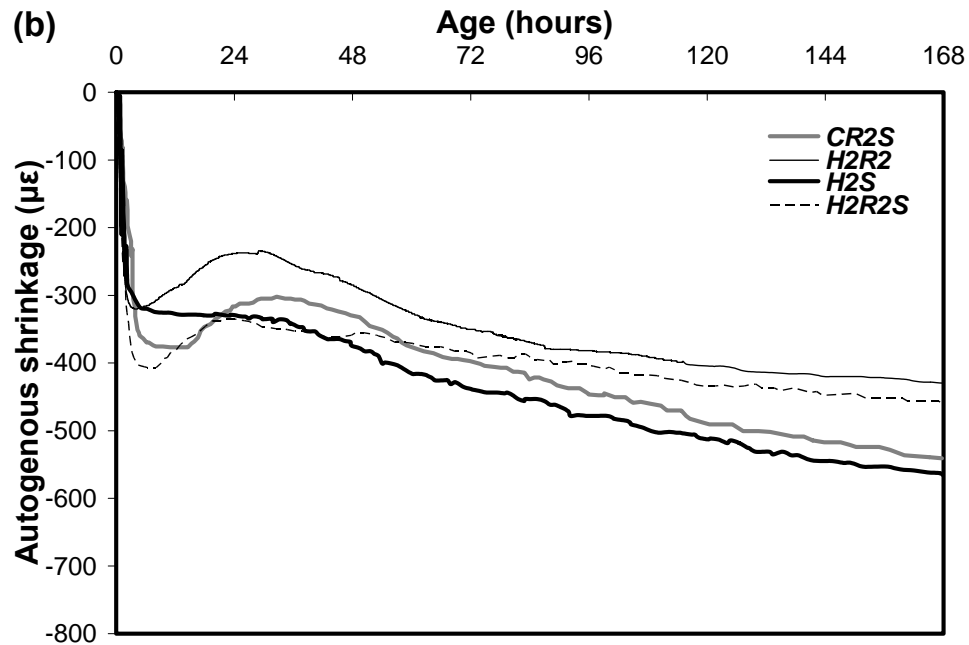
Figure 7-7 Contd': Autogenous shrinkage for mixtures incorporating a) single and b) combined shrinkage mitigation techniques.

Figure 7-7(b) shows the measured shrinkage for mixtures incorporating more than one shrinkage mitigation technique. Generally, the shrinkage behaviour of these mixtures depended on the interaction between the different shrinkage mitigation mechanisms of the combined techniques. This probably can lead to affirmative and/or negative effects on the final shrinkage behaviour.

As mentioned earlier, adding SRA leads to a lower shrinkage as a result of reducing capillary stresses, inducing early expansion, and retarding hydration reactions, which effectively reduces the rate of self-desiccation (i.e. autogenous shrinkage) development. Therefore, adding SRA to SAP and PHCM mixtures reduced the total and autogenous shrinkage significantly with about 19% and 25% with respect to SAP mixture

values, and by 26% and 17% with respect to PHCM values, respectively. In fact, the early expansion had a major contribution to the achieved reduction in the net autogenous shrinkage. Mixture incorporating SAR and SAP exhibited higher early expansion (about 74 μm) which is about one order of magnitude of that of SAP mixtures without SRA (32 μm). Moreover, adding SRA to PHCM led to an early-age expansion, distinct from mixture incorporating PHCM only, which showed a plateau in shrinkage development during the same period. This indicates that the early expansion effect of SRA was a dominate factor in the resultant shrinkage behaviour.

Conversely, adding either SAP or PHCM to *CR2* mixture increases the measured shrinkage compared to mixture incorporating SRA only. This can be attributed to the reduction in the SRA concentration due to the higher water content (Acker, 2004) and the ability of SAP particles to absorb SRA (Bentz, 2005). Moreover, SRA hinder CH formation (Matlese *et al*., 2005) which results in a lower amount of micro restraining crystals compared to PHCM mixture as shown in TGA curves (**Fig. 7-8**). PHCM mixture incorporating SRA showed an additional peak at about 340°C and smaller amount of CH decomposition compared to that of PHCM mixture without SRA. Previous studies (Sant, 2009) reported a reduction in the SRA peak with time, which was attributed to the reduction in SRA concentration in the pore solution due to being uptake by hydration products. This can explain the difference in the 12 and 24 hrs TGA results, where the peak corresponding to SRA was disappeared for *H2R2* mixture at 24 hrs and another peak seems to detected around 800°C, which is correspond to SRA taken in the CSH gel (Beaudoin *et al*., 2008).
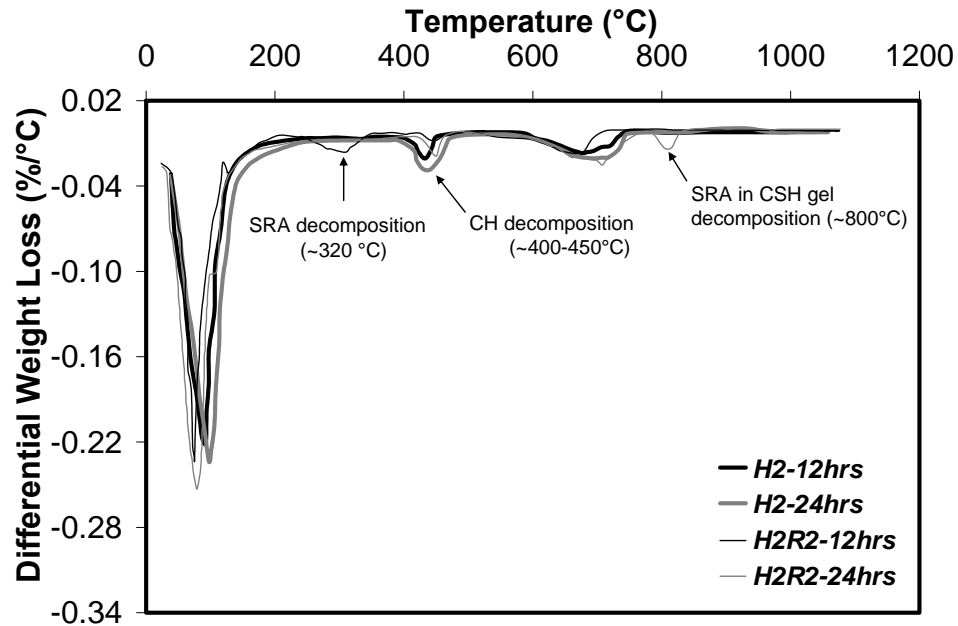
Figure 7-8: TGA curves at different ages for PHCM mixture with and without SRA.

On the other hand, adding PHCM to **SAP** mixture showed about 16% and 11% lower mass loss and total shrinkage, respectively compared to that the **SAP** mixture, and slightly higher shrinkage compared to that of the PHCM mixture. This can be explained as follows: the addition of PHCM accelerates hydration reactions, which increases water consumption and the rate of self-desiccation. Hence, the water stored inside the SAP particles will be released earlier to compensate for the water deficit. This leads to less evaporable water, more hydration products and stronger restraining skeleton in the **H2S** mixture compared to that of the **CS** mixture. This can be seen in TGA curves, where the peak of evaporable water (60-200°C) was higher in SAP compared to that of **H2S** mixture, while the CH peak (thus amount) was lower (**Fig. 7-9(a)**). This was also confirmed by DSC results, where **CS** mixtures showed lower CH enthalpy compared to that of mixture incorporating both PHCM and SAP (**Fig. 7-9(b)**). Hence, the absence of

the early expansion in **P-SAP** specimens compared to that of the SAP specimens (**Fig. 7-7(a,b)**) can be ascribed to the higher hydration progress and consequently higher autogenous shrinkage that likely offset the expansion induced by the released water. This is in agreement the previous heat of hydration results of *H2S* mixture (higher temperature peak and the absent of the second peak (**Fig. 7-3(b)**)).
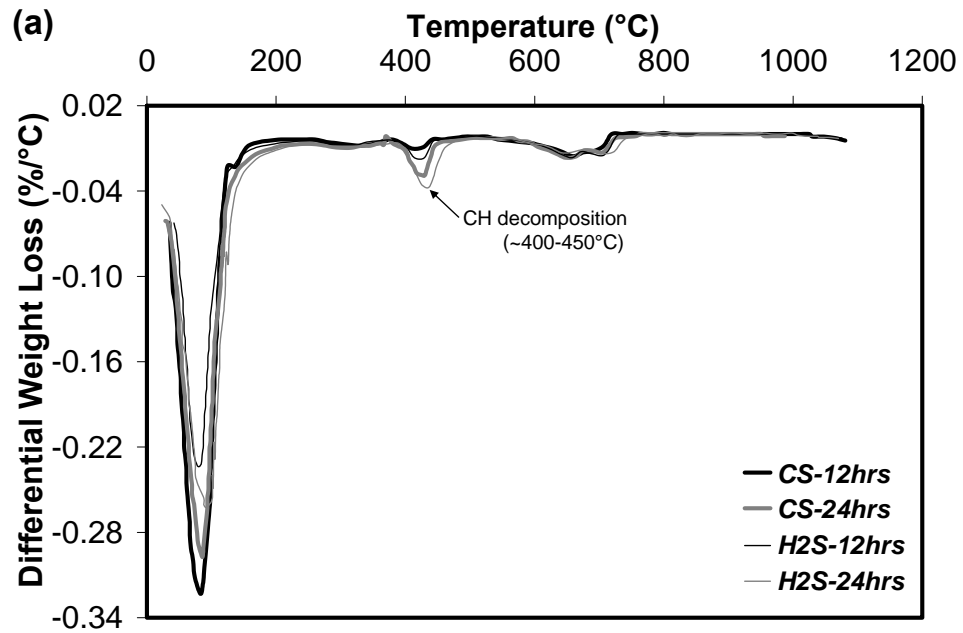
Figure 7-9: Thermal analysis at different ages for PHCM mixture with and without SAP a) TGA and b) CH content.
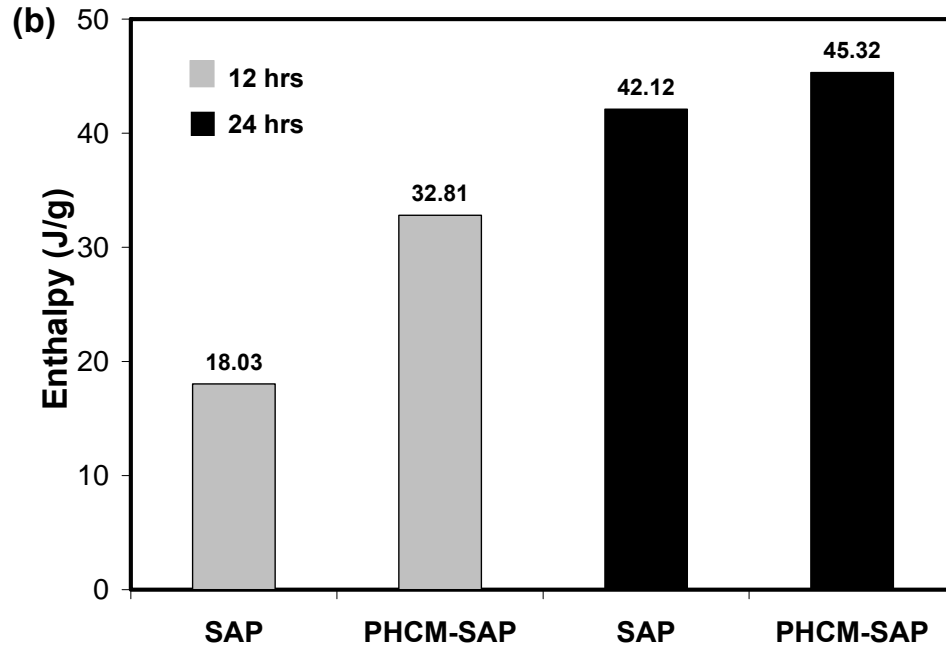
Figure 7-9 Contd': Thermal analysis at different ages for PHCM mixture with and without SAP a) TGA and b) CH content.

As expected, combining the three mitigation techniques showed a trend that can be a considered as the resultant of the different involved mechanisms. Adding SRA retarded hydration and induced higher early expansion (about 70 μm) compared to mixtures incorporating both PHCM and SAP, which showed a plateau in stead of expansion during the same period (**Fig. 7-7(b)**). Adding PHCM provided additional CH to the mixture, which enhanced the passive retraining system and eliminate the hindering of CH formation induced by SRA. This was confirmed based on DSC results, where the CH enthalpy in *CR2S* mixture, detected as early as 3 hrs from adding the mixing water, was increased with the addition of PHCM to about the double (i.e. 3.104 J/g).

The mass loss-shrinkage curves for mixtures incorporating combined shrinkage mitigation techniques are shown in **Fig. 7-6(b)**. Adding SRA to SAP and/or PHCM mixtures reduced the initial slope. This is expected due to the additional shrinkage reduction induced by SRA. Adding SAP to the *H2* mixture did not cause a significant change in the initial slope. This is consistent with the earlier explanation of the synergetic effect of PHCM and SAP.

Moreover, mass loss-shrinkage curves second slopes for all mixtures incorporating more than one mitigation technique were lower than those of mixtures incorporating one mitigation technique (**Fig. 7-6(b)**), indicating higher efficiency than their individual effects. For instance, the three mitigation techniques individually reduced the second slope with an average of 25% compared to 51% for the *H2R2S* mixture with respect to mixture *C* value.

7.5.   STATISTICAL ANALYSIS FOR EFFECT OF PHCM ADDITION ON SHRINKAGE

Analysis of variance (ANOVA) was used to analyze the experimental data. To investigate whether an experimental variable (e.g. PHCM addition) is statistically significant, an *F* value is determined as the ratio of the mean squared error between treatments (e.g. different PHCM addition ratio) to that of within treatments (due to using replicates rather than testing only one specimen). This value is then compared to a standard (critical) *F* value of an *F*-distribution density function obtained from statistical tables based on the significance level (α) and the degrees of freedom of error determined from the number of treatments and observations in an experiment. Exceeding the critical

value of an F-distribution density function reflects that the tested variable affects the mean of the results (Montgomery, 2009).

ANOVA at a significance level $\alpha = 0.05$, showed that variation in the addition rate of PHCM had an insignificant effect on the mean of total shrinkage measured after the first 24 hours. The calculated F value of 0.892 for the total shrinkage results was lower than the corresponding critical F value of 4.07 ($F_{0.05,3,8}$). Conversely, variation in the addition rate of PHCM showed a significant effect on the mean autogenous shrinkage measured from the final setting time; the associated value was 60.26, which is significantly larger than the corresponding critical F value ($F_{0.05,3,8}$).

According to previous studies (Aitcin, 1999, Zhang *et al.*, 2003), measuring the total shrinkage after 24 hours leads to overlooking the autogenous deformation contribution. Hence, the total measured shrinkage can be re-evaluated taking into account the autogenous shrinkage measured using the corrugated tube from the time of final setting until the beginning of drying at 24 hours (Weiss *et al.*, 2008). ANOVA for the total measured shrinkage after adding autogenous shrinkage showed that the variation in the addition rate of PHCM had a significant effect on the mean of the total shrinkage results. The calculated F value was 73.03, which is significantly larger than the corresponding critical F value ($F_{0.05,3,8}$). This emphasizes the significant role of autogenous shrinkage. Indeed, delays in measuring shrinkage can result in underestimating the actual deformation behaviour, in agreement with previous findings (Aitcin, 1999, Zhang *et al.*, 2003).

7.6.   CONCLUSIONS

The main conclusions that can be drawn from this experimental investigation are:

1) UHPC mixtures incorporating PHCM achieved higher early-age compressive strength results than those mixtures incorporating SRA and/or SAP.

2) SRA was the most effective shrinkage mitigation method compared to other mitigation techniques.

3) PHCM achieved excellent early-age shrinkage reduction in balance with other properties when used alone or combined with other shrinkage mitigation techniques.

4) Combining PHCM and SRA mitigated the drawbacks of SRA including delays in setting time and significant reduction in early-age compressive strength.

5) The addition of PHCM improved the shrinkage behaviour of mixtures incorporating SAP and overcame the SAP drawbacks including higher mass loss and porosity that usually lead to a reduction in early-age compressive strength.

6) Combining shrinkage mitigation techniques including SRA, SAP and PHCM showed better overall behaviour compared to their individuals effects. This includes enhanced compressive strength development and lower shrinkage.

7.7. REFERENCES

Acker, P., (2004), "Swelling, shrinkage and creep: a mechanical approach to cement hydration," *Materials and Structures*, Vol. 37, No. 4, pp. 237-243.

Aggoun, S., Cheikh-Zouaoui, M., Chikh, N. and Duval, R., (2008), "Effect of some admixtures on the setting time and strength evolution of cement pastes at early ages," *Construction and Building Material*, Vol. 22, No. 2, pp. 106-110.

Aitcin, P.C., (1999), "Demystifying autogenous shrinkage," *Concrete International*, Vol. 21, No. 11, pp. 54-56.

Anna, K., Leivo, M. and Sipari, P., (1995), "Experimental study on the basic phenomena of shrinkage and cracking of fresh mortar," *Cement and Concrete Research*, Vol. 25, No. 8, pp. 1747-1754.

Baroghel-Bouny, V., Mounanga, P., Khelidj, A., Loukili, A. and Rafaï, N., (2006), "Autogenous deformations of cement pastes: Part II. W/C effects, micro–macro correlations, and threshold values," *Cement and Concrete Research*, Vol. 36, No. 1, pp. 123-136.

Beaudoin, J., Drame, H., Raki, L., and Alizadeh, R., (2008), "Formation and properties of C-S-H-PEG nanostructures", *Materials and Structures*, Vol. 42, No.7, pp. 1003-1014.

Bentz, D.P., (2005), "Capitalizing on self-desiccation for autogenous distribution of chemical," *Proceedings of the 4th International Seminar on Self-Desiccation and Its Importance in Concrete Technology*, B. Persson, D. Bentz, and L.O. Nilsson (eds.), Lund University, USA, pp. 189-196.

Bentz, D.P., (2006), "Influence of shrinkage-reducing admixtures on early-age properties of cement pastes," *Journal of Advanced Concrete Technology*, Vol. 4, No. 3, pp. 423-429.

Bentz, D.P., (2008), "A review of early-age properties of cement-based materials," *Cement and Concrete Research*, Vol. 38, No. 2, pp. 196-204.

Bentz, D.P. and Jensen, O.M., (2004), "Mitigation strategies for autogenous shrinkage cracking," *Cement and Concrete Composites*, Vol. 26, No. 6, pp. 677-685.

Bentz, D.P., Hansen, K.K., Madsen, H.D., Vallee, F. and Griese, E.J., (2001a), "Drying/hydration in cement pastes during curing," *Materials and Structures*, Vol. 34, No. 9, pp. 557-565.

Bentz, D.P., Geiker, M.R. and Hansen, K.K., (2001b), "Shrinkage-reducing admixtures and early-age desiccation in cement pastes and mortars," *Cement and Concrete Research*, Vol. 31, No. 7, pp. 1075-1085.

Carde, C. and Francois, F., (1997), "Effect of the leaching of calcium hydroxide from cement paste on mechanical and physical properties," *Cement and Concrete Research*, Vol. 27, No. 4, pp. 539-550.

Eberhardt, A.B. and Kaufmann, J., (2006), "Development of shrinkage reduced self-compacting concrete," *ACI*, Special Publication, SP-235, pp. 13-30.

Hansen, T.C. and Nielsen, K.E.C., (1965), "Influence of aggregate properties on concrete shrinkage," *ACI Materials Journal*, Vol. 62, No. 7, 1965, pp. 783-794.

He, Z., Li, Z.J., Chen, M.Z. and Liang, W.Q., (2006), "Properties of shrinkage-reducing admixture-modified pastes and mortar," *Materials and Structures*, Vol. 39, No. 4, pp. 445-453.

Hobbs, D.W., (1974), "Influence of aggregate restraint on the shrinkage of concrete," *American Concrete Institution*, Vol. 71, pp. 445-450.

Holschemacher, K., Dehn, F., Klotz, S. and Weiße, D., (2005), "Experimental investigation on ultra high-strength concrete under concentrated loading," *Proceedings of the Seventh International Symposium on Utilization of high-strength/ high performance concrete*, Washington D.C., USA, Vol. 2, pp.1145-1158.

Ichinomiya, T., Hishiki, Y., Ohno, T., Morita, Y. and Takada, K., (2005), "Experimental study on mechanical properties of ultra high-strength concrete with low-autogenous-shrinkage," *ACI*, Special Publication, SP-228, pp. 1341-1352.

IUPAC, (1972). Manual of Symbols and Terminology, Appendix 2, Part 1. In: Colloid and Surface Chemistry, *Pure and Applied Chemistry*, Vol. 31**,** 578 p.

Jensen, O.M. and Hansen, P.F., (1996), "Autogenous deformation and change of relative humidity in silica fume modified cement paste," *ACI Materials Journal*, Vol. 93, No. 6, pp. 539-543.

Jensen, O.M. and Hansen, P.F., (2001), "Water-entrained cement-based materials: I. Principles and theoretical background," *Cement and Concrete Research*, Vol. 31, No. 4, pp. 647-654.

Jensen, O.M. and Hansen, P.F., (2002), "Water-entrained cement-based materials: II. Experimental observations," *Cement and Concrete Research*, Vol. 32, No. 6, pp. 973-978.

Kamen, A., Denarié, E., Sadouki, H. and Brühwiler, E., (2008), "Thermo-mechanical response of UHPFRC at early-age: Experimental study and numerical simulation," *Cement and Concrete Research*, V. 38, No. 6, pp. 822-831.

Kovler, K., (1996), "Why Sealed Concrete Swells," *ACI Materials Journal*, Vol. 93, No. 4, pp. 334-340.

Kovler, K. and Bentur, A., (2009), "Cracking sensitivity of normal and high strength concretes," *ACI Materials Journal*, Vol. 106, No. 6, pp. 537-542.

Ma, J., Orgass, M., Dehn, F., Schmidt, D and Tue, N.V., (2004), "Comparative investigations on ultra-high performance concrete with and without coarse aggregates," *Proceeding of the International Symposium on Ultra High Performance Concrete*, Germany, pp. 205-212.

Matlese, C., Pistolesi, C., Lolli, A., Bravo. A., Cerulli, T. and Salvioni, D, (2005), "Combined effect of expansion and shrinkage reducing admixture to obtain stable and durable mortars" *Cement and Concrete Research*, Vol. 35, No. 12, pp. 2244-2251.

Mikhail, R.S., Abo-El-Enein, S.A. and Gabr, N.A., (1977), "Hardened slag-cement pastes of various porosities I. Compressive strength, degree of hydration and total porosity," *Journal of Applied Chemistry and Biotechnology*, Vol. 24, No. 12, pp. 735-743.

Mönnig, S. and Lura, P., (2007), "Superabsorbent Polymers - An Additive to Increase the Freeze-Thaw Resistance of High Strength Concrete," In: *Advances in Construction Materials*, Part V, Springer, Berlin-Heidelberg, pp. 351-358.

Montgomery, D.C., (2009). Design and Analysis of Experiments, 7th Edition, John Wiley & Sons, Hoboken, New Jersey, USA, 656 p.

Odler, I. and Dörr, H., (1979), "Early hydration of tricalcium silicate I : Kinetics of the hydration process and the stoichiometry of the hydration products," *Cement and Concrete Research*, Vol. 9, No. 2, pp. 239-248.

Odler, I. and Rößler, M., (1985), "Investigations on the relationship between porosity, structure and strength of hydrated Portland cement pastes: II. Effect of pore structure and of degree of hydration," *Cement and Concrete Research*, Vol. 15, No. 3, pp. 401-410.

Powers, T.C., (1962), "A hypothesis on carbonation shrinkage," *Journal of Portland Cement Association Research and Development Labs*, Vol. 4, No. 2, 1962, pp. 40-50.

Rajabipour, F., Sant, G. and Weiss, J., (2008), "Interactions between shrinkage reducing admixtures (SRA) and cement paste's pore solution," *Cement and Concrete Research*, Vol. 38, No. 5, pp. 606-615.

Ramachandran, V.S., Haber, R.M., Beaudoin, J.J. and Delgado, A.H., (2002). Handbook of Thermal Analysis of Construction Materials, Noyes Publications/William Andrew Publishing, Norwich, 655 p.

Sant, G., (2009), "Fundumental investigation related to the mitigation of volume change in cement-based materials at early-ages," Ph.D thesis, *Purdue University*, Indiana, USA, 203 p.

Tazawa, E. and Miyazawa, S., (1999), "Effect of constituents and curing condition on autogenous shrinkage of concrete," *Proceedings of the International Workshop Autogenous Shrinkage of Concrete*, (ed.) Eichi Tazawa, Taylor & Francis, pp. 269-280.

Wang, F., Zhou, Y., Peng, B., Liu, Z. and Hu, S., (2009), "Autogenous Shrinkage of Concrete with Super-Absorbent Polymer," *ACI Materials Journal*, Vol. 106, No. 2, 2009, pp. 123-127.

Weiss, J., Lura, P., Rajabipour, F. and Sant, G., (2008), "Performance of shrinkage-reducing admixtures at different humidities and at early ages," *ACI Materials Journal*, Vol. 105, No. 5, pp. 478-486.

Xiao, L. and Li, Z., (2008), "Early-age hydration of fresh concrete monitored by non-contact electrical resistivity measurement," *Cement and Concrete Research*, Vol. 38, No. 3, pp. 312-319.

Zhang, M. H., Tam, C. T. and Leow, M.P., (2003), "Effect of water-to-cementitious materials ratio and silica fume on the autogenous shrinkage of concrete," *Cement and Concrete Research*, Vol. 33, No. 10, pp. 1687-1694.

CHAPTER EIGHT

INFLUENCE OF NATURAL WOLLASTONITE MICROFIBERS ON EARLY-AGE BEHAVIOUR OF UHPC*

In order to produce concrete characterized by lower early-age shrinkage and cracking risk along with reducing its environmental and economic impact, the concept of reusing waste concrete (i.e. partially hydrated cementitious materials) as a source for internal passive restraining system and its efficiency was discussed in Chapters 6 and 7. In this chapter, various sizes of natural wollastonite microfiber were added to the UHPC as a replacement for cement. The potential of using wollastonite microfiber, as a natural material, to improve early-age properties of UHPC along with achieving lower environmental impact was investigated.

8.1.   INTRODUCTION

Early-age cracking of cement based materials arises from the early rapid volume changes as a result of autogenous and drying shrinkage and thermal deformations (Bentz *et al*., 2008, Ma *et al*., 2007). Such volume changes induce tensile stresses within cement based materials. The tensile strength of such materials and its ability to resist tensile stresses increase with time (ACI Committee 231, 2010). Hence, a competition between the induced tensile stresses and the development of cement based materials tensile strength exists during early-ages. Once tensile stresses exceeded the tensile strength, micro-

---

*A version of this chapter has been submitted for review to the Journal of Materials in Civil Engineering, ASCE.

cracking develops and propagates leading to visible shrinkage macro-cracking (ACI Committee 231, 2010, Cusson, 2008). Shrinkage cracks later facilitate the penetration of aggressive substances to concrete, leading to a reduction in its performance, serviceability, and durability (Passuello *et al.*, 2009).

Several methods have been advocated to minimize the cracking potential of concrete, including using coarser cement particles, expansive additives, shrinkage reducing admixtures and/or improving curing conditions (Bentz and Peltz, 2008, Van Breugel and De Vries, 1998, Tazawa, 1998, Nmai *et al.*, 1998). These approaches primarily focus on reducing shrinkage strains in concrete, thereby reducing the level of residual stress that develops (Shah *et al.*, 1998). On the other hand, microfibers were reported to act as a local restraint for shrinkage (Zhang and Li, 2001). Microfibers generally bridge micro-cracks, leading to a reduction in crack widths and delaying the occurrence of cracking (Lawler *et al.*, 2003).

Different types of microfibers have been used as reinforcements for cementitious materials, including organic, mineral, metallic, or synthetic microfibers (Andiç *et al.*, 2008, Pierre *et al.*, 1997). Among these, metallic microfibers (e.g. steel) have been widely used in different UHPC applications (Hoang *et al.*, 2008). However, optimizing the use of other types of microfibers in UHPC applications can provide an effective and low-cost reinforcement method. A potential microfiber is wollastonite, which is widely used in other industrial applications (e.g. ceramics, plastics, paints, etc.) (Azaroy *et al.*, 1995).

Wollastonite is a naturally occurring, acicular, inert, white mineral (calcium meta silicate [β- CaO-SiO$_2$]), which is less costly than steel and carbon microfibers (Low and Beaudoin, 1992). Previous studies have shown the potential for using natural wollastonite microfibers as a reinforcing material in cementitious materials (Low and Beaudoin, 1992, Low and Beaudoin, 1993, Low and Beaudoin, 1994a). The addition of wollastonite in cement-silica fume matrices showed significant improvements in pre-peak and post-peak load, flexural toughness and ductility (Low and Beaudoin, 1993). Moreover, wollastonite microfibers imbedded in cementitious materials achieved high stability without surface or bulk deterioration with time (Low and Beaudoin, 1994b). However, there appears to be little or no information with regards to the early-age properties, shrinkage and cracking behaviour of UHPC reinforced with natural wollastonite microfibers. Moreover, the mechanism of microfiber/matrix interfacial bond in UHPC has not yet been fully characterized. Therefore, the aim of this study is to examine the feasibility of utilizing various small-size wollastonite microfibers in UHPC to control shrinkage cracking, and to investigate its effect on other early-age properties of UHPC.

8.2.   RESEARCH SIGNIFICANCE

With the increasing use of UHPC in the construction, strengthening and rehabilitation of different infrastructure, controlling the early-age shrinkage cracking of UHPC is essential for ensuring an enhanced long-term performance and longer service life. Added wollastonite microfibers acted as an internal restraint for shrinkage, reinforcing the microstructure at the micro-crack level leading to an enhancement of early-age engineering properties of UHPC matrix. From an environmental point of view, achieving

UHPC with comparable performance, yet with lower cement content, using natural wollastonite as partial replacement for cement can lead to a reduction in the cement factor and consequently lower CO_2 emissions. This can make the cement intensive UHPC more sustainable.

8.3.   EXPERIMENTAL PROGRAM

This experimental program aims to investigate the effect of wollastonite microfibers on early-age behaviour of UHPC and their role in controlling shrinkage cracking. This is of primary importance in order to achieve high performance and durable structures. In this study, the hydration and strength development (compressive strength, flexural toughness, heat of hydration, degree of hydration) and shrinkage behaviour have been investigated on UHPC mixtures incorporating different contents and sizes of wollastonite microfibers. All tests were conducted on UHPC specimens without heat curing in order to explore real effects that govern UHPC shrinkage existing in structural elements cast in-situ.

8.3.1.   Materials and Mixture Proportions

The materials used in this chapter were similar to that used in Chapter 3 (refer to Section 3.4.1). The chemical and physical properties of the used binders have been given in Chapter 3 (**Table 3-1**). Commercially available natural wollastonite microfibers were used at three dosages (4, 8 and 12%) as partial substitution for cement by volume. Three microfiber sizes were used in this study: MF1 (length 152 μm, diameter 8 μm), MF2 (length 50 μm, diameter 5 μm), and MF3 (length 15 μm, diameter 3 μm) (see **Fig. 8-1**).

The selected composition of the control mixture are shown in Chapter 3 (refer to **Table 3-2**). The characteristics of the tested mixtures are shown in **Table 8-1**.

(a) **(b)** **(c)**
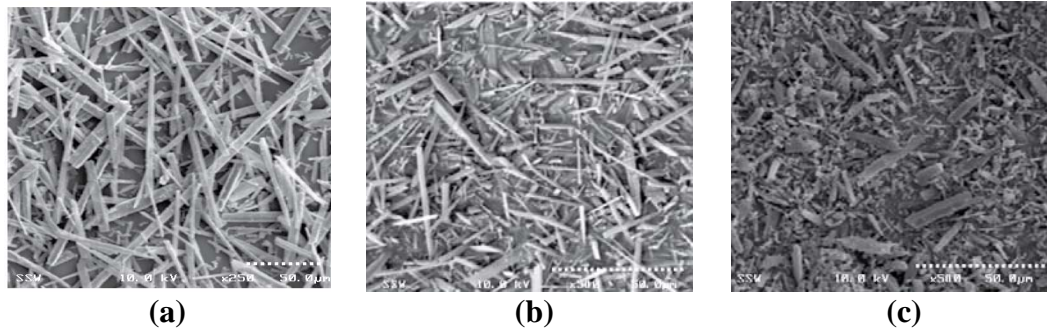
Figure 8-1: Different sizes of wollastonite microfibers a) MF1, b) MF2 and c) MF3.

Table 8-1: Tested mixtures

Mixture	MF1%	MF2%	MF3%
C	----	----	----
M14	4.0	----	----
M18	8.0	----	----
M112	12.0	----	----
M24	----	4.0	----
M28	----	8.0	----
M212	----	12.0	----
M34	----	----	4.0
M38	----	----	8.0
M312	----	----	12.0

8.3.2. Preparation of Test Specimens and Testing Procedures

The experimental methods used in this chapter are the cubic compressive strength test, flexural strength test, workability test, Semi-adiabatic calorimetry, TGA, MIP, measurements of total free shrinkage, mass loss, setting time, shrinkage restraining test

and   SEM/EDX analysis. The cubic compressive strength test, Semi-adiabatic

calorimetry, TGA, MIP, measurements of total free shrinkage, mass loss, setting time and

SEM/EDX analysis were previously explained in chapters 3, 5 and 7. The workability,

flexural strength test and shrinkage restraining test are explained in the following

sections.

The workability of mixtures was evaluated based on the flow index (*F*), which is

defined as follows (**Eq. 1**):

$$F(\%) = \frac{R_{25} - R_0}{R_0} \times 100$$
Eq. 1

where R_{25} is the radius of the mortar pile after the 25th drop and R_0 is the initial radius of

the mortar pile according to the ASTM C 1437 (Standard Test Method for Flow of

Hydraulic Cement Mortar).

Flexural strength testing was conducted on 35x35x200 mm UHPC prisms at the

ages of 3, 5 and 7 days (Pierre *et al*., 1997). The third-point loading flexural strength tests

were carried out using a computer controlled material testing system at a loading rate of

0.1 mm/min. Prior to the bending test, each beam specimen was maintained in a calcium

hydroxide saturated solution. A total of four specimens were tested for each mixture at

each age and the average result was reported.

An instrumented ring test was performed similar to previous work (See *et al*., 2003)

to quantify the restrained shrinkage behaviour, cracking age and width, for mixtures with

and without wollastonite microfibers. The dimensions of the concrete ring specimen used

in this evaluation are given in **Fig. 8-2**. The specimens were not allowed to dry from top

and bottom surfaces of the ring by sealing the circumference. Each ring specimen was equipped with four strain gages at the mid-height on the inner circumference of the steel ring. Steel ring strain measurements were monitored until the concrete ring cracked. After that, measurements of the cracking widths were taken every day for at least 7 days.
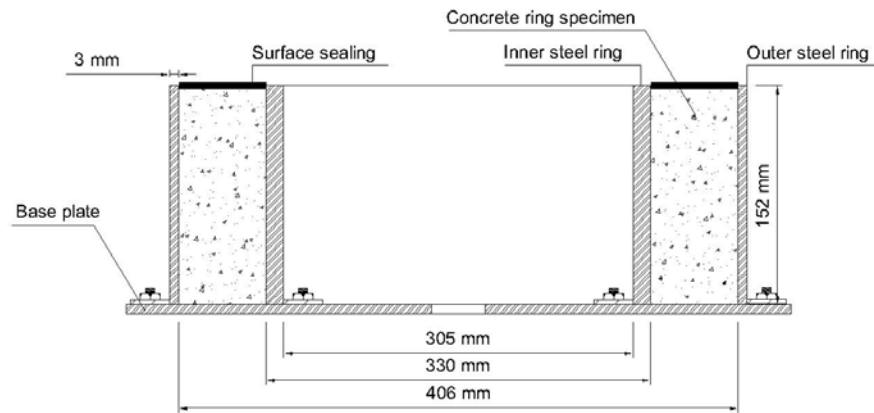
Figure 8-2: Concrete ring test.

8.4. RESULTS AND DISCUSSION

8.4.1. Workability

The workability of UHPC mixtures incorporating microfibers is highly affected by the microfiber content and its aspect ratio (Tatnall, 2006). **Figure 8-3** shows the relative change in the flowability of UHPC mixtures incorporating different sizes and contents of wollastonite microfibers with respect to that of the control mixtures. Incorporating MF1 and MF2 led to lower workability compared to that of mixtures without microfibers. The higher the MF1 or MF2 content, the lower was the workability achieved. This can be attributed to an increase in the microfibers interlocking due to its needle-like shape (Tatnall, 2006). However, this reduction in workability can be overcome through applying vibration during placing or using higher dosage of HRWRA (Tatnall, 2006,

Ransinchung and Kumar, 2010). Conversely, adding MF3 increased workability of UHPC mixtures compared to that of the control. The workability was better enhanced as the added amount of MF3 increased. MF3 microfibers have a very small size; thus it provides an internal lubricant effect by displacing water from voids between coarser particles, leading to lower water demand (Nehdi *et al.*, 1998, Schmidt, 1992).
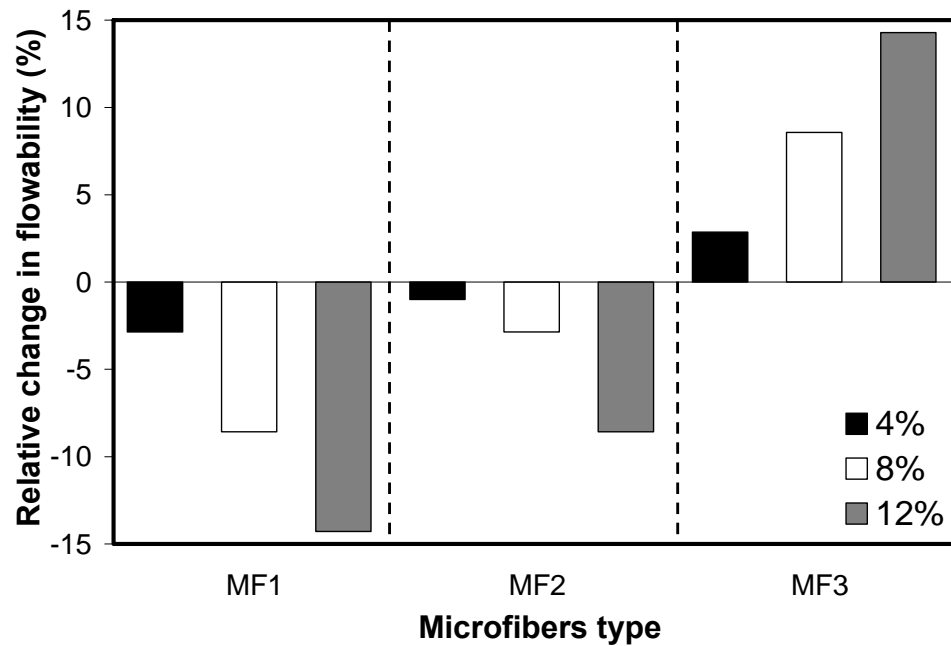
Figure 8-3: Relative change in flowability index for mixtures incorporating different content and sizes of wollastonite microfibers compared to that of the control mixture.

8.4.2. Early-Age Compressive Strength

Compressive strength is considered as a key property of UHPC. The addition of wollastonite microfibers affected the early-age compressive strength of UHPC, as shown in **Fig. 8-4(a,b,c)** and **Table 8-2**. The compressive strength development was mainly influenced by wollastonite microfibers content and size (i.e. aspect ratio). During the very early-age (i.e. ≤ 24 hrs), mixtures incorporating MF1 or MF2 exhibited compressive

strength comparable to or higher than that of the control mixture (**Fig. 8-4(a,b)**). This improvement in compressive strength was more significant at higher wollastonite microfibers content. Conversely, the greater the MF3 content, the lower was the early-age compressive strength (**Table 8-2**).

Table 8-2: Compressive strength results of UHPC mixtures incorporating different content and sizes of wollastonite microfibers.

Age (hrs)/ Variation (%)*	Microfibers Types								
	MF1 (%)			MF2 (%)			MF3 (%)		
	4	8	12	4	8	12	4	8	12
12(hrs)	11.4	12.1	15.2	10.0	10.4	12.0	9.8	6.7	4.7
(%)	(+21)	(+28)	(+61)	(+6)	(+10)	(+27)	(+4)	(-28)	(-50)
24(hrs)	37.6	38.0	39.1	36.9	37.5	38.1	36.4	33.0	29.3
(%)	(+14)	(+15)	(+19)	(+13)	(+15)	(+16)	(+11)	(0)	(-10)
168(hrs)	90.7	94.8	101.2	89.5	92.7	95.3	81.6	86.3	88.5
(%)	(-2)	(+2)	(+9)	(-3)	(0)	(+2)	(-12)	(-7)	(-4)

* Variation with respect to the control value at the same age
**All compressive strength results are in (MPa)

The improvement in very early-age compressive strength can be ascribed to the ability of microfibers to bridge micro-cracks, thus leading to a higher load carrying capacity (Ding and Kusterle, 2000). The size-dependent effect of wollastonite microfibers on early-age compressive strength can be explained as follows: The efficiency of microfibers in bridging cracks is a function of the content and length of the used microfibers and the fiber-paste interfacial bond strength (Hameed *et al*., 2009, Banthia and Sheng, 1996). During very early-age, the degree of hydration is low and consequently the microfiber/matrix bond strength is low (Chan and Li, 1997). Moreover, the addition of wollastonite microfibers as a partial replacement for cement can delay the bond strength development as a result of a dilution effect (Schmidt, 1992). Therefore,

microfibers with a larger aspect ratio will be more effective as it has larger specific surface area (i.e. contact area), thus resulting in sufficient anchorage length beyond the edges of micro-crack. Moreover, the longer the hydration period, the higher was the matrix strength and consequent improvement of the microfiber/matrix bond and bridging efficiency, leading to higher compressive strength (Chan and Li, 1997).
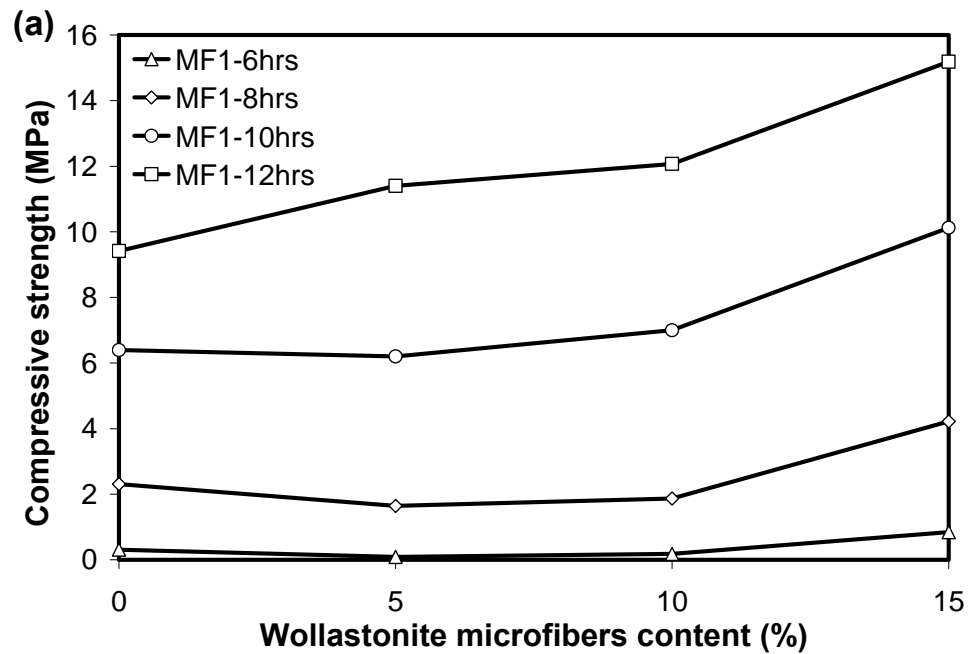
Figure 8-4: Very early-age compressive strength development for different wollastonite microfibers a) MF1, b) MF2 and c) MF3.
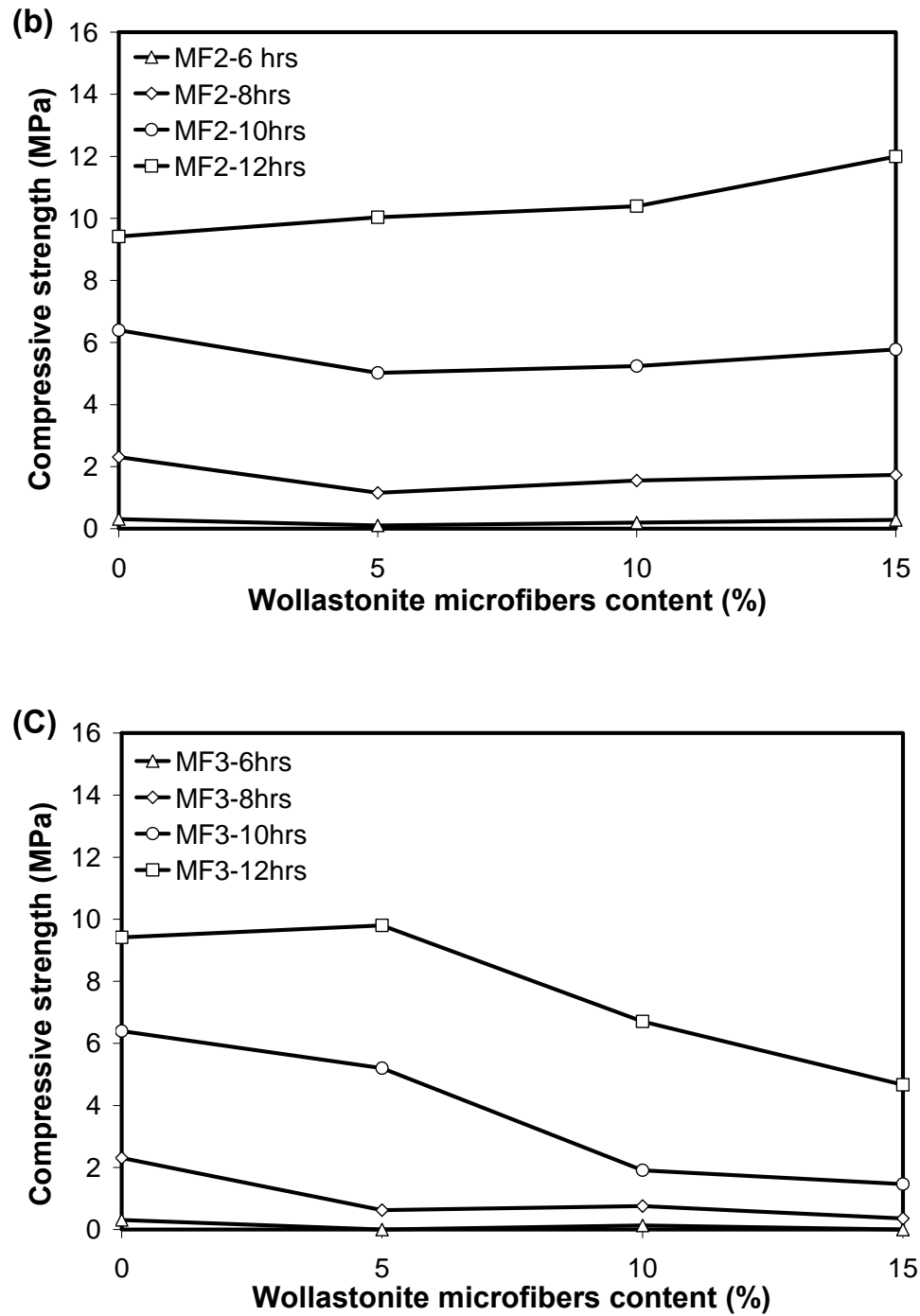
Figure 8-4 Contd': Very early-age compressive strength development for different wollastonite microfibers a) MF1, b) MF2 and c) MF3.

At later ages (i.e. > 24 hrs), mixtures incorporating low wollastonite microfibers content exhibited a slightly lower compressive strength compared to that of the control mixture. However, increasing the wollastonite microfibers content diminished and/or reduced the reduction in the compressive strength regardless of the microfiber size. For instance, increasing the wollastonite microfiber content from 4 to 12% improved the 7-days compressive strength from -2.0% to +9 % for MF1, -3% to +2% for MF2 and -12% to -4% for MF3 of their respective control values, as shown in **Fig. 8-5**. A similar trend, though with a smaller magnitude, was observed at 28-days. This can be attributed to an improvement of the microfiber-matrix-bond with age, especially at the low w/c of UHPC, which leads to higher microfiber crack-bridging efficiency (Chan and Li, 1997**,** Hamoush *et al.*, 2010). Moreover, adding very short microfibers (e.g. MF3) can enhance the compressive strength due to its packing effect (Lange *et al.*, 1997).
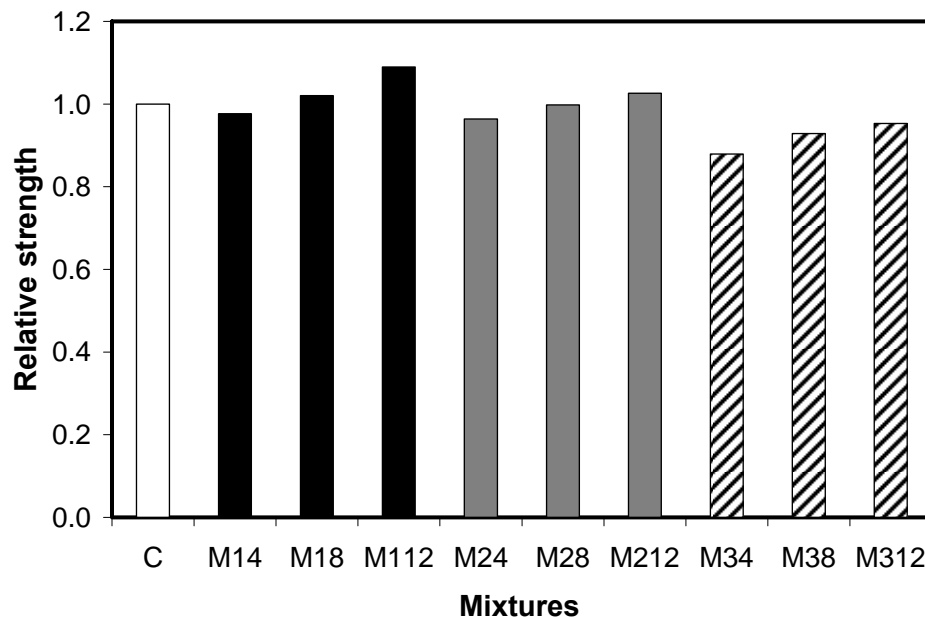
Figure 8-5: Relative early-age compressive strength of mixtures incorporating different content and sizes of wollastonite microfibers at age 7 days.

8.4.3. Heat of Hydration

A characteristic of cementitious materials is the heat generated due to the exothermic hydration reactions of cement. This heat is translated into a temperature increase from which the heat quantity developed can be evaluated (Chikh *et al.*, 2008). Test results were presented graphically in terms of semi-adiabatic temperature evolution versus time in the present study.

Wollastonite microfiber is a relatively inert material expected not to have a significant effect on the heat of hydration liberated during the hydration process (Low and Beaudoin, 1992). Contradictory to this previous finding in (Low and Beaudoin, 1992), the addition of wollastonite microfibers in UHPC modified the evolution of heat of hydration compared to that of the control mixture. Regardless of its size, adding 4% of wollastonite microfibers exhibited higher heat of hydration with respect to that of the control mixture (**Fig. 8-6(a)**). The higher the wollastonite microfibers content, the lower was the increase in temperature peak with respect to that of the control mixture. For instance, the temperature peak for incorporating 4 and 12% of wollastonite microfibers varied by +13% and +3% for MF1, +11% and +1% for MF2 and by +6% and -5.5% for MF3 of their respective control values (**Fig. 8-6(b)**)

In the present study, very small size wollastonite microfibers were used and different characterization of the hydration process was made compared to that in the previous study (Low and Beaudoin, 1992). Therefore, the discrepancy in the heat of hydration behaviour can be explained as follows: the added very fine inert particles (i.e. MF3) displaced some of the water from voids between cement particles, making it available; hence allowing more hydration reactions to take place (Schmidt, 1992). Simultaneously, adding these inert materials as a partial replacement for cement induced

a dilution effect, especially at higher dosages, leading to a lower hydration rate. UHPC is characterized by a very low w/c. Hence, the availability of space for hydration products to form is the main restriction on hydration development (Lea, 1988). Therefore, adding 4% MF3, which is finer than cement particles, displaced water from voids and led to a higher rate of hydration. Conversely, increasing the MF3 content (> 4%), reduced the active sites (i.e. dilution effect) and improved the packing density, thus limiting the available space for hydration products to form and leading to a lower hydration rate.

On the other hand, the addition of 4% of MF1 and MF2 induced higher porosity due to the percolation of microfibers (Bentz, 2000), which increased the space available for hydration products. Consequently, more hydration reactions took place and a higher temperature peak was reached. At higher contents, the dilution effect dominates the hydration rate, resulting in a lower heat of hydration.
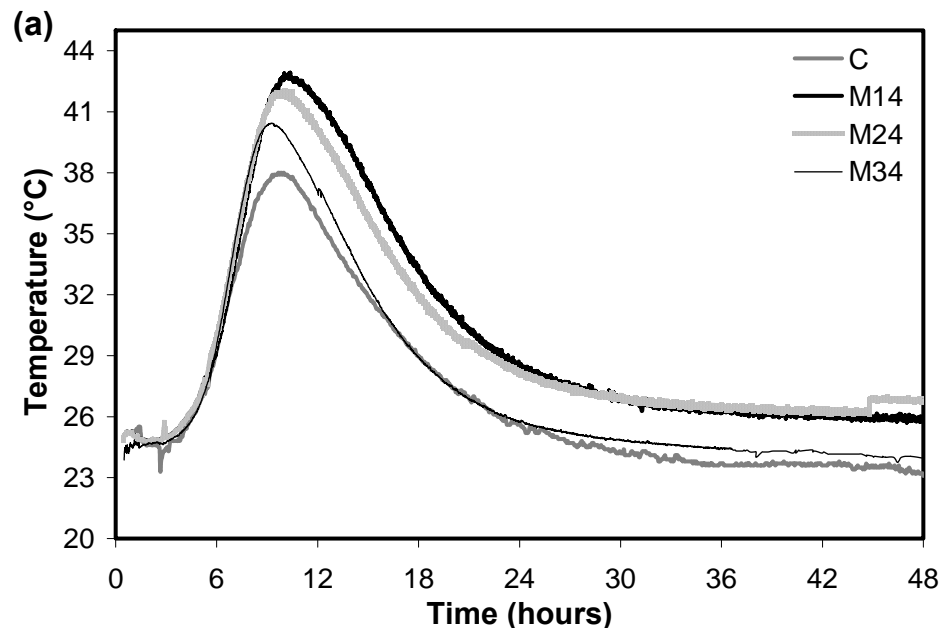
Figure 8-6: a) General trend of heat of hydration for wollastonite microfibers mixtures and b) variation in temperature peak of wollastonite mixtures Vs. control mixture.
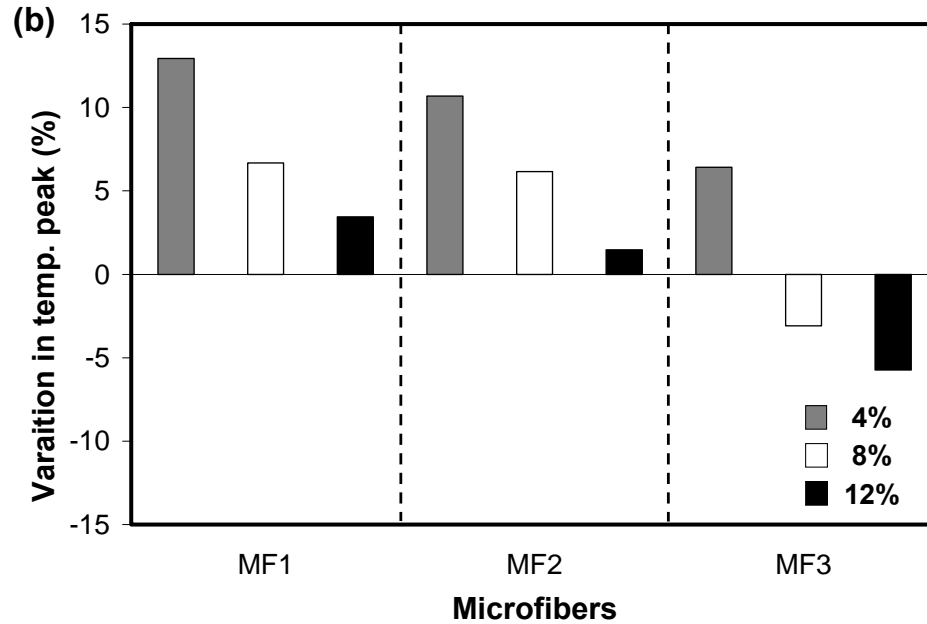
Figure 8-6 Contd': a) General trend of heat of hydration for wollastonite microfibers mixtures and b) variation in temperature peak of wollastonite mixtures Vs. control mixture.

Figure 8-7(a,b) shows the degree of hydration and porosity for mixtures incorporating different wollastonite microfiber sizes. It can be observed that, at the same wollastonite microfibers content, the degree of hydration increased with higher size of wollastonite microfibers, while the porosity did not change significantly. Hence, it is expected that extra hydration products filled the additional space induced by the incorporation of larger size of wollastonite microfibers. (Heat of hydration results for all wollastonite microfibers can be found in **Appendix D**).
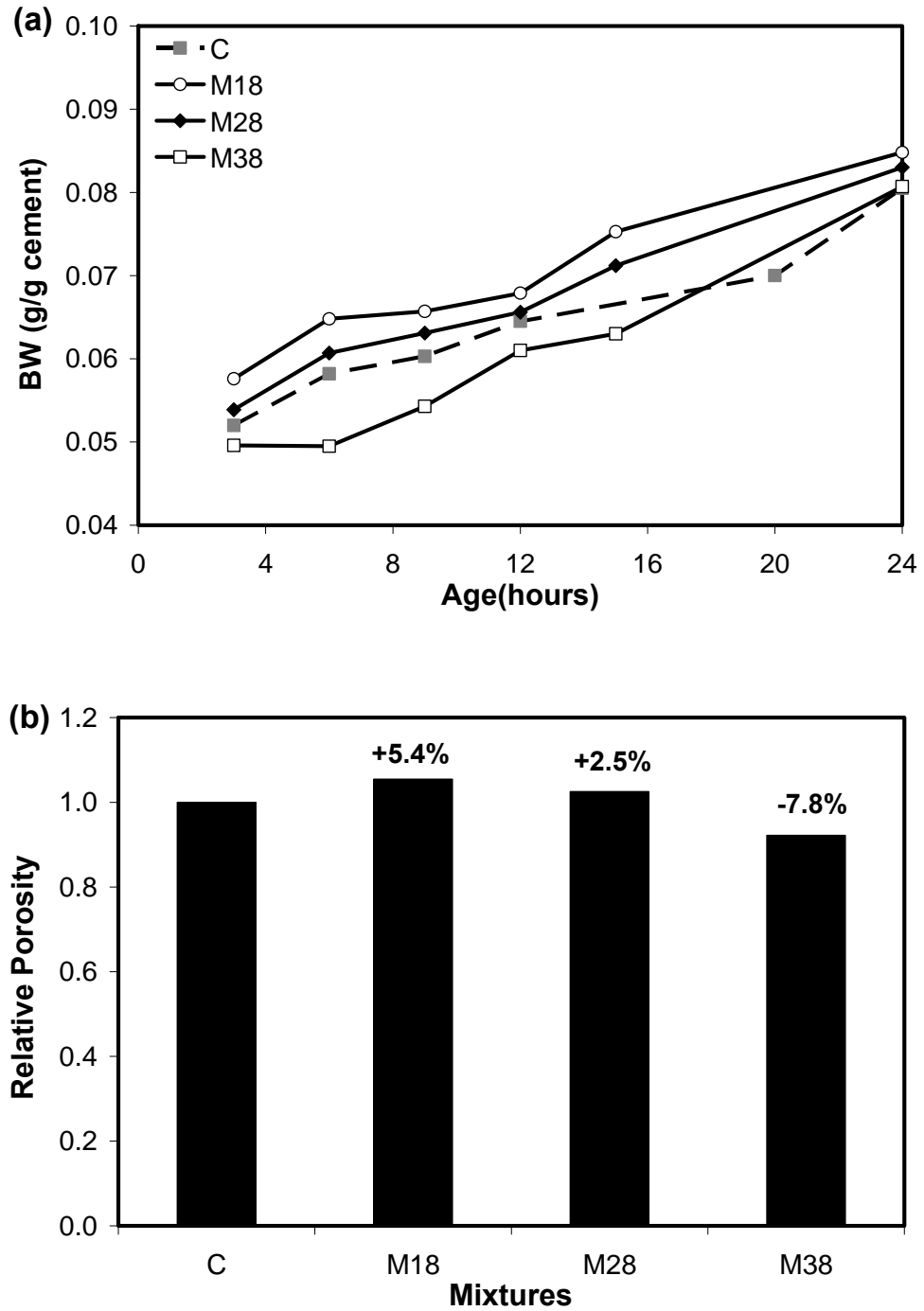
Figure 8-7: a) Development of degree of hydration and b) relative porosity for mixture incorporating 8% of wollastonite microfibers.

8.4.4. Free Shrinkage and Mass Loss

The mass loss and total shrinkage curves for mixtures incorporating wollastonite microfibers are shown in **Fig. 8-8 and 8-9**. The measured total shrinkage includes both drying and autogenous shrinkage (thermal deformation can be ignored due to the small cross-section of the specimens (Baroghel-Bouny *et al.*, 2006)). For very low w/c (Tazawa and Miyazawa, 1999), the contribution of autogenous shrinkage to the total shrinkage can be comparable to that of drying shrinkage.
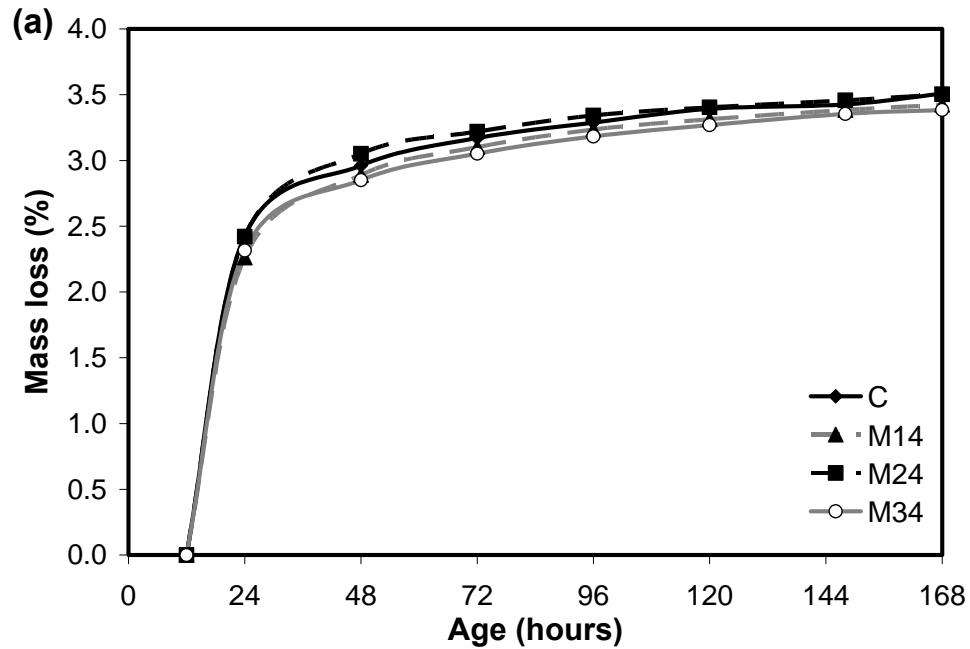
Figure 8-8: Mass loss for mixtures incorporating wollastonite microfibers with a) 4%, b) 8% and c) 12% contents compared to that of the control mixture.
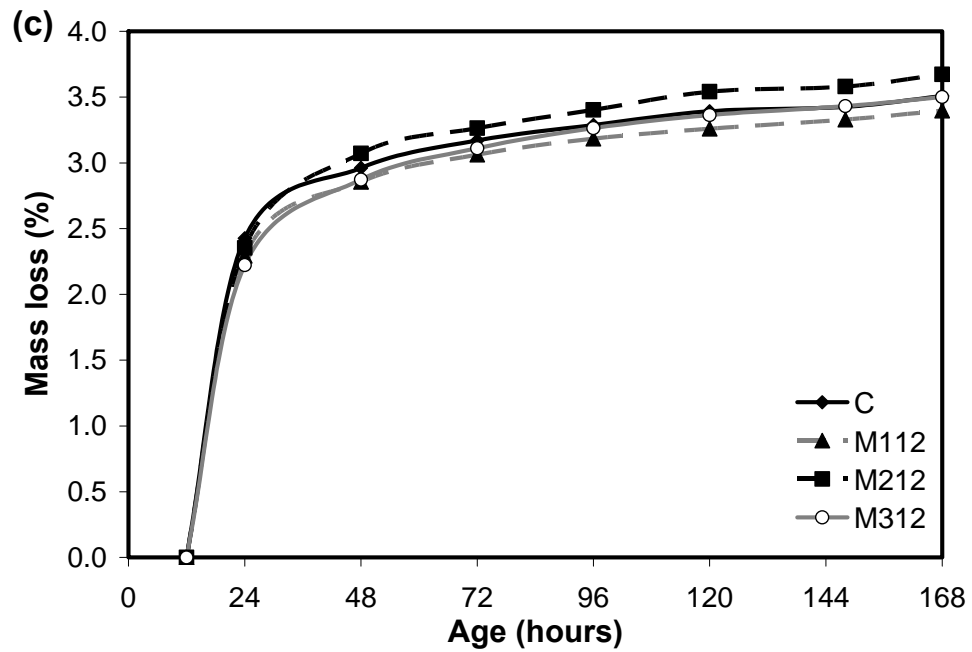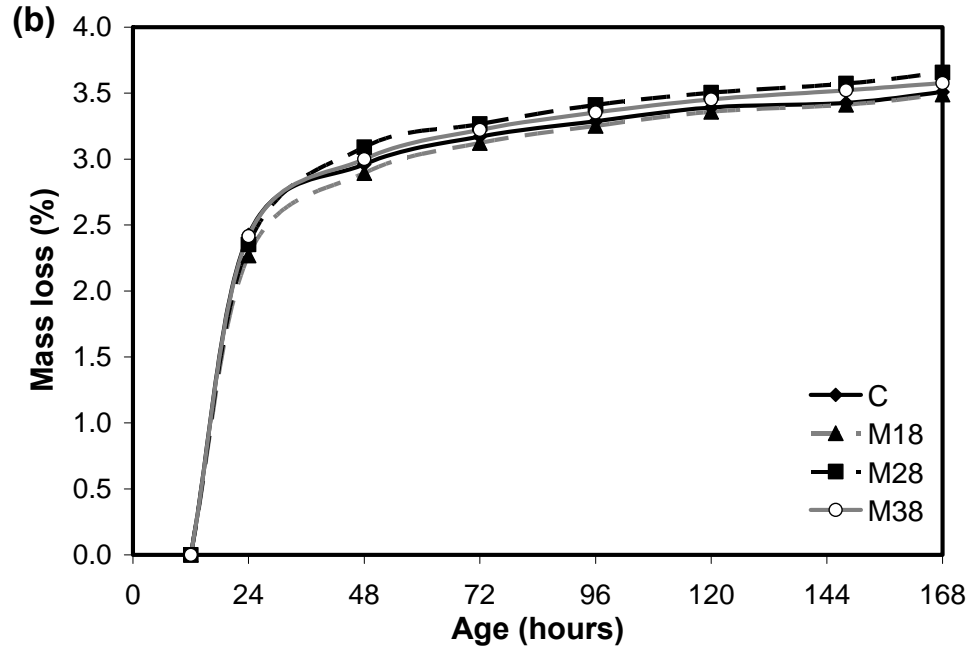
Figure 8-8 Contd': Mass loss for mixtures incorporating wollastonite microfibers with a) 4%, b) 8% and c) 12% contents compared to that of the control mixture.

Despite the higher porosity induced by wollastonite microfibers, mass loss did not change significantly compared to that of the control mixture with no microfibers. Variation in mass loss due to incorporating different contents and sizes of wollastonite microfibers, ranged between -3.5% to +4.6% with respect to that of the control mixture. This can be attributed to the discontinuity of the pore structure induced by wollastonite microfibers (Mathur *et al.*, 2007). Moreover, this confirms previous results which suggested that more hydration products were formed in the space induced by the incorporation of wollastonite microfibers, thus leading to a denser and a discontinuous pore structure.

The general trend of the total shrinkage results indicates a progressive reduction in total shrinkage with increasing content and aspect ratio of wollastonite microfibers, as shown in **Fig. 8-9**. As the microfibers content increased from 4% to 12%, the reduction in total shrinkage at 7-days increased from 11% to 16% for MF1 and from 2% to 9% for MF2 with respect to that of the control mixture. On the other hand, mixtures incorporating different contents of MF3 exhibited a less significant reduction in the total shrinkage compared to that of the control mixture.

Microfibers locally restrain shrinkage stresses in the cementitious matrix (Mangat and Azari, 1984). As the matrix around shrinks, shear stresses develop along microfibers, leading to compressive stresses in the microfibers and tensile stresses in the cementitious matrix (Zhang and Li, 2001). The efficiency of microfibers in restraining shrinkage depends on several parameters, including the elastic modulus of the microfibers and matrix, the microfiber content and its aspect ratio (Zhang and Li, 2001, Mangat and Azari, 1984). Hence, the shrinkage restraining efficiency of microfibers at

early-age is higher due to the low elastic modulus of the cementitious matrix (Zhang and Li, 2001). For instance, incorporating 4% of MF1 led to around 40% reduction in total shrinkage at 24 hrs, and about 16% at 7-days compared to that of the control mixtures, respectively. Moreover, for the same microfibers content, the higher the microfibers aspect ratio, the longer was the effective length leading to higher microfiber-matrix interfacial bond force and consequently higher restraint for shrinkage. For instance, at the same microfiber content of 12%, incorporating MF1 (aspect ratio 19) reduced the total shrinkage by about eight times greater than the reduction induced by MF3 (aspect ratio 5). Moreover, increasing the microfibers content led to better shrinkage reduction (Mangat and Azari, 1984, Swamy and Stavrides, 1979). This can be attributed to the smaller cross-sectional area of the matrix cylinder surrounding each microfiber needed to induce adequate interfacial bond strength and shrinkage restraining (Zhang and Li, 2001).
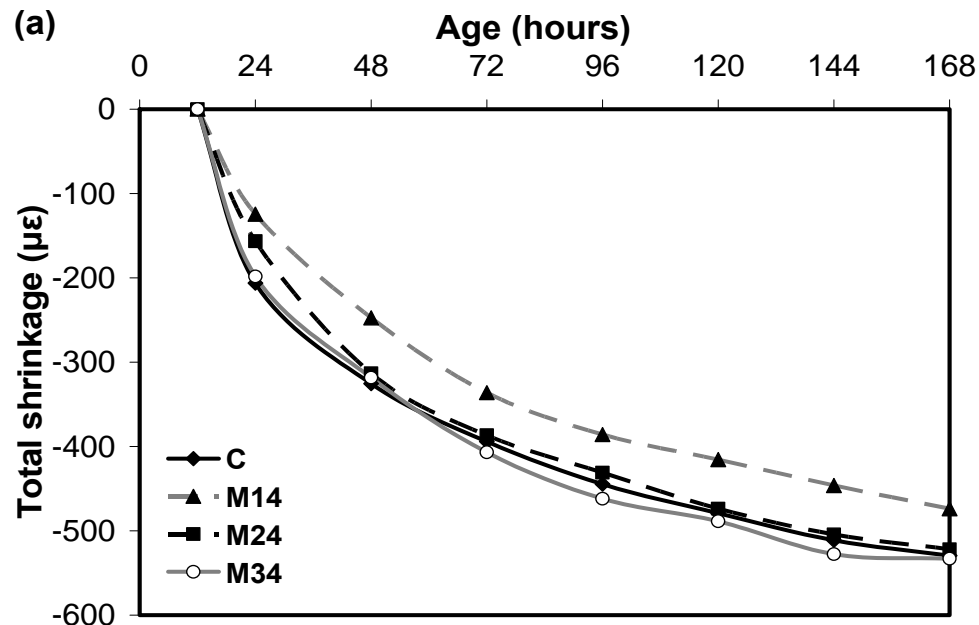
Figure 8-9: a) General trend of total shrinkage for wollastonite microfibers mixtures and b) variation in total shrinkage of wollastonite mixtures Vs. control mixture at 7-days.
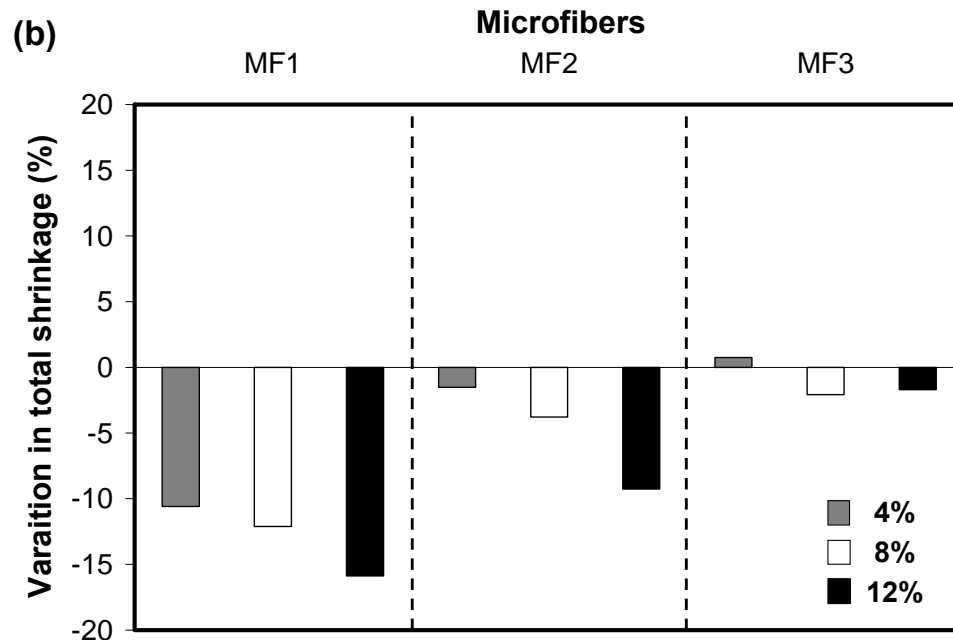
Figure 8-9 Contd': a) General trend of total shrinkage for wollastonite microfibers mixtures and b) variation in total shrinkage of wollastonite mixtures Vs. control mixture at 7-days.

Figure 8-10 shows the effect of adding wollastonite microfibers on autogenous shrinkage development. Generally, mixtures incorporating wollastonite microfibers exhibited lower autogenous shrinkage compared to that of the control mixture. In addition, the MF3 mixture achieved the lowest autogenous shrinkage compared to that of other wollastonite microfiber mixtures. Autogenous shrinkage is strongly related to hydration reactions in which water is consumed, leading to internal self-desiccation (without external water loss) (Powers and Brownyard, 1948). Adding wollastonite microfibers as a partial replacement for cement led to a lower hydration activity (i.e. dilution effect) (Bentz *et al*., 2008), and locally restrained shrinkage as shown earlier. Hence, increasing the wollastonite microfibers content increased the passive internal restraint along with reducing hydration activity. Consequently, lower autogenous

shrinkage occurred (Bentz *et al.*, 2008, Bentz and Peltz, 2008). Moreover, mixtures incorporating the very fine microfibers (i.e. MF3) exhibited early age expansion, which led to a lower net autogenous shrinkage. This expansion can be attributed to the development of disjoining pressure as a result of water absorption on these very fine microfiber surfaces (Craeye *et al.*, 2010). (Shrinkage results for all wollastonite microfibers can be found in **Appendix D**).
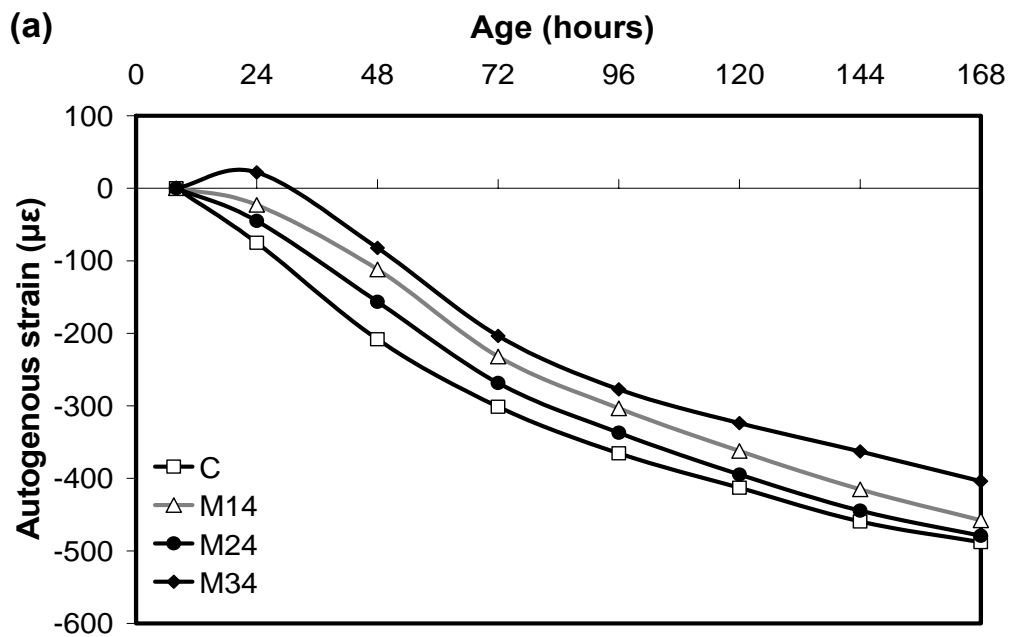
Figure 8-10: a) General trend of autogenous shrinkage for wollastonite microfibers mixtures and b) variation in autogenous shrinkage of wollastonite mixtures Vs. control mixture at 7-days.
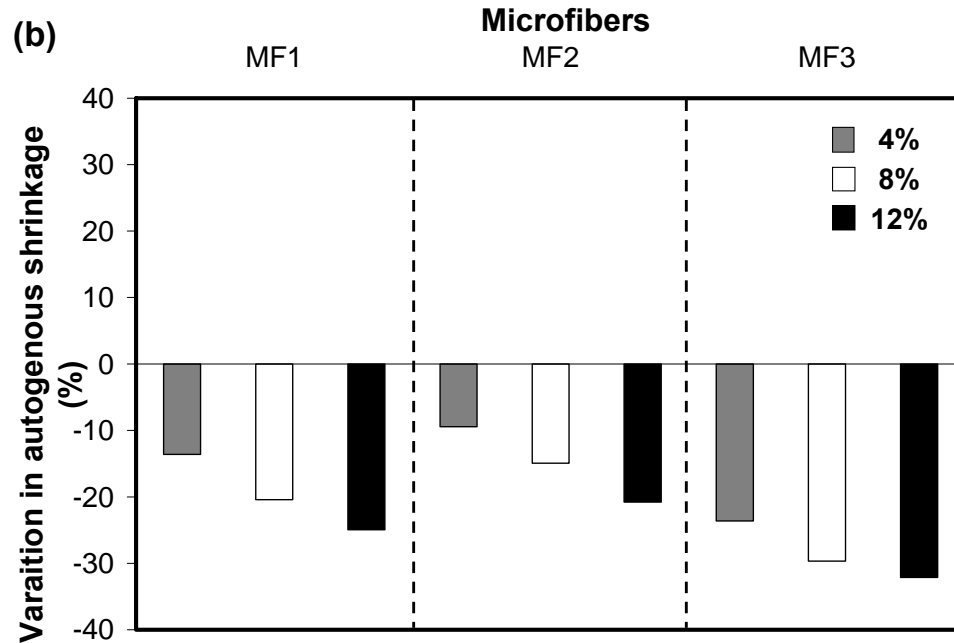
Figure 8-10 Contd': a) General trend of autogenous shrinkage for wollastonite microfibers mixtures and b) variation in autogenous shrinkage of wollastonite mixtures Vs. control mixture at 7-days.

8.4.5. Restrained Shrinkage

MF1 and MF2 wollastonite microfibers were found to enhance the shrinkage cracking resistance as it delayed the age at which the first crack occurred, compared to that of the control mixture. For instance, adding 4% of MF1 and MF2 delayed the cracking age by about 27% and 16% compared to that of the control mixture, respectively. The higher the MF1 or MF2 content, the later was the onset of cracking (**Fig. 8-11(a)**). Conversely, increasing the MF3 content reduced the cracking age (**Fig. 8-11(b)**). In the absence of microfibers, there is little resistance to crack propagation, while in a cementitious matrix incorporating microfibers, the weakest crack resistance point changes with time depending on the distribution of microfibers (Passuello *et al.*, 2009). Hence, microfibers

delayed the coalescence and propagation of cracks at early-age through better stress

transfer at micro-cracks (Banthia and Sheng, 1996, Swamy and Stavrides, 1979). Using

microfibers with a very small aspect ratio (i.e. MF3) jeopardized its crack bridging

efficiency, leading to lower shrinkage cracking resistance and earlier crack formation. On

the other hand, the increase in the cracking age with increasing microfiber content

implies a higher crack bridging efficiency and ability of larger size wollastonite

microfibers to overcome the reduction in matrix strength induced by dilution effect.
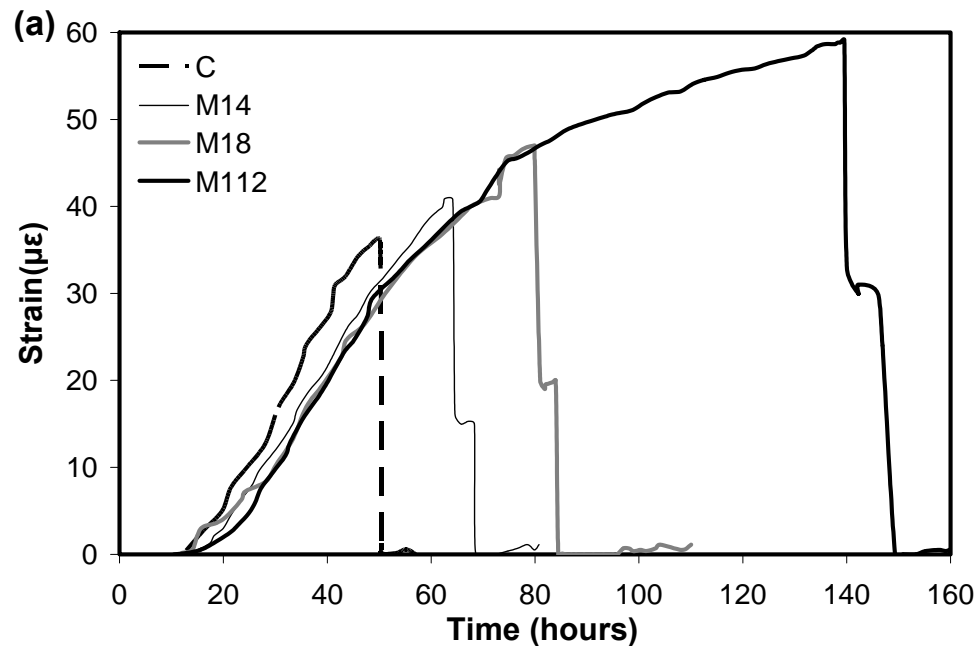
Figure 8-11: Strain measurements of the steel ring for mixtures incorporating different content of a) MF1 and b) MF3.
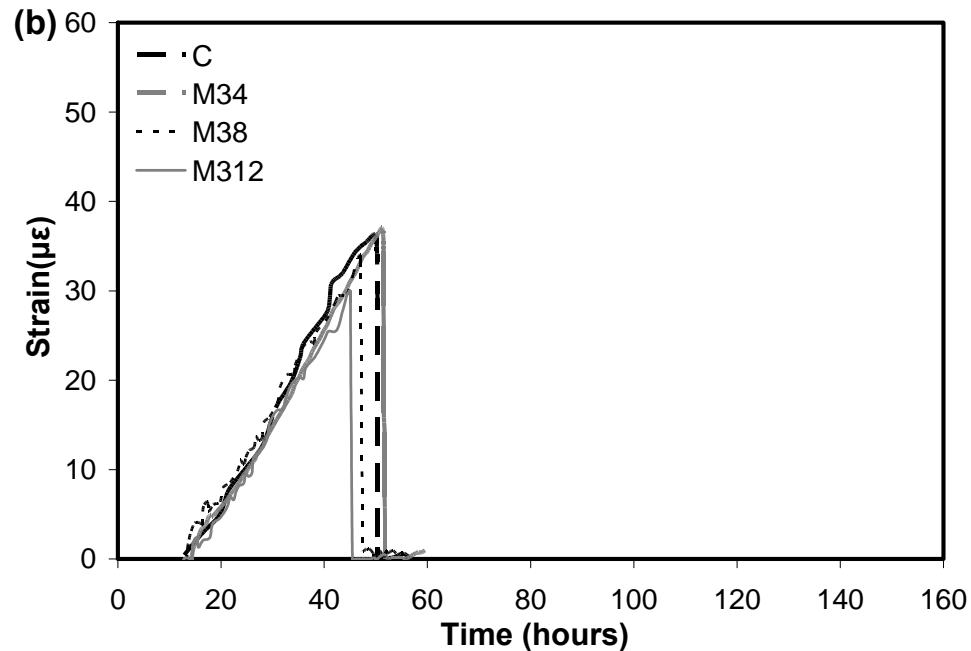
Figure 8-11 Contd': Strain measurements of the steel ring for mixtures incorporating different content of a) MF1 and b) MF3.

For all tested mixtures, cracking was first observed to occur after approximately 42 hours. Steel rings containing specimens with MF1 and MF2 microfibers tended to experience the development of two cracks, while those with MF3 or no microfibers exhibited only one large crack. The presence of multiple cracks is an expected result, since microfibers create internally several small restraints inside the matrix leading to lower crack width as the cracking opening is shared by all cracks (Passuello *et al*., 2009).

Moreover, the total width of the multiple cracks developed in MF1 and MF2 was lower than that of the control mixture single crack at the end of the investigated period (**Fig. 8-12**). The absence of multiple cracks in the control and MF3 mixtures can be attributed to the stress relief induced by the opening of single crack, since, unlike matrices with microfibers, there is no ability to transfer or redistribute stresses (Shah and

Weiss, 2006). Moreover, the crack width increased with increasing MF3 content. This can be ascribed to a reduction in the tensile strength of the matrix due to the cement dilution effect.
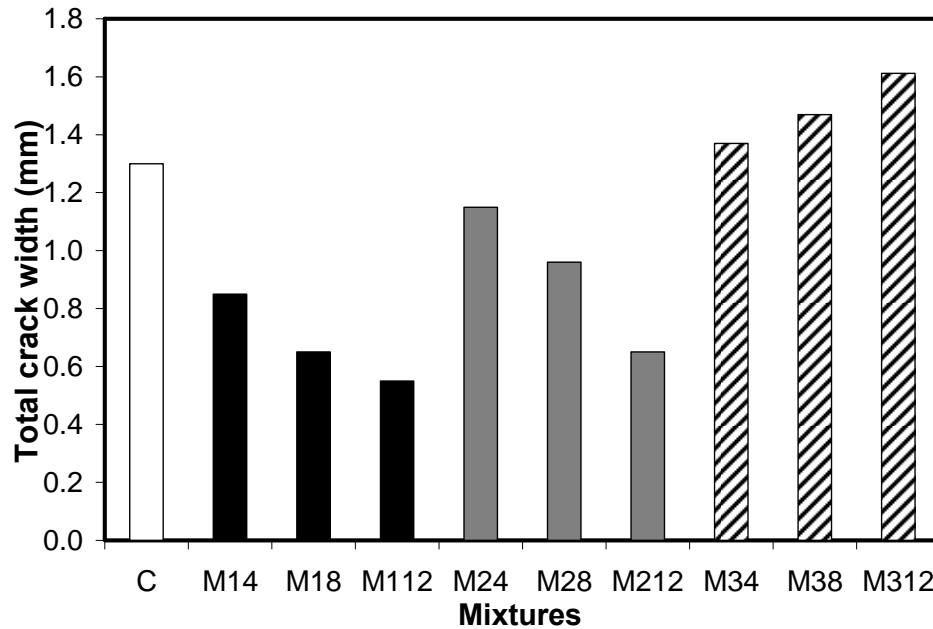
Figure 8-12: Total crack width for mixtures incorporating different content and sizes of wollastonite microfibers.

8.4.6. Flexural Strength

The addition of wollastonite microfibers in UHPC mixture significantly modified its flexural strength characteristics compared to that of the control mixture without microfibers. The flexural strength varied depending on the wollastonite microfibers content and aspect ratio and the hydration period of the cementitious matrix.

Figure 8-13 shows the variation in flexural strength for different wollastonite microfibers contents and aspect ratios relatively to that of the control mixture. At 3-days, the flexural strength increased as the content of the wollastonite microfibers and its

aspect ratio increased, except for MF3. Moreover, at 5 and 7-days, tested specimens of mixtures incorporating MF1 and MF2 did not display signs of distress during the initial portion of the test procedure. Popping and cracking sounds could be heard towards the end of the test as the load applied to the specimen continued to increase. Subsequently, a sudden and brittle failure similar to that of the control mixture without microfibers occurred.
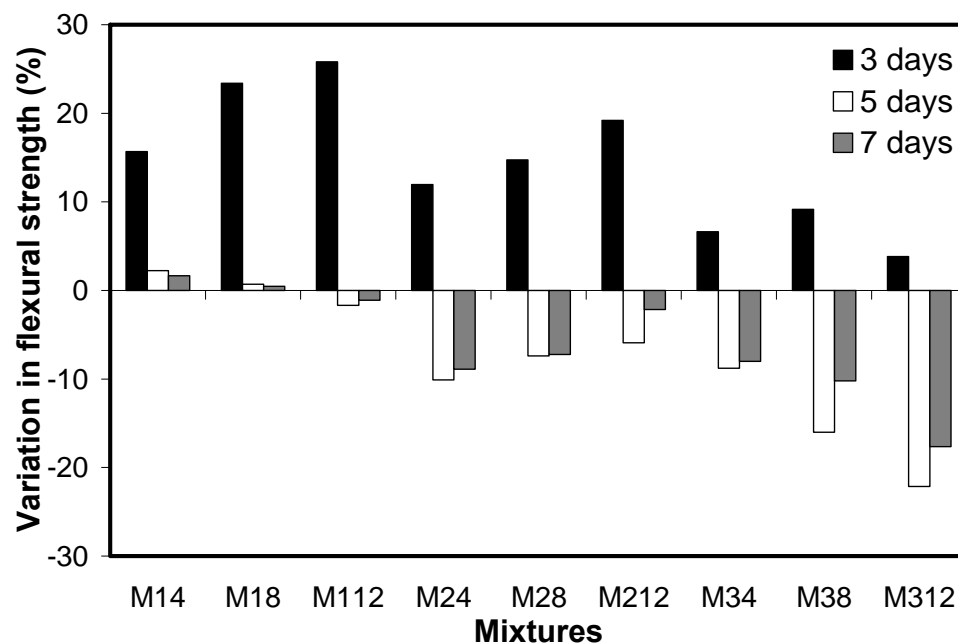
Figure 8-13: Relative flexural strength for mixtures incorporating different content and sizes of wollastonite microfibers compared to that of the control mixture.

The cracking process is believed to initiate as sub-micro cracks formed around flaws once the load is applied. Coalescence of these sub-micro cracks results in forming narrow micro-cracks. Microfibers hindered the widening of these narrow micro-cracks, though their lengths continued to increase. Eventually, the coalescence of narrow micro-

cracks localizes deformation, producing macro-cracks over the entire width of specimens (Lawler *et al*., 2003). Therefore, increasing the amount of microfibers increases the crack bridging efficiency (Lawler *et al*., 2003, Banthia and Sheng, 1996) and consequently delays the development of macro-cracks, which leads to a stronger material as observed for the mixtures incorporating MF1 and MF2 (Lawler *et al*., 2003). The microfiber/matrix interfacial bond and fiber length are important factors that can influence the effectiveness of microfibers as a medium of stress transfer (Banthia and Sheng, 1996). Hence, increasing the embedment length and the fiber perimeter increases the interfacial contact area between the fibers and matrix, leading to stronger interfacial bond (Pakravan *et al*., 2010). This can explain the increase in flexural strength as the aspect ratio of the added wollastonite microfibers increased. On the other hand, it seems that the very small size of MF3 and the expected reduction in the strength induced by the cement dilution effect significantly reduced the flexural strength of MF3 mixtures.

The very high strength of the UHPC matrix is expected to enhance the fiber-matrix interfacial bond, providing high resistance to fiber pullout. Previous studies (Ransinchung and Kumar, 2010, Low and Beaudoin, 1994) showed that wollastonite microfibers have the ability to react with cement and develop a strong chemical bond. This strong chemical adhesion will increase the bond strength, leading to fiber rupture rather than pull-out (Rathod and Patodi, 2010). Hence, the reduction in the flexural strength, at ages 5 and 7 days, can be attributed to sudden rupture of wollastonite microfibers under flexural load (Rathod and Patodi, 2010, Lawler *et al*., 2005). This was confirmed by SEM micrographs as shown in **Fig. 8-14**. Moreover, wollastonite microfibers have a relatively low modulus of elasticity (30 GPa) (Pierre *et al*., 1997) while the UHPC matrix has a very high

modulus (around 34 GPa after 3 days). This reduced the apparent strength of inclined microfibers (Zhang and Li, 2002). Thus, the amount of microfibers that pulled out instead of rupturing was reduced and the fracture toughness decreased.
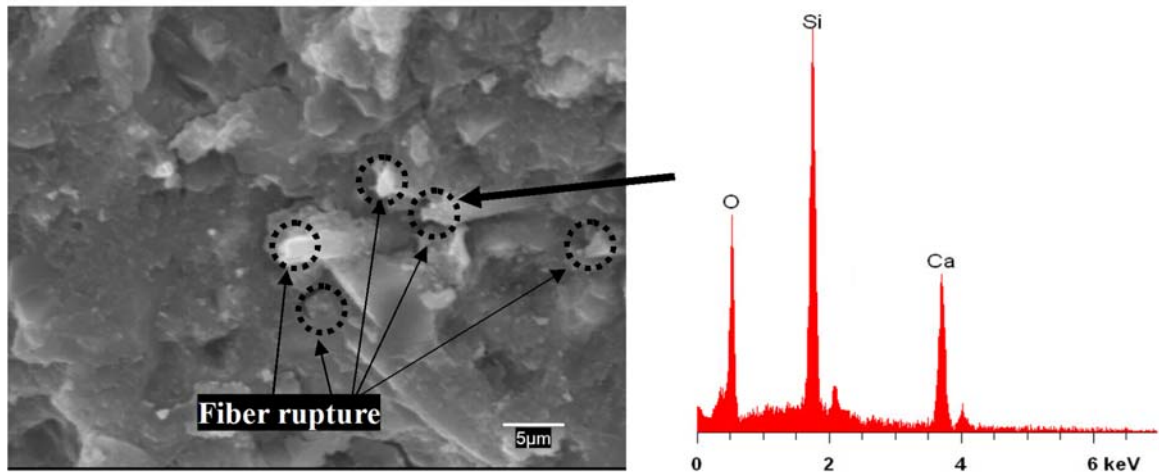
Figure 8-14: Scanning electron micrograph and energy dispersive X-ray element analysis for ruptured wollastonite microfibers.

8.6. CONCLUSIONS

The feasibility of utilizing various small-size wollastonite microfibers in UHPC to control shrinkage cracking and its effect on other early-age properties of UHPC were investigated. The main conclusions that can be drawn from this experimental are the following:

1) Influence of wollastonite microfibers addition on UHPC mixtures early-age compressive strength is highly influence by its bridging micro-cracks efficiency, packing and dilution effects.

2) Addition of high aspect ratio of wollastonite microfibers can improve UHPC hydration process through providing more space for hydration products to form.

3) Addition of wollastonite microfibers appears to promote pore discontinuity leading to lower mass loss and drying shrinkage.

4) Addition of wollastonite microfibers can act as passive internal restraint leading to lower measured shrinkage.

5) The low UHPC matrix elastic modulus at early-age increases the shrinkage restraining effect of wollastonite microfibers.

6) Addition of wollastonite microfibers retarded development of shrinkage cracks as it delay the coalescence of micro-cracks.

7) Addition of wollastonite microfibers increase the pre-peak load, however, no improvement in ductility was achieved due to rupture of wollastonite microfibers.

8.7.   REFERENCES

ACI Committee 231, (2010). Report on Early-Age Cracking: Causes, Measurement, and Mitigation, Technical committee document No. 231.R-10, American Concrete Institute, Farmington Hills, 48 p.

Andiç, Ö., Yardımcı, M.Y. and Ramyar, V., (2008), "Performance of carbon, polyvinylalcohol and steel based microfibers on alkali-silica reaction expansion," *Construction and Building Materials*, Vol. 22, No. 7, pp. 1527-1531.

Azarov, G.M., Maiorova, E.V., Oborina, M.A. and Belyakov, A.V., (1995), "Wollastonite raw materials and their applications (a review)," *Glass and Ceramics*, Vol. 52, No. 9, pp. 237-240.

Banthia, N. and Sheng, J., (1996), "Fracture toughness of microfiber reinforced cement composites," *Cement and Concrete Composites*, Vol. 18, No. 4, pp. 251-269.

Baroghel-Bouny, V., Mounanga, P., Khelidj, A., Loukili, A. and Rafai, N., (2006) "Autogenous deformations of cement pastes: Part II. w/c effects, micro-macro correlations, and threshold values," *Cement and Concrete Research*, Vol. 36, No. 1, pp.123-136.

Bentz, D.P., (2000), "Fibers, percolation, and spalling of high performance concrete," *ACI Materials Journal*, Vol. 97, No. 3, pp. 351-359.

Bentz, D.P., and Peltz, M.A., (2008), "Reducing thermal and autogenous shrinkage contributions to early-age cracking," *ACI Materials Journal*, Vol. 105, No. 4, pp. 414-420.

Bentz, D.P., Sant, G. and Weiss, J., (2008), " Early-age properties of cement-based materials I: influence of cement fineness," *Journal of Materials in Civil Engineering*, Vol. 20, No. 7, pp. 502-508.

Chan, Y.W. and Li, V.C., (1997), "Age effect on the characteristics of fiber/cement interfacial properties," *Journal of Materials Science*, Vol. 32, No. 19, pp. 5287-5292.

Chikh, N., Cheikh-Zouaoui, M., Aggoun, S. and Duval, R., (2008), "Effects of calcium nitrate and triisopropanolamine on the setting and strength evolution of Portland cement pastes," *Materials and Structures*, Vol. 41, No. 1, pp. 31-36.

Craeye, B., De Schutter, G., Desmet, B., Vantomme, J., Heirman, G., Vandewalle, L., Cizer, Ö., Aggoun, S. and Kadri, E.H., (2010), "Effect of mineral filler type on autogenous shrinkage of self-compacting concrete," *Cement and Concrete Research*, Vol. 40, No. 6, pp. 908-913.

Cusson, D., (2008), "Effect of blended cements on effectiveness of internal curing of HPC," *Proceedings of the Internal Curing of High-Performance Concretes: Laboratory and Field Experiences*, ACI SP-256, *American Concrete Institute*, Farmington Hills, pp. 105-120.

Ding, Y. and Kusterle, W., (2000), "Compressive stress-strain relationship of steel fiber-reinforced concrete at early-age," *Cement and Concrete Research*, Vol. 30, No. 10, pp. 1573-1579.

Hameed, R., Turatsinze, A., Duprat, F. and Sellier, A., (2009), "Metallic fiber reinforced concrete : effect of fiber aspect ratio on the flexural properties," *ARPN Journal of Engineering and Applied Sciences*, Vol. 4, No. 5, pp. 67-72.

Hamoush, S., Abu-Lebdeh, T., Cummins, T. and Zornig, B., (2010), "Pullout characterizations of various steel fibers embedded in very high-strength concrete," *American Journal of Engineering and Applied Sciences*, Vol. 3, No. 2, pp. 418-426.

Hoang, K.H., Phat, H.B., Hien, L.D. and Chanh, N.V., (2008), "Influence of types of steel fiber on properties of ultra high performance concrete," *Proceedings of the third ACF International Conference: Sustainable Concrete Technology and Structures in Local Climate and Environment conditions*, Ho Chi Minh city, Vietnam, pp. 347-355.

Lange, F., Mörtel, H. and Rudert, V., (1997), "Dense packing of cement pastes and resulting consequences on mortar properties," *Cement and Concrete Research*, Vol. 27, No. 10, pp. 1481-1488.

Lawler, J.S., Wilhelm, T., Zampini, D. and Shah, S.P., (2003), "Fracture processes of hybrid fiber-reinforced mortar," *Materials and Structures*, Vol. 36, No. 3, pp. 197-208.

Lawler, J.S., Zampini, D. and Shah, S.P., (2005), "Microfiber and macrofiber hybrid fiber-reinforced concrete," *Journal of Materials in Civil Engineering*, Vol. 17, No. 5, pp. 595-604.

Lea, F.M., (1988). Lea's Chemistry of Cement and Concrete, 4th Edition, (ed.) P.C. Hewlett, J. Wiley, New York, 1053 p.

Low, N.M.P. and Beaudoin, J.J., (1992), 'Mechanical properties of high performance cement binders reinforced with wollastonite microfibers," *Cement and Concrete Research*, Vol. 22, No. 5, pp. 981-989.

Low, N.M.P. and Beaudoin, J.J., (1993), "Flexural strength and microstructure of cement binders reinforced with wollastonite microfibers," *Cement and Concrete Research*, Vol. 23, No. 4, pp. 905-916.

Low, N.M.P. and Beaudoin, J.J., (1994a), "The flexural toughness and ductility of portland cement-based binders reinforced with wollastonite microfibers," *Cement and Concrete Research*, Vol. 24, No. 2, pp. 250-258.

Low, N.M.P. and Beaudoin, J.J., (1994b), "Stability of portland cement-based binders reinforced with natural wollastonite microfibers," *Cement and Concrete Research*, Vol. 24, No. 5, pp. 874-884.

Ma, B., Wang, X., Liang, W., Li, X. and He, Z., (2007), "Study on early-age cracking of cement-based materials with superplasticizer," *Construction and Building Materials*, Vol. 21, No. 11, pp. 2017-2022.

Mangat, P.S. and Azari, M.M., (1984), "A theory for the free shrinkage of steel fiber reinforced cement matrices," *Journal of Materials Science*, Vol. 19, No. 7, pp. 2183-2194.

Mathur, R., Misra, A.K. and Goel, P., (2007), "Influence of wollastonite on mechanical properties of concrete," *Journal of Scientific and Industrial Research*, Vol. 66, No. 12, pp.1029-1034.

Nehdi, M., Mindess, S. and Aïtcin, P.-C., (1998), "Rheology of high-performance concrete: effect of ultrafine particles," *Cement and Concrete Research*, Vol. 28, No. 5, pp. 687-697.

Nmai, C., Tomita, R., Hondo, F. and Buffenbarger, J., (1998), "Shrinkage reducing admixtures," *Concrete International*, Vol. 20, No. 4, pp. 31-37.

Pakravan, H. R., Jamshidi, M. and Latifi, M., (2010), "Performance of fibers embedded in a cementitious matrix," *Journal of Applied Polymer Science*, Vol. 116, No. 3, pp. 1247-1253.

Passuello, A., Moriconi, G. and Shah, S.P., (2009), "Cracking behavior of concrete with shrinkage reducing admixtures and PVA fibers," *Cement and Concrete Composites*, Vol. 31, No. 10, pp. 699-704.

Pierre, P., Pleau, R., Rhéaume, M. and Pigeon, M., (1997), "The influence of microfiber on the drying behaviour of cement paste and mortars," *Proceedings of Annual conference of the Canadian society for civil engineering*, Sherbrooke, Québec, pp. 123-131.

Powers, T.C. and Brownyard, T.L., (1948), "Studies of the physical properties of hardened portland cement paste," Bulletin No. 22., Research Laboratories of the Portland Cement Association. Reprinted from Journal of the American Concrete Institute, October 1946–April 1947, Proceedings 43, Detroit, pp. 971-992.

Ransinchung, G.D., and Kumar, B., (2010), "Investigations on pastes and mortars of ordinary portland cement admixed with wollastonite and microsilica," *Journal of Materials in Civil Engineering*, Vol. 22, No. 4, pp. 305-313.

Rathod, J.D. and Patodi, S.C., (2010), "Interface tailoring of polyester-type fiber in engineered cementitious composite matrix against pullout," *ACI Materials Journal*, Vol. 107, No. 2, pp. 114-122.

Schmidt, M., (1992), "Cement with inter-ground additives: capabilities and environmental relief (I)," *Zement Kalk Gips*, Vol. 45, No. 7, pp. 64-69.

See, H.T., Attiogbe, E.K. and Miltenberger, M.A., (2003), "Shrinkage cracking characteristics of concrete using ring specimens," *ACI Materials Journal*, Vol. 100, No. 3, pp. 239-245.

Shah, S.P., Weiss, W.J. and Yang, W., (1998), "Shrinkage cracking-can it be prevented?," *Concrete International*, Vol. 20, No. 4, pp. 51-55.

Shah, H. R. and Weiss, J., (2006), "Quantifying shrinkage cracking in fiber reinforced concrete using the ring test," *Materials and Structures*, Vol. 39, No.9, pp. 887-899.

Swamy, R.N. and Stavrides, H., (1979), "Influence of fiber reinforcement on restraining shrinkage and cracking," *ACI Journal*, Vol. 75, No. 3, pp. 443-460.

Tatnall, P.C. (2006), "Chapter 49: Fiber-Reinforced Concrete," In *Significance of Tests and Properties of Concrete and Concrete-Making Materials* (STP 169D), Lamond, J. F. and Pielert, J. H. (eds.), ASTM International, West Conshohcken, PA., pp. 578-594.

Tazawa, E., (1998). Autogenous Shrinkage of Concrete. *Proceedings of the International Workshop on Autogenous Shrinkage of Concrete*, Japan Concrete Institute, Hiroshima, Japan, E & FN Spon, New York, 358 p.

Tazawa, E. and Miyazawa, S., (1999), "Effect of constituents and curing condition on autogenous shrinkage of concrete," *Proceedings of the International Workshop Autogenous Shrinkage of Concrete*, Eichi Tazawa(ed.), Taylor & Francis, pp. 269-280.

Van Breugel, K. and De Vries, J., (1998), "Mixture optimization of low water/cement ratio high strength concretes in view of autogenous shrinkage," *Proceedings of International Symposium on High Performance and Reactive Powder Concrete*, Sherbrooke, Canada, pp. 365-382.

Zhang, J., and Li, V., (2001), "Influences of fibers on drying shrinkage of fiber-reinforced cementitious composite," *Journal of Engineering Mechanics*, Vol. 127, No. 1, pp. 37-44.

Zhang, J. and Li, V., (2002), "Effect of inclination angle on fiber rupture load in fiber reinforced cementitious composites," *Composite Science and technology*, Vol. 62, No. 6, pp. 775-781.

<div align="right">**CHAPTER NINE**</div>

SHRINKAGE BEHAVIOUR OF UHPC WITH SHRINKAGE REDUCING ADMIXTURE AND WOLLASTONITE MICROFIBERS*

In previous chapters, shrinkage reducing admixtures and wollastonite microfibers have been used to improve shrinkage behaviour and the cracking potential of UHPC. Shrinkage reducing admixture had shown a high efficiency in reducing early-age shrinkage, however, it delays development of mechanical properties. Wollastonite microfibers was found to act as an internal passive restraint for shrinkage, reinforcing the microstructure at the micro-crack level leading to an enhancement of early-age engineering properties of UHPC matrix. These results are based on previous independently analysis of SRA and wollastonite microfibers, without considering their combination. In this chapter, the improvement in early-age properties, shrinkage behaviour and reduction of cracking potential of UHPC due to the addition of the SRA and wollastonite microfibers, used separately or in a blend, were investigated and analyzed.

9.1.   INTRODUCTION

General background on the UHPC properties (high strength and enhanced durability) and characterization (homogeneity, stronger and higher packing density microstructure and its very low water to cement ratio) has been given in previous chapter 3. In addition, it has

---

*A version of this chapter has been submitted for review to Cement and Concrete Composites.

been illustrated that UHPC has high tendency to early-age cracking which probably affect its durability. Furthermore, UHPC has a serious environmental and economical impact due to its high cement content which increases energy consumption and CO_2 emissions.

In Chapter 8, it was outlined the potential of replacing cement with an inert natural material, such as wollastonite microfibers. Addition of wollastonite microfibers was found to improve the early-age properties of UHPC. This probably will lead to environmental and economic benefits.

Among the several methods that have been proposed to minimize cracking potential of concrete, shrinkage reducing admixture (SRA) was the most commonly used technique. SRAs directly influence shrinkage by decreasing the surface tension of the pore solution, leading to lower capillary stresses and consequently a reduced shrinkage (Nmai *et al*., 1998). However, possible disadvantages of these materials include effectiveness reduction over time (Schemmel *et al*., 1999), delaying setting time, reducing strength (Bentz, 2006) and washing out of SRA as illustrated in chapter 5.

Therefore, the aim of this research is to develop a strategy for producing UHPC with lower cracking propensity to traditional UHPC, while having a more positive environmental foot-print, through combining the benefits of SRA and wollastonite microfibers.

9.2.   RESEARCH SIGNIFICANCE

Reducing concrete shrinkage cracks is important for durability, as well as that of strength, particularly in structures such as slabs, bridge deck overlays, tunnel linings and

pavements. In this chapter, the reduction of cracking risk has been evaluated by the reduction of shrinkage and the increase of the crack opening resistance due to the addition of shrinkage reducing admixtures (SRA) and wollastonite microfibers. Both technologies have been considered individually and used in combination. Addition of wollastonite microfibers had jeopardize the reduction It has been noted that combining SRA and wollastonite microfibers has led to a better cracking behaviour compared to mixtures incorporating one of these techniques alone. Moreover, the combining effect gives better carking behaviour than the effect of increasing SRA or wollastonite microfibers dosages.

9.3.   EXPERIMENTAL PROGRAM

This experimental program aims to investigate the effect of SRA and wollastonite microfibers on early-age behaviour of UHPC and their role in controlling shrinkage cracking. This is of primary importance in order to achieve high performance and durable structures. In this study, monitoring of the strength development (compressive strength, heat of hydration, degree of hydration) and characterization of the shrinkage behaviour have been investigated on UHPC mixtures incorporating different dosages of SRA and/or wollastonite microfibers. All tests were conducted on UHPC specimens without heat curing in order to understand real effects that govern UHPC shrinkage in structural elements cast in situ.

9.3.1.   Materials and Mixture Proportions

The materials used in this chapter were similar to that used in Chapter 3 (refer to Section 3.4.1). The chemical and physical properties of the used binders have been given in

Chapter 3 (refer to **Table 3-1**). A poly-oxyalkylene alkyl ether shrinkage reducing admixture was used in this study. SRA dosages of 1% and 2% by mass of cement were added as a partial replacement of the mixing water. Commercially available natural wollastonite microfibers MF1 (length 152 µm, diameter 8 µm) were used at two concentrations (4 and 12%) as partial substitution for cement by volume. The selected composition of the control mixture are shown in Chapter 3 (refer to **Table 3-2**). The characteristics of the tested mixtures are shown in **Table 9-1**.

Table 9-1: Tested mixtures.

Mixture	SRA (%)	Wollastonite microfiber (%)
C	----	----
R1	1.0	----
R2	2.0	----
W4	----	4.0
W12	----	12.0
R1W4	1.0	4.0
R1W12	1.0	12.0
R2W1	2.0	4.0
R2W12	2.0	12.0

9.3.2. Preparation of Test Specimens and Testing Procedures

The experimental methods used in this chapter are the cubic compressive strength test, Semi-adiabatic calorimetry, TGA, MIP, measurements of total free shrinkage, mass loss, setting time, shrinkage restraining test, COD and SEM/EDX analysis. All tests were previously explained in chapters 3, 5, 7 and 8.

9.4.   RESULTS AND DISCUSSION

9.4.1.   Compressive Strength

Compressive strength is considered as a key property of UHPC. The addition of wollastonite microfibers was found to affect the early-age compressive strength of UHPC, as shown in **Fig. 9-1**. A detailed discussion on the effect of wollastonite microfibers addition on compressive strength was given in Chapter 8.

On the other hand, mixtures incorporating SRA achieved a lower early-age compressive strength compared to that of the control mixture (**Fig. 9-1**). The higher the SRA dosage, the lower was the achieved early-age compressive strength. This can be attributed to the retardation effect induced by SRA, in agreement with previous work (He *et al.*, 2006).
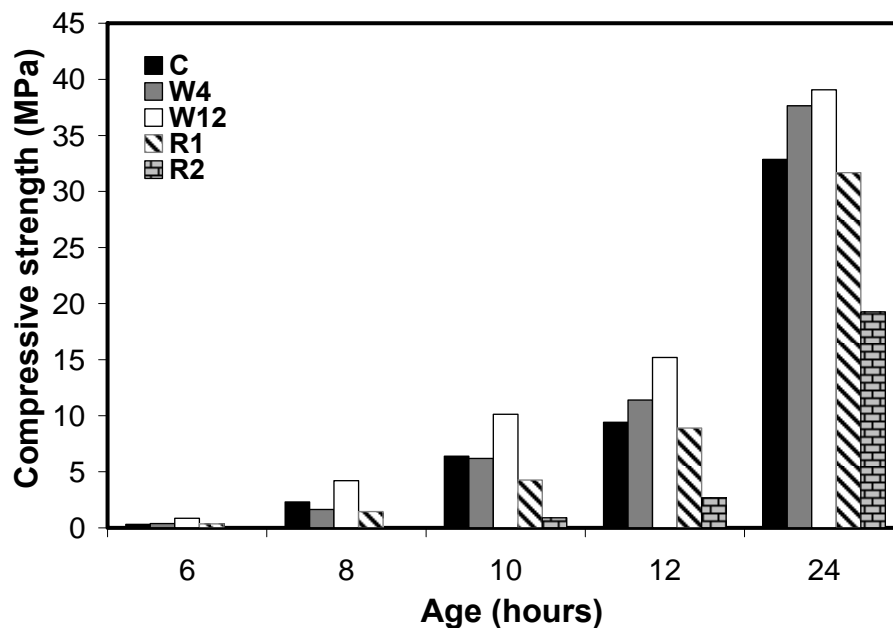
Figure 9-1: Development of early-age compressive strength of UHPC mixtures with and without different dosages of SRA or wollastonite microfibers.

Figure 9-2 illustrates the combined effect of SRA and wollastonite microfibers on the very early-age compressive strength. Generally, adding wollastonite microfibers to SRA mixtures improved the early-age compressive strength compared to that of mixtures incorporating SRA alone. The higher the wollastonite microfibers content, the higher was the improvement in compressive strength. For instance, adding 4% and 12% of wollastonite microfibers was found to increase the early-age compressive strength of mixture **R1** by 12% and 20%, respectively and by 55% and 70% at age 24 hrs, respectively for mixture **R2** (**Fig. 9-2(a)**). Compared to mixtures incorporating wollastonite microfibers alone, mixtures incorporating both SRA and wollastonite microfibers exhibited lower early-age compressive strength. The higher the added dosage of SRA, the higher was the reduction in the compressive strength. For instance, adding 1 and 2% of SRA was found to reduce the 24 hrs compressive strength for mixture **W4** by 6% and 16%, respectively and by 4% and 13% at age 24 hrs, respectively for mixture **W12** (**Fig. 9-2(b)**).

The combined effect of SRA and wollastonite microfibers on the very early-age compressive strength represents the net result of two conflicting effects: reinforcing and retardation. Wollastonite microfibers bridge micro-cracks and reinforce the microstructure, leading to higher strength (compared to that of the **R1** and **R2** mixtures). Concurrently, SRA retards the hydration process and consequently reduces the reinforcing efficiency of wollastonite microfibers (compared to that the **W4** and **W12** mixtures). The efficiency of microfibers in bridging micro-cracks is a function of the interfacial microfiber/matrix bond strength (Hameed *et al*., 2009, Banthia and Sheng, 1996). The lower the degree of hydration, the smaller is the microfiber/matrix bond

strength, and consequently the lower is the reinforcing efficiency (Chan and Li, 1997). This is shown in degree of hydration results discussed below.
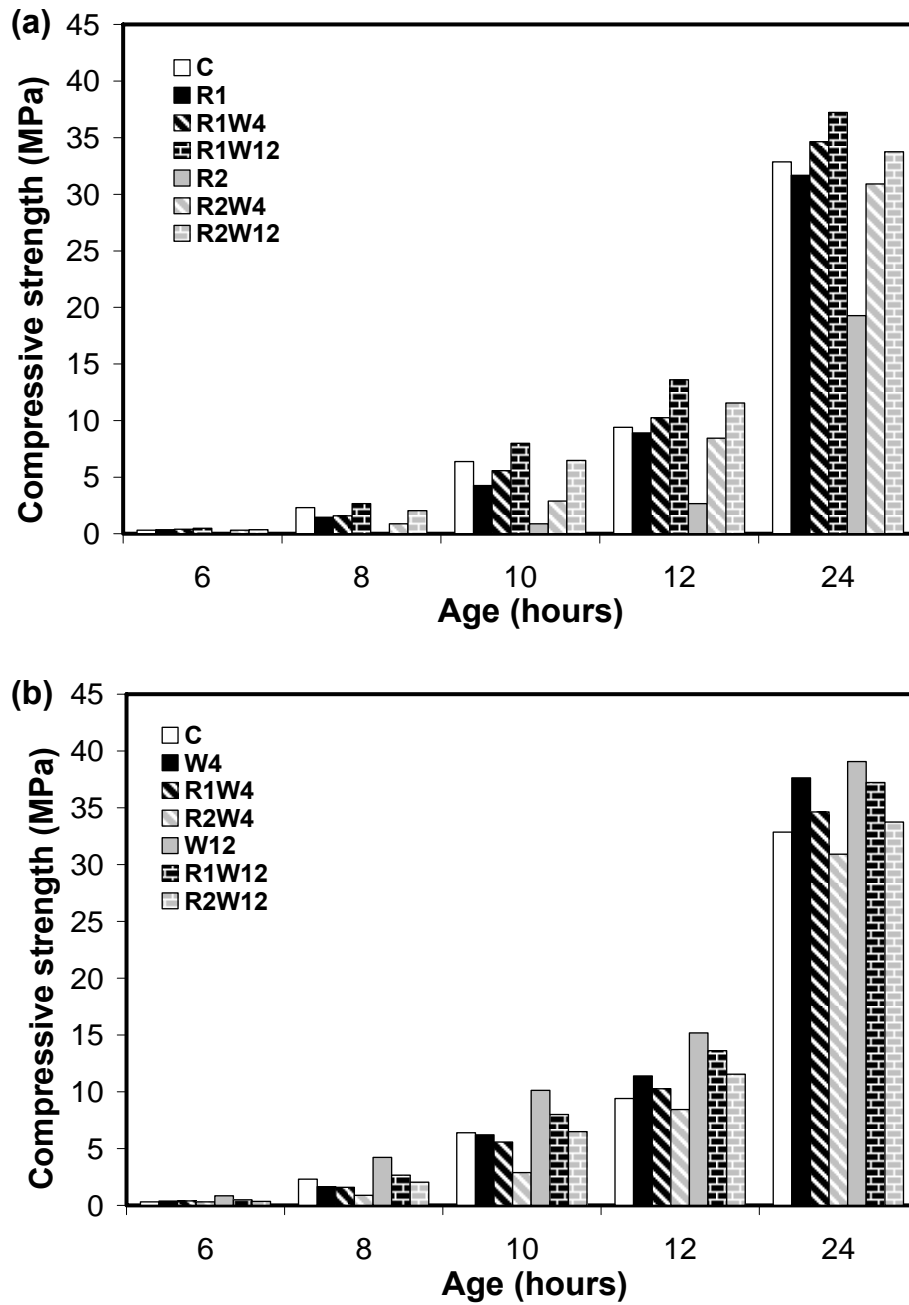
Figure 9-2: Effect of combing SRA and wollastonite microfibers on early-age compressive strength of UHPC with respect to a) SRA and b) wollastonite microfibers mixtures.

At later ages (i.e. >24 hrs), similar to very early-age results, the addition of wollastonite microfibers enhanced the compressive strength at late ages for SRA mixtures, as shown in **Fig. 9-3**. The micro-cracks bridging and reinforcing of the microstructure induced by wollastonite microfibers was able to reduce the negative effect induced by SRA and achieve acceptable compressive strength behaviour.
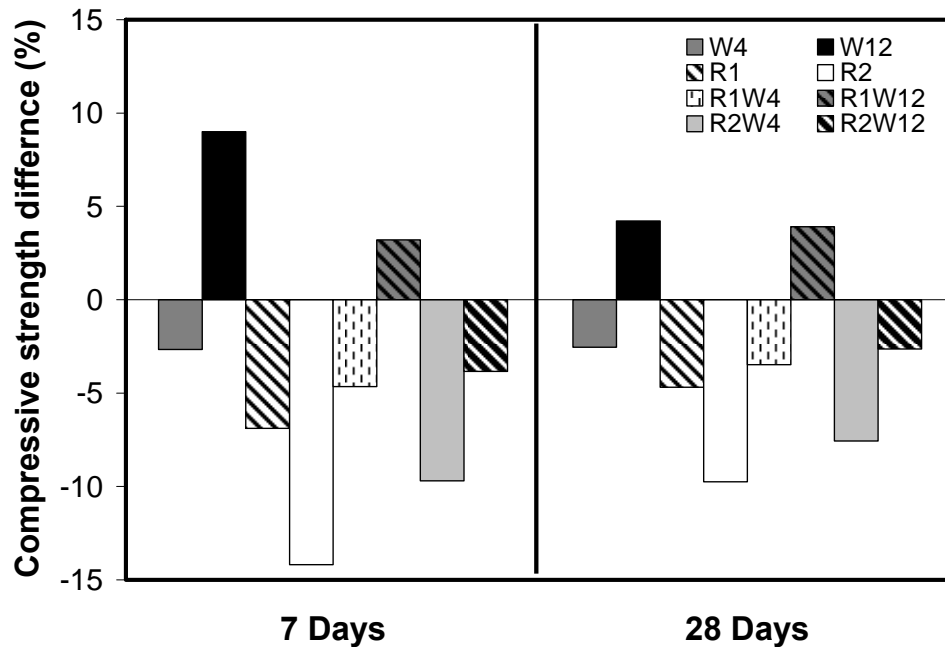
Figure 9-3: Variation in the compressive strength of UHPC mixture with different dosages of SRA and/or wollastonite microfibers compared to the control mixture.

9.4.2. Heat of Hydration

In chapter 8, the wollastonite microfibers effect on heat hydration was investigated and analyzed. It was concluded that addition wollastonite microfibers can alert the hydration process through inducing higher porosity, due to percolation of microfibers (Bentz, 2000)

and displacing water from pores. Adding wollastonite microfiber exhibited slightly higher heat of hydration with respect to that of control mixture (**Fig. 9-4(a)**).

It can be noted that adding SRA retarded hydration reactions and reduced the liberated heat compared to that of the control mixture without SRA, as shown in **Fig. 9-4(a)**. This is consistent with previous results (Eberhardt and Kaufmann, 2006). Furthermore, as the SRA dosage increased from 1 to 2%, the temperature peak decreased and occurred later in time compared to that of the 1% SRA mixture. This retardation effect can be attributed to a reduction in the ability of salts (e.g. alkali sulphates) to dissolve and ionize in the pore solution due to the lower polarity induced by SRA addition (Rajabipour *et al.*, 2008).

On the other hand, mixtures incorporating both wollastonite microfibers and SRA exhibited similar trend to that of mixtures incorporating SRA alone, regardless of the added amount of wollastonite microfibers, as shown in **Fig. 9-4(b)**. The higher the dosage of SRA, the smaller and later the temperature peaks occurred. Moreover, at the same dosage of SRA, on significant change in the heat of hydration was found as the content of wollastonite microfibers increased from 0% to 12%. For instance, the difference in the temperature peaks ranged between -0.9% to 1.8% and -1.3% to +1.6% for the 1% and 2% SRA mixtures, respectively. This indicates that the retardation of hydration process induced by SRA is the dominant factor.
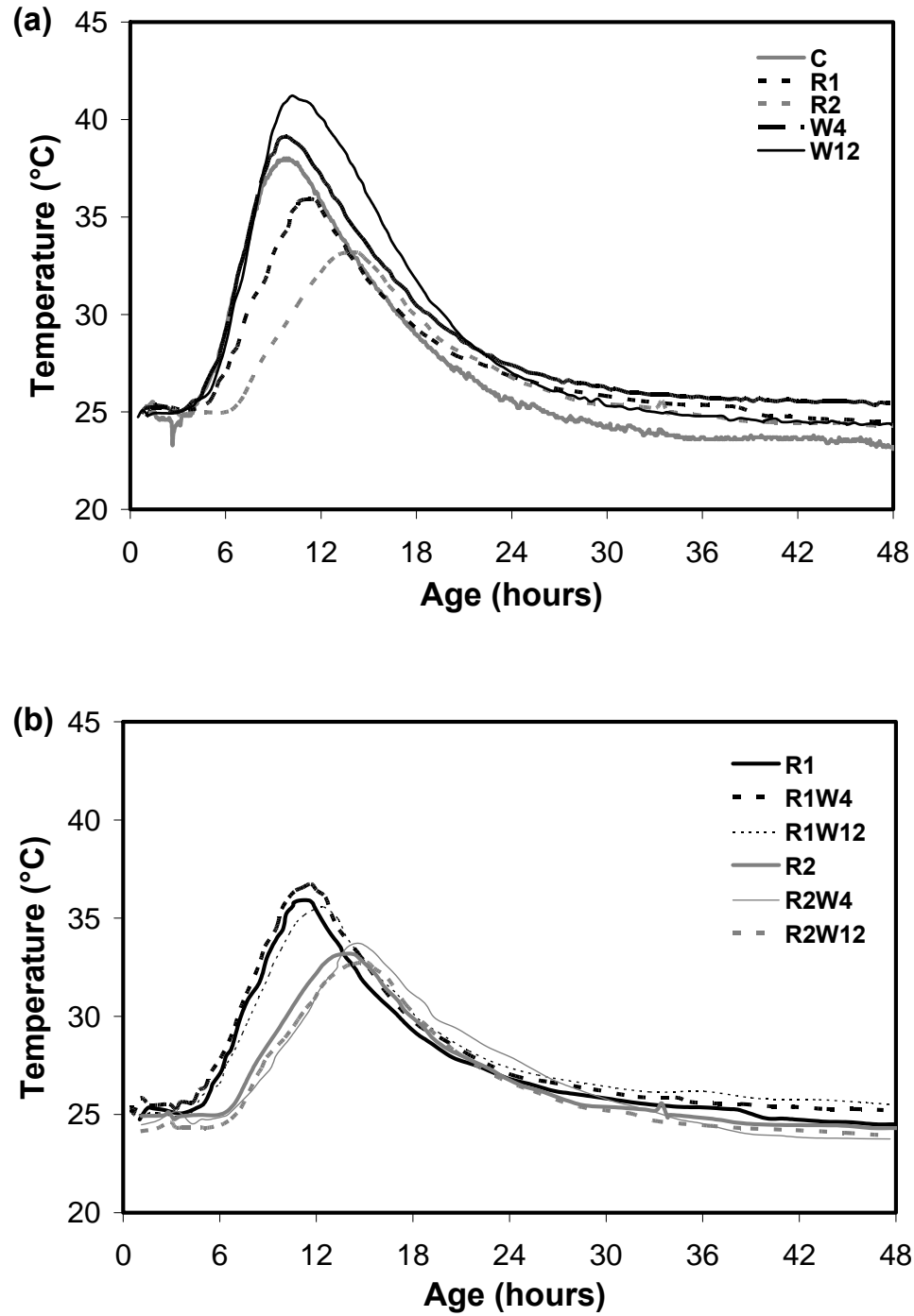
Figure 9-4: Heat of hydration for UHPC mixtures incorporating SRA and/or wollastonite microfibers a) individually and b) combined.

9.4.3. Degree of Hydration

Shrinkage mitigation techniques usually affect the rate of hydration reactions. Accordingly, the degree of hydration and amount of BW will be changed (Bentz, 2000). TGA was used to investigate the hydration evolution. The measured degree of hydration (represented by the relative BW) versus age is shown in **Fig. 9-5**.
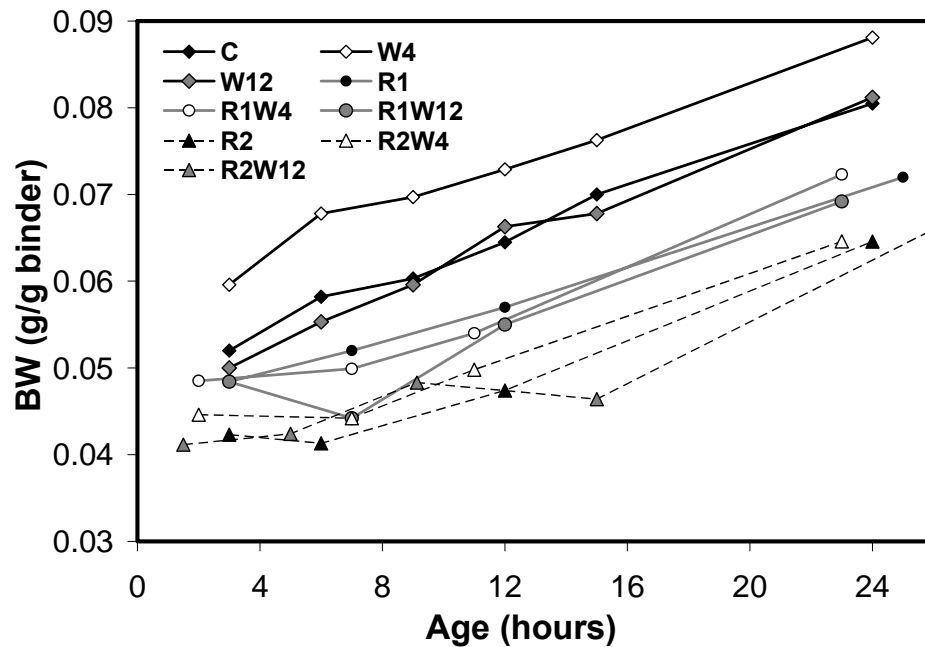
Figure 9-5: Change in degree of hydration during the first day for different UHPC mixtures.

It can be observed that all mixtures incorporating SRA exhibited lower degree of hydration with respect to that of the control mixtures without SRA. The higher the added SRA dosage, the lower was the degree of hydration. For instance; **R1W4** and **R2W4** mixtures exhibited about 18% and 27% lower amount of BW, respectively compared to that of the **W4** mixture without SRA. This is consistent with the retardation induced by

SRA and early-age compressive strength results (see **Fig. 9-1**). Moreover, mixtures with the same dosage of SRA exhibited a significant change in BW as the wollastonite microfibers content increased from 0% to 12%. For instance, at 2% SRA, the variation in the amount of BW between mixtures with and without wollastonite microfibers ranged between -4.4% and +1.8%. These results confirm heat of hydration results (see **Fig. 9-4(b)**).

9.4.4. Free Shrinkage and Mass Loss

The mass loss, autogenous and total shrinkage curves for mixtures incorporating SRA and/or wollastonite microfibers are shown in **Figs. 9-6** and **9-7**. The measured total shrinkage includes both drying and autogenous shrinkage (thermal deformation can be ignored due to the small cross-section of the specimens (Baroghel-Bouny *et al.*, 2006). Generally, for very low w/c (Tazawa and Miyazawa, 1999), the contribution of autogenous shrinkage to the total shrinkage can be comparable to that of drying shrinkage.

Despite the higher porosity induced by wollastonite microfibers (Bentz, 2000), no significant change in mass loss was observed compared to that of the control mixture with no microfibers. This can be attributed to the discontinuity of the pore structure induced by wollastonite microfibers (Mathur *et al.*, 2007) and the development of greater hydration products. This was also confirmed by MIP test results. For instance, mixture **W12** had a total porosity about 12.5% higher than that of the control mixture at 24 hrs. However, analysis of the MIP pore size distribution data at 24 hrs, according to the International Union of Pure and Applied Chemistry system (IUPAC) classification (Aligizaki, 2006), showed that **W12** had about 73% higher small mesopores (size range:

2.5 to 10 nm) than that of the control mixture, while it had 6% and 8% lower large

mesopores (size range: 10-50 nm) and macropores (size > 50 nm) with respect to values

for the control mixture, respectively. The higher small mesopores content indicates more

advance development of hydration (Antonio *et al*., 2010). On the other hand, electrostatic

interaction between the pore wall and pore liquid can hinder the pore liquid transfer

process in pore sizes below 50 nm, while it has no effect in macrospores (Aligizaki,

2006). Hence, the lower content of macropores in **W12**, probably affect the water

transport mechanism, thus leading to the lower mass loss compared to that in the control
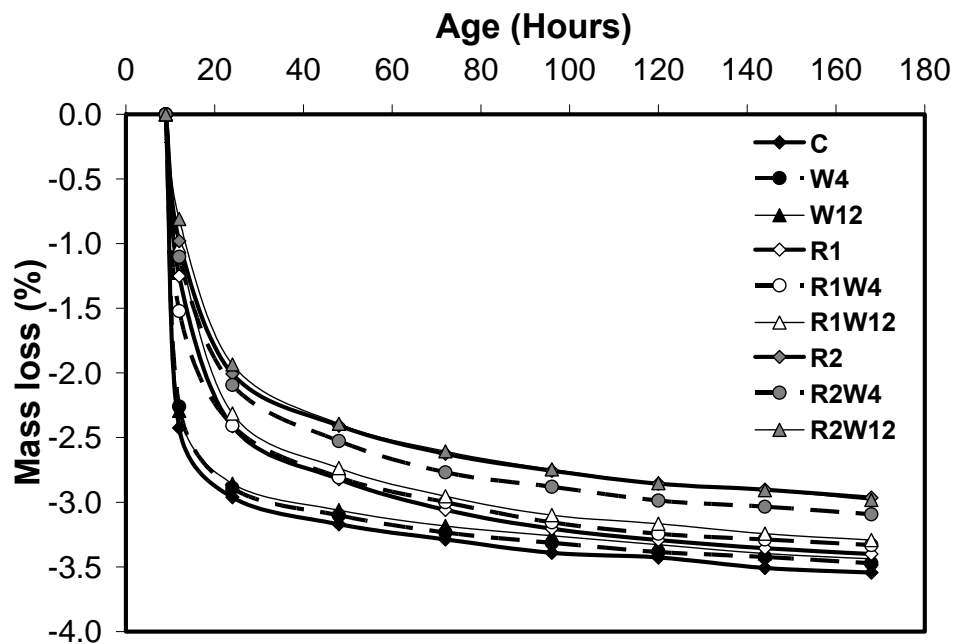
mixture.

Figure 9-6: Mass loss for UHPC mixtures with and without different dosages of SRA and/or wollastonite microfibers.

On the other hand, incorporating SRA slightly reduced mass loss with respect to

that of the control mixture. The higher the dosage of SRA, the greater was the reduction

in the mass loss. Moreover, adding SRA to mixtures incorporating wollastonite microfibers reduced the mass loss with respect to that of mixtures incorporating wollastonite microfibers alone. For instance, mixtures **R1W12** and **R2W12** exhibited about 7% and 16% lower mass loss compared to that of mixture **W12** (**Fig. 9-6**). This can be ascribed to the development of a drying front on the exposed top surfaces of specimens, which in turn restricted extracting more water from deeper within specimens (Bentz, 2006).

The general trend of total shrinkage results indicates a progressive reduction in total shrinkage with increasing content of wollastonite microfibers, as shown in **Fig. 9-7(a)**. A detailed discussion on the effect of wollastonite microfibers addition on shrinkage behaviour was given in chapter 8.

SRA induced a significant reduction in total shrinkage compared to that of the control mixture, in agreement with previous findings (He *et al*., 2006, Bentz, 2006, Powers and Brownyard, 1948). For instance, mixtures **R1** and **R2** exhibited about 39% and 48% lower total shrinkage, respectively, compared to that of the control mixture at 7-days. This can be attributed to a reduction in surface tension of the pore solution induced by SRA (Kovler and Bentur, 2006). As a result, lower capillary stresses developed and consequently lower total shrinkage was achieved. This reduction in capillary stresses also explains the lower autogenous shrinkage of mixtures **R1** and **R2** compared to that of the control mixture (about 41% and 59% reduction at 7-days, respectively) as shown in **Fig. 9-7(b)**. Moreover, SRA is believed to mitigate the drop in internal relative humidity, leading to lower self-desiccation and autogenous shrinkage (Bentz *et al*., 2001). A few hours after the final setting, **R1** and **R2** specimens exhibited an expansion (**Fig. 9-7(a)**).

This expansion played a significant role in reducing the net shrinkage along with the reduction in autogenous shrinkage induced by SRA compared to that of control specimens (Weiss *et al.*, 2008). Previous study (Sant, 2009) attributed this expansion to crystallization stresses as a result of amplifying portlandite super-saturation in the pore solution induced by SRA addition.

Figure 9-7 shows the effect of adding SRA to mixture incorporating wollastonite microfibers on the development of total and autogenous shrinkage. Adding SRA to mixtures incorporating wollastonite microfibers reduced the total and autogenous shrinkage significantly compared to that of mixtures incorporating wollastonite microfibers alone. For instance, mixtures **R1W12** exhibited about 37% and 20% reduction in autogenous and total shrinkage, respectively compared to that of mixture **W12**.
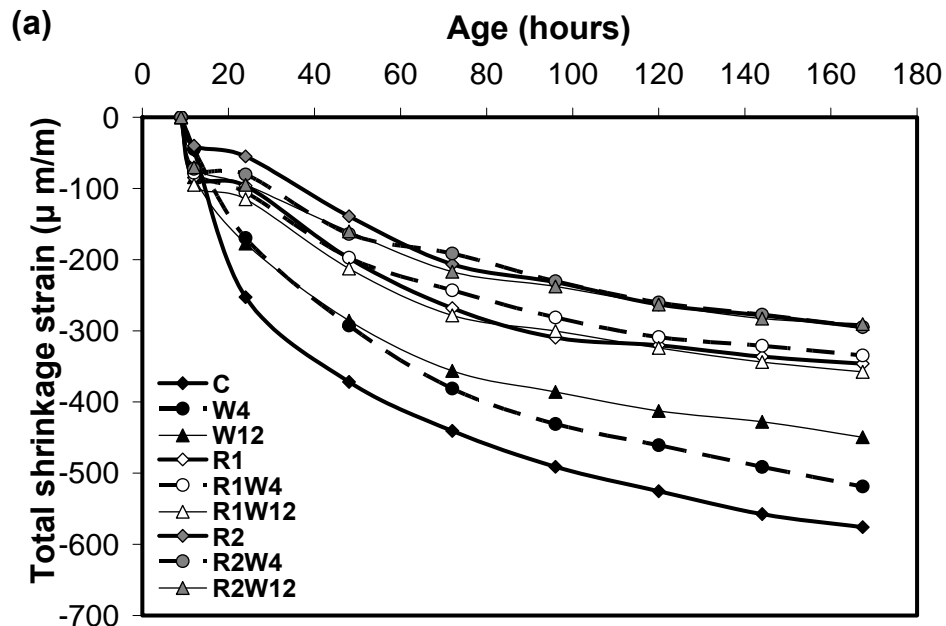
Figure 9-7: Shrinkage strains for UHPC mixtures with and without different dosages of SRA and/or wollastonite microfibers under a) drying and b) sealed conditions.

(b)
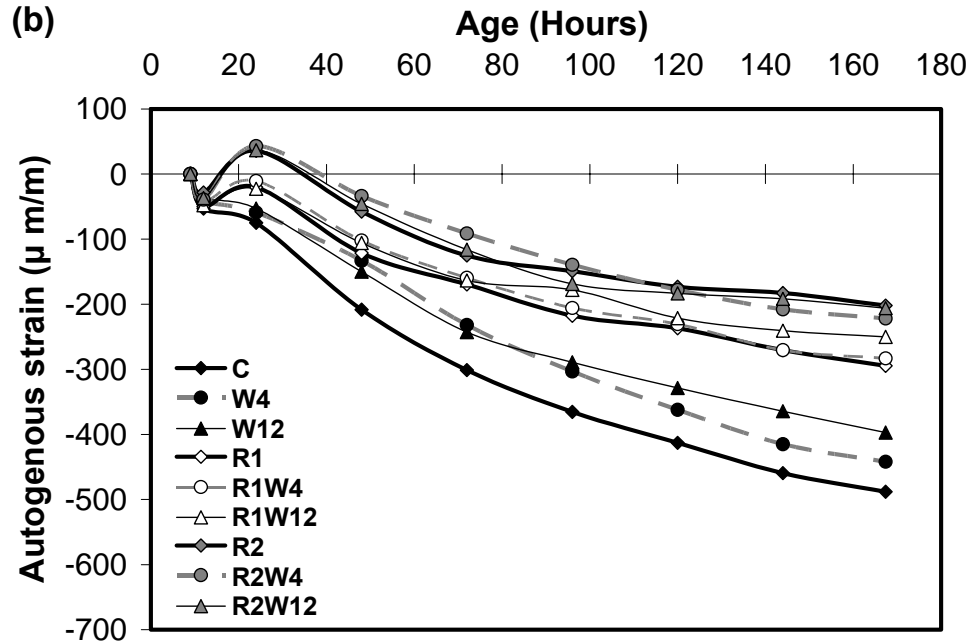
Figure 9-7 Contd': Shrinkage strains for UHPC mixtures with and without different dosages of SRA and/or wollastonite microfibers under a) drying and b) sealed conditions.

The reduction in total and autogenous shrinkage compared to that of control mixture was comparable for all mixtures incorporating the same SRA dosage, regardless of the added amount of wollastonite microfibers. Mixtures incorporating 2% SRA had 59%, 54% and 58% reduction in autogenous strain for 0%, 4% and 12% wollastonite microfibers content, respectively. This implies that SRA had a major effect on reducing shrinkage, while wollastonite microfibers have a minor or negligible effect. This is due in part to the retardation effect of SRA and early expansion. The major part of shrinkage occurred during the first 24 hrs (Pease *et al.*, 2005). The restraining effect of wollastonite microfibers during this period depends on the ability to transfer shear stresses between microfibers and the cementitious matrix, which is a function of the interfacial

microfiber/matrix bond strength (Hameed *et al*., 2009, Banthia and Sheng, 1996). Hence, the retardation of hydration reactions induced by SRA can lead to lower microfiber/matrix bond strength and consequently lower shrinkage restraining efficiency (Chan and Li, 1997). The pullout of wollastonite microfibers for the cementitious matrix is shown in **Fig. 9-8**. On the other hand, the high early expansion induced by SRA (i.e. between 12 and 24 hrs) could delay the development of contracting forces, which is considered as driving force for shrinkage development (Nawa and Horita, 2004).

Figure 9-8: SEM for wollastonite microfibers pullout from cementitious matrix incorporating SRA.

9.4.5.   Restrained Shrinkage

Figure 9-9 shows the steel ring measured strains for the **C**, **R1**, **R2**, **W4** and **W12** mixtures. The SRA mixtures had a time lag in the development of strain during the 24 hrs ring test and consequently a delay in the age at which the first crack occurred. The delay in cracking age was about 38% and 82% for mixtures **R1** and **R2**, respectively, compared to that of the control mixture (**Fig. 9-9(a)**), which is in agreement with previous studies (Weiss, 1997, Shah *et al*., 1997). This is a consequence of the slower development of the

shrinkage for these mixtures (see **Fig. 9-7**). The lower shrinkage development can be attributed to the retardation in hydration reactions and reduction in capillary stresses, along with the early expansion which compensated for shrinkage strains and cause the ring specimen to come out of contact with the inner steel ring thus generating no strains (Pease *et al.*, 2005).

Wollastonite microfibers enhanced the shrinkage cracking resistance as it delayed the cracking age compared to that of the control mixture (**Fig. 9-9(a)**). A detailed discussion on the effect of wollastonite microfibers addition on restrained shrinkage was given in chapter 8.

Figure 9-9(b) illustrates steel ring strain results for mixtures incorporating both SRA and wollastonite microfibers. Similar to mixtures with SRA, mixtures incorporating wollastonite microfibers had a time lag in strain development during the ring test. This is in agreement with previous shrinkage (see **Fig. 9-7**). Combining SRA and wollastonite microfibers improved the resistance to shrinkage cracking and significantly delayed the cracking age compared to that of the control mixture. For instance, combing 1% of SRA and 4% of wollastonite microfibers delayed the cracking age by about 84%, 33% and 43% compared to that of the control, **R1** and **W4** mixtures, respectively. This represents the net result of combining the reduction in capillary stresses induced by SRA and improvement of cracking resistance provided by wollastonite microfibers.

Mixtures **R1W4** and **R1W12** exhibited comparable strain behaviour to that of mixtures **R2** and **R2W4**, respectively, as shown in **Fig. 9-9(b)**. Hence, it appears that the

SRA dosage can be reduced while achieving better or comparable cracking behaviour with the aid of wollastonite microfibers.

Steel rings containing specimens with wollastonite microfibers tented to experience the development of two cracks, while those with no microfibers exhibited only one large crack.   The presence of multiple cracks is an expected result, since microfibers create internally several small restraints inside the matrix leading to lower crack width as the cracking opening is shared by all cracks (Passuello *et al*., 2009). The absence of multiple cracks in the control and SRA mixtures can be attributed to the stress relief induced by the opening of a single crack, since, unlike matrices with fiber, there is no ability to transfer or redistribute stresses (Shah and Weiss, 2006).
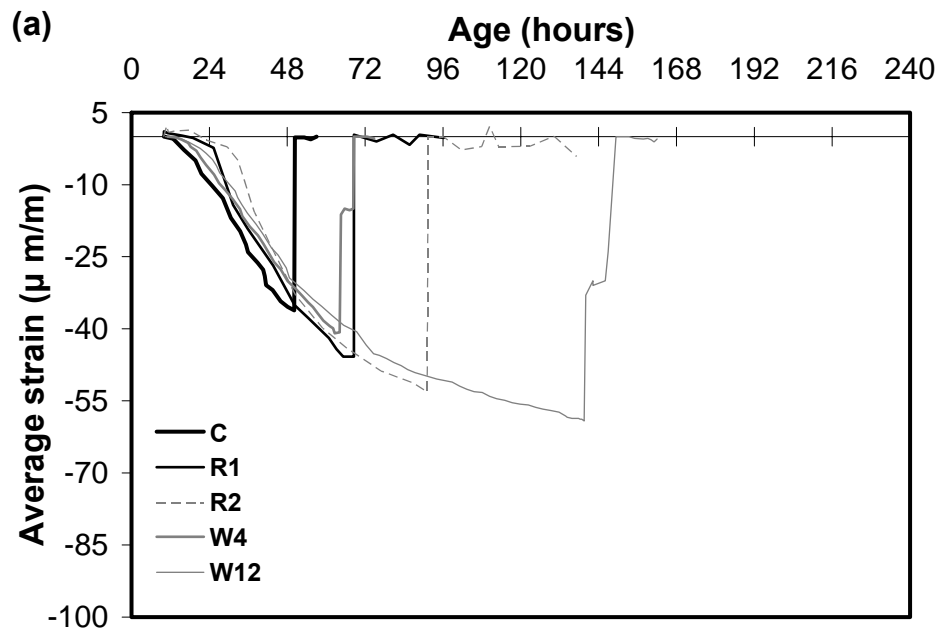
Figure 9-9: Strain measurements of the steel ring for UHPC mixtures incorporating SRA and/or wollastonite microfibers a) individually and b) combined.
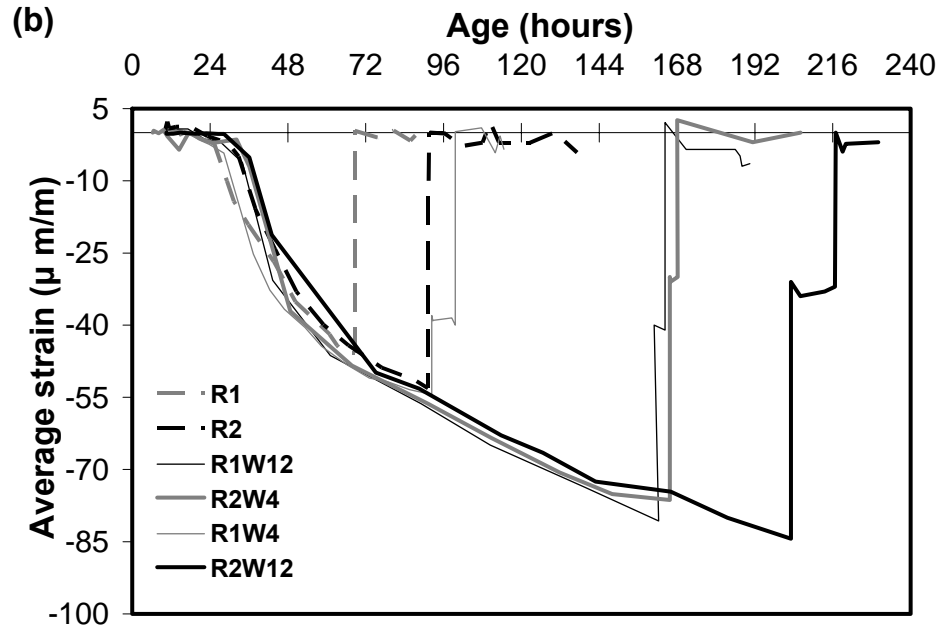
Figure 9-9 Contd': Strain measurements of the steel ring for UHPC mixtures incorporating SRA and/or wollastonite microfibers a) individually and b) combined.

9.4.6.   COD Results

Washing out of SRA from concrete, especially during early-ages, can significantly diminish its effectiveness in reducing shrinkage strains. SRA reduces the pore fluid surface tension in concrete but does not chemically combine with other hydration products (Rodden and Lange, 2004). Therefore, as SRA is washed out, higher shrinkage values develop. **Figure 9-10(a)** shows shrinkage results for the control, **R2**, **R2W4** and **R2W12** mixtures under submerged conditions.
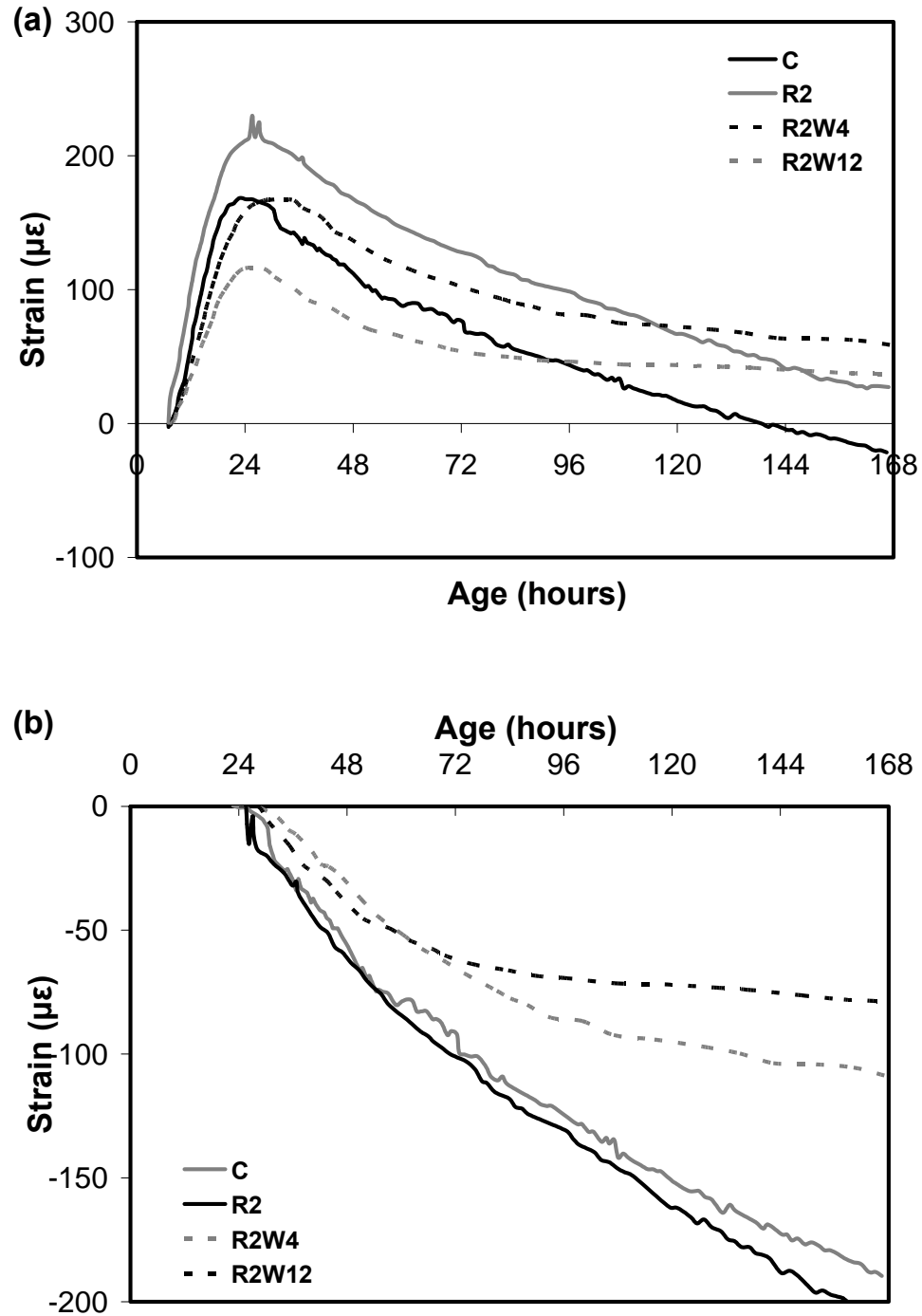
Figure 9-10: Measured strains under submerged condition for control, SRA and/or wollastonite microfibers UHPC mixtures: a) observed and b) initiated to zero after the early expansion.

Under submerged conditions, specimens continued to swell during the first 24 hrs, then started to shrink until the end of the investigated period. The early swelling resulted in a lower net shrinkage compared with that of sealed specimens (see **Fig. 9-10(a)**). The swelling of submerged specimens can be ascribed to the continuous supply of water, allowing the calcium silicate hydrate (CSH) to absorb water and expand (Neville, 1996). The reduction in the swelling strain with time can be explained by the fact that the progress of the hydration reactions reduced and depercolated the concrete capillary porosity, which interfered with water imbibing from the surrounding environment. Hence, no further expansion took place, while internal self-desiccation occurred as water was consumed by the hydration process. Mixtures incorporating wollastonite microfibers exhibited lower early-age expansion compared to that of the control and SRA mixtures. Moreover, the higher the wollastonite microfibers content, the lower was the early expansion. This can be attributed to the discontinuity of the pore structure induced by wollastonite microfibers (Mathur *et al*., 2007) which probably affected water movement within the concrete (Passuello *et al*., 2009).

In order to capture the shrinkage behaviour under submerged conditions, the strain curves were initiated to zero at the end of the swelling, as shown in **Fig. 9-10(b)**. Mixture **R2** had a comparable shrinkage strain to that of the submerged control specimens with no SRA, while mixtures **R2W4** and **R2W12** exhibited a lower shrinkage strain. Moreover, the reduction in shrinkage strain increased with higher content of wollastonite microfibers. It is hypothesized that SRA is washed out with migrating water from SRA mixtures, jeopardizing their shrinkage mitigation efficiency, while lower amounts of SRA were washed out from **R2W4** and **R2W12** mixtures.

To examine this hypothesis, chemical oxygen demand (COD) tests were conducted on water samples taken from the submersion tanks. The COD results in **Fig. - 11** for the **C**, **R2**, **R2W4** and **R2W12** mixtures confirm the existence of SRA in the submerging water. The cumulative level of leached SRA increased with time. However, mixtures **R2W4** and **R2W12** had lower COD values compared to that of mixture **R2**, which indicates a reduction in the amount of SRA washed out. The higher the content of wollastonite microfibers in specimens, the lower was the measured COD. This can be ascribed to the discontinuity of the pore structure of the wollastonite microfibers, which interfered with the washing out of SRA. Hence, a higher SRA content remained inside the pore solution, thus reducing capillary stresses induced by the internal self-desiccation and leading to lower shrinkage.
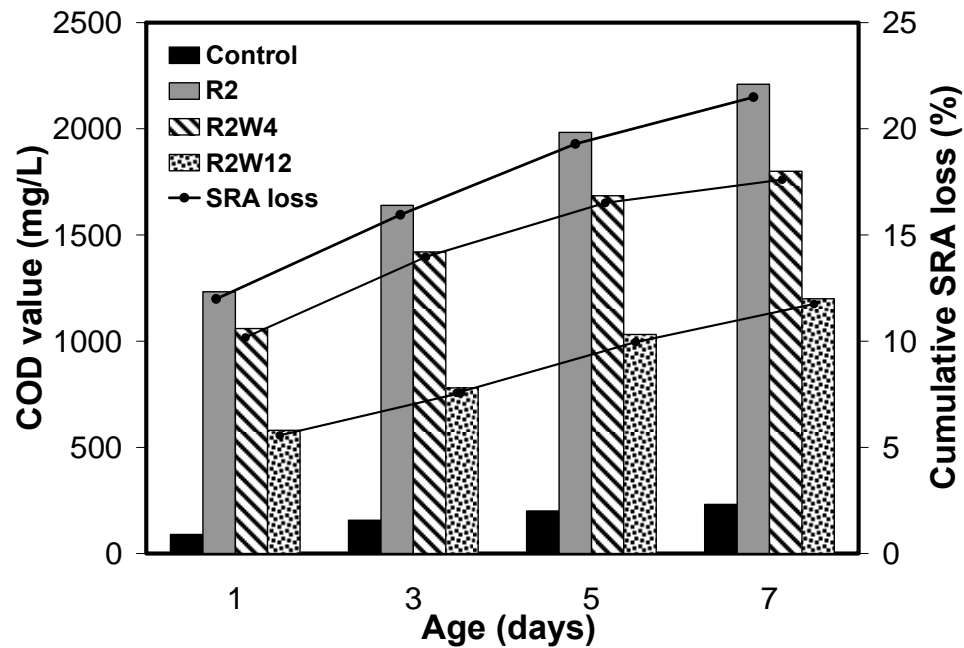
Figure 9-11: COD values for control, SRA and/or wollastonite microfibers UHPC mixtures.

9.6.   CONCLUSIONS

In this study, the shrinkage of UHPC mixtures with and without SRA and/or wollastonite microfibers was investigated under sealed, drying and submerged conditions. Based on this work, the following conclusions can be drawn:

1) Wollastonite microfibers addition in UHPC mixtures had a positive effect on the early-age compressive strength.

2) The addition of wollastonite microfibers enhanced compressive strength of UHPC mixtures incorporating SRA.

3) Incorporating both wollastonite microfibers and SRA in UHPC delayed the time of cracking through retarding the development of shrinkage strains and resisting the coalescence of micro-cracks.

4) The washout of SRA under submerged conditions can jeopardize its effectiveness in mitigating shrinkage strains.

5) Incorporating wollastonite microfibers in UHPC appears to promote pore discontinuity, thus leading to lower mass loss, less drying shrinkage and reduced SRA washing out.

9.7.   REFERENCES

Aligizaki, K.K., (2006). Pore Structure of Cement-based Materials: testing, interpretation and requirements. 1St Edition, Taylor & Francis, New York, USA, 388 p.

Antonio, A., Melo, N., Maria, A.C. and Wellington, R., (2010), "Mechanical properties, drying and autogenous shrinkage of blast furnace slag activated with hydrated lime and gypsum," *Cement and Concrete Composites*, Vol. 32, No. 4, pp. 312-318.

Banthia, N. and Sheng, J., (1996), "Fracture toughness of microfiber reinforced cement composites," *Cement and Concrete Composites*, Vol. 18, No. 4, pp. 251-269.

Baroghel-Bouny, V., Mounanga, P., Khelidj, A., Loukili, A. and Rafai, N., (2006), "Autogenous deformations of cement pastes: Part II. w/c effects, micro-macro correlations, and threshold values," *Cement and Concrete Research*, Vol. 36, No. 1, pp.123-136.

Bentz, D.P., (2000), "Fibers, percolation, and spalling of high performance concrete," *ACI Materials Journal*, Vol. 97, No. 3, pp. 351-359.

Bentz, D.P., (2006), "Influence of Shrinkage-Reducing Admixtures on Early-Age Properties of Cement Pastes," *Journal of Advanced Concrete Technology*, Vol. 4, No. 3, pp. 423-429.

Bentz, D.P., Geiker, M.R. and Hansen, K.K., (2001), "Shrinkage-reducing admixtures and early-age desiccation in cement pastes and mortars," *Cement and Concrete Research*, Vol. 31, No. 7, pp. 1075-1085.

Chan, Y.W. and Li, V.C., (1997), "Age effect on the characteristics of fiber/cement interfacial properties," *Journal of Materials Science*, Vol. 32, No. 19, pp. 5287-5292.

Eberhardt, A.B. and Kaufmann, J., (2006), "Development of shrinkage reduced self-compacting concrete," *ACI Journal*, Special addition NO. P-235, pp. 13-30.

Hameed, R., Turatsinze, A., Duprat, F. and Sellier, A., (2009), "Metallic fiber reinforced concrete: effect of fiber aspect ratio on the flexural properties," *ARPN Journal of Engineering and Applied Sciences*, Vol. 4, No. 5, pp. 67-72.

He, Z., Li, Z.J., Chen, M.Z. and Liang, W.Q., (2006), "Properties of shrinkage-reducing admixture-modified pastes and mortar," *Materials and Structures*, Vol. 39, No. 4, pp. 445-453.

Kovler, K. and Bentur, A., (2009), "Cracking sensitivity of normal and high strength concretes," *ACI Materials Journal*, Vol. 106, No. 6, pp. 537-542.

Lea, F.M., (1988). Lea's Chemistry of Cement and Concrete. 4th Edition, (ed.) P.C. Hewlett, J. Wiley, New York, 1053 p.

Low, N.M.P. and Beaudoin, J.J., (1992), "Mechanical properties of high performance cement binders reinforced with wollastonite microfibers," *Cement and Concrete Research*, Vol. 22, No. 5, pp. 981-989.

Mathur, R., Misra, A.K. and Goel, P., (2007), "Influence of wollastonite on mechanical properties of concrete," *Journal of Scientific and Industrial Research*, Vol. 66, No. 12, pp.1029-1034.

Nawa, T. and Horita, T., (2004), "Autogenous shrinkage of High- performance concrete," *Proceedings of the International Workshop on Microstructure and Durability to Predict Service Life of Concrete Structures,* Sapporo, Japan.

Neville, A.M., (1996). Properties of Concrete, 4th Edition, John Wiley &Sons, New York, 797 p.

Nmai, C., Tomita, R., Hondo, F. and Buffenbarger, J., (1998), "Shrinkage reducing admixtures," *Concrete International*, Vol. 20, No. 4, pp. 31-37.

Passuello, A., Moriconi, G. and Shah, S.P., (2009), "Cracking behavior of concrete with shrinkage reducing admixtures and PVA fibers," *Cement and Concrete Composites*, Vol. 31, No. 10, pp. 699-704.

Pease, B.J., Shah, H.R., and Weiss, W.J., (2005), "Shrinkage behavior and residual stress development in mortar containing shrinkage reducing admixture (SRA's)," *ACI-Special Publication on Concrete Admixtures*, Vol. 227, pp. 285–302

Powers, T.C. and Brownyard, T.L., (1948), "Studies of the physical properties of hardened portland cement paste," Bulletin No. 22, Research Laboratories of the Portland Cement Association. Reprinted from *Journal of the American Concrete Institute*, October 1946–April 1947, Proceedings 43, Detroit, pp. 971-992.

Rajabipour, F., Sant, G. and Weiss, J., (2008), "Interactions between shrinkage reducing admixtures (SRA) and cement paste's pore solution," *Cement and Concrete Research*, Vol. 38, No. 5, pp. 606-615.

Rodden, R.A. and Lange, D.A., (2004) "Feasibility of shrinkage reducing admixtures for concrete runway pavements," *Technical Note No. 4*, The Center of Excellence for Airport Technology (CEAT), 6 p.

Sant, G.N., (2009), "Fundamental investigations related to the mitigation of volume changes in cement-based materials at early ages," Ph.D. thesis, Purdue University, 227 p.

Schmidt, M., (1992), "Cement with inter-ground additives: capabilities and environmental relief (I)," *Zement Kalk Gips*, Vol. 45, No. 7, pp. 64-69.

Shah, S. P., Weiss, W. J., and Yang, W., (1997), "Shrinkage cracking in high performance Concrete." *Proceedings of the PCI/FHWA International Symposium on High Performance Concrete*, New Orleans, Louisiana, pp. 217-228.

Shah, S.P., Weiss, W.J. and Yang, W., (1998), "Shrinkage cracking-can it be prevented?," *Concrete International*, Vol. 20, No. 4, pp. 51-55.

Shah, H. R. and Weiss, J., (2006), "Quantifying shrinkage cracking in fiber reinforced concrete using the ring test," *Materials and Structures*, Vol. 39, No.9, pp. 887-899.

Tazawa, E. and Miyazawa, S., (1999), "Effect of constituents and curing condition on autogenous shrinkage of concrete," *Proceedings of the International Workshop Autogenous Shrinkage of Concrete*, (ed.) Eichi Tazawa, Taylor & Francis, Hiroshima, Japan, pp. 269-280.

Weiss, J., Lura, P., Rajabipour, F. and Sant, G., (2008), "Performance of shrinkage-reducing admixtures at different humidities and at early ages," *ACI Materials Journal*, Vol. 105, No. 5, pp. 478-486.

Weiss, J., (1997), "Shrinkage Cracking in restrained Concrete Slabs: Testing methods, material compositions, shrinkage reducing admixture and theoretical modeling," M.S. thesis, Northwestern University, Evanston, Illinois, USA, 128 p.

<div align="right">**CHAPTER TEN**</div>

ARTIFICIAL NEURAL NETWORK MODELING OF EARLY-AGE AUTOGENOUS SHRINKAGE OF CONCRETE*

In this chapter, an artificial neural networks (ANN) model for the early-age autogenous shrinkage of concrete is proposed. The model inputs include the cement content, water-to-cement ratio (w/c), type and percentage of supplementary cementitious materials, total aggregate volume, curing temperature, and hydration age. The autogenous shrinkage of concrete is the model output. Subsequent to model validation using experimental results of chapter 3, a parametric study was carried out to identify the effects of input variables on the evolution of autogenous shrinkage. Moreover, the autogenous shrinkage database assembled and used in the training of the proposed ANN is considered as a contribution to the state-of-the-art knowledge; it includes testing results on modern concretes under various environmental conditions.

10.1. INTRODUCTION

Concrete is the most widely used construction material world-wide (Vanikar, 2004). Shrinkage of concrete initiates cracks that can lead to the ingress of aggressive substances, which jeopardizes the durability of concrete structures (Lura *et al*., 2007). Hence, concrete shrinkage has been a matter of great concern in the design of durable concrete infrastructure (Toutanji *et al*., 2004). Shrinkage occurring over a long time

---

period is attributed to drying. Early-age drying shrinkage induces internal tensile stresses while the concrete has not yet gained sufficient tensile strength to withstand such stresses, which leads to cracking (Sivakumar and Santhanam, 2006).

At early-ages, another type of concrete shrinkage (so called "autogenous shrinkage") occurs without moisture exchange with the environment (Bentz and Jensen, 2004). Autogenous shrinkage is a mechanism whose importance has grown with the increasing use of low w/c concrete. For many years, autogenous shrinkage, which can mainly be attributed to internal self-desiccation due to the hydration of cement (Bentz and Jensen, 2004), had been neglected as it caused minor strains in conventional concrete members compared to that caused by drying shrinkage (Zhang *et al*., 2003). However, autogenous shrinkage was found to be too large to be neglected and to have critical effects on low w/c concrete members (Igarashi *et al*., 2000). The evolution of the autogenous shrinkage of concrete depends on many factors, including the w/c (Zhang *et al*., 2003), aggregate content, cement content (Tazawa *et al*., 1995), curing temperate (Mak *et al*., 1999), and type and percentage of supplementary cementitious materials (Zhang *et al*., 2003). Such parameters are highly interdependent and exhibit complex combined roles on the development of autogenous shrinkage.

Existing models for drying shrinkage do not normally perform well for autogenous shrinkage of modern concretes (ACI 209R-92 (ACI Committee 209, 1992), Model B3 (Bažant, 1995), CEB-FIP 1990 (CEB-FIP 1990, 1991), Gl2000 (Gardner and Lockman, 2001)), since they are limited to concretes with mean 28-days compressive strengths ranging from 20 to 70 MPa. They also cannot capture the effects of high

contents (more than 30%) of silica fume, fly ash and other natural pozzolans, and they do not take into account the faster evolution of properties at early-ages in very low w/c ratio systems (ACI Committee 209, 2008, Lṕez and Pacios, 2006). Such models generally use mathematical formulae relating variables by means of statistical coefficients calculated from certain databases. The characteristics of the databases, including component materials, age and environmental conditions, limit the validity and application range of such models (Lṕez and Pacios, 2006).

On the other hand, ANN is a powerful modeling tool for problems where the rules which govern the results are either not defined properly or too complex (Adeli, 2001, Flood and Kartam, 1994). A number of applications of ANN in concrete materials and structures have been proposed by several researchers (Bilgehan and Turgut, 2010, Rattapoohm and Pichai, 2009, Yeh, 2008, El-Chabib *et al*., 2005). ANN is an artificial intelligence technique that does not require mathematical relationships between variables. It has learning, self-organizing and auto-improving capabilities (Demir, 2008) allowing it to capture complex interactions among variables without any previous knowledge of the nature of these interactions. A properly trained ANN also has the ability to recall full patterns from incomplete or noisy data (Rafiq *et al*., 2001). Due to such exceptional capabilities, ANN has been used in a wide range of engineering applications.

This chapter demonstrates the potential for using artificial neural networks to predict the autogenous shrinkage of concrete under different curing temperatures. The assembled database, model architecture and training process of the ANN network are described. Moreover, the influence of important parameters including w/c, superplasticizer dosage and curing temperature on autogenous shrinkage were

quantitatively analyzed and evaluated with respect to knowledge available in the open literature.

10.2.   RESEARCH SIGNIFICANCE

For many years, the autogenous shrinkage of concrete associated with the internal consumption of water during cement hydration and the associated self-desiccation had not been regarded as a serious problem. However, with the increasing use of low w/c concrete, the importance of autogenous shrinkage has grown since it is too large to be neglected. Autogenous shrinkage can have a comparable value to that of drying shrinkage. Therefore, predicting the autogenous shrinkage is an important aspect in the service life analysis and design of durable concrete structures. In this study, an attempt was made to develop an artificial intelligence-based tool for accurately predicting the autogenous shrinkage of concrete based on its mixture design. A powerful modeling tool, artificial neural networks, was employed on a comprehensive database assembled from the open literature. The ANN model allows predicting autogenous shrinkage along with the influence of key parameters on the autogenous shrinkage behaviour of concrete.

10.3.   NEURAL NETWORK APPROACH

ANN has been used to relate the autogenous shrinkage of concrete and its mixture composition at different curing temperatures. ANN learns from input information similar to the operation of a biological brain (Haykin, 1999). It has the capability of generalization, classification, pattern recognition, function approximation and simulation of sophisticated operations (Haykin, 1999). ANN structure consists of parallel multiple layers of linear and nonlinear processing elements (i.e. neurons) which can be classified

into: an input layer, an output layer, and hidden layers (Demir, 2008), as shown in **Fig. 10-1**. These neurons are linked by variable weights. The input layer receives original data (x_i), which is adjusted by connection weights (w_{ij}) and biases (b). The adjusted inputs are subjected to a summation process to form a single input (net)$_j$ for all inputs received from the input layer (**Eq. 10-1**) (Sarıdemir, 2009).

$$(net)_j = \sum_{i=1}^{n} w_{ij} \cdot x_i + b$$ **Eq. 10-1**

This single input is modified by an activation function ($f(x)$) to generate an output value of the processing unit through the hidden layers. The error between the network outputs and desired targets is calculated and then propagated back to the network through a learning algorithm. The implementation of such an algorithm updates the network weights and biases in the direction in which the total network error decreases rapidly. ANN then synthesizes and memorizes the relationship between the inputs and outputs through a training process. Hence, the used data in the training process should be sufficient and representative to allow the ANN to recognize the underlying structure of the information involved. Once an ANN is established and well-trained, it will be capable of predicting outputs of any input set of data, and predicting the outcome of any unfamiliar set of input located within the range of the training data with an acceptable degree of accuracy.

In civil engineering, feed-forward neural networks along with back-propagation algorithms are widely used and have shown efficient performance (Demir, 2008, Sarıdemir, 2009, Venkiteela *et al*., 2010, Adhikary and Mutsuyoshi, 2006, Mukherjee and

Biswas, 1997). Hence, they were selected for constructing the proposed ANN model in this study.
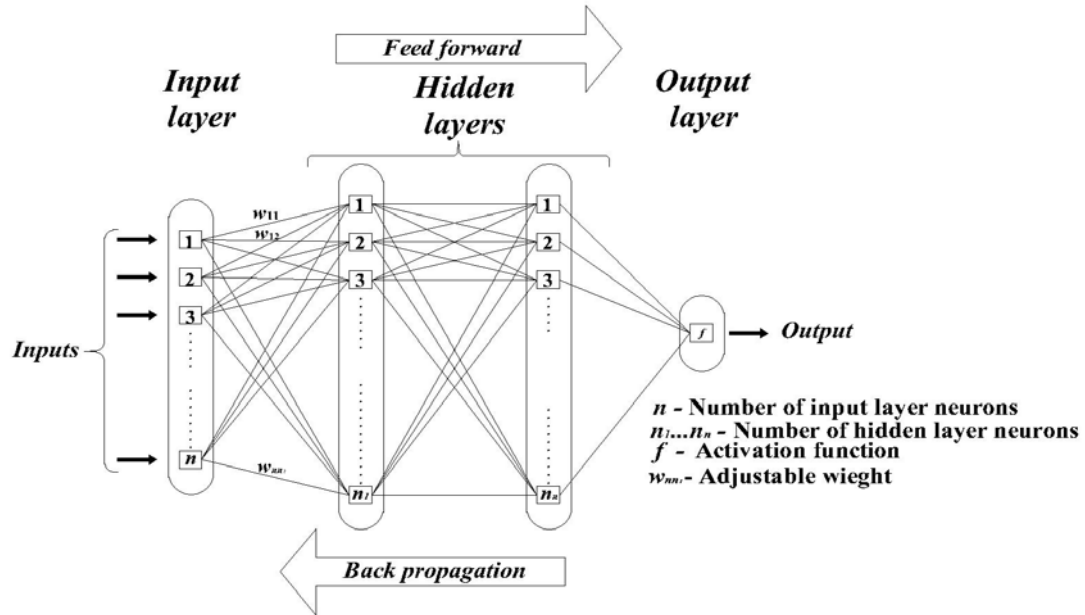
Figure 10-1: The architecture of ANN models.

10.3.1. Feed-Forward Neural Network

Feed-forward neural network (FFN) is the most widely used model in engineering applications. In FFN, neurons are arranged in layers and all the neurons in each layer are linked to all the neurons in the next layer (Adhikary and Mutsuyoshi, 2006). In general, the FFN consists of one input layer, one output layer and one or more hidden layers of neurons (Mukherjee and Biswas, 1997). The phrase "Feed-forward" indicates that the data move forward from one layer to the next during ANN modeling (Venkiteela *et al*., 2010). The input layer receives input information and passes it forward to the neurons of the hidden layer, which in turn passes the information to the output layer. The output from the output layer is the corresponding prediction of the model for the data set

supplied at the input layer. To construct a stable FFN for a particular problem, the optimum number of neural units in each layer was selected using a trial and error approach as recommended by (Rafiq *et al.*, 2001).

10.3.2. Back-Propagation Learning Algorithm

Learning algorithms are techniques used to establish connections (i.e. weights and biases) between neurons forming the network structure and to adjust both weights and biases to obtain the desired values. There are two broad categories of algorithms: unsupervised (weights and biases are modified in response to network inputs only) and supervised (weights and biases are modified in order to move the network outputs closer to the targets) (Haykin, 1999).

One of the well-known supervised training algorithms for the FFN is the back-propagation algorithm. In this algorithm a gradient descent technique is applied to minimize the error for a particular training pattern in which it adjusts the weights by a small amount at a time (Sarıdemir, 2009, Venkiteela *et al.*, 2010, Adhikary and Mutsuyoshi, 2006, Mukherjee and Biswas, 1997, Topçu and Sarıdemir, 2007, Ince, 2004). The learning error is calculated using the following equation (**Eq. 10-2**)

$$\text{Error} = \tfrac{1}{2} \sum_i (t_i - o_i)^2 \qquad \textbf{Eq. 10-2}$$

Where t_i is the target output and o_i is the predicted output at neuron (i), respectively. In the back-propagation phase, the error between the predicted and target output values is calculated and used to update the weights between neurons using the following equation (**Eq. 10-3**) (Ince, 2004):

$$\Delta w_{i,j}(t) = \eta \delta_j o_i + \beta \Delta w_{i,j}(t-1)$$ **Eq. 10-3**

where $\Delta w_{i,j}(t)$ is the weight change at the end of iteration (t), δ_j local error gradient, $\Delta w_{i,j}(t-1)$ is the weight change at iteration (*t*-1), η, β are learning and moment rate, respectively. Hence, the error serves as a feedback for the learning process. The iteration continues until a satisfactory convergence is achieved (Mukherjee and Biswas, 1997).

10.4.   PROPOSED ANN MODEL

A multilayered feed-forward neural network with a back-propagation algorithm was used to model the autogenous shrinkage behaviour in the present study. Two hidden layers with a Tansigmoid (*tansig* **Eq. 10-4**) transfer functions were used, while a pure linear transfer function (**Eq. 10-5**) was used in the output layer.

$$tan \, sig \, (n) = \frac{2}{1 + e^{(-2n)}} - 1$$ **Eq. 10-4**

$$purelin \, (n) = n$$ **Eq. 10-5**

During the training process, the design of network architecture starts with fewer hidden neurons, and then the number of hidden neurons is adjusted by assessing the network error through applying a trial and error approach (Nehdi *et al.*, 2007). In order to improve generalization, the regularization method was applied. This involves modifying the performance function, which is normally chosen to be the sum of squares of the network errors on the training set (Demuth and Beal, 1998). The new performance function measures the network performance as the weight sum of two factors: the mean squared error and the mean squared weight and bias values (**Eq. 10-6**). Using this modified

performance function causes the network to have smaller weights and biases, which forces the network response to be smoother and less likely to over fit.

$$msereg = \gamma mse + (1-\gamma)msw$$ **Eq. 10-6**

Where (*msereg)* is the mean squared error with a regularization performance function, (γ) is the performance ratio which gives weight to the mean square errors (*mse*) (**Eq. 10-7**) and the mean square weights (*msw*) (**Eq. 10-8**).

$$mse = \frac{1}{N} \sum_{i=1}^{N} (t_i - o_i)^2$$ **Eq. 10-7**

Where N is the number of iterations, t_i is the target output and o_i is the predicted output at neuron (i), respectively.

$$msw = \frac{1}{n} \sum_{j=1}^{n} w_j^2$$ **Eq. 10-8**

Where n is the number of neurons, w is the weight value for neuron (j).

To simplify the learning process and reduce the required time for training, the back-propagation Levenberg-Marquardt Algorithm (LMA) was adopted as the learning algorithm (Nehdi *et al.*, 2001). The LMA operates in a batch mode at which the weights and biases of the network are updated only after the entire training set has been applied to the network (Demuth and Beal, 1998). LMA propagates back the errors computed at the output layer to the network based on the Jacobian matrix J, which contains the first derivatives of the network errors with respect to weights and biases. An iteration of such algorithm can be written as follows (**Eq. 10-9**)

$$w_{j+1} = w_j - \left[J^T J + \mu I\right]^{-1} J^T e \qquad \qquad \textbf{Eq. 10-9}$$

where w_j is a vector of current weights and biases, μ is a learning rate, J is the Jacobian matrix, J^T is the transpose matrix of J, I is the identity matrix, and e is a vector of network errors. Parameters of the established ANN model are shown in **Table 10-1**.

The available set of data is divided into three subsets, namely, training, validation, and testing. The training data is used to train the model to recognize the patterns between input and output data. The validation data is used to evaluate the effectiveness of the designed model in generalizing the underlying relationships and achieving a good performance when new data are introduced. The final model is tested with the testing data set, not presented to the model before, to ensure that predictions are real and not artifacts of the training process (Demuth and Beal, 1998). Before training, all data (i.e. inputs and targets) were scaled so that they fall in the range [-1,1]. This pre-processing step increases the efficiency of the ANN training (Rafiq *et al*., 2001).

Table 10-1: The values of parameters used in the ANN model.

Parameters	ANN
Number of input layer neurons	8
Number of hidden layer	2
Number of first hidden layer neurons	12
Number of second hidden layer neurons	8
Number of output layer neurons	1
Minimum gradient	1×10^{-10}
Goal	1×10^{-5}

10.5.   MODEL DATABASE

The ability of the ANN model to predict the autogenous shrinkage behaviour of concrete mixtures will largely depend on how comprehensive the database is. In other words, it will depend on the availability of experimental data that are capable to teach the ANN relationships between the concrete mixture variables and its measured autogenous shrinkage. An extensive literature review identified a great amount of published data on concrete shrinkage. However, in many cases there is insufficient information regarding the exact concrete mixture composition, testing methodology, curing conditions, incomplete or graphically presented data, and the absence of other important parameters needed to properly characterize autogenous shrinkage (e.g. age at which the measuring of autogenous shrinkage started). The exclusion of such incomplete data reduced the extent of the database available for training the network.

It should also be highlighted that autogenous shrinkage of concrete has not been researched as extensively as drying shrinkage until Tazawa and Miyazawa (Tazawa and Miyazawa, 1993) emphasized its importance for low w/c mixtures. To avoid further complexity, only experimental data having mixture components with comparable physical and chemical properties were identified for the training and testing of the network. Using the aforementioned criteria, a number of data sets were selected from different studies and used to train, validate and test the ANN model, as summarized in **Table 10-2**. For ANN training, eight input variables were selected: w/c, cement content, silica fume percentage, fly ash percentage, superplasticizer content, total aggregate volume, curing temperature and hydration age. The measured autogenous shrinkage of concrete was the single output.

Table 10-2: Database sources and variables range of input and output.

	Source	No. of mixtures	Variables	Maximum	Minimum	Unit
1	Zhang *et al.*, 2003	9	Cement	924	292	kg/m^3
2	Igarashi *et al.*, 2000	4				
3	Lura *et al.*, 2007	1	w/c	0.60	0.16	-----
4	Mak *et al.*, 1999	4				
5	Yang *et al.*, 2005	3	SF	30	0.0	% cement
6	Loukili *et al.*,2000	1				
7	Bentur *et al.*, 2001	1	FA	50	0.0	% cement
8	Lee *et al.*, 2006	4				
9	Akkaya *et al.*, 2007	3	TA	72	40	% total volume
10	Pipat *et al.*, 2005	5				
11	Yun *et al.*, 2006	4	SP	4	0	% cement
12	Mazloom *et al.*, 2004	4				
13	Meddah and Sato, 2010	1	Temp.	65	10	°C
14	Nassif *et al.*, 2007	5				
15	Konsta *et al.*, 2003	3	Age	360	0.5	hours
16	Meddah *et al.*, 2006	7				
17	Guangcheng *et al.*, 2006	4	Autogenous shrinkage	-1012	+20	με
18	Akcay and Tasdemir,2009	1				
19	Daniel and Ted, 2008	1	TA: Total aggregate volume;			
20	Ma *et al.*, 2003	4	SF: Silica fume;			
21	Brook *et al.*, 1999	8	FA: Fly ash;			
Total No. of mixtures		77	SP: Superplasticizer			

10.6.   RESULTS AND DISCUSSION

Since there is no precise method for partitioning the database, the ANN model was trained with randomly selected 60% of the total database, while 20% was used for validation and the other 20% for testing (West *et al.*, 1997). The performance of an ANN model depends on the success of the training process. A successfully trained ANN model should give accurate output predictions, not only for input data used in the training

process, but also for new testing data unfamiliar to the model within the range of the

training database. Moreover, very good ANN models normally have only slight

difference between their validating and testing errors (Amegashie *et al.*, 2006). At the

training stage, the performance of the ANN model was assessed statistically based on

root-mean-squared (*RMS*) error, absolute fraction of variance (R^2), and mean absolute

percentage error (*MAPE*) between model and experimental results which are expressed in

the following equations (**Eq. 11,12** and **13**) , respectively (Sarıdemir, 2009, Topçu and

Sarıdemir, 2008)

$$RMS = \sqrt{\frac{1}{n} \sum_{i=1}^{n} (t_i - o_i)^2} \qquad \textbf{Eq. 11}$$

$$R^2 = 1 - \left(\frac{\sum_{i=1}^{n} (t_i - o_i)^2}{\sum_{i=1}^{n} (t_i)^2} \right) \qquad \textbf{Eq. 12}$$

$$MAPE = \frac{1}{n} \frac{\sum_{i=1}^{n} |t_i - o_i|}{\left| \sum_{i=1}^{n} t_i \right|} \qquad \textbf{Eq. 13}$$

Where t_i is the target output, o_i is the predicted output, and *n* is the number of data points.

Satisfactory performance of the training process was verified by requiring the

ANN model to predict the autogenous shrinkage of concrete mixtures from the training

data set using the eight input variables. Predictions of the ANN model are shown in **Fig.

10-2**. The figure includes the equity line, as a reference, which represents the condition of

equal values for the predicted and measured autogenous shrinkage strains. It can be noted

that the ANN model had captured the input-output relationships since the points are mostly located on or slightly under/above the equity line between the experimental and predicted expansion values. The *RMS*, R^2 and *MAP*E values were 29 με, 0.98 and 12.2%, respectively, which indicates that the performance of ANN is satisfactory.

To examine the generalization capacity of the ANN, it was tested using the testing data (20% of the original database). Such testing points were not previously presented to the model, and thus the predictive capacity of the model for new data can be evaluated. The eight input parameters of the testing data points were introduced to the ANN model and the response (predicted autogenous shrinkage) is shown in **Fig. 10-2**. Similar to the case of the training data, the model achieved good predictions relative to the actual experimental data; testing data points were mostly located on or slightly deviated from the equity line (**Fig. 10-2**). The *RMS*, R^2 and *MAPE* of the testing data points were 42 με, 0.965 and 15.1%, respectively. Hence, it can be deduced that the ANN had a satisfactory generalization capacity for predicting the autogenous shrinkage of similar concrete mixtures exposed to various curing temperatures. In addition, statistical parameters for the model validation data were comparable to that of the training and testing data (i.e. *RMS* =39 με, R^2=0.95 and *MAPE*= 13.2%) indicating an excellent performance of the model (Shang *et al*., 2004).
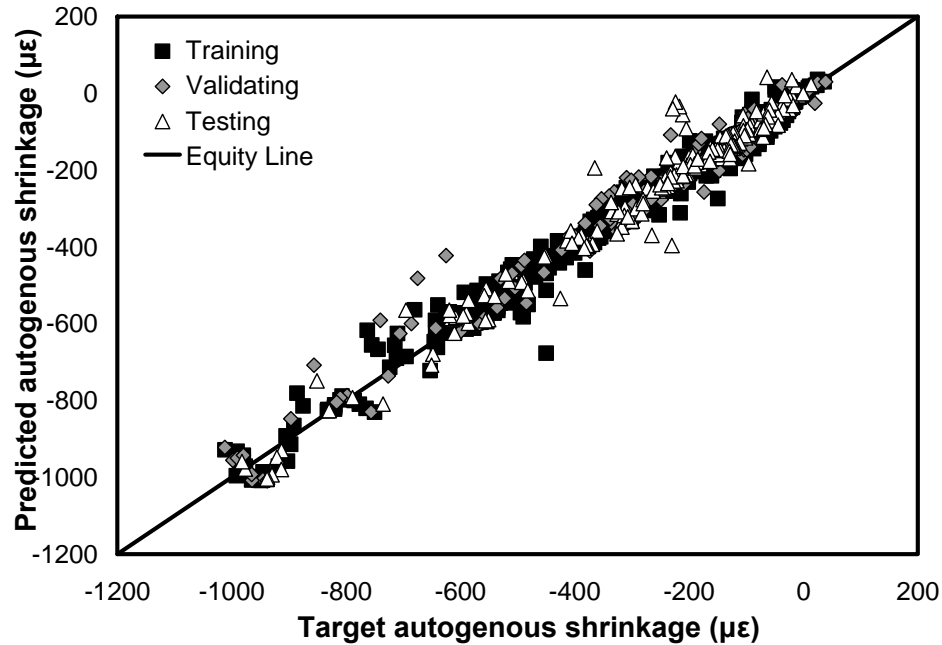
Figure 10-2: Response of ANN model in predicting autogenous shrinkage of concrete.

10.6.1. Validating ANN Using Experimental Work

To demonstrate the utility of the proposed ANN model, experimental measurements from Chapter 3 for UHPC mixtures with w/c=0.22 and 0.25 cured at different temperatures, namely, 10, 20, 40 °C were collected and compared to that predicted by the trained ANN model. Details for the experimental program, materials, specimens and testing procedure were given in Chapter 3.

The measured and predicted autogenous shrinkage curves are illustrated in **Fig. 10-3**. It can be observed that the ANN predictions were in good agreement with the measured results throughout the entire range of the shrinkage behaviour. A comparison between the measured and ANN model-predicted autogenous shrinkage values shows a

deviation of about ±20%, which is quite reasonable according to (ACI Committee 209, 2008) (**Fig. 10-4**).
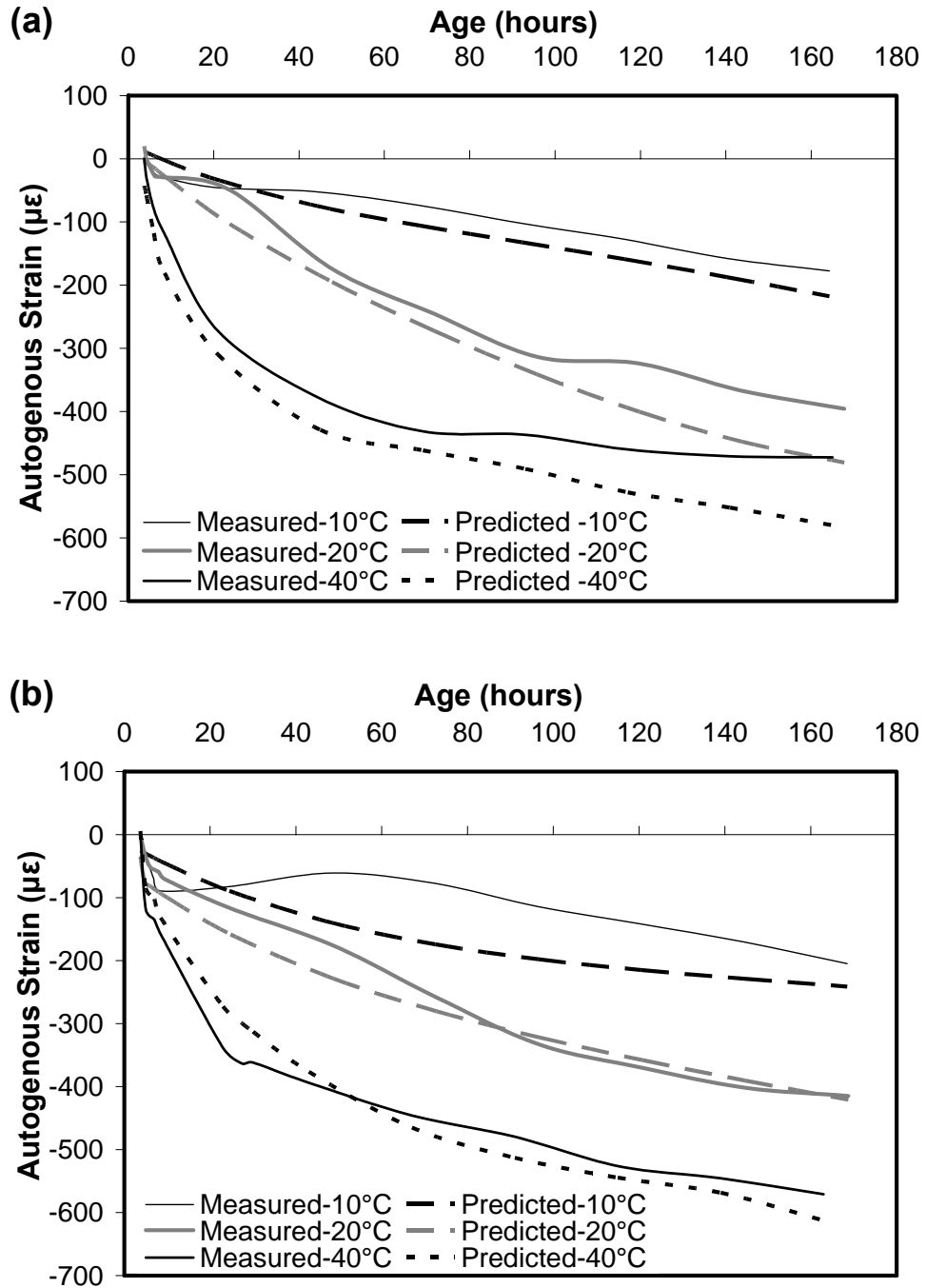
Figure 10-3: Measured autogenous shrinkage values compared with predicted a) w/c=0.22 and b) w/c=0.25.
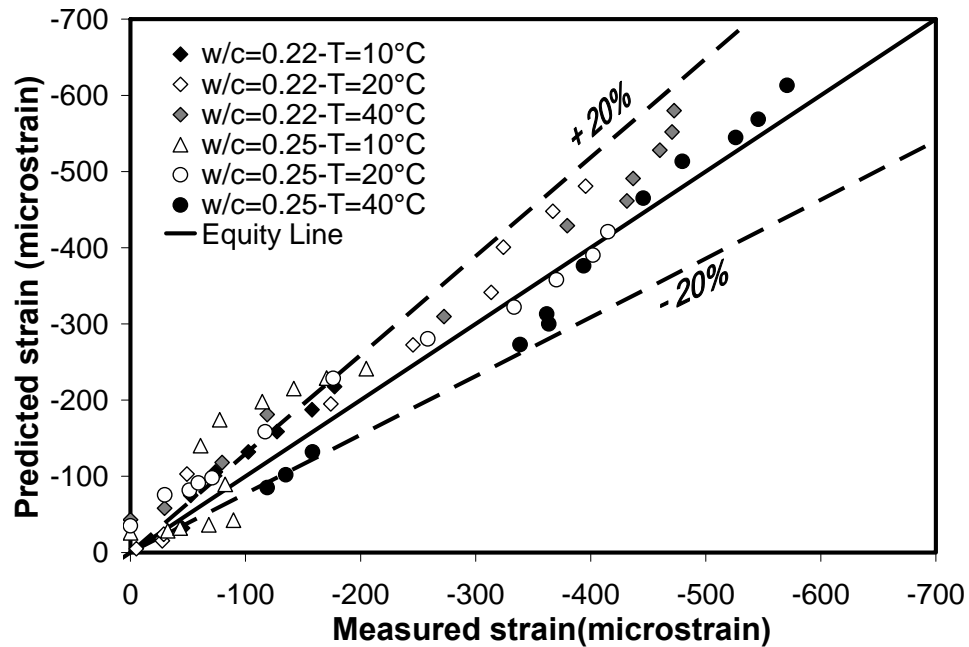
Figure 10-4: Deviation between measured and predicted autogenous shrinkage values.

Moreover, residual analysis was applied to evaluate the performance of the ANN models. The residual value R is defined as the difference between the measured and ANN-predicted shrinkage strains (**Eq. 10-14**).

$$R = \text{Predicted value} - \text{Measured value}$$

Eq. 10-14

The residuals of tested mixtures at the different curing temperature are plotted in **Fig. 10-5**. Positive residuals indicate that the model underestimated the shrinkage strains and negative residuals indicate that the model overestimates them. The distributions of the residuals in the negative region are greater than that in the positive range, indicating that the ANN model slightly overestimated autogenous shrinkage. However, about 97% of residuals are within a low range of ±100 με, which indicates a reasonable performance of the ANN model.
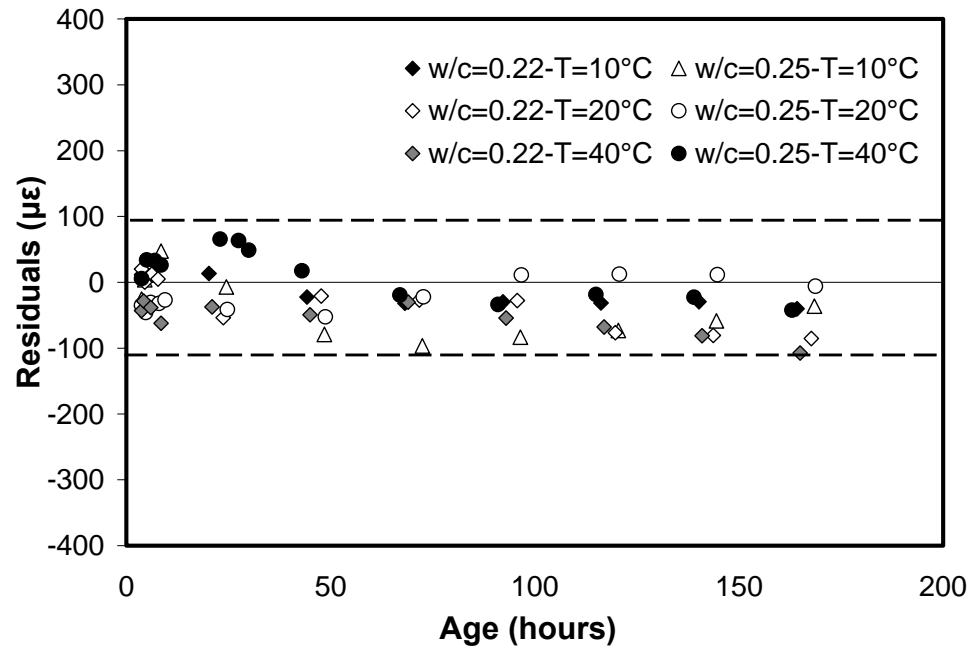
Figure 10-5: Residual values for ANN model.

10.6.2. Parametric Analyses

The ANN model showed a satisfactory performance and demonstrated its ability to predict autogenous shrinkage strains for a wide range of concrete mixture designs under different curing temperatures. The purpose of this section is to exploit the abilities of the ANN model in capturing the influence of individual input parameters on autogenous shrinkage development. The analysis was done by randomly selecting a concrete mixture to create multiple new mixtures (not previously presented to the model) with various levels (within the range of training data) of the parameter of interest. Among the model inputs, the w/c, superplasticizer content and curing temperature were selected due to limited and/or conflicting results about their effects on autogenous shrinkage.

10.6.2.1 *Effect of Water-to-Cement Ratio*

The w/c has a great influence on the autogenous shrinkage behaviour of a concrete mixture. To investigate changes in the autogenous shrinkage magnitude due to variation of the w/c ratio, the w/c ratio was changed while the water amount was held constant. This corresponds to an increasing cement content and paste content while the aggregate amount remains constant. A constant dosage of superplasticizer was added; hence workability of the tested mixtures varied. As expected, the mixture with the lowest w/c ratio had the greatest amount of autogenous shrinkage. Moreover, autogenous shrinkage increased with a drop of the w/c as shown in **Fig. 10-6**. Increasing the cement content increases chemical shrinkage, which is a main driving force behind autogenous shrinkage. In agreement with previous work (Baroghel-Bouny *et al*., 2006), the magnitude of the predicted autogenous shrinkage at a given age increased linearly as the w/c decreased. The w/c is likely to be below 0.25 for ultra-high-performance concrete (UHPC). However, limited data is available on the relationship between the autogenous shrinkage behaviour and w/c for w/c values below 0.25. Therefore, with the aid of the ANN generalization capability, this relationship was successfully investigated.

Below w/c = 0.24, the relationship of autogenous shrinkage and w/c exhibited a similar linear trend but with a higher slope. This indicates that the rate of autogenous shrinkage development is faster and more sensitive to w/c ratio reduction below 0.25 compared to that at higher w/c (> 0.25). Reviewing the limited test results for mixtures with w/c below 0.25, a good agreement between model predictions and experimental data was found. For instance, results reported by (Tazawa *et al*., 2000) show that reducing the w/c from 0.23 to 0.17 led to about 1.5 times higher rate of autogenous shrinkage

compared to that induced by reducing the w/c from 0.4 to 0.3. Therefore, a polynomial

relationship was proposed to capture the behaviour over a wider w/c range from 0.16 to

0.44 (**Fig. 10-7**).
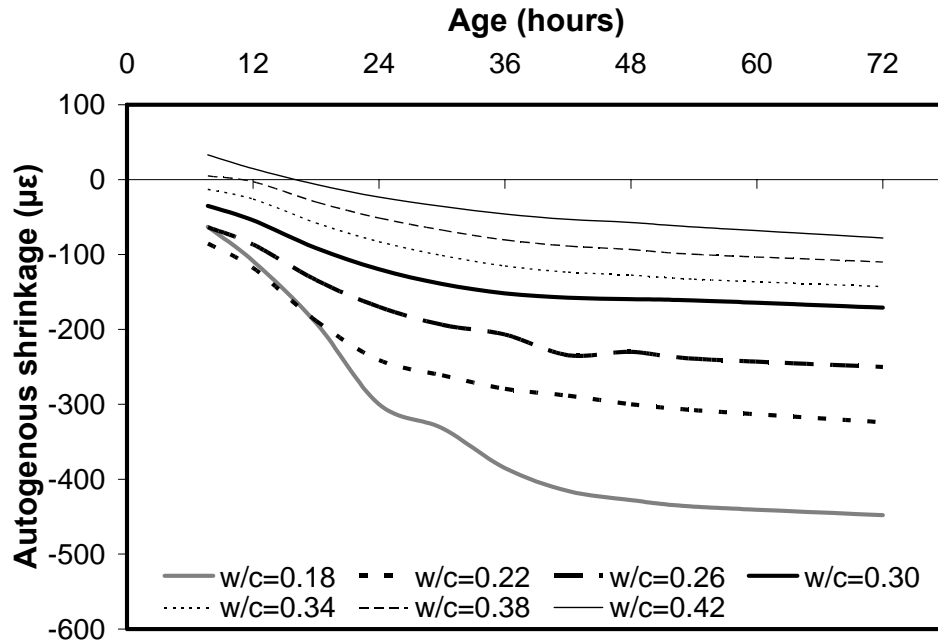
Figure 10-6: Sensitivity of ANN model to the w/c in predicting autogenous shrinkage.
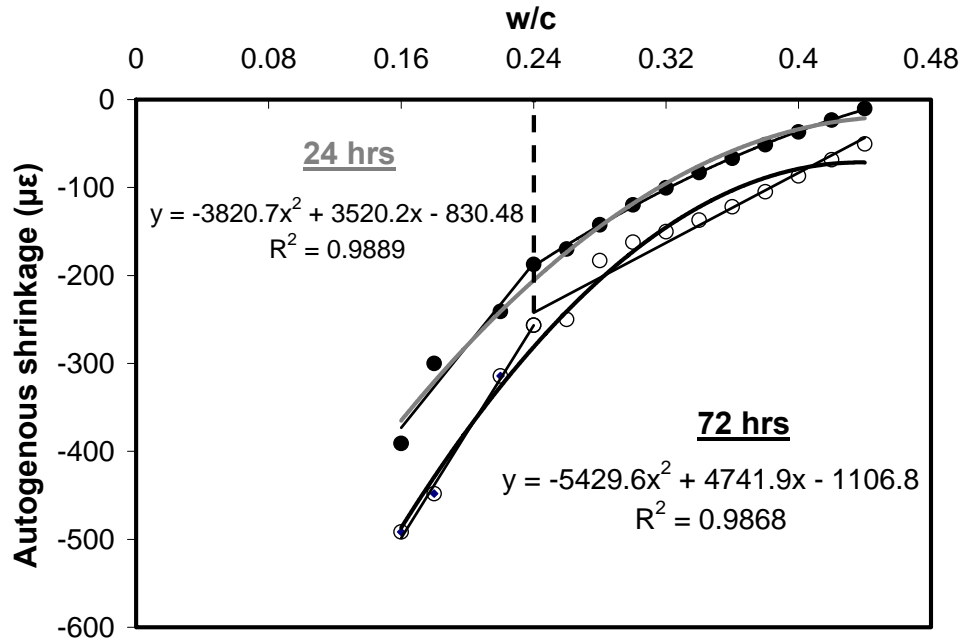
Figure 10-7: Correlation between autogenous shrinkage of concrete measured at T=20°C and w/c at ages 24 and 72 hours.

10.6.2.2 *Effect of Superplasticizer*

Superplasticizer (SP) is a key component in modern concretes. It is used to improve workability and allow for adequate placement on site. In the literature, there is conflicting observations about the effect of superplasticizer on autogenous shrinkage. An increasing trend was reported (e.g. Holt and Leivo, 2004, Holt, 2005), as well as a reducing trend (e.g. Tazawa and Miyazawa, 1995, Nawa and Horita, 2004). In order to demystify such discrepancies, the ANN model was used to capture the effect of the SP dosage on the autogenous shrinkage behaviour. **Figure 10-8** illustrates the effect of the SP amount on the autogenous shrinkage of concrete mixtures with a w/c = 0.26 used with various cement contents. It can be observed that the autogenous shrinkage of concrete increased

with increasing SP dosage until reaching a threshold dosage, beyond which autogenous shrinkage decreased. This threshold dosage increased with increasing cement content.

This behaviour can be explained as follows: Chemical shrinkage, which is a reduction in the volume of hydration products compared to that of the reacting constituents, is a main driving mechanism behind autogenous shrinkage (Tazawa *et al*., 1995). Adding SP deflocculated cement particles, leading to better dispersion, and consequently faster rate of hydration reactions. This ultimately led to a higher rate of autogenous shrinkage (Holt and Leivo, 2004, Holt, 2005). Conversely, a higher SP dosage was found to have the side effect of slowing the chemical activity of hydration through provoking an ionic double layer around cement grains (Morin *et al*., 2001). Therefore, it can be argued that as long as the added SP dosage is less than the threshold dosage, SP improves cement dispersion leading to higher chemical activity. Once the SP dosage exceeds the threshold, SP starts slowing down the chemical activity of hydration reactions. This threshold dosage was found to increase with increasing cement content since more cement particles need to be dispersed. However, at very high cement content, a lower SP dosage may be required since a higher percentage of cement grains acts as a filler rather than a reacting material, as shown in **Fig. 10-8**.
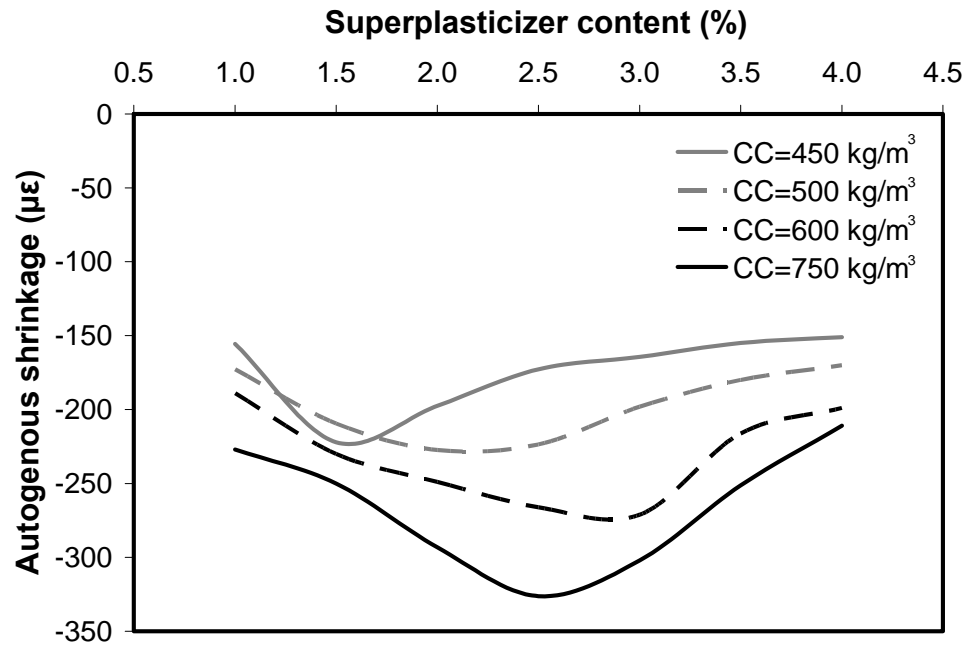
Figure 10-8: Effect of superplasticizer dosage on autogenous shrinkage of concrete measured at T=20°C and w/c=0.26.

10.6.2.3 *Effect of Curing Temperature*

The ANN model was used to predict the autogenous shrinkage curves of concrete mixtures with a w/c = 0.26 that were cured at various temperatures ranging from 10°C to 40°C. These curves were plotted versus the age up to 72 hours in **Fig. 10-9**. It is observed that the initial slope of these curves increased with increasing curing temperature, indicating a higher rate of autogenous shrinkage development. Moreover, the higher the curing temperature, the earlier the curve started to flatten. At that flatten point (known as the knee-point) a significant reduction in autogenous shrinkage occurred (Mounanga *et al.*, 2006). This reduction in autogenous shrinkage is frequently ascribed to the formation of a load-bearing microstructure (self-supporting skeleton), which resists contracting forces (Sellevold *et al.*, 1994). Hence, increasing the curing temperature had two

compensating influences: accelerated hydration reactions leading to a higher rate of autogenous shrinkage, but at the same time accelerated the development of a self-supporting skeleton that resisted autogenous shrinkage. The autogenous shrinkage is the net resultant of these two compensating processes. Therefore, as the curing temperature increased, a delay in starting autogenous shrinkage measurements will result in a significant underestimation of its real value.
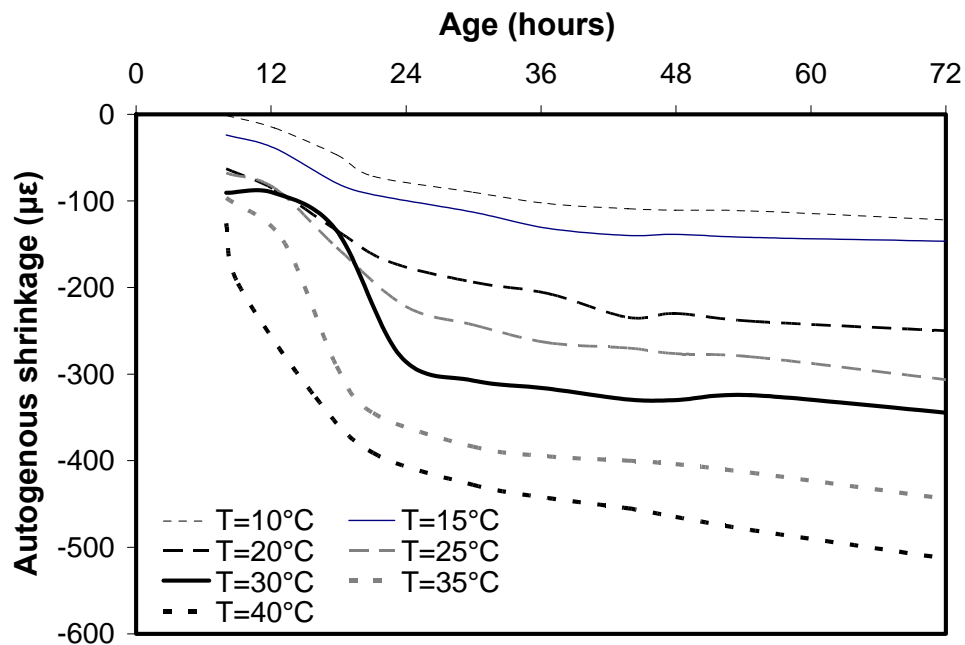
Figure 10-9: autogenous shrinkage vs. age for concrete w/c=0.26 and cured at various temperature ranges from 10 to 40°C.

10.7.   CONCLUSIONS

Autogenous shrinkage is a highly complex mechanism that makes modeling its behaviour a difficult task. This study aimed at demonstrating the possibility of adapting artificial neural networks to predict the autogenous shrinkage of concrete as a function of its mixture design under different curing temperatures. A database for autogenous shrinkage

was developed and used for training, validating and testing the ANN model. The results support the following conclusions:

1) The ANN model thus developed is a viable method for predicating autogenous shrinkage strains of concrete. It showed an excellent ability to capture the interrelationships amongst key system variables.

2) Using the generalization capabilities of the ANN, the effects of several parameters on the early-age autogenous shrinkage development could be quantified.

3) At a given age, the magnitude of autogenous shrinkage increased linearly as the w/c was reduced. Below a w/c = 0.24, the rate of autogenous shrinkage became more sensitive to w/c reduction. A polynomial relationship can capture the autogenous shrinkage behaviour for w/c values ranging from 0.16 to 0.42.

4) A superplasticizer threshold dosage has been proposed at which the effect of the SP on autogenous shrinkage switches from a motivator to chemical hydration reactions to a deterrent. This threshold dosage changes according to the mixture proportions.

5) The higher the curing temperature, the earlier the knee-point was reached where the shrinkage curve started to flatten.

6) Hence, particularly at high curing temperatures, measuring autogenous shrinkage should start as early as possible in order to capture its real value.

7) The proposed ANN is not capable of extrapolation beyond the domain of the data used in its training. However, it can be extended beyond the current domain and to include other experimental variables should sufficient data needed for such an extension becomes available in the future.

10.8. REFERENCES

ACI Committee 209, (1992), "Prediction of creep, shrinkage, and temperature effects in concrete structures (ACI 209R-92)," *American Concrete Institute*, Farmington Hills, MI, 47 pp.

ACI Committee 209, (2008), "Guide for modeling and calculating shrinkage and creep in hardened concrete (ACI Report 209.2R-08)," *American Concrete Institute,* Farmington Hills., 44 p.

Adeli, H., (2001), "Neural networks in civil engineering: 1989-2000," *Computer-Aided Civil and Infrastructure Engineering*, Vol. 16, No. 2, pp. 126-142.

Adhikary, B. and Mutsuyoshi, H., (2006), "Prediction of shear strength of steel fiber RC beams using neural networks," *Construction and Building Materials*, Vol. 20, No. 9, pp. 801-811.

Akcay, B. and Tasdemir, M., (2009), "Optimisation of using lightweight aggregates in mitigating autogenous deformation of concrete," *Construction and Building Materials*, Vol. 23, No.1, pp. 353-363.

Akkaya, Y., Ouyang, C. and Shah, S., (2007), "Effect of supplementary cementitious materials on shrinkage and crack development in concrete," *Cement and Concrete Composites*, Vol. 29, No. 2, pp.117-123.

Amegashie, F., Shang, J.Q., Yanful, E.K. Ding, W., Al-Martini, S. (2006), "Using Complex Permittivity and Artificial Neural Networks to Identify and Classify Copper, Zinc and Lead Contamination in Soil," *Canadian Geotechnical Journal*, Vol. 43, pp. 100-109

Baroghel-Bouny, V., Mounanga, P., Khelidj, A., Loukili, A. and Rafaï, N., (2006), "Autogenous deformations of cement pastes: Part II. W/C effects, micro–macro correlations, and threshold values," *Cement and Concrete Research*, Vol. 36, No. 1, pp. 123-136.

Bažant, Z. P., (1995), "Creep and shrinkage prediction models for analysis and design of concrete structures—Model B3," *Materials and Structures*, Vol. 28, No. 6, pp. 357-365.

Bentur, A., Igarashi, S. and Kovler, K., (2001), "Prevention of autogenous shrinkage in high-strength concrete by internal curing using wet lightweight aggregates," *Cement and Concrete Research*, Vol. 31, No. 11, pp. 1587-1591.

Bentz, D. and Jensen, O., (2004), "Mitigation strategies for autogenous shrinkage cracking," *Cement and Concrete Composites*, Vol. 26, No. 6, pp. 677-685.

Bilgehan, M. and Turgut, P., (2010), "The use of neural networks in concrete compressive strength estimation," *Computers and Concrete*, Vol. 7, No. 3, pp. 271-283.

Brook, J., Cabrera, J. and Johari, M., (1999), "Factors affecting autogenous shrinkage of silica fume high strength concrete," *In: Autogenous shrinkage of concrete: proceedings of the international workshop*, Japan Concrete Institute, Tazawa E.(ed.), Taylor & Francis, pp. 195-202.

CEB-FIP 1990, (1991), "Model code for concrete structures," *Bulletin Information*, No. 199, 201 pp.

Daniel, C. and Ted, H., (2008), "Internal curing of high-performance concrete with pre-soaked fine lightweight aggregate for prevention of autogenous shrinkage cracking," *Cement and Concrete Research*, Vol. 38, No. 6, pp. 757-765.

Demir, F., (2008), "Prediction of elastic modulus of normal and high strength concrete by artificial neural networks," *Construction and Building Materials*, Vol. 22, No. 7, pp. 1428-1435.

Demuth, H., and Beal, M., (1998). Neural Network Tool Box for Use with MATLAB Version 3.0, The Math Works Inc., pp. 5.37-5.39.

El-Chabib, H., Nehdi, M. and Said, A., (2005), "Predicting shear capacity of NSC and HSC slender beams without stirrups using artificial intelligence," *Computers and Concrete*, Vol. 2, No. 1, pp. 79-96.

Flood, I., and Kartam, N., (1994), "Neural networks in civil engineering I: principles and understanding," *Journal of Computing in Civil Engineering*, Vol. 8, No. 2, pp. 131-148.

Gardner, N., and Lockman, M., (2001), "Design provisions for drying shrinkage and creep of normal-strength concrete," *ACI Materials Journal*, Vol. 98, No. 2, pp. 159-167.

Guangcheng, L., Youjun, X. and Zhengwut, J., (2006), "Volume changes of very-high-performance cement-based composites," *Magazine of concrete research*, Vol. 58, No. 10, pp. 657-663.

Holt, H. and Leivo, M., (2004), "Cracking risks associated with early age shrinkage," *Cement and Concrete Composites*, Vol. 26, No. 5, pp. 521-530.

Holt, H., (2005), "Contribution of mixture design to chemical and autogenous shrinkage of concrete at early ages," *Cement and Concrete Research*, Vol. 35, No. 3, pp. 464-472.

Haykin, S., Neural Networks: A Comprehensive Foundation, 2nd Edition, Upper Saddle River, NJ: Prentice-Hall, 1999, 700 p.

Igarashi, S., Bentur, A., Kovler, K., (2000), "Autogenous shrinkage and induced restraining stresses in high-strength concretes," *Cement and Concrete Research*, Vol. 30, No. 11, pp. 1701-1707.

Ince, R., (2004), "Prediction of fracture parameters of concrete by artificial neural networks," *Engineering Fracture Mechanics* , Vol. 71, No. 15, pp. 2143-2159.

Konsta, m., Dattatreya, J. and Shah, S., (2003), "Influence of mineral admixtures on the autogenous shrinkage and porosity of high strength concrete," In: *Sixth CANMET/ACI International Conference on Durability of Concrete*, Malhotra V.M. (ed.), ACI-SP 212, pp. 227-238.

Lee, K., Lee, H., Lee, S. and Kim, G., (2006), "Autogenous shrinkage of concrete containing granulated blast-furnace slag," *Cement and Concrete Research*, Vol. 36, No. 7, pp. 1279-1285.

Loukili, A., Chopin, D., Khelidj, A. and Le Touzo, J., (2000), "A new approach to determine autogenous shrinkage of mortar at an early age considering temperature history," *Cement and Concrete Research*, Vol. 30, No. 6, pp. 915-922.

Lṕez, V. and Pacios, A., (2006), "Modeling the influence of SRA on properties of HPC," *Proceedings of International symposium on Measuring, monitoring and modeling concrete properties*, Konsta-Gdoutos (eds.), Springer Netherlands, Part 5, pp. 441-447.

Lura, P., Pease, B., Mazzotta, G., Rajabipour, F. and Weiss, J., (2007), "Influence of shrinkage-reducing admixtures on development of plastic shrinkage cracks," *ACI Materials Journal*, Vol. 104, No. 2, pp. 187-194.

Ma, J., Dietz, J. and Dehn, F., (2003), "Ultra high performance self-compacting concrete," *Proceedings of 3rd International Symposium on Self-compacting Concrete*, Ólafur W. and Indriði N. (eds.) , RILEM Publications, pp. 136-142.

Mak, S., Ritchie, D., Taylor, A. and Diggin, R., (1999), "Temperature effects on early age autogenous shrinkage in high performance concretes," *In: Autogenous shrinkage of concrete: proceedings of the international workshop, Japan Concrete Institute*, Tazawa E.(ed.), Taylor & Francis, pp. 155-166.

Mazloom, M., Ramezanianpour, A. and Brooks, J., (2004), "Effect of silica fume on mechanical properties of high-strength concrete," *Cement and Concrete Composites*, Vol. 26, No. 4, pp. 347-357.

Meddah, M., Aitcin, P. and Petrov, N., (2006), "A new approach for the determination of the starting point of autogenous shrinkage strain," *Proceedings of Seventh CANMET/ACI International Conference on Durability of Concrete*, Malhotra V.M. (ed.), ACI-SP 234, pp. 473-484.

Meddah, M. and Sato, R., (2010), "Effect of curing methods on autogenous shrinkage and self-induced stress of high-performance concrete,' *ACI Materials Journal*, Vol. 107, No. 1, pp. 65-74.

Morin, V., Tenoudji, F., Feylessoufi, A. and Richard, P., (2001), " Superplasticizer effects on setting and structuration mechanisms of ultra high-performance concrete," *Cement and Concrete Research*, Vol. 31, No. 1, pp. 63-71.

Mounanga, P., Baroghel-Bouny, V., Loukili, A. and Khelidj, A., (2006), "Autogenous deformations of cement pastes: Part I. Temperature effects at early age and micro–macro correlations," *Cement and Concrete Research*, Vol. 36, No. 1, pp. 110-122.

Mukherjee, A. and Biswas, S., (1997), "Artificial neural networks prediction of mechanical behavior of concrete at high temperature," *Nuclear Engineering and Design*, Vol. 178, No. 1, pp. 1-11.

Nassif, H., Suksawang, N. and Mohammed, M., (2007), "Effect of curing methods on early-age and drying shrinkage of high-performance concrete," *Transportation Research Record: Journal of the Transportation Research Board*, Vol. 1834, pp. 48-58.

Nawa, T. and Horita, T., (2004), "Autogenous shrinkage of high-performance concrete," *Proceedings of the International Workshop on: Microstructure and Durability to Predict Service Life of Concrete Structures*, Sapporo, Japan, pp. 29-38.

Nehdi, M., El-Chabib, H. and El-Naggar, M., (2001), "Predicting performance of self-compacting concrete mixtures using artificial neural networks," *ACI Materials Journal*, Vol. 98, No. 5, pp. 394-401.

Pipat, T., Toyoharu, N., Masashi, N. and Toshiki, S., (2005), "Effect of fly ash on autogenous shrinkage," *Cement and Concrete Research*, Vol. 35, No. 3, pp. 473-482.

Rattapoohm, P. and Pichai N, (2009), "An integrated approach for optimum design of HPC mix proportion using genetic algorithm and artificial neural networks, " *Computers and Concrete*, Vol. 6, No. 3, pp. 253-268.

Rafiq, M., Bugmann, G. and Easterbrook, D. "Neural network design for engineering applications," Computers *and Structures*, Vol. 79, No. 17, 2001, pp. 1541-1552.

Sarıdemir, M., (2009), "Predicting the compressive strength of mortars containing metakaolin by artificial neural networks and fuzzy logic," *Advances in Engineering Software*, Vol. 40, No. 9, pp. 920-927.

Sellevold, E., Bjøntegaard, Ø., Justnes, H. and Dahl, P., (1994), "High-performance concrete: early volume change and cracking tendency," *Proceedings of the International RILEM Symposium on Thermal Cracking at Early Ages*, Springenschmid R. (ed.), Munich, Germany, E. & F.N. Spon, London, pp. 229-236.

Shang, J., Ding, W., Rowe, R. and Josic, L., (2004), "Detecting heavy metal contamination in soil using complex permittivity and artificial neural networks," *Canadian Geotechnical Journal*, Vol. 41, No. 6, pp. 1054-1067.

Sivakumar, A. and Santhanam, M., (2006), "Experimental methodology to study plastic shrinkage cracks in high strength concrete," *Proceedings of International symposium: Measuring, monitoring and modeling concrete properties*, Konsta-Gdoutos (ed.), Springer Netherlands, Part 3, pp. 291-296.

Tazawa, E. and Miyazawa, S., (1993), "Autogenous shrinkage of concrete and its importance in concrete technology," *Proceedings of Fifth International Symposium on Creep and Shrinkage of Concrete*, Bažant Z. and Carol I. (eds.), RILEM, Barcelona, pp. 159-168.

Tazawa, E., Miyazawa, S. and Kasai, T., (1995), "Chemical shrinkage and autogenous shrinkage of hydrating cement paste," *Cement and Concrete Research*, Vol. 25, No. 2, pp. 288-292.

Tazawa, E. and Miyazawa, S., (1995), "Influence of cement and admixture on autogenous shrinkage of cement paste," *Cement and Concrete Research*, Vol. 25, No. 2, pp. 281-287.

Tazawa, E., Sato, R., Sakai, E. and Miyazawa, S., (2000), "Work of JCI committee on autogenous shrinkage" *Proceedings of international RILEM workshop: Shrinkage of concrete –Shrinkage 2000*, V. Baroghel-Bouny and P.-C. Aitcin (eds.), RILEM publications S.A.R.L., Paris, France, pp. 21-40.

Topçu, I and Sarıdemir, M., (2007), "Prediction of properties of waste AAC aggregate concrete using artificial neural networks," *Computational Materials Science*, Vol. 41, No. 1, pp. 117-125.

Topçu, I. and Sarıdemir, M., (2008), "Prediction of mechanical properties of recycled aggregate concretes containing silica fume using artificial neural networks and fuzzy logic," *Computational Materials Science*, Vol. 41, No. 1, pp. 74-82.

Toutanji, H., Delatte, N., Aggoun, S., Duval, R. and Danson, A., (2004), "Effect of supplementary cementitious materials on the compressive strength and durability

of short-term cured concrete," *Cement and Concrete Research*, Vol. 34, No. 2, pp. 311-319.

Vanikar, S., (2004), "The advances and barriers in application of new concrete technology," *Proceedings of the international workshop on sustainable development and concrete technology*, Kejin Wang (ed.), Beijing, China, pp. 25-33.

Venkiteela, G, Gregori, A., Sun, Z. and Shah, S., (2010), "Artificial neural network modeling of early-age dynamic young's modulus of normal concrete," *ACI Materials Journal*, Vol. 107, No. 3, pp. 282-290.

West, P., Brockett, P. and Golden, L., (1997), "A comparative analysis of neural networks and statistical methods for predicting consumer choice," *Marketing Science*, Vol. 16, No. 4, pp. 370-391.

Yang, Y., Sato, R. and Kawai, K., (2005), "Autogenous shrinkage of high-strength concrete containing silica fume under drying at early ages," *Cement and Concrete Research*, Vol. 35, No. 3, pp. 449-456.

Yeh, I-C., (2008), "Modeling slump of concrete with fly ash and superplasticizer," *Computers and Concrete*, Vol. 5, No. 6, pp. 559-572.

Yun, L., Seong, Y., Min, K. and Jin, K., (2006), "Evaluation of a basic creep model with respect to autogenous shrinkage," *Cement and Concrete Research*, Vol. 36, No. 7, pp. 1268-1278.

Zhang, M., Tam, C. and Leow, M., (2003), "Effect of water-to-cementitious materials ratio and silica fume on the autogenous shrinkage of concrete," *Cement and Concrete Research*, Vol. 33, No. 10, pp. 1687-1694.

CHAPTER ELEVEN

SUMMARY, CONCLUSIONS AND RECOMMENDATIONS

11.1.   SUMMARY AND CONCLUSIONS

Despite the current knowledge and specifications for the early-age shrinkage of concrete and its mitigation techniques, numerous early-age shrinkage cracking problems in various concrete structures have been reported, indicating the existence of high shrinkage. Yet, the issue of early-age shrinkage and how to mitigate it has not been fully resolved and there are clear gaps between theory, research and practice.

This dissertation attempted to overcome some of these gaps through providing a series of fundamental investigations related to volume changes in cementitious materials at early-age and strategies used to mitigate it, taking into consideration the ambient environmental conditions. Moreover, new strategies for producing concrete with lower shrinkage and cracking risk although, which is also more environmentally friendly, were proposed. These include the use of partially hydrated cementitious materials and wollastonite microfibers as partial replacement for cement.

At the start of this research, Chapter 2 provides a comprehensive review for the early-age properties of concrete. It was found that the reported research on the early-age properties and shrinkage of concrete considering the exposure environmental conditions is rather limited. The development of early-age shrinkage for cementitious materials can be particularly sensitive to exposure conditions in the field, including temperature and

relative humidity. Yet, existing research studies on early-age shrinkage had a limited scope and relied mostly on constant curing conditions. It is anticipated that if research on the early-age shrinkage of new generations of concrete (e.g. ultra-high performance concrete (UHPC)) continue using classical testing approaches, a similar situation to that of normal concrete would prevail in the near future; i.e. cracking, expensive rehabilitation and accusations of unfounded science. This will defeat the purpose of UHPC that has been introduced as an "ultimate" building material for the construction, strengthening and rehabilitation of bridges and other transportation infrastructure. Thus, this dissertation introduces an integrated testing approach that allows capturing the actual mechanisms governing shrinkage of structural elements and the role of shrinkage mitigation techniques under simulated field-like conditions.

Chapter 3 adopts a more fundamental approach based on the progress of hydration in an attempt to capture the effect of drying conditions on the autogenous shrinkage of ultra-high performance concrete (UHPC) at early-ages. UHPC specimens were exposed to different temperatures, namely, 10, 20 and 40°C under a relative humidity (RH) ranging from 40 to 80%. Results show that autogenous and drying shrinkage are dependent phenomena. Assuming the validity of the conventional superposition principle between drying and autogenous shrinkage led to overestimating the actual autogenous shrinkage under drying conditions; the level of overestimation increased with decreasing RH. Therefore, the behaviour of autogenous strains under sealed conditions will differ from that under drying conditions.

The findings from Chapter 3 motivated research on investigating the role and efficiency of different shrinkage mitigation techniques under field-like conditions. For

this purpose, new UHPC mixtures incorporating a shrinkage-reducing admixture (SRA) and a superabsorbent polymer (SAP) as shrinkage mitigation methods were also investigated in Chapter 4. Results show that the SRA and SAP effectiveness in reducing autogenous shrinkage under sealed conditions differ than that under drying conditions. Adding SRA effectively reduced drying strains, which are the dominant strains in UHPC specimens under low RH conditions. At higher RH conditions, SRA reduced autogenous strains, which in turn are the dominant strains in high RH environments. Under sealed conditions, early-age expansion of SAP mixtures had a significant effect in reducing the net strains. Under drying conditions, adding SAP resulted in higher drying strains, which disturbed the curing process and diminished the effect of SAP as a shrinkage mitigating method. Generally, adequate external curing is essential to mitigate early-age deformation in UHPC even when internal curing mechanisms are provided, since it guarantees a suitable environment for shrinkage mitigation methods to work properly.

Chapters 3 and 4 provided fundamental knowledge for the interaction mechanisms between drying and autogenous shrinkage under various curing conditions that simulate field-like conditions, including arid, normal and cold conditions. The second level of the fundamental investigation covered the behaviour under the effect of outdoor environmental conditions in which structures are subjected to moisture cycles and/or submerged conditions (simulating submerged parts of marine and offshore structures). This was done in chapter 5 by continuing research on the early-age shrinkage along with applying environmental loading, including drying/wetting cycles and submerged condition. Results show that applying the environmental load alters the shrinkage behavior of UHPC with and without shrinkage mitigation methods. It was

discovered that exposure to drying/wetting cycles and submerged conditions jeopardize the effectiveness of using SRA through a washing out mechanism. Using a combination of SRA and SAP creates a synergistic effect whereby the benefits of these shrinkage mitigation methods are optimized. This allows overcoming their individual deficiencies under different exposure conditions, which is promising for developing a new generation of high-performance shrinkage mitigation admixture with a dual effect. It is concluded that adequately considering in-situ conditions in testing protocols of UHPC should allow gaining a better understanding of shrinkage mitigation mechanisms and developing suitable performance specifications before a wide implementation of UHPC in full-scale field constructions.

Fundamental investigations described in this dissertation proved that relying on constant and standard curing conditions alone to evaluate the early-age shrinkage behaviour and efficiency of shrinkage mitigation techniques is risky since ignoring the realistic field-like exposure conditions may yield misleading conclusions. Obviously, concerted efforts from concrete researchers, professional organizations and standardization agencies are needed. In addition to the current standard tests, much research should be conducted on developing and standardizing new series of early-age shrinkage performance tests that concomitantly take other variables (temperature, relative humidity, wetting-drying, immersion, aggressive media, etc.) into consideration. These combined performance tests are better able to capture synergistic actions of chemical and physical mechanisms in concrete structures, which can occur under real field-like exposure conditions. Such an integrated testing approach is essential for the development of consistent performance-based standards and specifications for concrete. Also, it should

lead to producing more reliable data and knowledge on the early-age shrinkage behaviour of normal and emerging concrete types with inevitable improvements in the modelling of concrete structures.

The second core theme of this research is to achieve concrete with lower early-age shrinkage and reduced cracking risk, along with reducing its environmental and economic impact. UHPC has a high carbon-footprint and environmental impact due to its high cement content, leading to high energy consumption and CO_2 emissions associated with cement production. In chapter 6, a new concept for reducing early-age shrinkage in hardening cement-based materials is introduced. The concept consists of adding partially hydrated cementitious materials (PHCM) as a concrete admixture. Reusing disposal concretes in producing PHCM will yield significant economical and environmental benefits. Results showed a high potential for PHCM to reduce concrete shrinkage. The addition of PHCM provides hydration product micro-crystals and a pre-existing hydrated cement paste structure, which act as passive internal restraining clusters within the fresh concrete. Consequently, the developed passive restraining system resists bulk deformations and acts as a load bearing structure, thus leading to lower shrinkage. Hence, the concept of a self-restraining shrinkage system was proposed and its mechanism was demonstrated. In addition, results show that PHCM can potentially be used for several other purposes, including as an accelerator for concrete instead of chloride-based accelerators that induce a risk of corrosion in reinforced concrete. A dedicated experimental study was conducted to providence evidence for aforementioned observation (see Appendix B).

To complement the findings of Chapter 6, the efficiency of PHCM as a shrinkage reducing technique, when PHCM is used separately or combined with SRA and SAP, was investigated in Chapter 7. Results indicate that SRA was the most effective in reducing shrinkage; however, PHCM achieved excellent early-age shrinkage reduction when used alone or combined with other shrinkage mitigation techniques. PHCM mitigates undesirable behaviour induced by SRA and/or SAP. Combining PHCM and SRA mitigated the drawbacks of SRA including preventing delays in setting time and mitigating significant reductions in early-age compressive strength. The addition of PHCM to a mixture incorporating SAP improved the shrinkage behaviour and overcame the SAP drawbacks including higher mass loss and porosity, which led to preventing the reduction in early-age compressive strength induced by SAP.

Making concrete a more environmentally friendly material can be achieved in several ways. In Chapter 6 and 7, the production of low shrinkage environmentally friendly UHPC through using PHCM is proposed. This reduces the amount of portland cement in the mixture by partially replacing it with other suitable more environmentally friendly materials, thus reducing the amount of energy consumed and CO_2 emitted. In a low w/c concrete, a high fraction of cement particles remain un-hydrated due to limitation of the available water and space. In chapter 8, the potential for using wollastonite microfibers as partial replacement for cement by volume and it capability to reduce shrinkage and improve the cracking resistance was investigated.

Commercially available natural wollastonite microfibers were used at three concentrations (4, 8 and 12%) as partial substitution for cement by volume. Three microfiber sizes were used in this study: MF1 (length 152 μm, diameter 8 μm), MF2

(length 50 µm, diameter 5 µm), and MF3 (length 15 µm, diameter 3 µm). Results show that the early-age properties of UHPC mixtures incorporating wollastonite microfibers are highly affected by the microfiber aspect ratio and content, along with the hydration age of the cementitious matrix. Wollastonite microfibers were found to reduce shrinkage strains and increase the cracking resistance. It acts as an internal restraint for shrinkage, reinforces the microstructure at the micro-crack level and promotes pore discontinuity, thus leading to lower mass loss and less drying shrinkage. Incorporating wollastonite microfibers enhanced the early-age engineering properties of the UHPC matrix along with reducing its cement factor, which represents economic and environmental benefits.

The promising results of using wollastonite microfibers introduced in Chapter 8 encouraged the combination of wollastonite microfibers and SRA to optimize the gained benefit. In chapter 9, the effects of incorporating SRA and/or wollastonite microfibers on the early-age shrinkage behaviour and cracking potential of UHPC has been evaluated. Wollastonite microfibers were added at rates of 0, 4 and 12% as partial volume replacement for cement, while SRA was added at 1% and 2% by cement weight. Results show that the reinforcing effect induced by wollastonite microfibers mitigated the reduction in mechanical properties induced by SRA. Addition of wollastonite microfibers to SRA mixtures did not impart a significant change in the measured free shrinkage strain, while it enhanced the cracking resistance compared to that of mixtures incorporating SRA alone. Moreover, adding wollastonite microfibers promoted pore discontinuity, thus reducing the washing out of SRA from concrete under submerged conditions. Consequently, the efficiency of SRA in reducing shrinkage under submerged conditions was improved owing to the presence of wollastonite microfibers.

In Chapter 10, an original approach based on artificial neural networks (ANN) was proposed to assist engineers and quality control personnel in developing adaptable inference systems for the early-age shrinkage assessment of concrete. This is practically effective to select optimum concrete mixtures for specific exposure conditions. The ANN model inputs include the hydration age, water-to-cement ratio, total aggregate volume, cement content, curing temperature, and type and percentage of supplementary cementitious materials, while the autogenous shrinkage of concrete was the single model output. In such an ANN system, combining the effects of concrete mixture proportions and performance criteria with respect to a certain field-like exposure condition could simplify the decision-making process and improve the reliability of assessment.

The ANN model developed in Chapter 10 was trained using a newly assembled database. These data can be considered as an enhancement for the existed concrete shrinkage database, since it included testing results for modern concretes under various environmental conditions. The ANN model showed high capability to accurately predict the autogenous shrinkage behaviour under different exposure conditions and exhibited a good generalization capacity beyond the training stage as validated by results obtained on new testing data within the range of training database.

This model could be used in the design and prequalification stage of a construction project to reduce the need for exhaustive trial batches and experimental programs, thus facilitating the decision-making process. The developed ANN model is versatile and can be re-trained to encompass wider ranges of input variables, different mixture proportions, other environmental conditions, etc., when such data becomes available.

Among the model inputs, the w/c, superplasticizer content and curing temperature were selected due to limited and/or contradictory results about their effect on autogenous shrinkage. Thus, the generalization capabilities of the ANN model were used to resolve this issue and clarify the influences of these parameters on the early-age autogenous shrinkage development.

11.2.   RECOMMENDATIONS FOR FUTURE WORK

1. Based on the findings of the current thesis, it is suggested that other early-age properties of cement-based materials, such as their mechanical properties, be re-examined using an integrated testing approach in which chemical, physical and structural aspects are assessed under a field-like exposure. Such an approach can elucidate synergistic actions of multiple mechanisms and better capture performance risks of cement-based materials that might be overlooked by current single-parameter standard test methods.

2. On-site cracking of concrete is usually attributed to drying shrinkage and evaporation of water from the concrete surface. However, mechanisms and causes of cracking differ depending on the exposure conditions, type of the concrete element, etc. It is recommended that field tests be conducted to better quantify the actual source of cracking stresses and to quantify the benefits imparted by different shrinkage mitigation techniques.

3. Tests conducted under drying/wetting cycles and submerged conditions introduced in the current thesis used a single curing temperature and a regular water immerging

solution. Following a similar integrated testing approach, further research is needed on UHPC using different curing temperatures and more aggressive immersing solutions.

4. Given further research, the integrated testing procedures developed in this dissertation can be improved and refined. Investigations of reproducibility, inter- and multi-laboratory errors should also be conducted for such combined performance tests.

5. To develop shrinkage performance-based standards and specifications for concrete, there is an essential need to improve the shrinkage measuring techniques. Moreover, standardizing multi-factor performance tests could capture synergistic shrinkage mechanisms that can not be identified by current testing procedures which consider only one single factor at a time. Thus, it is recommended that standardization agencies such as CSA and ASTM motivate research programs in this theme in the near future.

6. It was shown that the PHCM can be a very effective technique for reducing concrete shrinkage. However, to become a more versatile technique, further research and development are required. This includes: (i) investigating the effectiveness of the PHCM technique with different mixture proportions including various types of binders, w/c values and chemical admixtures; (ii) investigating the effect of adding PHCM as a paste without aggregate, which should reduce the volume of the added PHCM, making it a more practical tool for precast-plants, (iii) developing a mixture design procedure to include the PHCM, and (iv) investigating the long-term properties of concrete incorporating the PHCM.

7. The feasibility of implementing wollastonite microfibers in UHPC to resist shrinkage cracking has been proven in the current dissertation. However, to become an effective and applicable technique, further research and development are required. This includes investigating: (i) the effectiveness of the wollastonite microfibers in UHPC incorporating steel microfibers; (ii) the hybrid effect of adding wollastonite micro and microfibers. (iii) and the long-term properties of concrete incorporating wollastonite microfibers.

8. This research demonstrated the promising application of artificial intelligence in modeling the complex early-age shrinkage behaviour of concrete. Such a versatile modeling tool should be established based on reliable databases derived from integrated performance tests. Indeed, more information on the early-age behaviour of concrete with various materials proportions combined with environmental conditions and/or structural loading is still needed. Once this information becomes available, the artificial intelligence inference system can be further developed and be commercially used to facilitate the decision-making process in the design/prequalification stage of construction projects.
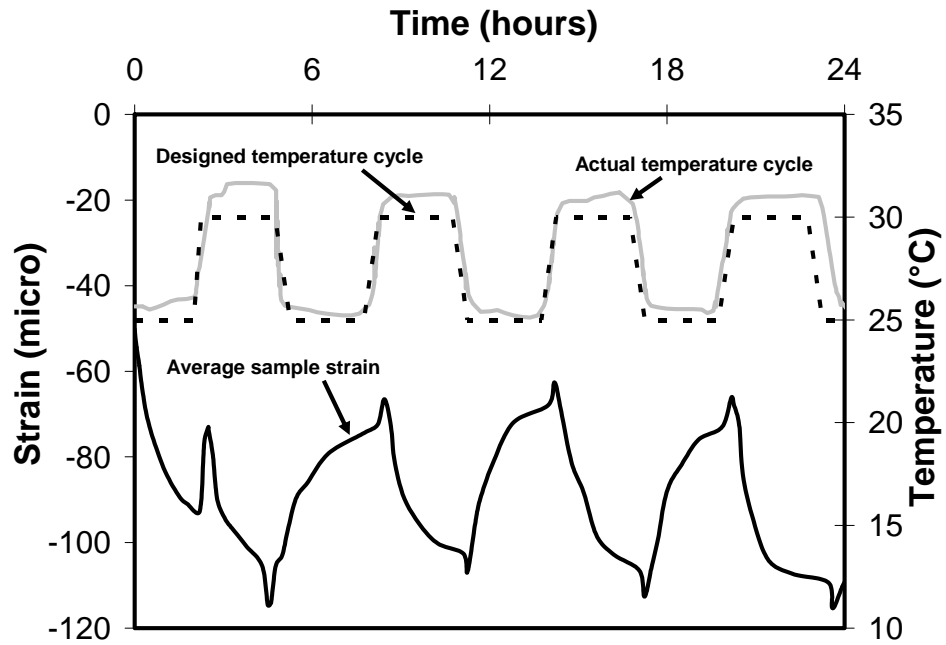
Figure A-1: Detailed temperature and total strain measured in concrete samples over 24 hours.
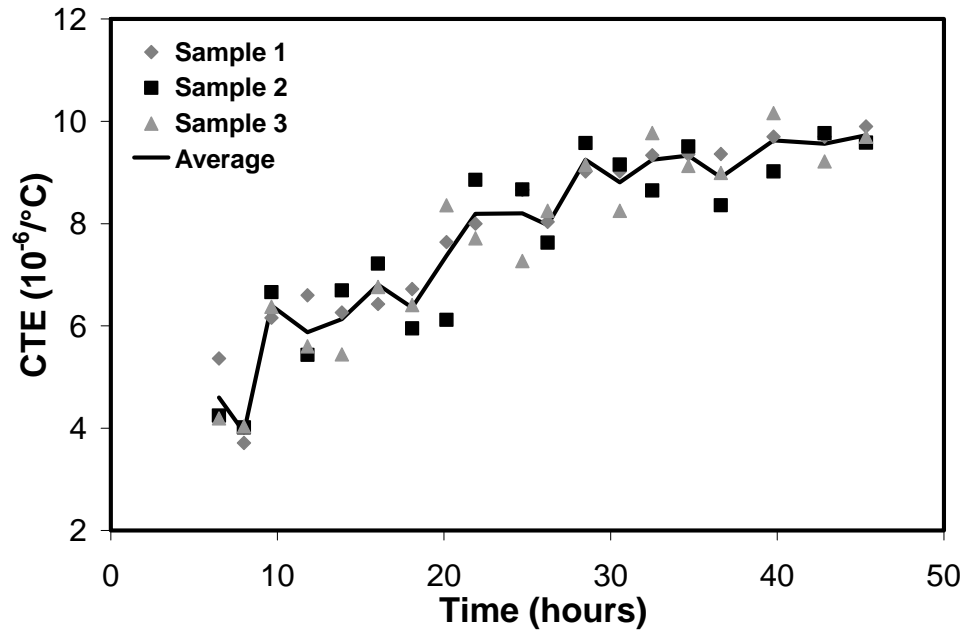
Figure A-2: Time-evolution of coefficient of thermal expansion.

SELF-ACCELERATED CONCRETE USING PARTIALLY HYDRATED CEMENTITIOUS MATERIALS

B.1.   INTRODUCTION

This study pioneers the concept of self-accelerated concrete. The effect of adding partially hydrated cementitious materials (premade or from returned/unused concrete) on the setting and hardening process of concrete cured at various temperatures was investigated. The partially hydrated cementitious materials (*PHCM*) were added at rates of 25, 33 and 50% of the overall batch weight. Similar mixtures incorporating chloride- (*CA*) and non-chloride- (*NCA*) based accelerating admixtures were also tested for comparison. The results indicate that the added *PHCM* alert the hydration kinetics and act as a setting and hardening accelerator. Mixtures incorporating *PHCM* showed comparable to and/or higher early-age compressive strength than that of both the control and mixtures incorporating accelerating admixtures. Therefore, using *PHCM* paves the way for self-accelerated concrete, without the need for accelerating admixtures, providing a safe and cost effective method for precast and cast in place concrete. Using left-over and unused concrete in this process enhances the sustainability of concrete and minimizes disposal in ready mixed concrete operations.

B.2.   EXPERIMENTAL PROGRAM

This experimental program aims to produce a self-accelerated concrete without need for accelerating admixtures. This Appendix was devoted to validating the addition of *PHCM* as an accelerating technique and to evaluating its efficiency compared to that of different accelerating admixtures. The characteristics of the tested mixtures are shown in **Tables B-1**.

Table B-1 Tested mixtures

Mixture	Accelerating method	PHCM (% of the batch weight)	Admixture Dosage (% of cement mass)
MC	----	0.0	----
MP1		25.0	----
MP2	PHCM	33.0	----
MP3		50.0	----
MAC1	Chloride	----	2.0
MAC2	Admixture	----	4.0
MANC1	Non-Chloride	----	1.5
MANC2	Admixture	----	3.0

B.3.   RESULTS AND DISCUSSION

B.3.1.   Setting Time and Compressive Strength

B.3.1.1 PHCM technique

Regardless of the added amount of PHCM, the PHCM technique significantly enhanced the development of early-age compressive strength. All PHCM mixtures consistently produced higher early-age compressive strengths compared to that of *MC* cured at 10 and 20°C, as shown in **Fig. B-1(a,b)**. The increase in compressive strength was directly proportional to the added amount of *PHCM*. For instance, the 24 hrs compressive strength at 10 and 20°C increased by 70% and 30% for *MP1*, 85% and 40% for *MP2* and

by 140% and 45% for *MP3* of their respective *MC* values. At 10°C, *PHCM* addition

induced higher increase in compressive strength compared to that at 20°C. This is likely

due to the acceleration effect induced by *PHCM* addition. Hence, the slow rate of

hydration and strength development at the low temperature of 10°C were compensated

for, leading to more hydration products and stronger microstructure (ACI Committee E-

701, 2001). Compared with the *MC* setting time, the *PHCM* technique also reduced the

setting time significantly as shown in **Table B-2**. These results demonstrate that the

PHCM technique can be considered as an effective setting and hardening accelerating

method.
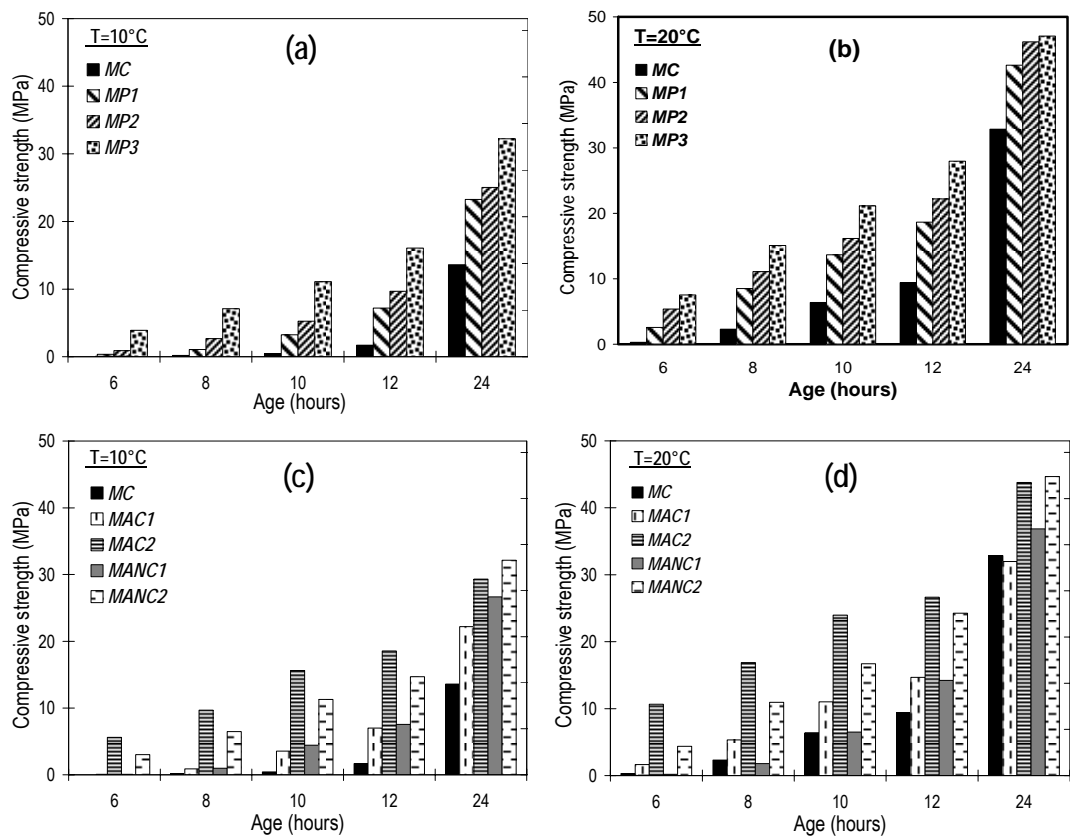
**Figure B-1: Early-age compressive strength of UHPC mixtures incorporating
PHCM cured at a) 10°C and b) 20°C and UHPC mixtures incorporating *CA* and
NCA cured at c) 10°C and d) 20°C.** [Maximum COV (10°C, 20°C): *MC* (0.9%, 2.0%),
MP1 (1.9%, 4.8%), *MP2* (2.3%, 5.6%), *MP3* (2.7%, 2.2%), *MAC1* (1.7%, 0.9%), *MAC2*
(4.2%, 4.7%), *MANC1* (4.9%, 0.9%), *MANC2* (3.8%, 6.8%)].
Table B-2: Initial and final setting times for different mixtures.

Mixture	Temperature °C			
	10		20	
	Setting time (min)			
	Initial	Final	Initial	Final
MC	510	715	460	520
MP1	450	495	340	420
MP2	405	465	220	270
MP3	245	280	170	210
MAC1	425	475	240	285
MAC2	160	205	150	190
MANC1	475	540	350	395
MANC2	240	300	260	295

The improvement in compressive strength and reduction in setting time induced by *PHCM* addition cannot be solely attributed to the effect of the older material. For instance, for mixture *MP3* after 6 hours of curing at 10°C, 50% of the mixed cementitious material is 6 hours older. Hence, 50% of the cementitious material has an age of 12 hours, while the other 50% has an age of 6 hours. Summing up 50% of the *MC* compressive strength at age 6 hours (0.0 MPa) and 12 hours (1.68 MPa) results in a compressive strength of about (0.84 MPa), which is much lower than that of *MP3* at 6 hours (3.90 MPa). On the other hand, the setting time of the normal paste starts at about 510 min at 10°C, hence, adding 50% of 6-hour older paste material should theoretically reduce the setting to about 150 min. However, the setting time was only reduced to about 245 min (which represents about 52% reduction with respect to the *MC* value). The longer setting time for *MP3* than the theoretical value (150 min) can be attributed to the effect of remixing on the already developed microstructure. Remixing breaks down the formed connections between hydration products (Lea, 1988), hence, the *MP3* paste will initially have a lower stiffness than that of the paste mixed 6 hours earlier.

B.3.1.2 Chloride-based accelerating admixture (CA)

The compressive strength results of mixtures incorporating different dosages of *CA* are shown in **Fig. B-1(c,d)**. The higher the dosage, the higher the rate of hydration reactions, and consequently the higher the early-age compressive strength achieved, which is in agreement with previous results (Cheeseman and Asavapisit, 1999). As shown in **Fig. B-1(c,d)**, *MAC2* exhibited about six times higher early-age compressive strength compared to that of *MAC1* after 6 hrs from mixing, regardless of the curing temperature. In addition, the *CA* improved the compressive strength more effectively at 10°C compared to that at 20°C. This is probably due to the higher heat liberated from the accelerated hydration reactions, offsetting the prolonged strength gain induced by the low curing temperature (Shideler, 1952). Adding the *CA* reduced the initial and final setting times significantly (**Table B-2**). For instance, *MAC2* exhibited initial and final setting times at 10 and 20°C more than 60% shorter than that of *MC*.

B.3.1.3 Non-chloride based accelerating admixture (NCA)

The compressive strength results for mixtures incorporating different dosages of the *NCA* are shown in **Fig. B-1(c,d)**. Mixture *MANC1* did not show a significant improvement in very early-age compressive strength. During the first 10 hrs, *MANC1* showed a lower compressive strength than that of *MC* at 20°C. However, *MANC1* exhibited initial and final setting times about 24% shorter than that of *MC*. *MANC1* showed a different strength gain rate at 10°C compared to that at 20°C, with a significant increase in compressive strength (about double that of *MC*). On the other hand, *MANC2* had higher early compressive strength and shorter setting time compared to that of *MC*. For instance, *MANC2* exhibited about 136% and 36% higher compressive strength than to that of *MC*

after 24 hrs at 10 and 20°C, respectively. Hence, the *NCA* can generally be considered as a setting accelerator, confirming results reported by others (Chikh *et al*., 2008), while its effect on early-age strength gain can vary depending on the added dosage.

B.3.1.4 Comparison between different acceleration techniques

To evaluate the efficiency of the *PHCM* accelerating technique versus accelerating admixtures, the differences between the compressive strength gain achieved by mixtures incorporating *PHCM* and that incorporating accelerating admixtures were calculated, as shown in **Fig. B-2**. Generally, the *PHCM* mixtures exhibited higher compressive strength compared to that of **MAC1** and **MANC1**. For instance, the differences in early-age compressive strength between *PHCM* mixtures and **MAC1**, over the investigated period, ranged respectively from -0.6 to +10 MPa at 10°C, and from +1 to +15 MPa at 20°C, respectively. A similar trend was observed between *PHCM* mixtures and **MANC1**, as shown in **Fig. B-2(c)**.

On the other hand, mixtures incorporating *PHCM* showed lower early-age compressive strength compared to that of **MAC2** mixtures. The gap in compressive strength decreased with increasing the added amount of *PHCM*. However, the mixture *MP3* incorporating 50% *PHCM* showed early-age compressive strength comparable to and/or higher than that of **MANC2** at 10 and 20°C over the investigated period. Moreover, *MP3* exhibited a compressive strength at the end of the investigated period higher than that of **MAC2** as shown in **Fig. B-2(b)**. In simple terms, it takes the maximum dosage of *CA* to compete with the acceleration induced by the *PHCM* method.
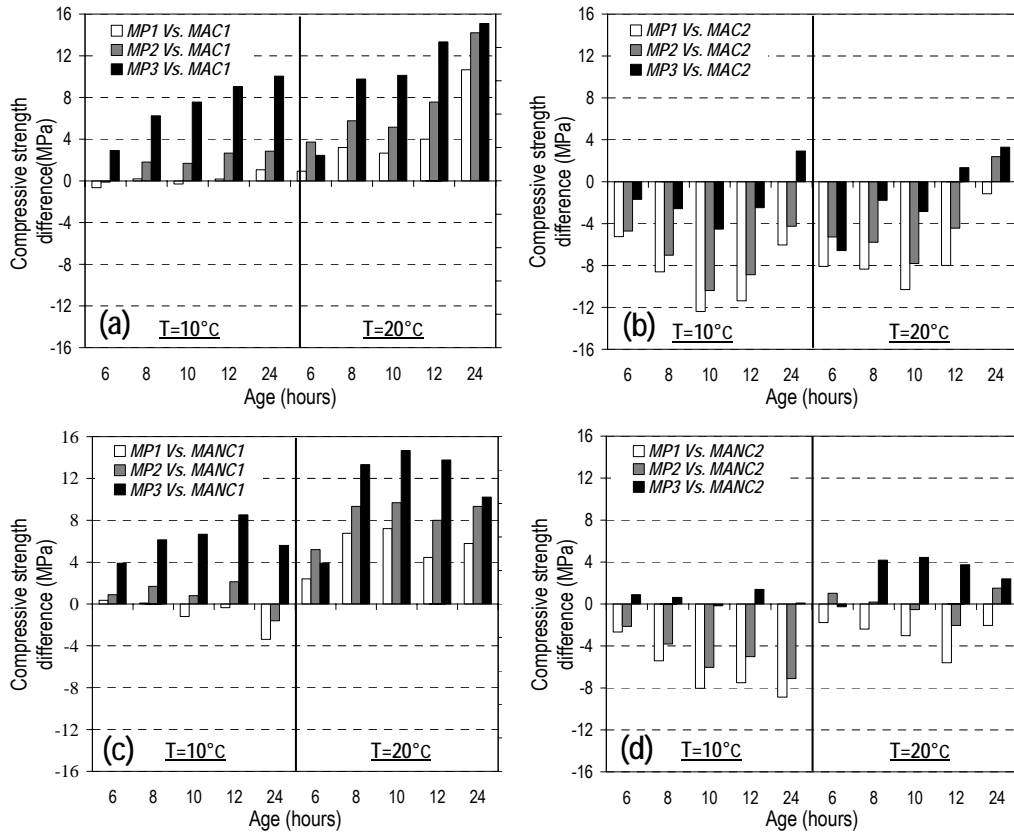
Figure B-2: Compressive strength difference between UHPC mixtures incorporating *PHCM* and that incorporating *CA* [a) *MAC1*, and b) *MAC2*] and *NCA* [c) *MANC1*, and d) *MANC2*] at different curing temperatures.

Figure B-3 shows the compressive strength results for different mixtures at age 28-days. Generally, all mixtures incorporating different acceleration techniques exhibited 28-days compressive strength comparable to that of *MC*, regardless of the curing temperature. For instance, the difference in 28-days strength between the control mixture without accelerating technique and mixtures with accelerating techniques at 10°C and 20°C, ranged from -1% to +6.5% and from -4% to +2.5% with respect to the *MC* value, respectively. This slight variation in the 28-days compressive strength can be attributed to the fact that at low w/c ratio, the hydration progress is mainly controlled by the availability of sufficient space for hydration products to form (Lea, 1988).
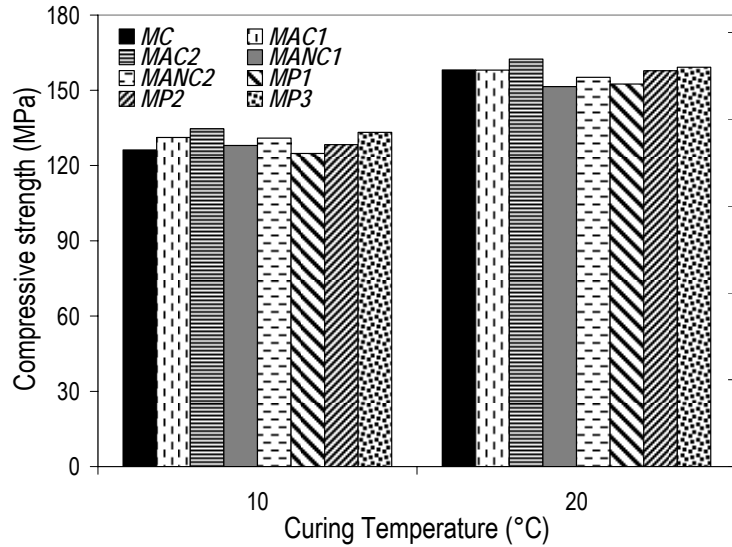
Figure B-3: 28 days compressive strength of UHPC mixtures incorporating *PHCM* , *CA* and *NCA* cured at 10°C and 20°C.

The effectiveness of the *PHCM* technique as a setting accelerator increased with increasing the added amount of *PHCM*, as shown in **Fig. B-4**. The lower the temperature, the higher the relative acceleration induced by the *PHCM* technique. Mixtures incorporating *PHCM* achieved longer setting time compared to that of ***MAC2*** (see **Fig. B-4(b)**). However, ***MP2*** and ***MP3*** exhibited similar and/or shorter setting time compared to ***MAC1*** (see **Fig. B-4(a)**). On the other hand, *PHCM* mixtures exhibited shorter setting time compared to that of ***MANC1***, while longer compared to that of ***MANC2,*** except for ***MP3*** (see **Fig. B-4(c,d)**).
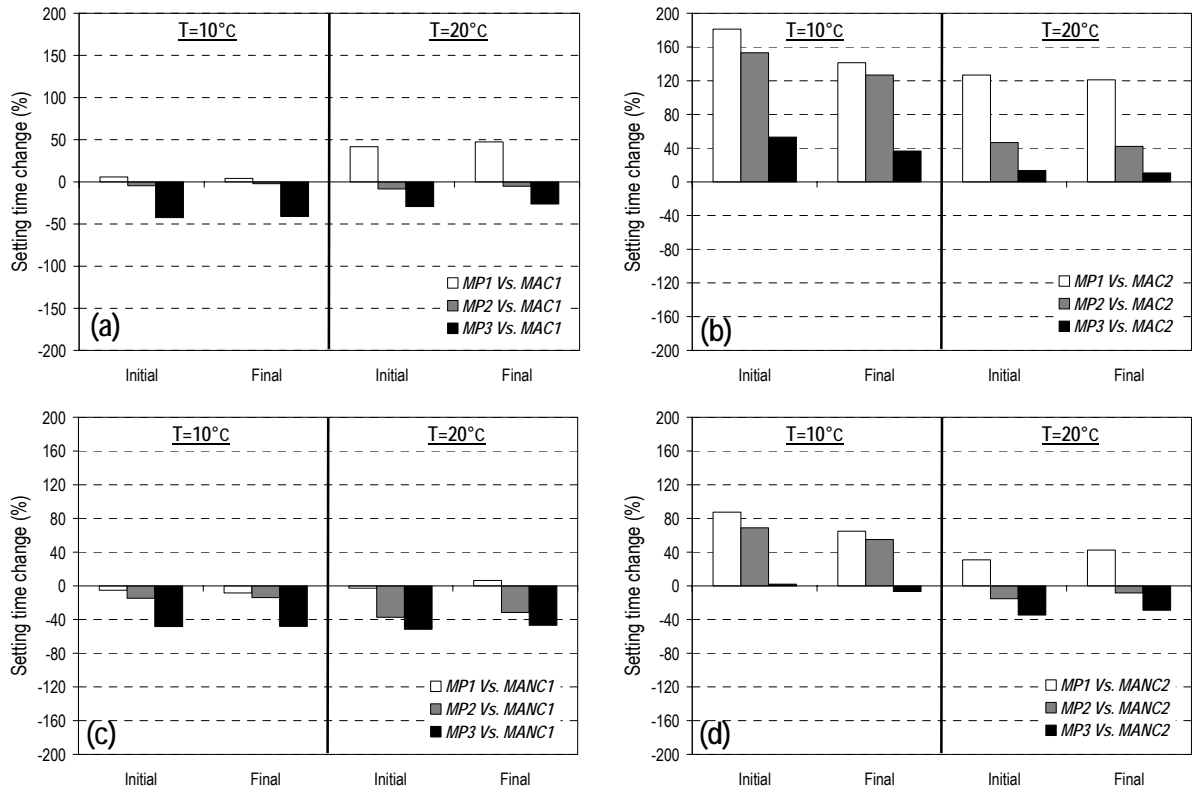
Figure B-4: Change in initial and final setting times for UHPC mixtures incorporating *PHCM* and that incorporating *CA* [a) *MAC1*, and b) *MAC2*] and *NCA* [c) *MANC1*, and d) *MANC2*] at different curing temperatures.

B.3.2. Degree of Hydration

Early-age strength development of concrete mixtures highly relies on the degree of hydration achieved (Xiao and Li, 2008). The correlation between the compressive strength and degree of hydration (represented by the amount of BW) is plotted in **Fig. B-5**. It can be observed that the relationship exhibits a linear trend for mixtures incorporating *PHCM* and *CA* (with R^2 = 0.97 and 0.94, respectively). Conversely, combining data points for *MANC1* and *MANC2* mixtures indicates a very poor linear trend (R^2 = 0.67), while separating these two sets of data leads to a linear trend with R^2 = 0.97 and 0.95 for *MANC1* and *MANC2*, respectively, as shown in the upper left corner of

Fig. B-5. This linear relationship between compressive strength and degree of hydration has been reported in previous works (Xiao and Li, 2008, Powers, 1948). It indicates a proportional relationship between the added dosages of *PHCM* and *CA* and the development of hydration and strength. Conversely, the *NCA* behaves differently from one dosage to another, in compliance with previous studies (Rear and Chin, 1990).
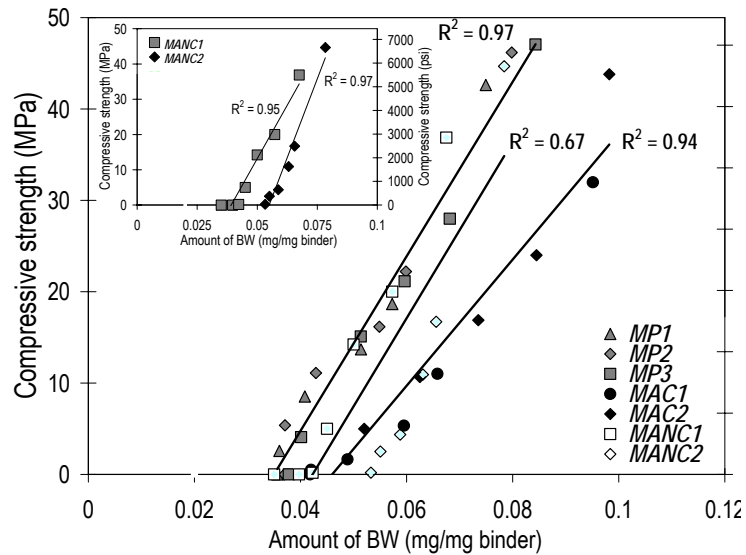
Figure B-5: Relation between degree of hydration (amount of BW) and compressive strength development for the tested mixtures.

B.3.3. Heat of Hydration

Mixtures incorporating *PHCM* had similar temperature evolution curves that differed from that of the control *MC*, as shown in **Fig. B-6(a)**, indicating a variation in the hydration kinetics. Initially, the temperature for *PHCM* mixtures rised rapidly after casting the specimen in the semi-adiabatic cell (20 min from water addition) and did not exhibit an induction period (period in which the rate of hydration reactions slows down significantly (Ramachandran et al., 2002). Temperature rised up until reaching a peak of about 42°C after about 7.5 hrs for *MP3*, 38°C and 39°C after about 8 hrs for *MP1* and

MP2, respectively. On the other hand, *MC* hydration exhibited induction and acceleration periods as shown in **Fig. B-6(a)**. The acceleration period for *MC* was initiated at about 6 hrs later than that of *PHCM* mixtures and had a temperature peak of about 36°C at around 12 hrs from water addition. Hence, the *PHCM* technique effectively diminished the induction period, leading to a continuous progress of hydration reactions and consequently shorter setting time and higher early-age compressive strength as discussed earlier.

Figure B-6: Heat of hydration for UHPC mixtures incorporating a) *PHCM***, b)** *CA***, and c)** *NCA***.**

The general profile of temperature evolution curves for mixtures incorporating *CA* was similar to that of *MC* but with different rates. In general, as the dosage of the

admixture increased, hydration reactions were accelerated. This is apparent in the heat of hydration curves in **Fig. B-6(b)**. With increased admixture dosage, the curves shifted upward and to the left, which is in agreement with previous work (Cheeseman and Asavapisit, 1999, Ramachandran et al., 2002).
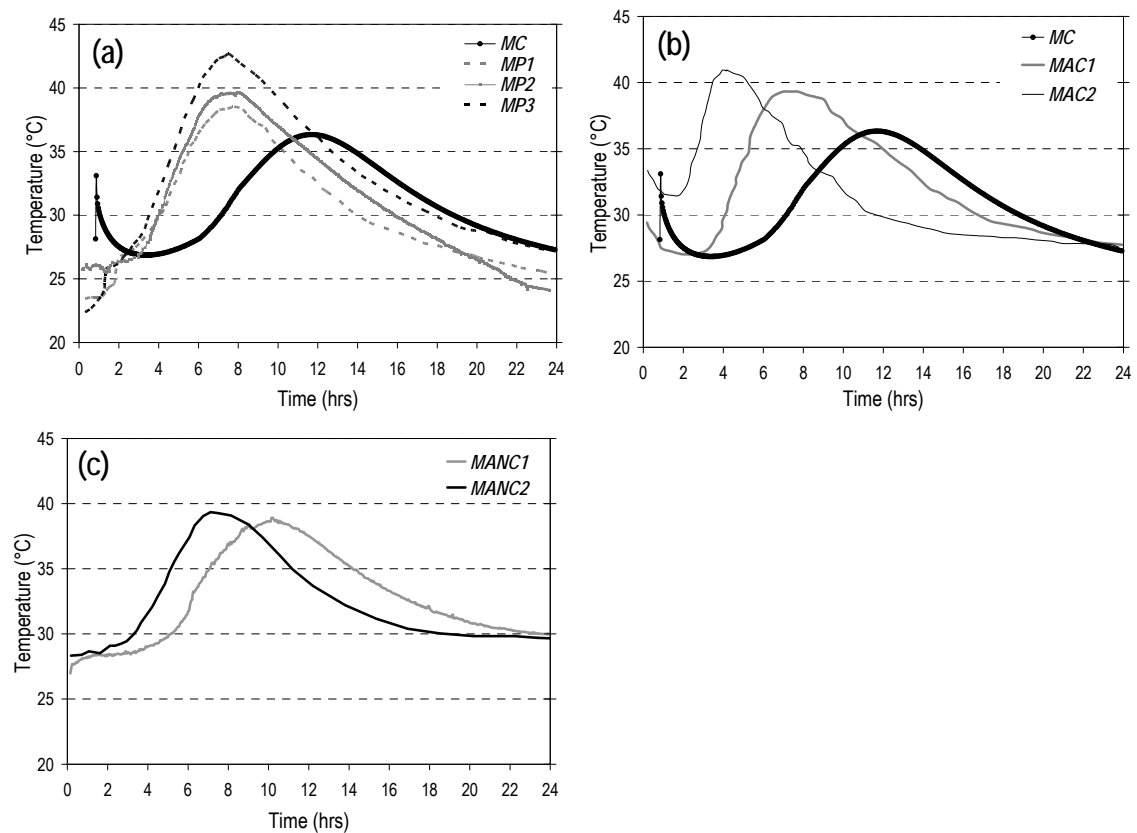
For mixtures incorporating the *NCA*, a similar trend of temperature evolution curves to that of the *PHCM* mixture was observed, as shown in **Fig. B-6(c)**. The dormant period was overlapped by the acceleration period, in agreement with previous results (Hill and Daughert, 1996). However, mixtures incorporating the *NCA* showed lower temperature peaks compared to that of the *PHCM* mixtures. This suggests higher reactivity at early-age for the *PHCM* mixtures with respect to that incorporating the *NCA*.

B.3.4.   Shrinkage

Shrinkage results for mixtures incorporating *PHCM* and accelerating admixtures are shown in **Fig. B-7**. All mixtures incorporating accelerating admixtures showed a significant increase in the measured shrinkage (about 31, 10, 12 and 23% for *MAC1*, *MAC2*, *MANC1* and *MANC2*, respectively), while no significant mass change was measured, which is in agreement with previous works (Shideler, 1952, Rixom, M.R. and Mailvaganam, 1999) (**Fig. B-8**). Conversely, *PHCM* mixtures showed lower shrinkage and mass loss compared to that of the control *MC* (**Figs. B-7 and B-8**). This can be attributed to the fact that the measured shrinkage includes drying and autogenous shrinkage (thermal deformation can be ignored due to the small cross-section of the samples (Baroghel-Bouny *et al.*, 2006). Autogenous shrinkage is strongly related to hydration reactions in which water is consumed, leading to internal self-desiccation

(without external water loss) (Powers, 1948). For low w/c mixtures, the amount of autogenous shrinkage can be comparable to that of drying shrinkage (Tazawa, E. and Miyazawa, 1999). Using accelerating admixtures increases the rate of hydration and consequently refines and changes the size distribution of capillary pores, which in turn eliminates water loss (ACI Committee 301, 2005). Conversely, the accelerated hydration reactions and finer porosity will increase self-desiccation, and consequently increase the autogenous shrinkage contribution to the measured shrinkage.
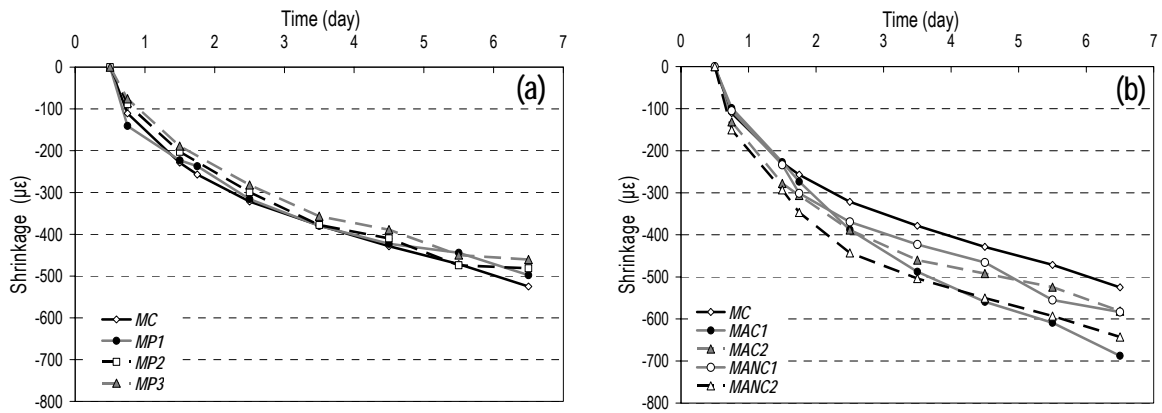
Figure B-7: Drying shrinkage for a) *PHCM* **mixtures and b) mixtures incorporating accelerating admixtures** [Maximum **COV**: *MC* (4.5%), *MAC1* (4.8%), *MAC2* (1.9%), *MANC1* (5.9%), *MANC2* (4.3%), *MP1* (3.1%), *MP2* (1.5%), *MP3* (4.6%)].
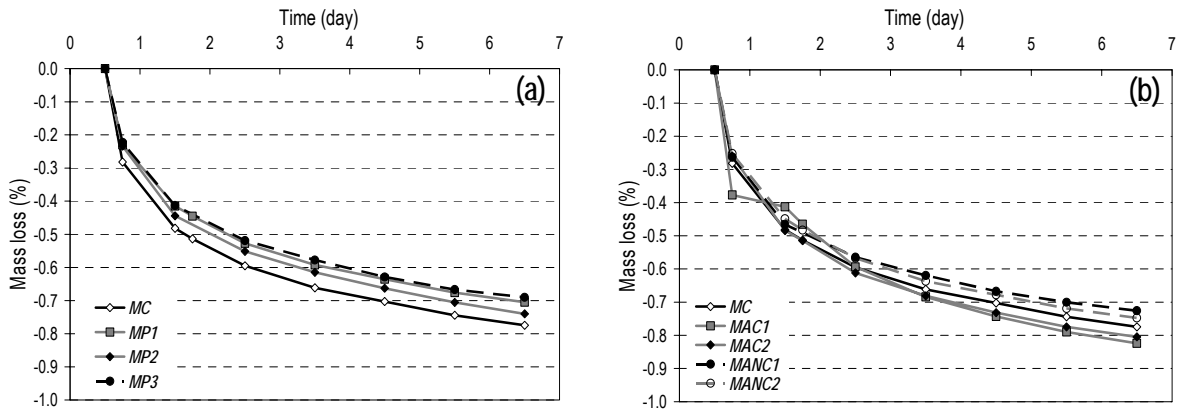
Figure B-8: Mass loss for a) *PHCM* **mixtures, and b) mixtures incorporating accelerating admixtures.**

In *PHCM* mixtures, a similar process takes place; however, the added *PHCM* can act as a passive internal restraint, thus reducing the amount of deformation developed, along with accelerating the hydration reactions. At the micro-level, the added *PHCM* provides CH crystals that can act as a passive restraint and reduce the measured physical shrinkage (Jensen and Hansen, 1996). The hypothesis that CH crystals can provide restraint was proposed by (Bentz and Jensen, 2004) based on results reported in (Carde and Francois, 1997, Powers, 1962) which indicate a significant effect of leaching and dissolution of CH crystals on mechanical and deformation properties. This explanation is consistent with autogenous shrinkage results shown in **Fig. B-9**, and with DSC results presented below. Increasing the amount of added *PHCM* increased the passive internal restrain and consequently reduced the amount of autogenous shrinkage. Accelerating admixtures initially increase the rate of autogenous shrinkage, as a result of increasing the rate of hydration, until reaching adequate stiffness to withstand shrinkage as reported by (Anna *et al*., 1955).
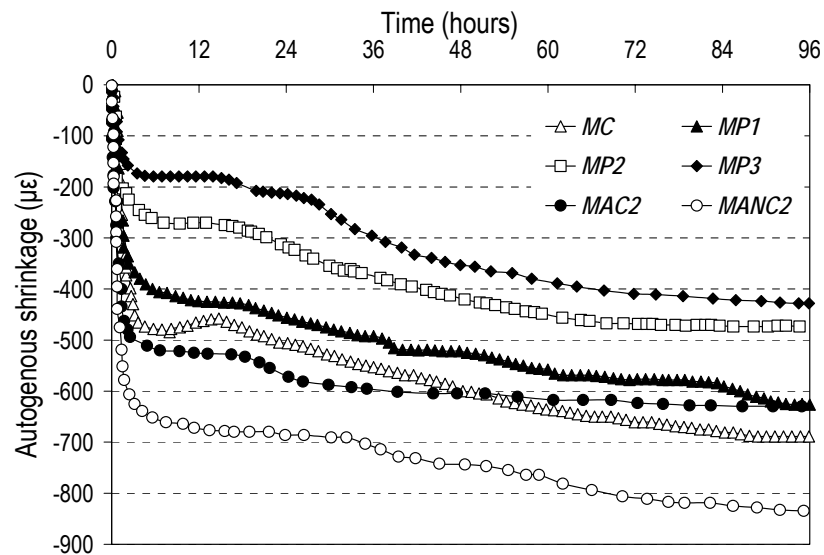
Figure B-9: Autogenous shrinkage for a) *PHCM* mixtures and b) mixtures incorporating accelerating admixtures.

Furthermore, the evaporable water content in *PHCM* mixtures is probably less than that in the control **MC** and mixtures incorporating accelerating admixtures at the onset of drying. This can be explained as follows: all mixtures initially have the same amount of mixing water, however, the added mixing water before casting the specimens for *PHCM* mixtures (i.e. mixing water at the second stage) is less than that of the ordinary mixture. For instance, for the mixture **MP3**, half of the mixing water is added in the first mixing stage, while the other half is added at the second stage before casting the shrinkage specimens. Hence, *PHCM* mixtures possess lower evaporable water and consequently lower mass loss as shown in **Fig. B-8**.

B.4.   CONCLUSIONS

The main conclusions that can be drawn from this experimental investigation are the following:

1) The addition of *PHCM* had a strong acceleration effect on the early-age setting and hardening process for concrete, hence, it can be considered as a setting and hardening accelerator.

2) Mixtures incorporating *PHCM* showed comparable and/or better early-age compressive strength results than that of the control and mixtures incorporating accelerating admixtures at cold (10°) and normal (20°C) temperatures.

3) The higher the added portion of *PHCM*, the higher was the acceleration effect.

4) Mixtures incorporating *PHCM* achieved a high potential for reducing autogenous shrinkage through providing internal passive restraint, compared to mixtures

incorporating accelerating admixtures. This is a clear advantage compared to conventional accelerating admixtures, which generally increase shrinkage strains.

5) The addition of *PHCM* mainly affects the nucleation and renewal process of CSH.

6) The *PHCM* technique pioneers the concept of self-accelerated concrete, which has a paramount potential, particularly in the pre-cast industry. It resolves the two major drawbacks associated with chloride-based accelerators; corrosion related to chlorides and increased shrinkage.

7) Concrete sustainability can be enhanced through using left-over and returned concrete in producing self-accelerated concrete, thus preventing wastage and disposal costs.

B.5.   REFERENCES

ACI Committee E-701, (2001) Cementitious Materials for Concrete, ACI Education Bulletin E3-01, American Concrete Institute, Farmington Hills, Michigan, 25 p.

ACI Committee 301, (2005) Specifications for Structural Concrete (ACI 301-05)," American Concrete Institute, Farmington Hills, MI, 49 p.

Anna, K., Leivo, M. and Sipari, P., (1995), "Experimental study on the basic phenomena of shrinkage and cracking of fresh mortar," *Cement and Concrete Research*, Vol. 25, No. 8, pp. 1747-1754.

Baroghel-Bouny, V., Mounanga, P., Khelidj, A., Loukili, A. and Rafaï, N., (2006), "Autogenous deformations of cement pastes: Part II. W/C effects, micro–macro correlations, and threshold values," *Cement and Concrete Research*, Vol. 36, No. 1, pp. 123-136.

Bentz, D.P. and Jensen, O.M., (2004), "Mitigation strategies for autogenous shrinkage cracking," *Cement and Concrete Composites*, V. 26, No. 6, pp. 677-685.

Carde, C. and Francois, F., (1997), "Effect of the leaching of calcium hydroxide from cement paste on mechanical and physical properties," *Cement and Concrete Research*, Vol. 27, No. 4, pp. 539-550.

Cheeseman, C.R. and Asavapisit, S., (1999), "Effect of calcium chloride on the hydration and leaching of lead-retarded cement," *Cement and Concrete Research*, Vol. 29, No. 6, pp. 885-892.

Chikh, N., Cheikh-Zouaoui, M., Aggoun, S. and Duval, R., (2008), "Effects of calcium nitrate and triisopropanolamine on the setting and strength evolution of Portland cement pastes," *Materials and Structures*, Vol. 41, No. 1, pp. 31-36.

Hill, R. and Daughert, K., (1996), "The interaction of calcium nitrate and a class C fly ash during hydration," *Cement and Concrete Research*, V. 26, No. 7, pp. 1131-1143.

Jensen, O.M. and Hansen, P.F., (1996), "Autogenous deformation and change of relative humidity in silica fume modified cement paste," *ACI Materials Journal*, Vol. 93, No. 6, 1996, pp. 539-543.

Lea, F.M., (1988). Lea's Chemistry of Cement and Concrete, 4th Edition, (ed.) P.C. Hewlett, J. Wiley, New York, 1053 p.

Powers, T.C. and Brownyard, T.L., (1948), "Studies of the physical properties of hardened portland cement paste," Bulletin No. 22., Research Laboratories of the Portland Cement Association. Reprinted from Journal of the American Concrete Institute, October 1946–April 1947, Proceedings 43, Detroit, pp. 971-992.

Powers, T.C., (1962), "A hypothesis on carbonation shrinkage," *Journal of the Portland Cement Association Research & Development Laboratories*, Vol. 4, No. 2, 1962, pp. 40-50.

Ramachandran, V.S., Haber, R.M., Beaudoin, J.J. and Delgado, A.H., (2002). Handbook of Thermal Analysis of Construction Materials, Noyes & William Andrew Publishing, Norwich, 655 p.

Rear, K. and Chin, D. (1990), "Non-chloride accelerating admixtures for early compressive strength," *Concrete International*, Vol. 12, No. 10, pp. 55-58.

Rixom, M.R. and Mailvaganam, N.P., Chemical Admixtures for Concrete, 3rd Edition, Brunner-Routledge, New York, 1999, 431 p.

Shideler, J.J., (1952), "Calcium cholride in concrete," ACI Materials Journal, Vol. 48, No. 3, pp. 537-559.

Tazawa, E. and Miyazawa, S., (1999), "Effect of constituents and curing condition on autogenous shrinkage of concrete," In: Autogenous Shrinkage of Concrete: Proceedings of the International Workshop, (ed.) Eiichi Tazawa, Taylor & Francis, pp. 269-280.

Xiao, L. and Li, Z., (2008), "Early-age hydration of fresh concrete monitored by non-contact electrical resistivity measurement," *Cement and Concrete Research*, Vol. 38, No. 3, pp. 312-319.

APPENDIX C

Table C -1*:* Sample for data used in ANN Model

Ref.	W/C	A/C	C.C.	SF	FA	HRWRA	Temp.	Age	Shrinkage strain
	-----	----	Kg	(%)*	(%)*	(%)*	(°C)	(Hours)	(μ m/m)
[3]	0.28	2.82	576	10	0	1.8	20	5.5	-17.4334
	0.28	2.82	576	10	0	1.8	20	6	-153.995
	0.28	2.82	576	10	0	1.8	20	7	-161.743
	0.28	2.82	576	10	0	1.8	20	8	-167.554
	0.28	2.82	576	10	0	1.8	20	9	-175.303
	0.28	2.82	576	10	0	1.8	20	10	-178.208
	0.28	2.82	576	10	0	1.8	20	11	-183.051
	0.4	4.14	424	10	0	1.8	20	11	-107.506
	0.4	4.14	424	10	0	1.8	20	12	-106.538
	0.4	4.14	424	10	0	1.8	20	13	-107.506
	0.4	4.14	424	10	0	1.8	20	14	-106.538
	0.4	4.14	424	10	0	1.8	20	15.574	-104.977
	0.5	5.36	340	10	0	1.4	20	12	-84.2615
	0.5	5.36	340	10	0	1.4	20	13	-84.2615
	0.5	5.36	340	10	0	1.4	20	14	-84.2615
	0.5	5.36	340	10	0	1.4	20	15	-87.1671
	0.5	5.36	340	10	0	1.4	20	15.5185	-88.4956
	0.5	5.36	340	10	0	1.4	20	17	-88.4956
	0.5	5.36	340	10	0	1.4	20	18.4815	-90.2655
	0.5	5.36	340	10	0	1.4	20	30.037	-99.115
[4]	0.22	2.036	750	0	0	1.4	20	1.27434	-20.9129
	0.22	2.036	750	0	0	1.4	20	2.23009	-28.7028
	0.22	2.036	750	0	0	1.4	20	3.13274	-60.1828
	0.22	2.036	750	0	0	1.4	20	3.66372	-96.9667
	0.22	2.036	750	0	0	1.4	20	4.61947	-146.862
	0.22	2.036	750	0	0	1.4	20	5.68142	-178.324
	0.22	2.036	750	0	0	1.4	20	7.43363	-214.974

- w/c: water to cement ratio
- a/c: aggregate to cement ratio
- CC: Cement Content
- SF: Silica fume
- FA: Fly Ash
- HRWRA: High range water reducing admixture
- * : % of the cement weight.

(a)

(b)

Figure D-1: Heat of hydration for mixtures incorporating wollastonite microfibers with a) 8% and b) 12% contents compared to that of the control mixture.

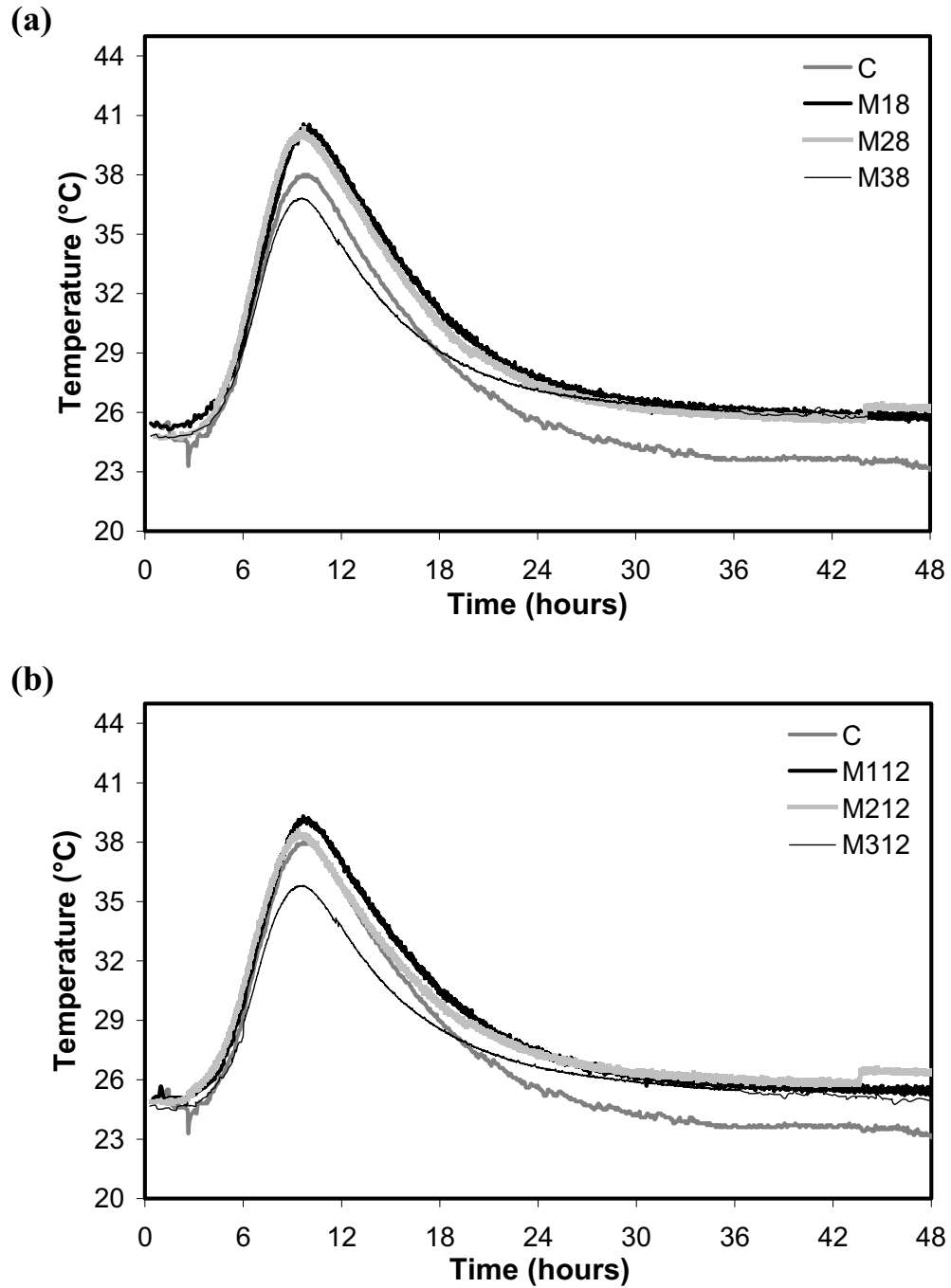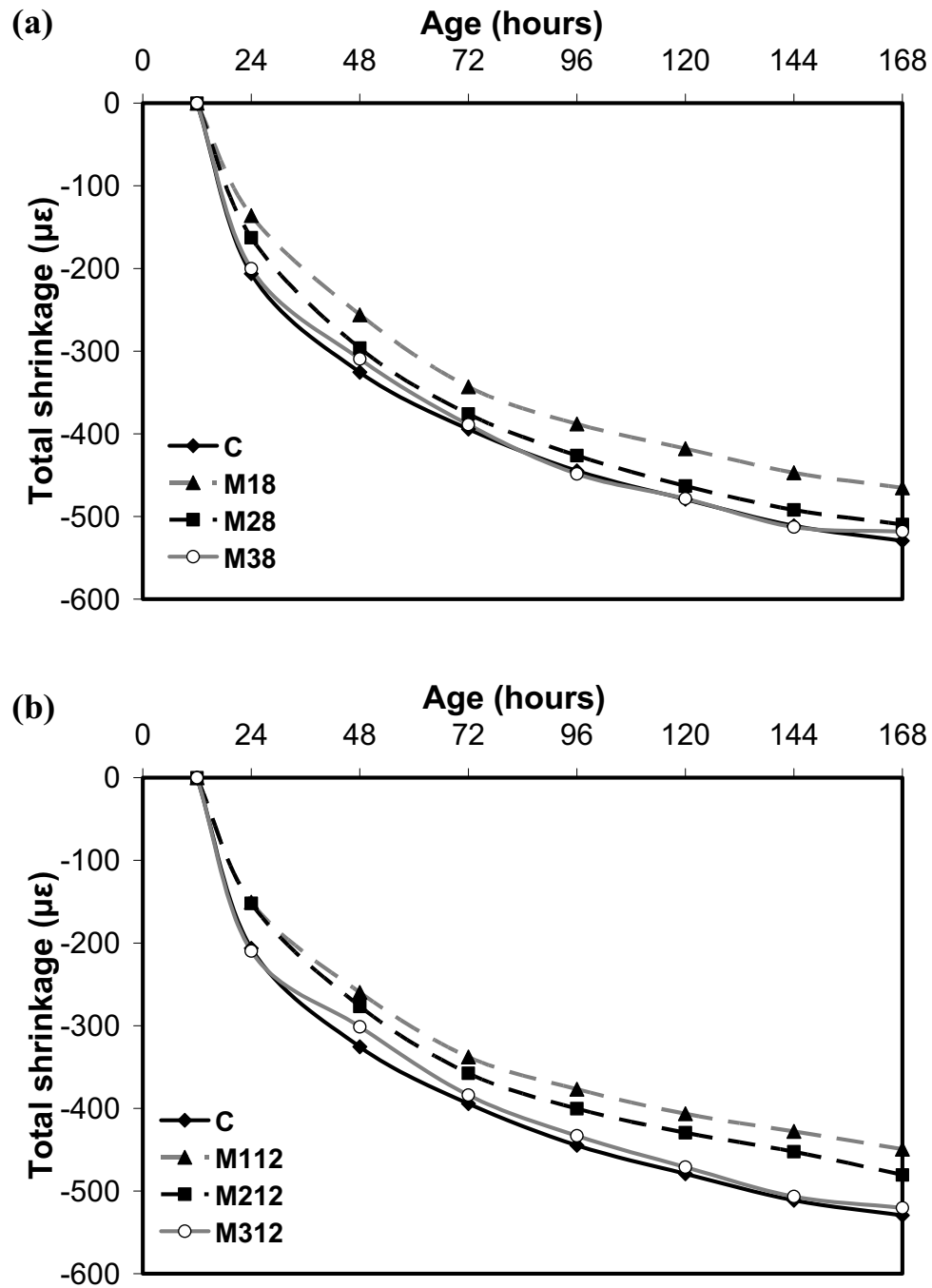**Figure D-2: Total shrinkage for mixtures incorporating wollastonite microfibers with a) 8% and b) 12% contents compared to that of control mixture.**
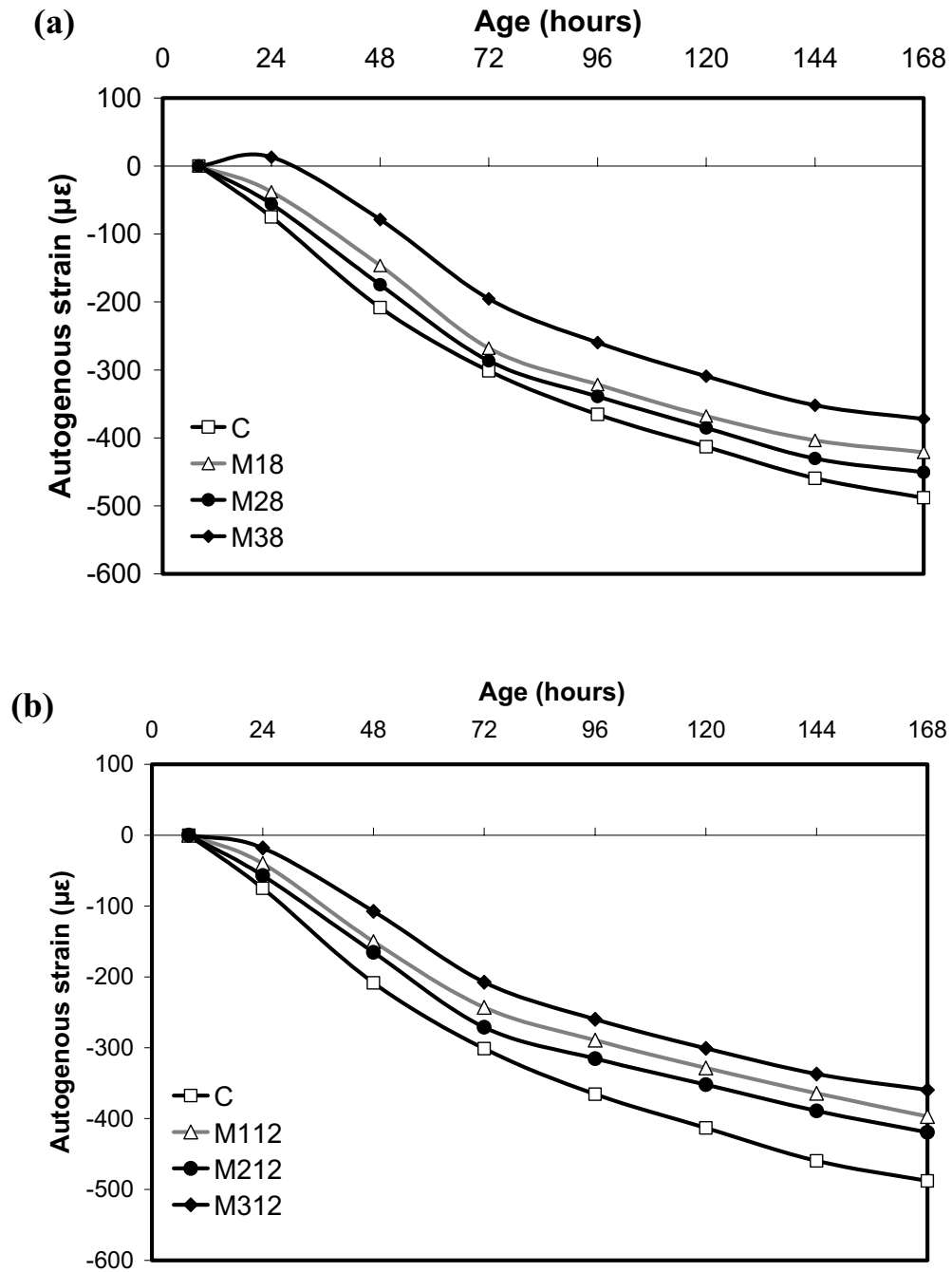
Figure D-3: Autogenous shrinkage for mixtures incorporating wollastonite microfibers with a) 8% and 6) 12% contents compared to that of the control mixture.

APPENDIX E

Table E -1*:* Trial Mixtures Composition

No.	Cement Content (kg)	Silica Fume (kg)	Quartz Sand (kg)	Quartz Powder (kg)	Water (kg)	HRWRA (kg)
1	720	210	1020	232	110	31
2	650	165	779	560	237	23
3	800	200	871	463	150	25
4	930	104	930	451	155	24
5	820	92	798	622	155	13
6	1114	169	611	305	212	40
7	1290	350	462	90	220	35

VITA

Name: Ahmed Mohammed Salah El-Din Mohammed Soliman

Post Secondary Education and Degrees:

Ain Shams University
Cairo, Egypt
1997-2002 B.Sc. (Civil Engineering)

Ain Shams University
Cairo, Egypt
2002-2005 M.Sc. (Civil Engineering/Materials)

The University of Western Ontario
London, Ontario, Canada
2007-2011, Ph.D. (Civil Engineering/Materials)

Related Work Experience:

Research and Teaching Assistant
The University of Western Ontario
2007-2011

Research and Teaching Assistant
Ain Shams University
2002-2007

Quality Control, Planning and Controls Engineer
Concrete Material Unit, Ain Shams University, Egypt
2002-2007

PUBLICATIONS

1. Nehdi, M. L. and **Soliman, A. M.** (2009) " Early-age properties of concrete: Overview of fundamental concepts and state-of-the art research," Construction Materials, ICE, Vol. 164, Issue CM2, April 2011, pp. 55-77.

2. **Soliman, A. M.** and Nehdi, M. L. (2009) "Effect of drying conditions on autogenous shrinkage of ultra-high performance concrete at early-age," Materials and Structures, RILEM, **In Press** (published on line in 2011- DOI: 10.1617/s11527-010-9670-0).

3. **Soliman, A. M.** and Nehdi, M. L. (Accepted 2011) "Early-age shrinkage of ultra high- performance concrete under drying/wetting cycles and submerged conditions," ACI Materials Journal, American Concrete Institute, **Accepted**.

4. **Soliman, A. M.** and Nehdi, M. L. (Accepted 2010) "Self-accelerated reactive powder concrete using partially hydrated cementitious materials," ACI Materials Journal, American Concrete Institute, **In Press** (to appear in 2011).

5. **Soliman, A. M.** and Nehdi, M. L. (2010) "Self-restraining concrete: mechanisms and Evidence," Cement and Concrete Research, Elsevier Science, **Submitted**

6. **Soliman, A. M.** and Nehdi, M. L. (2010) "Can partially hydrated cementitious materials mitigate early-age shrinkage in ultra-high Performance concrete?," Cement and Concrete Research, Elsevier Science, **Submitted**

7. **Soliman, A. M.** and Nehdi, M. L. (2010) "Influence of natural wollastonite microfiber on early-age behaviour of ultra-high performance concrete," Journal of Materials in Civil Engineering, ASCE, **Submitted**

8. **Soliman, A. M.** and Nehdi, M. L. (2011) "Shrinkage behaviour of ultra high-performance concrete with shrinkage reducing admixture and wollastonite microfiber," Cement and Concrete Composite, Elsevier Science, **Submitted.**

9. **Soliman, A. M.** and Nehdi, M. L. (2011) "Artificial neural network modeling of early-age autogenous shrinkage of concrete," ACI Materials Journal, American Concrete Institute, **Submitted**

10. **Soliman, A. M.** and Nehdi, M. L. (2010) "Performance of shrinkage reducing admixture under drying/wetting cycles and submerged conditions," Proceedings of 2nd International Structures Specialty Conference, Winnipeg, Manitoba, Canada, pp. (ST-30-1: ST-30-7).**Published**

11. **Soliman, A. M.** and Nehdi, M. L. (2010) "Effect of shrinkage mitigation methods on early-age shrinkage of UHPC under simulated field conditions," Eighth International Conference on. Short and Medium Span Bridges, Niagara Falls, Ontario, Canada, 2010, pp. (83-1 :83-8) **Published**

12. J. Camiletti, **Soliman, A.M.** and M.L. Nehdi (2010). "Performance of nano-limestone as a cement hydration accelerator" Proceedings of 2nd International Structures Specialty Conference, Winnipeg, Canada, pp. (ST-31-1 - ST-31-7). International Conference. **Published** (Co-supervising Work).

13. **Soliman, A. M.** and Nehdi, M. L. (2012) "Early-age behaviour of wollastonite microfiber UHPC" Twelfth International Conference on Recent Advances in Concrete Technology and Sustainability Issues, Prague, Czech Republic, 2012. **Submitted.**

14. **Soliman, A. M.** and Nehdi, M. L. (2012) "Performance of concrete shrinkage mitigation admixtures under simulated field conditions," Proceedings of the Tenth International Conference on Superplasticizer and Other Chemical Admixtures in Concrete to be held in Prague, Czech Republic, October 28 to 31, 2012. **Submitted.**

15. **Soliman, A. M.** and Nehdi, M. L. (2011), "Environmentally friendly self-accelerated concrete," Proceedings of 2nd International Engineering Mechanics and Materials Specialty Conference, Ottawa, Ontario, Canada. **Submitted.**

16. **Soliman, A. M.** and Nehdi, M. L. (2011), "Early-age behaviour of shrinkage reducing admixture and wollastonite microfibers in UHPC," Proceedings of

2nd International Engineering Mechanics and Materials Specialty Conference, Ottawa, Ontario, Canada. **Submitted.**

17. **Soliman, A. M.** and Nehdi, M. L. (2011), "Effect of exposure conditions on early-age shrinkage of UHPC thin elements," Proceedings of 2nd International Engineering Mechanics and Materials Specialty Conference, Ottawa, Ontario, Canada. **Submitted.**

18. J. Camiletti, **Soliman, A.M.** and M.L. Nehdi (2010). "Early age behaviour of UHPC incorporating micro-limestone," Proceedings of 2nd International Engineering Mechanics and Materials Specialty Conference, Ottawa, Ontario, Canada. **Submitted** (Co-supervising Work).

HONOURS AND AWARDS

- **2010-2011:** Graduate Research Thesis Award: University of Western Ontario, London, Ontario, Canada

- **2009-2010:** Graduate Research Thesis Award: University of Western Ontario, London, Ontario, Canada

- **2009-2010:** Graduate scholarship in structure Engineering Research award, The University of Western Ontario, London, Ontario, Canada

- **2007-Present:** Western Engineering Graduate Entrance Scholarship (WEGES), The University of Western Ontario, London, Ontario, Canada

- **1997-2002:** The Government Award of Excellence in Undergraduate Studies, Ain Shams University, Cairo, Egypt.

TEACHING EXPERIENCES

- **2008-2010:** Instructing a number of lectures in undergraduate courses: Mechanics of Materials [Second year course] & Materials for Civil Engineering [Third year course], The University of Western Ontario

SUPERVISORY EXPERIENCES

- **2009- 2011:** Co-supervising a Master student working on "The application of nano-limestone in concrete" at The University of Western Ontario [Publication is mentioned above].
- **2008-2009:** Supervising three summer students working at the Concrete Laboratory in the Faculty of Engineering at The University of Western Ontario.

OTHER RELATED EXPERIENCE

- **2004-2007** **Designer**, (Part Time)
  Engineering Consulting Center, Ain Shams University, Cairo, Egypt. *Duties:* Design concrete and steel structures, analysis for several normal and medium-rise buildings (up to 12 story), modeling and preparing structural drawings. Studying different problems in the area of industry and engineering and create solution methods.

- **2002-2007** **Laboratory and quality control engineer**,
  Materials laboratory, Ain Shams University, Cairo, Egypt
  Duties: supervision and conducting experiments, site visiting, test results analysis and writing technical reports.

- **2007-Present** **Teaching Assistant and Research Assistant,**
  The University Of Western Ontario, London, Ontario, Canada

- **2002-2007** **Teaching Assistant and Research Assistant**,
  Ain Shams University, Cairo, Egypt
  Courses: Properties & Testing of Materials (1&2), New Construction Materials, Special Concrete Types, Concrete Durability, Repair & Strengthening of Structures.

- **2006** **Research Assistant,** (Part-Time)
  National Research Center, Cairo, Egypt
  Duties: Studying the behavior of fiber reinforced concrete exposed to fire.

ELECTED POSITIONS

- **2009- 2011:** Councilor for the Faculty of Engineering for the Society of Graduate Students (SOGS)-4000 members, The University of Western Ontario.

- **2010- 2011:** Councilor for the Graduate Engineering Society-1500 members, The University of Western Ontario.

VOLUNTEER WORK

- **2009-2010:** Concrete Canoe 2009: provide information and advice to team members on different concrete practices.
- **2008-2009:** Concrete lab assistant: casting concrete samples to be used for demonstration purposes for undergraduate and postgraduate students.
- **2009-Present:** Steward for Civil and Environmental Engineering Department at the Graduate Teaching Assistant Union, The University of Western Ontario.
- **2009-Present:** Social Activities Coordinator at the Egyptian Student Association in North America (ESANA), London, Ontario, Canada.

MEMBERSHIPS:

- (CSCE) The Canadian Society for Civil Engineering.
- (ACI) The American Concrete Institute.
- (ASCE) American Society of Civil Engineers.
- (ESE) Egyptian Syndicate of Engineers.